



University of Reading

Clustering and stalling of North Atlantic cyclones: The influence on precipitation in England and Wales

Author:
Ruari I. RHODES

Supervisors:
Prof. Len C. SHAFFREY
Prof. Sue L. GRAY

*A thesis submitted in fulfilment of the requirements
for the degree of Doctor of Philosophy*

in the

Department of Meteorology

June 2017

Declaration of Authorship

I confirm that this is my own work and the use of all material from other sources has been properly and fully acknowledged.

Ruari I. Rhodes

Abstract

Recently, several large-scale flooding events in England and Wales have been caused by multiple cyclones in a short period of time (clustering), or slow moving storms (stalling).

The question of how much precipitation is associated with clustered or stalled extratropical cyclones is addressed using continuous areas of precipitation to associate extreme precipitation events to specific extratropical cyclones. This method is applied to ERA-Interim/HadUKP data and the HadGEM2-ES Historical and RCP8.5 climate model experiments for 1, 7, 13 and 31-day precipitation accumulations.

In ERA-Interim, extreme wet events ($p \geq 0.98$) in England and Wales are associated with 20% to 45% more cyclones than wet events ($p \geq 0.5$) in winter, spring and autumn. Mean cyclone residence times are generally longer in extreme wet events than wet events for all seasons. Longer residence times are associated with a quasi-stationary wavenumber 6 planetary wave in spring, summer and autumn.

Clustering is a less important process for extreme England and Wales precipitation events in HadGEM2-ES than in ERA-Interim. Stalling is important for summer extreme wet events in HadGEM2-ES as in ERA-Interim, however, stalling in winter extreme events is under-represented. Projected increases in extreme winter England and Wales precipitation events in HadGEM2-ES are primarily associated with increased atmospheric moisture availability rather than changes to clustering or stalling.

The ability of reanalyses to represent extreme England and Wales precipitation is also evaluated. ERA-Interim and 20CR only identify 45% to 55% of observed daily p98 precipitation events over England and Wales.

Clustering and stalling are significant influences on England and Wales precipitation, mainly affecting winter and summer precipitation events respectively. However, future changes in England and Wales precipitation are likely to be governed more by thermodynamic changes than changes in circulation patterns.

Acknowledgements

I owe thanks to more people than could possibly be listed here.

Len Shaffrey and Sue Gray have dedicated a vast amount of time to help guide and develop this project. I thank them not only for their time and expertise, but also for their patience and support. I could not have asked for better supervisors.

Monitoring committee meetings with John Methven and David Brayshaw were always a pleasure, and I invariably left our meetings with a new found enthusiasm and brimming with new ideas. Kevin Hodges and Giuseppe Zappa also both dedicated a great deal of time to helping me with the TRACK software.

I have been afforded many opportunities to discuss and develop my research with the team at Lloyds Banking Group, and our meetings have presented a valuable opportunity to put my research into wider context. Particular thanks go to Jack Oakshatt and Jessica Turner for our constructive meetings.

There are too many friends to name individually, but my thanks go to the runners, the cyclists and the weight-lifters; the climbers, walkers, singers and philosophers; the drinkers of tea, coffee, beer and gin; the dancers and board-gamers and karaoke-ists, and everyone who made the department such a wonderful place to be. My particular thanks go to my housemates past and present; those who spent long hours with me keeping stress at bay with exercise; those who spent long hours undoing all the hard work with pizza (often the same people); and those special few who were always there to drag me away for a cup of tea or a pint of beer and a good old-fashioned rant.

A few people deserve special mention. Kate has been endlessly patient and encouraging, despite my estimates of “just another couple of months” for over a year now. Sue and John kindly put a roof over my head for some time, as did Sam and Steph, for which I am sincerely grateful.

Finally to my family: I couldn't have done this without you. You have an ability to thrust me back into the real world with a cold, wet walk; a fleet of small children; or a casual little bike ride to Paris. I look forward to being able to spend more time with you all. My greatest thanks of all go to my dad. I owe everything that brought me to this point to his infectious enthusiasm and relentless belief in me.

Contents

Declaration of Authorship	ii
Abstract	iii
Acknowledgements	iv
Table of contents	v
Abbreviations	ix
Symbols	xi
1 Introduction and Literature Review	1
1.1 Introduction and motivation	1
1.2 Precipitation in England and Wales	3
1.2.1 Trends in England and Wales precipitation	3
1.3 Extratropical cyclones	6
1.3.1 Extratropical cyclone formation	6
1.3.2 Classification of extratropical cyclones	10
1.3.3 Extratropical cyclone structure	11
1.3.4 Objective cyclone tracking	13
1.3.5 Key features of the North Atlantic storm track	16
1.4 Importance of cyclones and fronts for precipitation	18
1.5 Climate change	22
1.5.1 Projected changes to North Atlantic cyclones and the storm track	23
1.5.2 Projected changes to precipitation from extratropical cyclones . .	26
1.6 Extratropical cyclone clustering and stalling in the present and future climate	27
1.6.1 Clustering	27
1.6.2 Stalling	32
1.7 Thesis structure and aims	33

2	Data and Methods	35
2.1	Observational datasets	35
2.1.1	England and Wales Precipitation (EWP)	35
2.1.2	Global Precipitation Climatology Project (GPCP)	36
2.2	Reanalysis	37
2.2.1	NOAA-CIRES Twentieth Century Reanalysis	37
2.2.2	ECMWF Reanalysis (ERA) Interim	38
2.3	Climate models	39
2.3.1	HadGEM2-ES	39
2.4	Extratropical cyclone tracking	42
2.5	Time-series analysis	43
2.6	Quantification of periods of cyclone clustering and stalling	45
3	Can reanalyses represent extreme precipitation over England and Wales?	47
3.1	Introduction	47
3.2	Data and Methods	49
3.2.1	Hit Rate analysis method	49
3.2.2	Accumulation time-scales	49
3.3	Analysis	50
3.3.1	Spatial analysis of precipitation data	50
3.3.2	Statistical analysis	51
3.3.3	Intensity of precipitation accumulations in reanalysis	51
3.3.4	Hit rate analysis for an example time-series	52
3.3.5	Hit rate analysis	53
3.4	Conclusions	55
4	Development of the Continuous Precipitation Area storm association algorithm	57
4.1	Introduction	57
4.2	Evaluation of established methods	58
4.3	Criteria for storm association algorithm	60
4.4	Development of CPA algorithm	61
4.4.1	Identification of Continuous Precipitation Areas	61
4.4.2	Language and structure	64
4.5	Comparison with established methods	65
4.6	Parameter sensitivity	67
4.6.1	Precipitation threshold evaluation	67
4.6.2	Cyclone proximity radius evaluation	69

4.7	Summary: CPA algorithm development and evaluation	71
5	Clustering, stalling, and England and Wales precipitation events in the recent climate	73
5.1	Introduction	73
5.2	Data	73
5.2.1	England and Wales precipitation	74
5.2.2	The North Atlantic storm track in ERA-I	75
5.2.3	250-hPa vector winds	76
5.3	Clustering, stalling, and extreme precipitation events in ERA-Interim . .	81
5.3.1	Relationship of cyclone clustering to extreme events	81
5.3.2	Relationship of cyclone stalling to extreme events	85
5.3.3	Precipitation intensity in extratropical cyclones	90
5.4	Discussion and conclusions	93
6	Evaluation of clustering, stalling and England and Wales precipitation events in HadGEM2-ES	97
6.1	Introduction	97
6.2	England and Wales precipitation in HadGEM2-ES	98
6.3	The North Atlantic storm track in HadGEM2-ES	100
6.3.1	Seasonal mean vector winds	101
6.3.2	Storm track density in the North Atlantic	103
6.3.3	Number and speed of extratropical cyclones in the Eastern North Atlantic	104
6.3.4	North Atlantic extratropical cyclone propagation speeds	106
6.4	Clustering, stalling, and precipitation events in HadGEM2-ES Historical .	108
6.4.1	Extreme England and Wales precipitation events	108
6.4.2	Clustering in HadGEM2-ES	113
6.4.3	Stalling in HadGEM2-ES	120
6.4.4	Extratropical cyclone precipitation intensity in HadGEM2-ES . . .	124
6.5	Discussion and conclusions	127
7	Climate change projection of clustering, stalling, and England and Wales precipitation events	131
7.1	Introduction	131
7.2	England and Wales precipitation in HadGEM2-ES RCP8.5	132
7.3	Projected changes to the North Atlantic storm track	134
7.3.1	Seasonal mean vector winds	135
7.3.2	Mean 250-hPa winds associated with extreme England and Wales precipitation events in RCP8.5	135

7.3.3	Frequency and propagation speed of North Atlantic Storms	137
7.3.4	Thermodynamic changes in the North Atlantic	142
7.3.5	Relationship between precipitation changes and storm track dynamics	144
7.4	Changes to clustering, stalling, and precipitation events in RCP8.5	145
7.4.1	Clustering in RCP8.5	145
7.4.2	Stalling in RCP8.5	148
7.4.3	Extratropical cyclone precipitation intensity in RCP8.5	151
7.5	Discussion and conclusions	153
8	Discussion and conclusions	159
8.1	Overview	159
8.2	Discussion and conclusions	161
8.2.1	How well are historical England and Wales precipitation events represented in reanalyses?	161
8.2.2	What is the best way to associate precipitation with extratropical cyclones?	162
8.2.3	To what extent is precipitation in England and Wales influenced by clustering and stalling of extratropical cyclones?	164
8.2.4	How well do climate models represent observed relationships between extratropical cyclones and England and Wales precipitation events?	166
8.2.5	How can we expect extreme precipitation events caused by extratropical cyclones to change in the future?	168
8.3	Future work	169
8.3.1	How does the influence of extratropical cyclone clustering and stalling on precipitation events vary throughout Europe?	170
8.3.2	What causes extratropical cyclones to stall?	170
8.3.3	How is the influence of clustering and stalling of extratropical cyclones on precipitation represented in CMIP5 models?	171
	Bibliography	173

Abbreviations

20CR	NOAA-CIRES Twentieth Century Reanalysis
CMIPx	Coupled Model Intercomparison Project - Phase x
CPA	Continuous Precipitation Area
ERA-I	ECMWF Reanalysis - Interim
EWP	England and Wales Precipitation
GCM	General Circulation Model
GIS	Geographic Information System
HadGEM2-ES	Hadley Centre Global Environment Model 2 - Earth System
HadUKP	Hadley Centre United Kingdom Precipitation
NCEP	National Centres for Environmental Prediction
NetCDF	Network Common Data Form
NOAA	National Oceanographic and Atmospheric Administration (US)
POT	Peaks-Over-Threshold
PV	Potential Vorticity
SLP	Sea Level Pressure
SST	Sea Surface Temperature
DJF	December, January, February
MAM	March, April, May
JJA	June, July, August
SON	September, October, November

Symbols

$p(x)$	x^{th} percentile	
\mathbf{u}_p	Wind speed vector (p hPa)	ms^{-1}
U_p	Zonal wind velocity (p hPa)	ms^{-1}
V_p	Meridional wind velocity (p hPa)	ms^{-1}
Z_p	Geopotential height (p hPa)	m
$\hat{\phi}$	Dispersion statistic	
ξ_p	Relative Vorticity (p hPa)	s^{-1}

To the luckiest man alive.

Chapter 1

Introduction and Literature Review

1.1 Introduction and motivation

Maritime regions of Western Europe are susceptible to extremes of rainfall generated by extratropical cyclones. Extreme accumulations of rainfall generate a high risk of pluvial and fluvial flooding, with wide-reaching socio-economic impacts. In recent years, several high-impact flooding events in England and Wales have been associated with particular patterns in the movement of extratropical cyclones. During 13–15th and 25th June 2007, two intense, slow moving extratropical cyclones caused high precipitation accumulations and extensive flooding across England and Wales. These were followed by an especially intense, stalled (slow moving) storm on 20 July 2007, recording 157.4 mm rainfall in 48 hours in Worcestershire (Blackburn et al., 2008). The effect of an intense, stalled storm producing rainfall on saturated ground was the rapid flooding of large parts of south-western England, leading to failures of water and power supplies. The town of Tewkesbury in Gloucestershire was entirely cut off (Figure 1.1a); 7,000 people needed to be rescued from the flood waters, and 13 people died (Pitt, 2008). Insured loss estimates are currently £2.5–3.5 billion, with a further £1bn of uninsured loss (Met Office 2011, Hughs and Gambrill 2012, Chatterton et al. 2010).

The winter of 2013-2014 was characterised by a series of highly mobile storms, which crossed the British Isles at regular intervals. Although only a few of these storms were particularly intense, the cumulative effect led to extensive flooding across England and Wales, with large-scale floods occurring on the Somerset Levels (Figure 1.1b) and the



FIGURE 1.1: (a) Tewkesbury Abbey, 2007-07-01 (Pitt, 2008). (a) Somerset levels, 2014-02-02 (Met Office, 2015).

River Thames. Insured flood losses only reached £500 million due to the sparse population of the Somerset Levels and the high level of flood protection in the Thames catchment; however, the combination of flood, storm surge and wind caused widespread damage to infrastructure (Met Office 2015, DEFRA 2014, RMS 2014).

The events of recent years have highlighted the need to better understand how extremes of accumulated precipitation are generated by extratropical cyclones. In particular, the relationship between the movement patterns of extratropical cyclones, particularly clustering and stalling, and extremes of accumulated precipitation over England and Wales is currently poorly understood. England and Wales is chosen as a study region due to the availability of a long-running, homogeneous precipitation dataset; its location at the eastern end of the North Atlantic storm track, and insurance industry interest in the region.

The aim of this thesis is to address gaps in our knowledge of how the movement of cyclones, specifically patterns of clustering and stalling, influences precipitation accumulations on time-scales from one day to one month over the England and Wales region. The following sections of this chapter will evaluate the current state of knowledge on matters relevant to this aim, structured as follows: the nature of precipitation over England and Wales is discussed in Section 1.2; the structure, formation, and precipitation characteristics of extratropical cyclones are discussed in Section 1.3; the importance of extratropical cyclones for precipitation in the North Atlantic storm track is discussed in Section 1.4; the influence of climate change on England and Wales precipitation and

extratropical cyclones in the North Atlantic is discussed in Section 1.5; clustering and stalling characteristics of extratropical cyclones are discussed in Section 1.6; and finally, the structure of this thesis, and its objectives, is described in Section 1.7.

1.2 Precipitation in England and Wales

England and Wales has a varied precipitation climatology, with annual totals dominated by orographically enhanced precipitation over the high ground of the Pennines, the Cambrian Mountains and the south-western moors (Figure 1.2). Hand et al. (2004) investigated the types of weather phenomena responsible for the most extreme precipitation over the United Kingdom. Extreme events from 1900–1960 were identified from publications of *Meteorological Magazine* and *British Rainfall*, and later events (1960–2005) were identified from on the Met Office *Daily Weather Report* series and other published reports. Extreme events were identified based on a variable threshold which considers both accumulated rainfall and event duration. Events were categorised based on descriptions given in the aforementioned publications, combined with station data, surface charts, and satellite imagery where available. Events were categorised as convective, convective (frontal forcing), orographic, frontal (embedded instability) and frontal. This study found that short duration (< 6 hours) precipitation extremes were predominantly caused by convective storms, whilst longer duration events (6–60 hours) were predominantly caused by frontal and orographically-enhanced events (Figure 1.3a). Where frontal rainfall was identified, 80% of cases were associated with a depression to the south/east of the British Isles, and a slow moving frontal system. The highest precipitation risk from slow-moving extratropical cyclones was identified as the north-western quadrant of the storm (Figure 1.3b). This high risk region in slow-moving extratropical cyclones is due to the rotating motion of the fronts as they wrap around a slow-moving low centre, causing the region in the north-western quadrant of the storm to experience rainfall from the cloud head, both fronts, and a region of likely convective storm development.

1.2.1 Trends in England and Wales precipitation

It is important to identify whether any long-term trends in precipitation exist, as these may be early evidence of the impact of climate change. Osborn et al. (2000) used a set of 110 precipitation station records to analyse trends and variation in daily precipitation intensity across the UK over the period 1961–1995. This study identified a significant

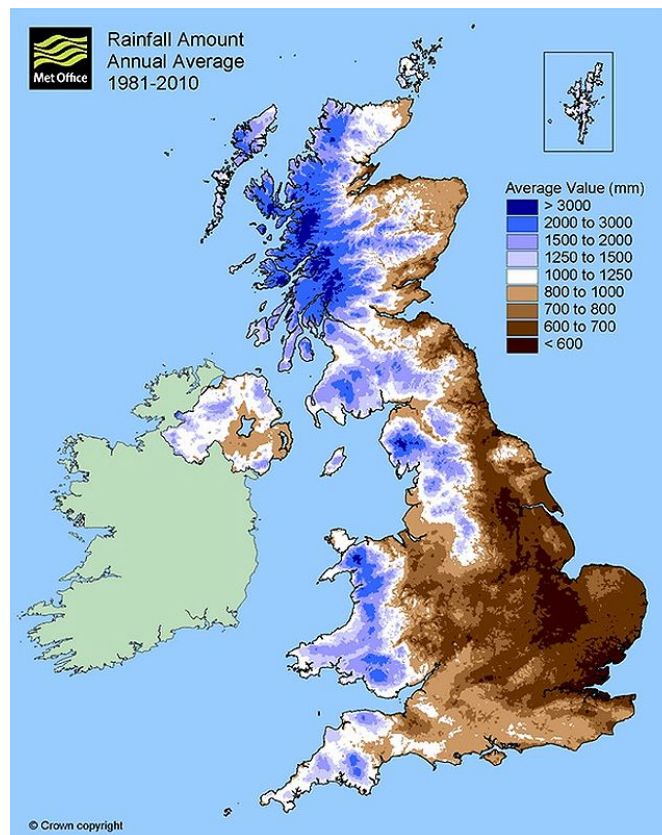


FIGURE 1.2: United Kingdom annual precipitation climatology, 1981–2010.

increase in winter daily precipitation intensity. The magnitude of this increase varies greatly by region, with higher trends identified in regions of high orography. A study by Alexander and Jones (2000) using the England and Wales precipitation time-series (Legg, 2011) also identified an increase in DJF (December, January, February) precipitation totals over the period 1931–1999. This increase was identified in the north-west region of England and Wales, which corresponds to the high orography region identified as having the strongest trend in Osborn et al. (2000). No significant increase was identified in daily 95th percentile precipitation intensity in England and Wales; however, an increase was identified during October–March (ONDJFM) in Scotland during the period 1931–2000 (Osborn et al., 2000). Mills (2016) demonstrates that trends in the England and Wales precipitation time-series are characterised by linear seasonal trends, interrupted by regime shifts in 1828, 1871, 1917, and 1976. When the data are re-modelled to allow for regime shifts, the current regime (1976–present) is found to follow the previously identified trend for drier summers, but no trend is found in winter precipitation.

Changes in flood risk in England and Wales are an important consideration when considering precipitation extremes. Flood risk has a great deal of spatial variation, and

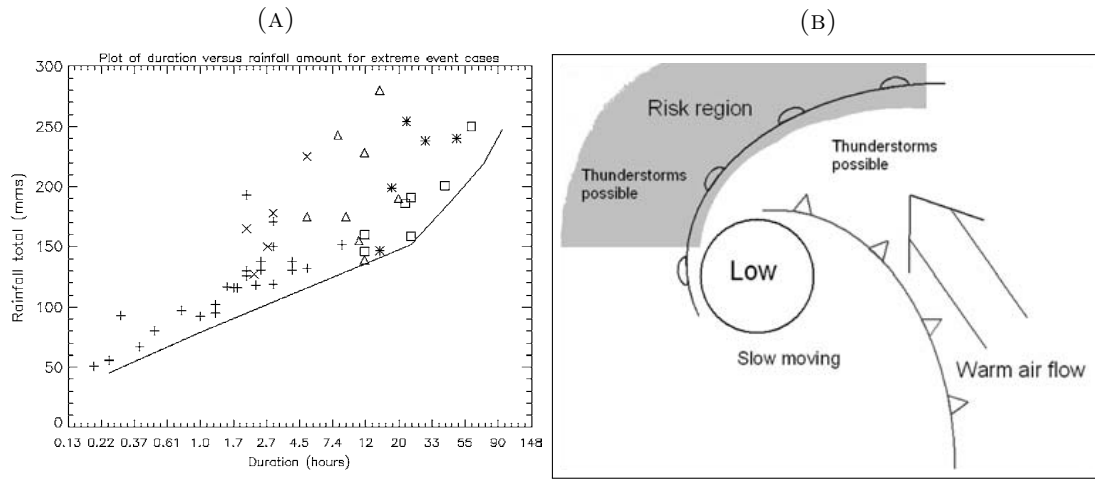


FIGURE 1.3: (A) Plot of point rainfall amount (mm) versus duration (h) (on a logarithmic scale) for each of five event categories: +=convective, x=convective*** (frontal forcing), * = orographic, Δ = frontal*** (with embedded instability) and \square = frontal. From Hand et al. (2004), Figure 1. (B) Schematic diagram of regions of high precipitation risk from extratropical cyclones from Hand et al. (2004), Fig. 12.

depends on the level of ground saturation at the time of a major precipitation event. Catchments vary greatly in their response times (Smith et al., 2013), and steeper catchments in rocky areas respond very much more quickly to a precipitation event than shallow catchments in porous areas. Robson et al. (1998) uses a Peaks-Over-Threshold method to examine river gauging stations around the UK for evidence of trends in flood magnitude and frequency. No trends in flood behaviour were identified for the period 1941–1980, but the authors identify the magnitude of inter-annual variability and the paucity of data as sources of uncertainty in identifying significant trends and long-term variation.

It is useful to identify changes in recent precipitation patterns in England and Wales which may be attributed to climate change. The winter of 2013–14 was exceptionally stormy in the UK, being characterised by a persistent area of low pressure to the north of the British Isles, an anomalous eastward extension of the jet stream, and a regular succession of extratropical cyclones moving across southern England from the North Atlantic. An attribution study was performed by Schaller et al. (2016) to determine whether climate change was likely to have influenced the chance of such an event occurring in the present climate. A large ensemble of a regional climate model simulated DJF 2013–14 under current climate conditions, and was compared against a “Natural” simulation with a pre-industrial atmospheric composition. An increased incidence of persistent low pressure to the north of the British Isles was identified in the current climate relative to the “Natural” simulation. A small but significant increase in days

with westerly flow over the UK was also identified. The risk of heavy precipitation was found to be increased over southern England, leading to a higher chance of extreme 30-day flow on the River Thames than in the pre-industrial climate. Whilst a single event cannot directly be attributed to climate change, this study shows that the likelihood of similar extreme precipitation events has increased due to a combination of a stronger hydrological cycle and altered circulation patterns.

1.3 Extratropical cyclones

To better understand reasons for England and Wales precipitation climatology and projected future trends, a good understanding of the structure and formation of extratropical cyclones is required. In Section 1.3.1, the formation of extratropical cyclones is discussed. Classifications of extratropical cyclones based on their structure and manner of cyclogenesis are outlined in Section 1.3.2. The main structural features of extratropical cyclones are discussed in Section 1.3.3. Techniques used for the analysis of extratropical cyclones and cyclone tracks in the North Atlantic are discussed in Section 1.3.4. Large-scale features of the North Atlantic storm track are discussed in Section 1.3.5.

1.3.1 Extratropical cyclone formation

The idealised structure of an extratropical cyclone in the mid-stages of its development was first described by Bjerknes and Solberg in 1919 (Bjerknes, 1919), and was updated in 1922 to include idealised descriptions of cyclones throughout several developmental stages (Bjerknes and Solberg, 1922). The “Norwegian model” describes cyclones as disturbances along a constant global boundary between warm and cold air masses (the “polar front”) (Figure 1.4). The Norwegian Model remains a commonly used descriptor of the life-cycle of extratropical cyclones, despite numerous refinements since its publication.

The Norwegian Model depicts four stages of cyclone development, as shown in Figure 1.4. Stage I is the development of a wave along the boundary of a warm, tropical air mass to the south and a cold, polar air mass to the north. Bjerknes and Solberg (1922) suppose that the two air masses must be moving in opposing directions, hence initiating a wave. As the wave propagates eastward, its amplitude is increased and the cold air mass begins to curve behind the wave, initiating a circulating motion in Stage II. The cyclone develops warm- and cold- fronts in Stage III due to the extension of the discontinuity between the two air masses to the south of the cyclone and the development of a warm sector to the south. In the final stage of development, the cold front

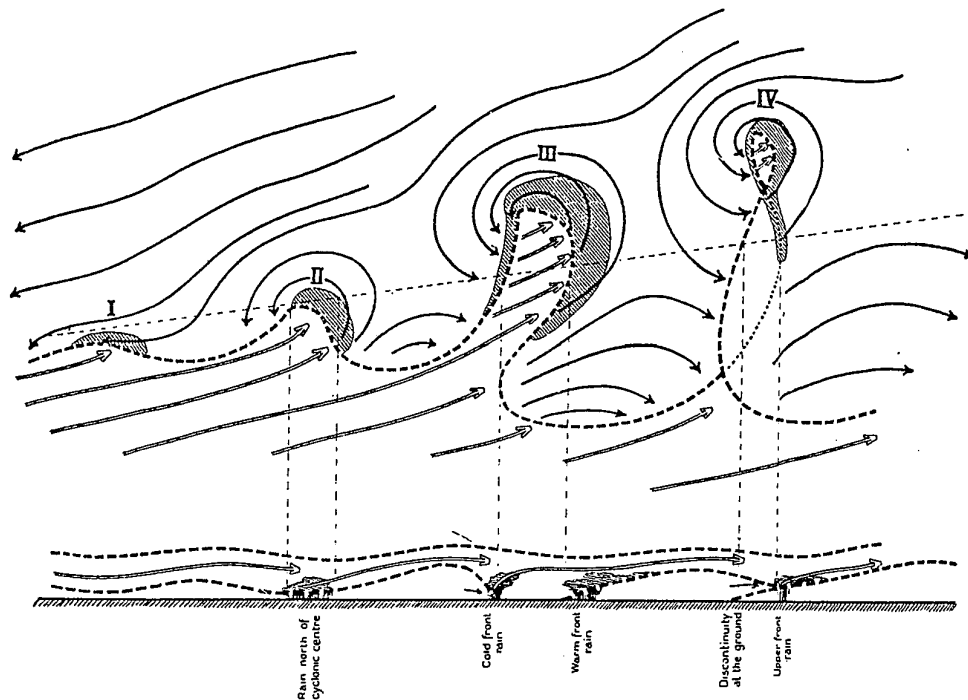


FIGURE 1.4: The Norwegian model of extratropical cyclone development (adapted from Bjerknes and Solberg 1922). Shaded areas indicate likely regions of precipitation. Arrows indicate wind flow. Dashed lines indicate the location of the polar front. Stages I to IV (left to right) show stages in the development of a cyclone from a frontal wave, through immature and mature stages of development, to the filling and occlusion of the cyclone. From Shapiro and Keyser (1990), Fig. 10.12

over-runs the warm front and develops an occluded front, “secluding” the cyclone centre and replacing any remaining warm sector air in the centre of the cyclone with cold air. This marks the decay of the cyclone and the filling of the low pressure region at the core.

A theory to describe a different development of the extratropical cyclone life-cycle was proposed in 1990 by Shapiro and Keyser. The Shapiro-Keyser model was based on the advances in observations and theory since the Norwegian model, and proposes a new type of cyclone with a characteristic frontal fracture which has been observed in explosive marine cyclogenesis.

As shown in Figure 1.5, the Shapiro-Keyser conceptual model retains the four stages of development shown in the Norwegian Model (Figure 1.4), with some modifications to the frontal structure. The cyclone begins with a broad, continuous frontal gradient in Stage I, and develops a wave form similar to the Norwegian Model. During Stage II, a discontinuity in the fronts is developed (“frontal fracture”), which evolves into a

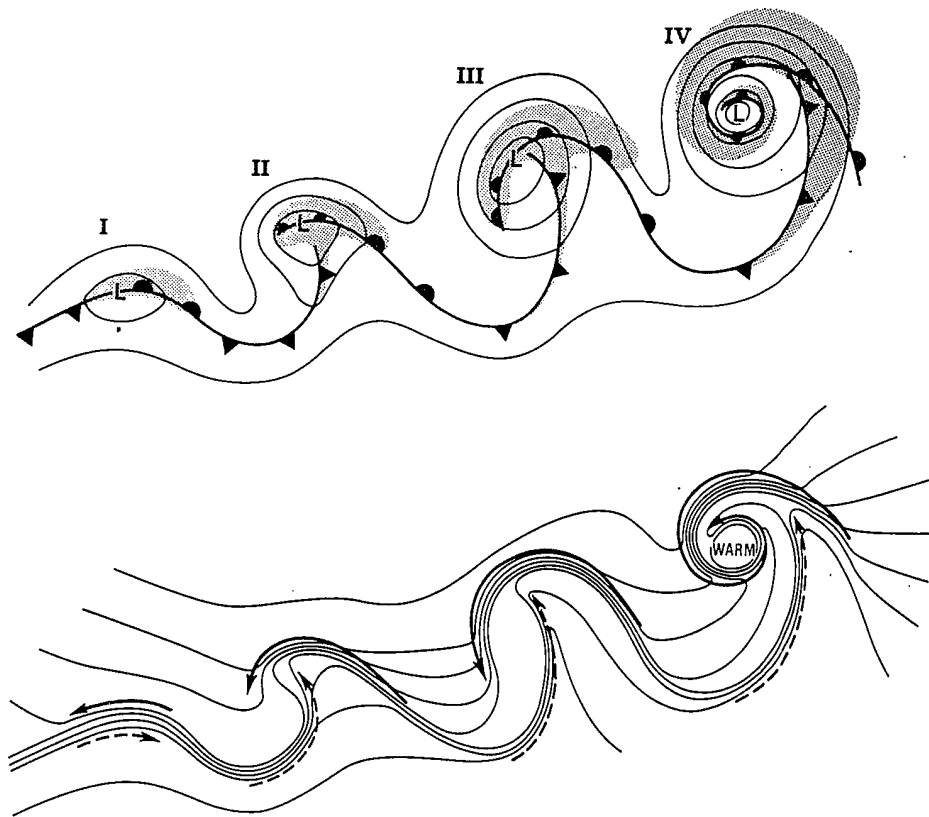


FIGURE 1.5: The Shapiro-Keyser model of extratropical cyclone development. Cyclones are shown in increasing stages of maturity from left to right: (I) incipient frontal cyclone; (II) frontal fracture; (III) bent-back warm front and frontal T-bone; (IV) warm-core frontal seclusion. Upper: sea-level pressure, solid lines; fronts, bold lines; and cloud signature, shaded. Lower: temperature, solid lines; cold and warm air currents, solid and dashed arrows, respectively. From (Shapiro and Keyser, 1990), Fig. 10.27.

bent-back warm front with frontal T-bone in Stage III. The cyclone then matures and develops a secluded core in Stage IV, consistent with the Norwegian Model.

Extratropical cyclones predominantly form in regions of baroclinic instability, where the zonal wind is highly sensitive to small perturbations. The Eady model (Eady, 1949) represents the initial stages of the amplification of a wave in an adiabatic environment against a baroclinic mean state. This model represents a small-amplitude perturbation to a basic state (zonal flow, constant vertical shear, constant Coriolis parameter (f) and no horizontal shear). The Eady model is held to be a good approximation of the initial development of an atmospheric wave, however it is only valid for small perturbations to the background state. The Charney model (Charney, 1947) assumes a similar basic state to the Eady model, but the fixed Coriolis parameter is replaced by a beta plane

approximation. This approximates the variation of the Coriolis parameter with latitude. Unlike the Eady model, no rigid upper boundary is specified. The Charney model and the Eady model produce similar growth rates.

Due to the lack of moist processes in both the Eady and Charney models, both predict cyclones of significantly larger length-scale than is observed. In addition to the amplifying frontal wave model of cyclogenesis, as predicted by the Eady and Charney models, perturbations may be induced by the presence of an upper-level Rossby wave. The influence of the upper-level wave extends to the surface, inducing a small perturbation in the θ gradient and creating a low-level wave that is 90° out of phase with the upper-level Rossby wave, and propagating eastward relative to the mean flow. As the low-level instability grows, it in turn acts to reinforce the upper-level wave, thus generating a self-perpetuating wave amplification. In the case where, due to the vertical gradient of zonal wind, the two waves remain synchronised at 90° out of phase, the resulting disturbance will continue to amplify and initiate cyclogenesis.

The concept of frontal wave cyclogenesis was first described by Bjerknes and Solberg (1922), who noted that some cyclones were observed to develop on the trailing fronts of existing, mature cyclones, especially toward the eastern end of the North Atlantic storm track, and proposed the theory that cyclones initiate as waves on a frontal boundary between warm and cold air masses. Thorncroft and Hoskins (1990) investigated the mechanisms responsible for the development of frontal waves, finding that cyclogenesis is initiated by the interaction of a surface frontal zone with a positive tropospheric potential vorticity (PV) anomaly. Such an anomaly may be caused by tropopause folding, bringing stratospheric high PV to the mid-troposphere, or by the presence of a jet streak over the frontal zone, or by a combination of the two. Where multiple sources of positive PV anomaly were present, explosive cyclogenesis was often found to occur.

Further to Thorncroft and Hoskins (1990), Renfrew et al. (1997) discusses the causes of instability in the front, finding that where stretching deformation is present along the axis of the front, the structure of the front remains stable to external influences. Rivals et al. (1998) modifies the method of Renfrew et al. (1997), and investigates the mechanism behind the (in)stability of a front lying underneath a strong upper-level jet. This study finds that the presence of the jet both stabilises the front by inducing low-level convergence, and de-stabilises the front by causing a redistribution of diabatically generated PV.

A climatology of frontal wave cyclogenesis in the North Atlantic is presented by Schemm and Sprenger (2015). In this study, frontal wave cyclogenesis is defined as the time of first occurrence of an extratropical cyclone (defined by a closed MSLP contour with a minimum lifespan of 24 hours) on an objectively identified front. For all seasons, frontal-wave cyclogenesis is found to occur most regularly over the Gulf Stream and the east coast of North America. Frontal-wave cyclogenesis in the eastern North Atlantic is identified most frequently in SON and DJF, when approximately 4–14% of cyclogenesis in the eastern North Atlantic occurs on a trailing front.

1.3.2 Classification of extratropical cyclones

The majority of extratropical cyclones may be classified into three distinct groups, based on the synoptic conditions leading to their cyclogenesis. The first two of these classifications, types “A” and “B”, were described by Petterssen and Smebye (1971), based on analysis of cyclones forming over North America, east of the Rocky Mountains. Type “A” cyclones are described as the “traditional” amplifying frontal wave within a baroclinic mean state, such as is indicated in the Eady model (Eady, 1949) and the Norwegian model of cyclogenesis (Bjerknes and Solberg, 1922). These are characterised by low levels of vorticity advection in the upper troposphere and high levels of thermal advection in the lower troposphere. In this case, the development of an upper-level trough is driven predominantly by thermal advection in the lower troposphere against a baroclinically unstable background state. Type “B” cyclones develop in the vicinity of an existing upper-troposphere disturbance, for example a Rossby wave, which creates strong vorticity advection in the upper troposphere. This vorticity enhances weak thermal advection in the lower troposphere during cyclogenesis, with thermal advection strengthening as the cyclone intensifies. Type “B” cyclones exhibit a westward tilt with height during the intensification phase, which decreases as the cyclone reaches maturity.

Both type “A” and “B” cyclones end their life-cycles in an occlusion as described by Bjerknes and Solberg (1922) and Shapiro and Keyser (1990). A third classification, type “C”, was proposed by Deveson et al. (2002), and supported by Plant et al. (2003), to account for cases found in the Fronts and Atlantic Stormtrack EXperiment (FASTEX; Joly et al. 1997) that did not conform to either type “A” or type “B” classification. Type “C” cyclones (not to be confused with a previous proposal for this designation by Radinovic (1986), for cyclones of an orographic origin based on studies of the Alpine region) are largely driven by diabatic and upper-level processes. These cyclones demonstrate low correlation between westward tilt and intensity, unlike type “B” cyclones, and the westward tilts of some type “C” cyclones have been observed to increase as

the cyclones mature. Type “C” cyclones occur predominantly in high latitude regions where an upper-level trough moves over an organised region of convection (Deveson et al., 2002). However, they are also observed frequently in cyclones originating over the eastern North Atlantic, in the vicinity of the British Isles (Dacre and Gray, 2009).

1.3.3 Extratropical cyclone structure

Within extratropical cyclones, several distinct structures have been identified through observational and modelling studies (e.g. Browning and Roberts 1994; Deveson et al. 2002). Figure 1.6 shows the major air movements within an idealised extratropical cyclone, including the warm conveyor belt (WCB), cold conveyor belt (CCB), and dry intrusion. The WCB was initially identified by Harrold (1973) as a broad (~100 km) flow ahead of the surface cold front, with ascent within the warm sector. Objectively identifiable WCB structures are found in the majority of DJF North Atlantic cyclones within 1,000 km of a cyclone centre, and are associated with a high rate of precipitation (Eckhardt et al., 2004). Carlson (1980) identified that the WCB ascends rapidly as it crosses the surface warm front, before turning anticyclonically and merging with the upper level jet stream. Browning and Roberts (1994) also identified a lower-level, cyclonic branch of the WCB in a case-study of an intense extratropical cyclone, which separates from the upper-level, anticyclonic branch and terminates within the cloud head.

The CCB flows ahead of the surface level warm front, passing beneath the WCB before ascending and diverging into two distinct flows; a low-tropospheric cyclonic branch, and a mid-tropospheric anticyclonic branch. (Carlson, 1980). Schultz (2001) identifies that, depending on the structure of the individual cyclone and the CCB identification method used, one of these paths may appear to be weak or non-existent. The cyclonic branch of the CCB may be more frequently identified in observational studies due to its greater width, and its prominence in intense extratropical cyclones (Schultz, 2001). Hewson and Neu (2015) presents a broad conceptual model of extratropical cyclone development from a wind storm risk perspective, identifying that whilst damaging winds may be present from the WCB during nearly the full life cycle of the cyclone, CCB winds tend to be stronger, but damaging only in the mature stages of cyclone development when the flow at the tip of the CCB is aligned with the direction of movement of the cyclone.

The dry intrusion (or “dry slot”) is a region of descending cold dry air of tropospheric origin, often associated with a tropopause fold (Browning, 1997). Whilst the ascending

Simplified Structure of an Extra-Tropical Cyclone

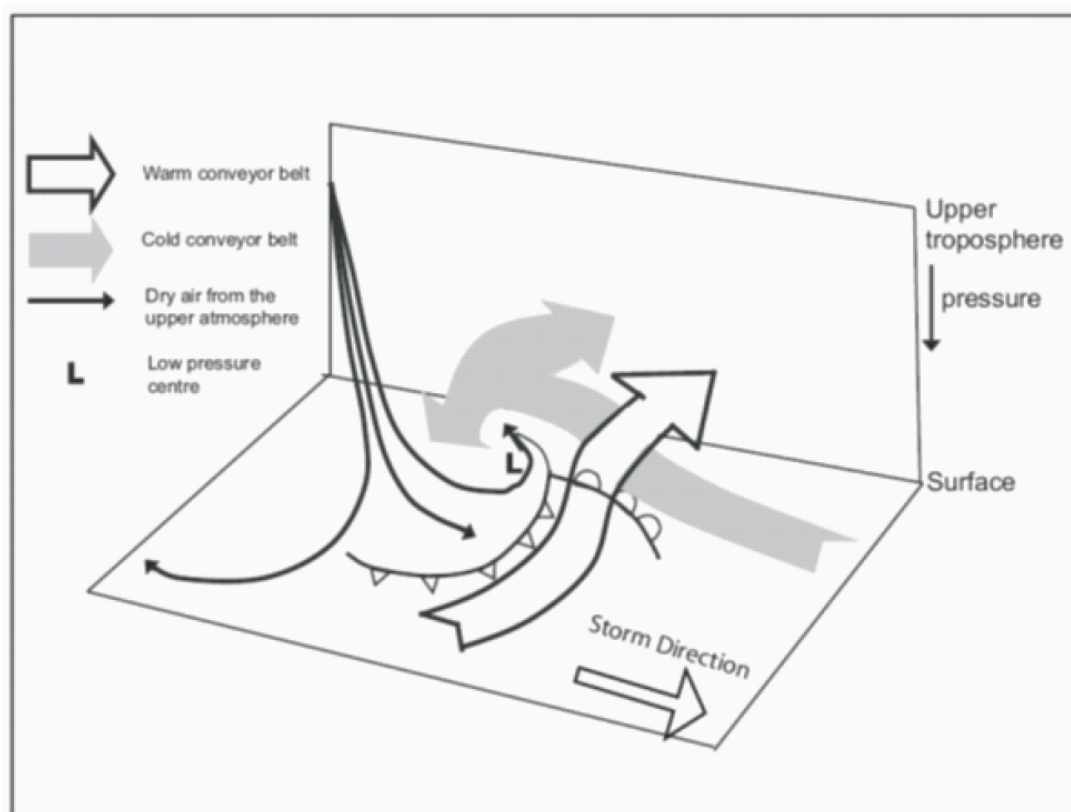


FIGURE 1.6: Schematic of warm conveyor belt, cold conveyor belt, and dry intrusion flows within an idealised extratropical cyclone. From Catto (2010), adapted from Browning (1997)

motion of the WCB is primarily responsible for generating the cloud head (Eckhardt et al., 2004), its comma shape and the distinct dry slot surrounding the cloud head is created by the dry intrusion. Browning (1997) identifies that, near the centre of the cyclone, the descending dry intrusion overruns part of the moist flow in the WCB, creating potential instability and the conditions for convective activity in the vicinity of the surface cold front. As noted by Hand et al. (2004), frontal precipitation with embedded convection has been responsible for several identified extreme rainfall events in the UK on time-scales of 5–25 hours. The interaction of the WCB and dry intrusion may therefore be considered to be highly relevant for the forecasting of precipitation extremes from extratropical cyclones.

In addition to the main structural features of extratropical cyclones as described above, atmospheric rivers are strongly linked with heavy precipitation events from extratropical cyclones. Atmospheric rivers are filaments of high water vapour transport which originate in the tropics and interact with the warm conveyor belt, giving the impression of a

“river” of moisture-laden air flowing from the tropics (Dacre et al., 2015). Lavers et al. (2011) identified the presence of an atmospheric river concurrently with the ten largest winter flooding events (based on river flow records) since 1970 in a range of basins across the UK. Dacre et al. (2015) finds that atmospheric rivers are formed by local moisture convergence around the cold front as it advances on the warm front. Moisture is thus sourced locally from the warm sector, not transported long distances from the tropics. Intense extratropical cyclones are found to produce a net export of water as they intensify, producing a filament-like water vapour footprint as they advance, which is identified from satellite imagery as an atmospheric river. Atmospheric rivers are therefore related to the intensity and warm sector humidity of previous cyclones, which indicates that moisture availability may be greater for cyclones forming part of a cluster. Ramos et al. (2016) analyses the representation of atmospheric rivers in six CMIP5 climate models, finding that the models represent atmospheric rivers well for the historical climate. The major source regions for atmospheric moisture in summer precipitation events in England and Wales were identified by de Leeuw (2014) using a back-trajectory analysis. Summer precipitation was identified as originating predominantly from coastal regions of western Europe; the east coast of North America, and in a region corresponding approximately to the North Atlantic storm track. Changes in the hydrological cycle or circulation patterns in these regions therefore are likely to influence precipitation over England and Wales in the summer months.

1.3.4 Objective cyclone tracking

Whilst historically storms were tracked subjectively (see for example Hinman 1888), the advent of gridded datasets, has created opportunities to develop automated, objective cyclone tracking algorithms. These algorithms allow the analysis of large numbers of cyclone tracks as found in reanalysis and climate model data, and ensure that consistent rules are applied for the identification of cyclones. By removing subjectivity from cyclone tracking, it is possible to generate objective statistical analyses and inter-comparisons of datasets. Reanalysis products, which assimilate historical observations to create a representation of the historical atmospheric state which conforms to physical principles, and climate models, which simulate historical and future climate scenarios using prescribed energy balance scenarios and model physics, output various atmospheric data onto a regular grid. This allows for objective algorithms to identify features associated with the presence of extratropical cyclones.

An early attempt at objective storm track analysis in gridded data, using an Eulerian approach, was made by Blackmon (1976). By applying a low band pass (2.5–6 day) filter to gridded 500 hPa geopotential height data, the Northern Hemisphere storm tracks were identified as regions of maximum variance. The Eulerian 2–6-day bandpass filtered variance analysis has been used in many studies to identify the storm tracks as regions of high synoptic variability, and can identify large-scale statistical features of the storm track (e.g. Hoskins and Hodges 2002; Hodges et al. 2003; Harvey et al. 2012).

Increasingly, objective feature tracking algorithms are being applied to gridded datasets to provide both large-scale statistical information regarding the overall storm track (e.g. Hoskins and Hodges 2002; Zappa et al. 2013a,b), as well as studies focussed on the behaviour of individual cyclones within the storm track (e.g. Dacre and Gray 2009; Hawcroft et al. 2012; Pfahl and Wernli 2012). Several objective feature tracking schemes are available, most commonly identifying features as maxima of 850-hPa relative vorticity (ξ_{850}), minima of mean sea level pressure (MSLP), and ∇^2 MSLP. Hodges et al. (2003) determines ξ_{850} to be more sensitive to smaller spatial scale features, such as developing cyclones, frontal waves, secondary cyclogenesis, and orographically generated cyclones. MSLP is identified as most appropriate for large spatial-scale systems, such as mature extratropical cyclones.

Neu et al. (2013) compared the performance of a variety of commonly used objective feature tracking methods in the IMILAST project (with the notable exception of Hodges 1994, 1995). 15 tracking methods from participating research centres were applied to a common reanalysis dataset (ERA-Interim, 1.5°, 6 hour time-steps). All algorithms tracked features of MSLP or ξ_{850} . Large differences in total hemispheric track count were found, with some tracking schemes even disagreeing on the sign of the seasonal change in track count between winter and summer. These discrepancies were attributed to characteristics of the methods such as the exclusion of features without a closed MSLP contour, or the choice of minimum distance between storms. In general, the tracking methods were found to agree more readily for the northern hemisphere than the southern hemisphere; for winter than summer; and for stronger storms than weaker. Importantly however, the various tracking methods usually agreed on the sign of the trend in regions with a strong trend in cyclone count.

As well as the characteristics of the cyclone tracking scheme used, it is essential to consider the ability of reanalysis datasets and climate models to accurately represent

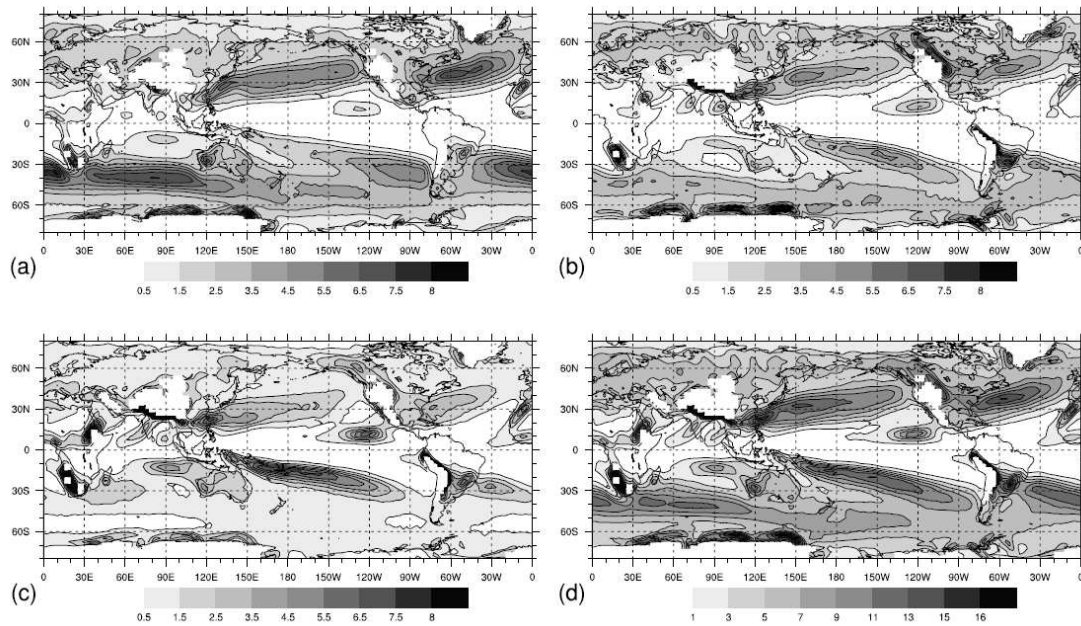


FIGURE 1.7: Global climatology of (a) cold; (b) warm; (c); quasi-stationary; and (c) all fronts. Units are percentage of time during which an objectively identified front was present within each $2.5^\circ \times 2.5^\circ$ grid box. From Berry et al. (2011), Fig. 2.

extratropical cyclones. Hodges et al. (2003) applied the Hodges (1994, 1995) tracking algorithm to four reanalysis products (ECMWF 15-year reanalysis, NCEP-NCAR 40-year reanalysis, NCEP-DOE reanalysis, and NASA-DAO 14-year reanalysis). The inter-model analysis was found to be highly consistent for the well-constrained northern hemisphere, particularly for extratropical cyclones with a large spatial scale. Higher variability was found in small spatial scale systems, such as immature cyclones and frontal wave cyclogenesis. Wang et al. (2016) provided an inter-comparison project using the latest generation of reanalysis products, with a feature tracking algorithm based on unfiltered MSLP with minimum lifetime and maximum distance limitations (4x6hr time-steps, 500 km straight-line respectively). Reanalysis products with higher resolutions produced higher cyclone densities. As with Neu et al. (2013), more agreement was found between the reanalysis products in the northern hemisphere than the southern hemisphere; in DJF than JJA; and in intense cyclones than weak cyclones. In long time-scale reanalysis products, the agreement between products was much greater in the satellite era (1979–present day). An increase in northern hemisphere cyclone count was identified for the period 1958–2010 in all reanalysis products except MERRA; however no change in mean intensity or in the count of intense cyclones was found.

Whilst the aforementioned cyclone tracking studies give information regarding the “centre” of extratropical cyclones in the storm tracks, precipitation over a given region is

also dependent on the location and intensity of the fronts associated with the extratropical cyclone. Global climatologies of frontal activity were derived by Berry et al. (2011) using the methodology described in Hewson (1997), with an additional algorithm to connect point features into spatially contiguous line features. By applying the Hewson (1997) methodology to 850 hPa wet bulb potential temperature (θ_{850}) from the ECMWF ERA-40 reanalysis product (Uppala et al., 2005), a global climatology of frontal activity for the period January 1958 – December 2001 was produced (Figure 1.7). When the North Atlantic storm track is gridded to 2.5° boxes, fronts occur in up to 15% of the time in each box, with a maximum located in the region of maximum baroclinicity in the western North Atlantic. This maximum is found to coincide with the maximum of cyclonic vorticity centres found in Hodges et al. (2003).

1.3.5 Key features of the North Atlantic storm track

Storm tracks are regions of high cyclone density found in the mid-latitude ocean basins in both hemispheres. The North Atlantic storm track extends from the east coast of North America to the west coast of Europe (Figure 1.8). The storm track indicates the frequency distribution of many individual cyclone paths, and does not indicate a likely length or trajectory for an individual cyclone track over its lifespan (Dacre and Gray, 2009).

The location and angle of the storm tracks relative to the Earth's rotation are influenced by the interaction between the atmosphere and major landmasses and orography. The North Atlantic storm track can be considered to start downstream of the Rocky Mountains of North America, with a region of intense cyclogenesis over the Gulf Stream in the western North Atlantic (Hoskins and Valdes, 1990). The strong gradient of sea surface temperature (SST) over the Gulf Stream creates a baroclinic environment which, coupled with a high level of upper-tropospheric vorticity advection as created by the airflow over and around the Rocky Mountains, generates optimal conditions for cyclogenesis. High rates of cyclogenesis are also observed downstream of Greenland, where upper-tropospheric vorticity is generated by interaction with the high orography.

In a study of the northern hemisphere storm tracks based on Eulerian and system-centred storm tracking techniques, Hoskins and Hodges (2002) identifies many of the key features associated with the North Atlantic storm track. This study identifies the importance of the confluence of thermal anomalies, with the interaction of cold air masses from the

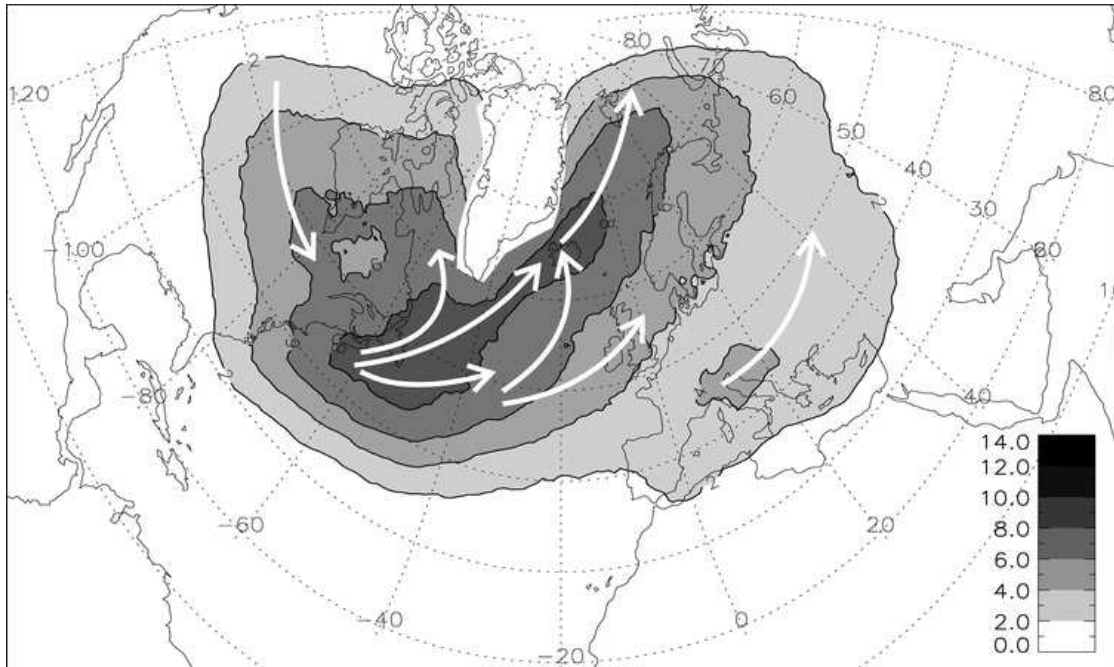


FIGURE 1.8: The North Atlantic storm tracks. Contours are track density every 2 cyclones / $10^6 km^2 month^{-1}$. White arrows indicate likely directions of propagation relative to point of cyclogenesis. From Dacre and Gray (2009), Fig. 5. © American Meteorological Society. Used with permission.

Canadian Arctic and the northward flow of warm waters from the subtropical North Atlantic being essential for the genesis of North Atlantic storms.

Cyclogenesis mechanisms vary spatially within the North Atlantic storm track, and this changes the structure of cyclones commonly found in different regions of the North Atlantic. Gray and Dacre (2006) developed an objective method to classify extratropical cyclones by the conditions of their genesis and development, using classifications analogous with the subjective threefold classification scheme described in Section 1.3.2. Using the method of Gray and Dacre (2006), Dacre and Gray (2009) describes the characteristics of cyclones originating in various regions of the North Atlantic, using an objective feature tracking method based on $\nabla\theta_w$ (Hewson, 1997). It was found that the distribution of type “A”, “B” and “C” cyclones (see Section 1.3.2 for descriptions) varied between the western- and eastern- North Atlantic, distributed as per Table 1.1. Cyclones affecting western Europe were found predominantly to originate in the eastern North Atlantic, where baroclinicity and sea surface temperature gradients are weaker than in the western North Atlantic. A higher prevalence of type C cyclones was found in the eastern North Atlantic, associated with frontal cyclogenesis, and a higher proportion of type A cyclones in the western North Atlantic, associated with baroclinic cyclogenesis.

	A	B	C
West	24%	51%	25%
East	11%	50%	39%

TABLE 1.1: Spatial distribution of cyclone classifications in the North Atlantic (Dacre and Gray, 2009)

Wernli and Schwierz (2006) found that most of the extratropical cyclones which track over western Europe originate in the east Atlantic region, with only 10–20% of cyclones crossing the UK originating in the western North Atlantic. This finding was confirmed by Dacre and Gray (2009) (see Figure 1.8 for schematic). This leads to the hypothesis that since this corresponds to a lysis region for west Atlantic cyclones, many of the storms tracking across western Europe may have formed on the trailing fronts of mature west Atlantic cyclones. This hypothesis is supported by their findings of higher relative vorticity at the point of genesis in the east Atlantic than the west Atlantic, indicating that vorticity may have been advected by the passage of a previous cyclone. Dacre and Gray (2009) also demonstrates that cyclones originating in the eastern North Atlantic tend to be shorter-lived and intensify more rapidly than cyclones developing over the western North Atlantic. In addition, as per Table 1.1, the majority of cyclones developing in the eastern North Atlantic were found to be types “B” and “C”, indicating that upper-level vorticity advection and mid-tropospheric latent heat release are more important for development in this region than lower-level baroclinicity.

1.4 Importance of cyclones and fronts for precipitation

A large proportion of accumulated precipitation in the UK is generated by extratropical cyclones and fronts. As discussed in Section 1.2, North Atlantic storms are associated with a large proportion of extreme UK rainfall events on time-scales of approximately six hours to three days (Hand et al., 2004), whereas convective storms are predominantly associated with shorter duration events. Convective precipitation occurs predominantly in the summer months in England and Wales, and leads to short-duration, high-intensity precipitation events. Conversely, extratropical cyclones occur predominantly in the winter months in England and Wales, and usually generate long-duration, lower-intensity precipitation events.

Several methods have been employed to identify the source of precipitation in the North Atlantic and Europe, primarily with the objective of quantifying the contribution of extratropical cyclones and fronts to climatological mean precipitation and precipitation

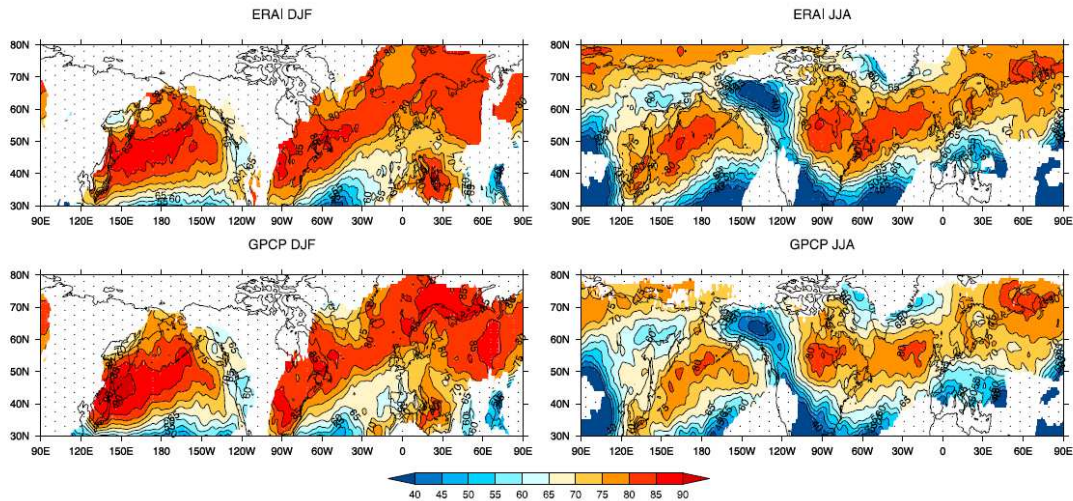


FIGURE 1.9: Percentage of climatological precipitation associated with an extratropical cyclone, in (top) ERA-Interim, (bottom) GPCP. Storms identified using Hodges (1994, 1995) algorithm on ξ_{850} . From Hawcroft et al. (2012), Fig. 3.

extremes. Hawcroft et al. (2012) identifies storms in ERA-Interim using the Hodges (1994, 1995) method on ξ_{850} , and assigns precipitation within a radial cap of $5/10/12^\circ$ (extreme storms/DJF/JJA respectively) of the tracked storm, thus creating a storm-centric method. Precipitation contribution from cyclones is found to be sensitive to the size of the radial cap used, introducing some uncertainty to the total cyclone precipitation contribution statistics. However, good agreement in total storm contribution is found between ERA-Interim and GPCP for the northern hemisphere storm tracks, and storms with a high peak precipitation intensity are found to produce disproportionately more precipitation throughout their lifetimes than storms with lower peak precipitation intensities. The authors speculate that this higher precipitation contribution from intense storms may be of relevance in future climate scenarios, as there is some indication that extratropical storms may become more intense, but less frequent, under a warming climate (e.g. Held 1993; Trenberth et al. 2003; Zappa et al. 2013b).

Pfahl and Wernli (2012) investigated the relevance of cyclones for extreme precipitation, utilising a cyclone tracking algorithm which estimates the area of extratropical cyclones based on closed MSLP (mean sea level pressure) contours. Approximately 60% of 99th percentile precipitation events (calculated per grid cell in ERA-Interim) were associated with extratropical cyclones in the North Atlantic storm track region. This is considered to be an unlikely association rate in reality, as the majority of precipitation accumulated in the North Atlantic storm track region is linked to extratropical cyclones and their fronts. The region of highest association rates extends rather to the north of the region of Western Europe which is regularly affected by extratropical cyclones,

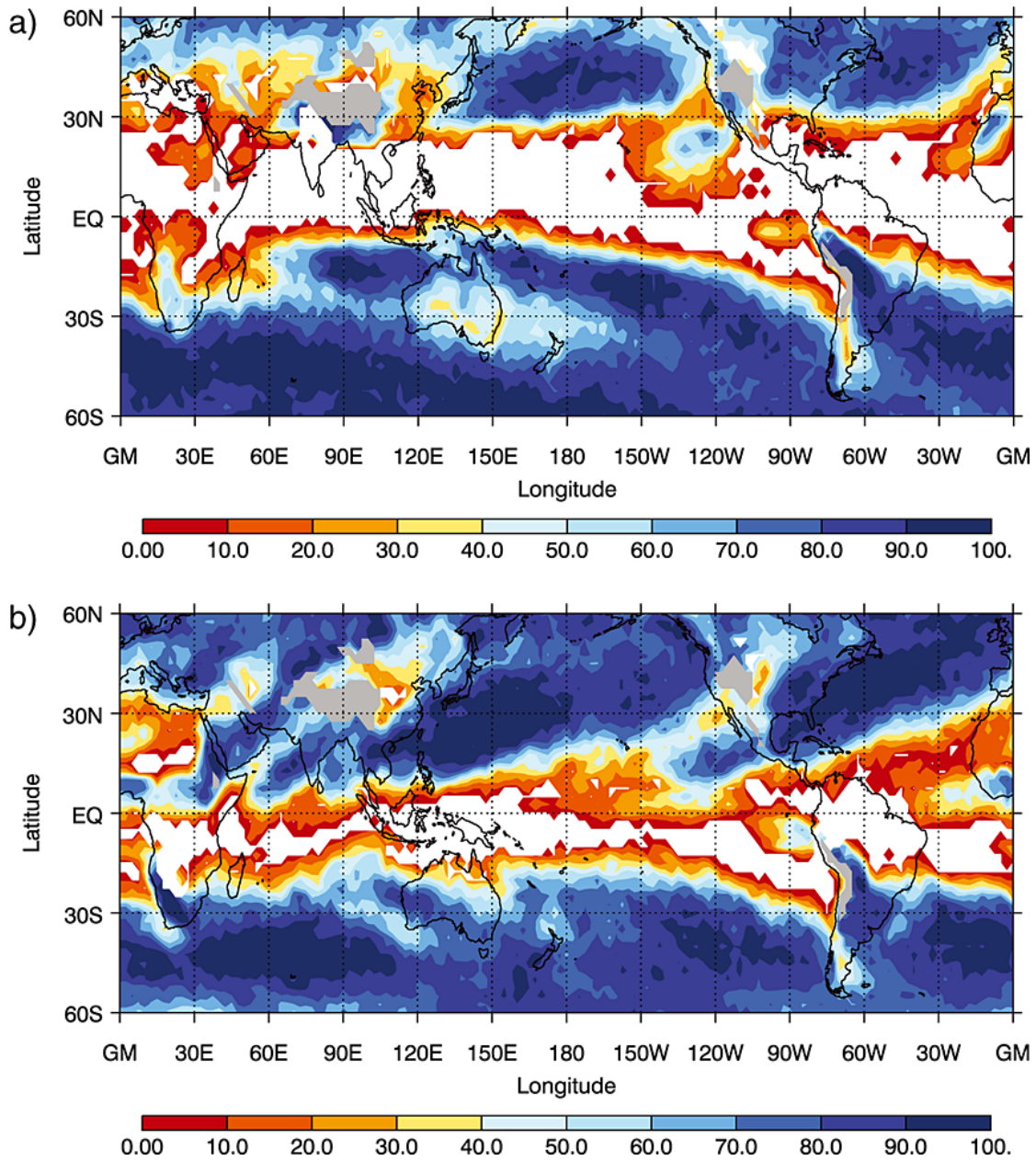


FIGURE 1.10: The proportion of 6-hourly ERA-Interim extreme precipitation events associated with fronts (1979–2011) for (a) JJA and (B) DJF. Regions where the link between fronts and precipitation is not statistically highly significant for that season are blanked out in which and high orography is blanked out in grey. From Catto and Pfahl (2013), Fig. 4.

which may be due to the lack of inclusion of front tracking, thus discounting the role of trailing fronts on precipitation extremes. Use of MSLP as a cyclone tracking metric also favours large, mature storms and quasi-stationary low pressure regions such as the Icelandic Low. It is also rather insensitive to small, developing cyclones which may produce extreme levels of precipitation in the eastern North Atlantic (e.g. Dacre and Gray 2009).

Whilst previous studies had focussed on the contribution of storm centres to precipitation accumulations, Catto et al. (2012) addresses the importance of fronts for precipitation. Using an objective front identification algorithm (Berry et al., 2011) on a thermal front parameter (Renard and Clarke, 1965; Hewson, 1998), combined with precipitation data from GPCP (Huffman et al., 1997), a global climatology of front-associated precipitation was developed. When precipitation is taken to be associated with a front given the presence of an objectively identified front within a surrounding 5° grid box, 90% of precipitation within the storm tracks was found to be related to a front. Catto and Pfahl (2013) expands on this analysis by investigating the role of fronts and cyclones, tracked using the Wernli and Schwierz (2006) method on closed MSLP contours, on the generation of extreme precipitation. A strong correlation was identified between the intensity of a front (as measured by the gradient of wet bulb potential temperature on the 850 hPa surface, $\Theta_{w(850)}$, across the front), and the intensity of precipitation near that front. A seasonal cycle in the importance of fronts to precipitation extremes was found, with lower association rates identified in JJA in the northern hemisphere (Figure 1.10), likely to be associated with the increased rate of extreme precipitation events generated by convective systems in the summer months. In total, however, less than 10% of extreme precipitation events within the North Atlantic storm track were identified as being associated with neither a front nor a cyclone, indicating a very high importance of extratropical cyclones for precipitation extremes in this region.

It is important to note that the definition of “extreme” precipitation varies considerably in the published literature, with little consistency between analyses. The extremity of an event depends on the time-period of the event, its spatial scale, and its intensity relative to local climatology. Extreme events are often defined relative to climatology, as events where precipitation exceeds a threshold percentile relative to the climatological rainfall distribution for the area, season, and time-scale in question. Of studies which use this method, the area concerned may vary from individual rain gauge stations (e.g. Wilby et al. 2008) to a regional average (e.g. Pfahl and Wernli 2012; Beniston et al. 2007; Catto and Pfahl 2013), varying the properties of associated precipitation greatly. Other studies use a Peaks-Over-Threshold method to identify extremes in a time-series of precipitation data. Extreme precipitation events may be defined according to impact; for example, precipitation which is associated with river catchment flooding (e.g. Wilby et al. 2008; Lavers et al. 2011). This method is highly dependent on the nature of the catchments in question, including its existing level of saturation. Furthermore, any of these methods may be applied to temporally aggregated data, for example a running sum or running mean. The definition of an “extreme” event therefore must be chosen

carefully to yield useful results for the type of precipitation event being studied.

1.5 Climate change

One of the key questions surrounding almost every study of precipitation is “How might this change in the future?”. There is no doubt that the climate is warming, and it is extremely likely that the dominant cause of climate warming is human influence (Stocker et al., 2013). As the Clausius-Clapeyron theorem indicates that a warmer atmosphere allows for an increased saturation water vapour pressure (by $\sim 7\%$ per $^{\circ}\text{C}$ under mean atmospheric conditions), moisture availability in the atmosphere is expected to increase on average, allowing increases in both mean and intense precipitation (Held and Soden, 2006). However, Allen and Ingram (2002) identified that in the CMIP2 (Coupled Model Inter-comparison Project, Phase 2, Meehl et al. 2000) climate models the rate of increase of precipitation with a warming climate is disproportionately skewed towards extreme precipitation events. In the Allen and Ingram (2002) study, mean climate model precipitation increased linearly by 3.5% per $^{\circ}\text{C}$, whilst regions in the tropics where precipitation accumulations are highest showed increases of up to 25% per $^{\circ}\text{C}$. Altered thermodynamics in the atmosphere also affects the position and intensity of the storm tracks, and it is likely that northern hemisphere storm tracks will be affected, generating regional uncertainties in precipitation projections. It is therefore vital to consider a wider range of literature around the theory and implications of climate change to better understand potential changes in precipitation events.

Recently, much analysis of climate projections has been performed under various emissions scenarios to identify biases inherent in the models. Analysis has been performed using the CMIP5 (Taylor et al., 2012) ensemble of climate models, as well as models from CMIP5’s predecessor, CMIP3 (Meehl et al., 2007). CMIP5 brings together model data from 29 modelling groups worldwide, all of which have been used to run a uniform set of experiments. This creates an ensemble of climate projections, with the ability to inter-compare models from different agencies to evaluate their strengths and weaknesses. Greenhouse gas concentrations for CMIP5 climate projections are provided by four Representative Concentration Pathways (RCP2.6, RCP4.5, RCP6, RCP8.5) (van Vuuren et al., 2011), where the number indicates the expected radiative forcing value in Wm^{-2} in the year 2100, relative to pre-industrial values. The RCPs are intended to relate to a range of likely anthropogenic greenhouse gas emissions scenarios, with RCP2.6 representing rapid climate change mitigation and reduction of emissions, and

RCP8.5 representing little to no change in future greenhouse gas emissions or mitigation strategies.

1.5.1 Projected changes to North Atlantic cyclones and the storm track

As discussed in Section 1.4, extratropical cyclones within the North Atlantic storm track are the main source of precipitation across western Europe, and the England and Wales region in particular. Regardless of the atmospheric moisture content under a future climate, the location and intensity of the storm track is vitally important for understanding the regional precipitation response.

Held (1993) suggested that the weakening of the equator–pole temperature gradient (caused by disproportionate warming in the polar regions due to loss of sea ice) could induce a poleward shift in the storm tracks. The author noted, however, that this change was most pronounced in models with highly simplified continents and topography. The poleward shift of the storm tracks was also identified in CMIP3 by Yin (2005). This poleward shift was identified most strongly in the upper troposphere. Pinto et al. (2007) identifies a general decrease in mid-latitude cyclone track densities, with an increase in track intensity over the British Isles, in an ensemble analysis of ECHAM5 using SRES A1B, A2, and B1 scenarios. Ulbrich et al. (2008) identifies a poleward shift in some regions (e.g. the North Pacific) in the CMIP3 models. However, this study was unable to replicate the clear upper-level poleward shift observed by Yin (2005), and concludes that the response of the storm tracks to climate change is sensitive to both the models and the analysis method. Harvey et al. (2012) found little evidence of a poleward shift in the wintertime storm tracks of the CMIP3 and CMIP5 ensembles (A1B and RCP4.5 scenarios respectively), with an increase in storm activity near the British Isles. In a multi-model assessment of CMIP5 ensemble members, Zappa et al. (2013b) identified a tri-polar response to climate change in the DJF North Atlantic storm track, with an increased track density over the British Isles and a reduced track density over the Norwegian Sea and the Mediterranean under RCP4.5 (Figure 1.11). Zappa et al. (2013b) identified a poleward shift in the multi-model mean JJA North Atlantic storm track under RCP4.5. The response of the location of the storm tracks to climate change therefore varies by season and basin, but can be summarised in the North Atlantic as a poleward shift in summer, and a tri-polar pattern in winter.

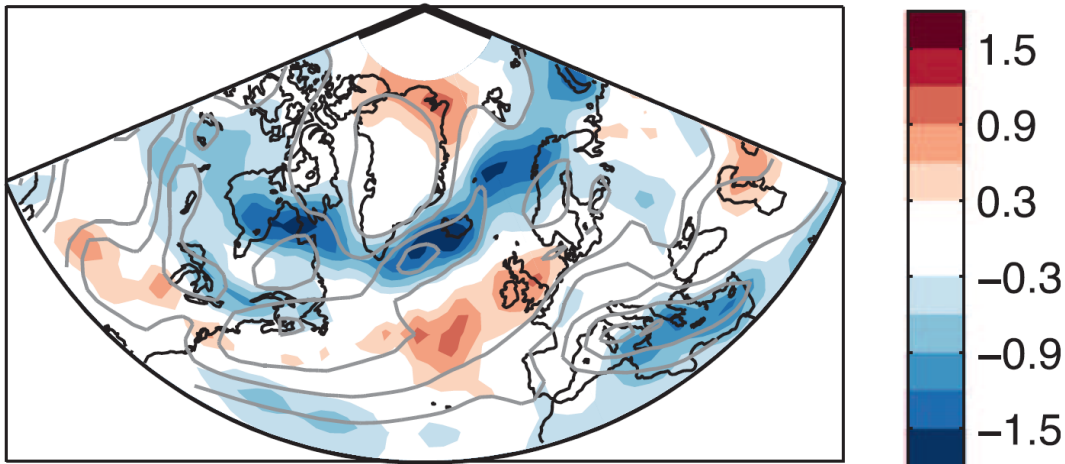


FIGURE 1.11: Mean DJF track-density response (RCP4.5 minus HIST) computed for the four models with the best representation of the location and tilt of the North Atlantic storm track in CMIP5. Units are in number of cyclones per month per unit area. Gray contours show the mean historical track density with isolines every four cyclones per month per unit area. From Zappa et al. (2013b), Fig. 3. © American Meteorological Society. Used with permission.

Zappa et al. (2013b) notes that the reduction in track density over the Norwegian Sea and increase in track density over the British Isles is characteristic of storm track with a reduced meridional tilt and an eastward extension, which is also the main pattern of North Atlantic storm track bias within the CMIP5 models (Zappa et al., 2013a). However, this spatial pattern is consistent when the analysis is performed only on those models with the lowest bias to the storm track tilt (HadGEM2-ES, EC-Earth, MRI-CGCM3; see Figure 1.12, models 13, 8, and 19 respectively).

In addition to the direction and location of the storm track, the intensity of individual storms in the future climate is of importance. Measures of intensity vary greatly; many studies use minimum MSLP or maximum ξ_{850} as metrics for intensity, which provide information regarding the circulation of a storm, but not necessarily its ability to produce precipitation. Bengtsson et al. (2009) analysed a high-resolution climate model (ECHAM5) for changes to the pressure, vorticity, wind speed and precipitation associated with extratropical cyclones, finding a small reduction on cyclone counts and a large increase in the total accumulated precipitation per cyclone. Precipitation was also identified as coming disproportionately from extreme events, with an increase in intensity of 21.4% for 99th percentile events in the North Atlantic storm track. Zappa et al. (2013b) shows that the mean CMIP5 precipitation response to the RCP4.5 scenario indicates increased precipitation near the British Isles and north-western Europe in DJF, with a

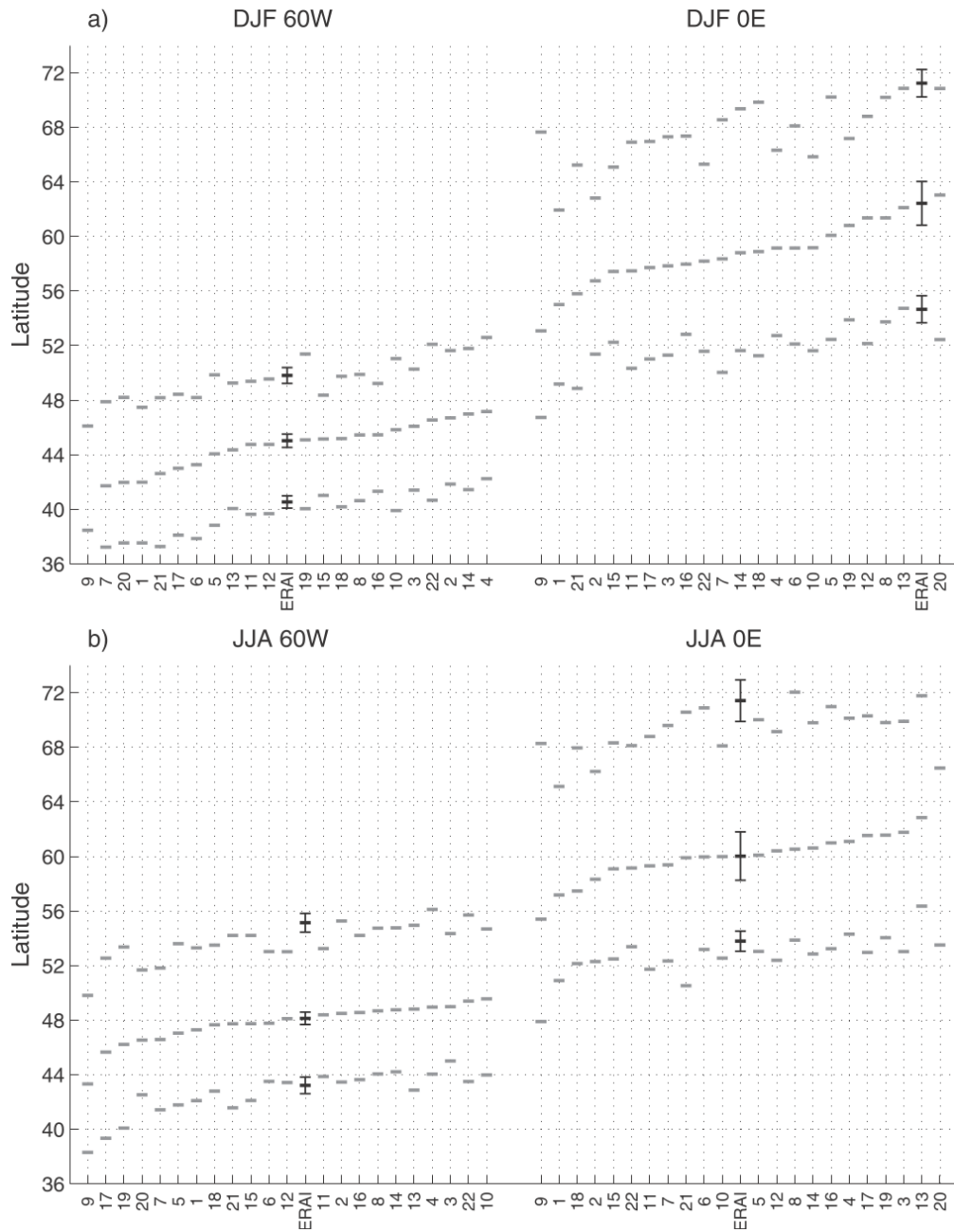


FIGURE 1.12: Latitudinal distribution of cyclone tracks for (a) DJF and (b) JJA at (left) 60°W and (right) 0° . Each column corresponds to a CMIP5 model and the three grey dashes indicate the 25th, 50th (median), and 75th percentiles of its latitudinal distribution of tracks. The models can be identified by the labels on the x axis. Values from ERA-Interim are displayed in the column with the black dashes. The 2σ confidence intervals are also indicated by error bars for ERA-Interim. From Zappa et al. (2013a),

Fig. 4: © American Meteorological Society. Used with permission.

weaker response in JJA. Li et al. (2014) identified that cyclones tend to produce more precipitation in a warmer climate, but that this does not always affect their dynamical intensity. This study also notes that moist processes are not always well represented in climate models, leading to errors in the intensity of cyclones due to diabatic processes. In an analysis of the dynamical intensity of extratropical cyclones in the A1B and A2 scenarios of CMIP3, Della-Marta and Pinto (2009) found that the return period of extreme cyclones as measured by minimum MSLP remained unchanged in the future climate, whilst a large reduction in the return period of extreme cyclones as measured by maximum ξ_{850} was identified. This highlights that measurements of dynamical intensity in the future climate are likely to be sensitive to the method of analysis.

1.5.2 Projected changes to precipitation from extratropical cyclones

Under a warmer global climate, it is highly likely that global mean precipitation will increase (Held and Soden, 2006), due to the increased availability of water vapour as described by the Clausius-Clapeyron relationship, as described in Section 1.5. In CMIP5, all models predict an increase in global mean precipitation ranging from 2% to 5% by 2100 in RCP2.6 and RCP8.5 scenarios respectively (Stocker et al., 2013). Trenberth et al. (2003) identifies that an increase in available moisture produces a non-linear storm intensity increase, as the additional latent heat released acts to intensify the storm. This increase in available moisture is considered to be robust across the CMIP3 climate model ensemble projections (Held and Soden, 2006).

Whilst there is high confidence in an intensified water cycle in the future global climate, there is much less confidence in regional projections of average precipitation, and lower confidence still in regional projections of extreme precipitation (Allen and Ingram, 2002; Huntington, 2006). Based on analysis of the CMIP3 models by Beniston et al. (2007), supported by Lehtonen et al. (2014), Northern Europe is projected to become wetter and Southern Europe drier, with less certainty around the central latitudes, including the British Isles. Dai (2006) identifies an excessive drizzle relative to reanalysis in the extratropical regions in a study of historical runs of 18 coupled climate models. This bias is identified in historical runs of the CMIP5 models by Liu et al. (2014), when compared with average precipitation over land from the CRU Global Land Precipitation Dataset (Hulme, 1992; Hulme et al., 1998).

Under the RCP8.5 scenario, a robust increase in precipitation is projected to occur in Northern Europe, and a robust decrease in precipitation is projected to occur in southern Europe, for all seasons 2081–2100 (Stocker et al., 2013). A region of high uncertainty

projected precipitation change is found near the flanks and exit region of the North Atlantic storm track, including the British Isles. Projected precipitation changes are higher in winter than summer in the northern hemisphere mid- and high-latitude regions. Zappa et al. (2013b) finds that projected DJF precipitation increases across the British Isles and much of Europe in the CMIP5 RCP4.5 experiment, with a strong signal-to-noise ratio. An increase is also found in JJA, but with a lower magnitude and higher uncertainty. Zappa et al. (2013b) finds that accumulated precipitation is predominantly generated by more intensely precipitating cyclones in the RCP4.5 scenario than in the historical model runs, with fewer weakly precipitating cyclones being identified in the North Atlantic storm track.

1.6 Extratropical cyclone clustering and stalling in the present and future climate

Clustering and stalling of extratropical cyclones are two mechanisms which may lead to extreme rainfall accumulations. Several studies have addressed the nature of clustering of extratropical cyclones in the North Atlantic storm track (e.g. Mailier et al. 2006; Vitolo et al. 2009; Pinto et al. 2013, 2014, 2016; Priestley et al. 2016). Extratropical cyclone clustering in western Europe is currently an area of interest for insurance companies concerned with the cumulative risk of wind and flood damage. Clustering of extratropical cyclones is discussed in Section 1.6.1. Although stalled, or slow-moving, extratropical cyclones are known to be related to some severe flood events (Blackburn et al., 2008; Met Office, 2012; Stadtherr et al., 2016), relatively little research has been published which directly addresses causes of extratropical cyclone stalling in the North Atlantic storm track, or the relationship between stalling and regional precipitation. Stalling of extratropical cyclones is discussed in Section 1.6.2.

1.6.1 Clustering

The first mechanism by which cyclones may be expected to cluster, frontal wave cyclogenesis, was first described by Bjerknes and Solberg (1922). That the passage of one storm may create ideal conditions for the creation of a second storm is an important concept in the consideration of clustering. In recent years, extratropical cyclone clustering has again come to prominence after large insured losses and damage to infrastructure caused by storm clusters across maritime regions of western Europe.

Mailier et al. (2006) modelled storm transits statistically by monitoring the passage of storms identified in the NCEP-NCAR reanalysis (Kalnay et al., 1996) using the Hodges (1994, 1995) tracking scheme on ξ_{850} across $\pm 10^\circ$ meridional gates. Each transit was considered to be a point process. Cyclone transits were modelled according to a dispersion statistic derived from the Poisson process as follows.

For a Poisson distributed process with fixed rate λ , the probability of number N of events occurring during a time interval Δt is given by:

$$P(N = n) = \frac{(\lambda \Delta t)^n e^{-\lambda \Delta t}}{n!}, n = 0, 1, 2, \dots \quad (1.1)$$

and the index of dispersion (ϕ) is given by:

$$\phi = \frac{\text{Var}(N)}{E(N)} \quad (1.2)$$

where $E(N)$ and $\text{Var}(N)$ are the mean and variance of N respectively. Where cyclone transits are distributed according to a homogeneous Poisson process, $\phi = 1$. Where cyclone transits are over (under-) dispersed, $\phi > 1$ ($\phi < 1$). Therefore the dispersion statistic $\hat{\psi}$ may be defined such that:

$$\hat{\psi} = \hat{\phi} - 1 = \frac{s_n^2}{\bar{n}} - 1 \quad (1.3)$$

For each grid point, Mailier et al. (2006) calculated a dispersion statistic $\hat{\psi}$ was calculated per Equation 1.3 (where s_n^2 is the sample variance of monthly total cyclone transits, and \bar{n} is the sample mean). This dispersion statistic was modelled against a Poisson process (Cox and Isham, 1980) with constant rate, signifying a purely random process. In locations where $\hat{\psi} > 0$, the passage of cyclones is found to be over-dispersed with respect to a fixed-rate Poisson process, indicating that passages are more clustered than a purely random process. Conversely, where $\hat{\psi} < 0$, cyclone passages are under-dispersed with respect to a fixed-rate Poisson process, indicating that passages are more regular than a purely random process.

By comparing the dispersion statistic for a given grid point with a fixed-rate Poisson process, Mailier et al. (2006) was able to identify regions of more regular or more clustered storm transit than a purely random process. The entrance region of the North Atlantic storm track was identified as a region of highly regular storm transit, whilst the exit region of the North Atlantic storm track was identified as a region of highly clustered

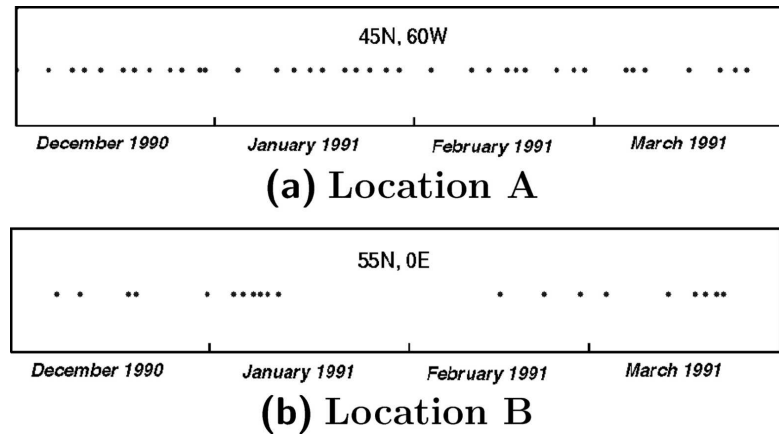


FIGURE 1.13: Storm dispersion at North Atlantic storm track (a) entrance, (b) exit regions, December 1990 – March 1991. From Mailier et al. (2006), Fig. 6. © American Meteorological Society. Used with permission.

storm transit (Figure 1.13). The majority of clustering was attributed to variations in the large-scale flow causing cyclones to group as they transit the Atlantic from west to east, with a smaller amount of clustering being due to cyclogenesis in the eastern North Atlantic. However, as per Dacre and Gray (2009), the majority of intense cyclones that affect the UK are generated in the eastern North Atlantic, which may increase the relevance of the latter mechanism for more damaging clusters of storms in this region. The modelling of cyclone transits as point processes is a highly useful method for statistical analysis; however, extratropical cyclones are large (radius $\approx 1,000$ km) features with highly asymmetrical precipitation distributions. These considerations must be made before conclusions are drawn with regards to the influence of clustering on precipitation events in a given region.

The work of Mailier et al. (2006) was expanded on by Vitolo et al. (2009), using the same data and dispersion statistic to investigate the effect of cyclone intensity on serial clustering. Clustering is found to increase considerably for more intense cyclones (where an “intense cyclone” is defined as one with a relative vorticity at 850 hPa (ξ_{850}) greater than the 80th percentile of climatological ξ_{850} at that grid-point), and is found to be highly sensitive to the size of the “gate” across which cyclones are tracked. The increased clustering for intense extratropical cyclones was found to be greatest near the exit region of the North Atlantic jet; a region which affects north-western Europe and the British Isles. This indicates that for England and Wales we may expect clustered storms to be especially intense in terms of relative vorticity.

Relative vorticity is a useful measure of cyclone activity, but is not directly related

to precipitation intensity. Indeed, a less intense extratropical cyclone with access to a continuous supply of moist air may precipitate more heavily than a fast-rotating extratropical cyclone with poor access to moisture. To date, no studies have investigated the link between clustering and precipitation intensity, leaving a gap in the research that could usefully be addressed.

Pinto et al. (2013) applies the dispersion statistic (Equation 1.3) to a range of reanalysis products and climate models, to verify the conclusions of Mailier et al. (2006) and Vitolo et al. (2009), to test the robustness of the observed clustering patterns to different reanalysis products, and to investigate the likelihood of changes to clustering behaviour under future climate conditions. The dispersion statistic methodology was applied to three reanalysis products (NCEP/NCAR 50-year reanalysis, Kistler et al. 2001; ERA-40 (Uppala et al., 2005); ERA-Interim, Dee et al. 2011), with cyclones tracked using the Murray and Simmonds (1991) method on MSLP. All three reanalysis products yielded serial regularity in the western North Atlantic, with serial clustering in the eastern North Atlantic. Clustering was found to be greater for intense cyclones (minimum core pressure $> 95^{\text{th}}$ percentile). This indicates that the observed clustering patterns are robust in multiple reanalysis products and with two cyclone tracking methodologies.

Future climate scenarios are also addressed in Pinto et al. (2013), using an ensemble of simulations using the coupled ECHAM5/MPI-OMI General Circulation Model (GCM) forced with historical conditions for 1860–2000 (20C) and the Special Report on Emissions Scenarios (SRES) A1B scenario for 2001–2100. A single-model ensemble was chosen to evaluate the statistical robustness of this method, rather than to specifically evaluate climate sensitivity. The GCM was found to represent historical clustering patterns well, but with a zonal bias to the storm track (consistent with larger studies of climate model synoptic-scale features such as Zappa et al. 2013a). Future changes to clustering behaviour were not found to be statistically significant.

Further analysis of the ability of climate models to represent the serial clustering of extratropical cyclones was performed by Economou et al. (2015), bringing the work of Pinto et al. (2013) up to date with the use of a CMIP5 model ensemble of 17 members, using the RCP4.5 scenario. Most models were able to qualitatively represent the 250-hPa jet axis, and dispersion statistic patterns for tracks identified using the Hodges (1994, 1995) method on ξ_{850} . Little agreement was identified between the models with respect to the sign and location of spatial trends in dispersion statistic, indicating a low level of confidence in the effect of climate change on serial clustering of extratropical

cyclones. Future changes in serial clustering of extratropical cyclones were found to be small, with a large sampling uncertainty between models.

A specific focus on the dynamical situations behind extratropical cyclone clustering affecting the British Isles is presented in Pinto et al. (2014). Using ERA-Interim (Dee et al., 2011) data for 1980–2012, Rossby wave breaking events were identified based on potential temperature, θ , on the 2 Potential Vorticity Unit surface (the dynamical tropopause). Storm tracks were identified using the Murray and Simmonds (1991) method, as per Pinto et al. (2013), and storms affecting the British Isles were identified using a 700-km radius around 55°N, 5°W. Clustering episodes were defined as periods with four or more consecutive cyclones within a seven-day period, with four winter months identified as clustered, with four or more 95th percentile cyclones. A stable, intensified jet was identified during all analysed clustering periods, and it is hypothesised that higher wind speeds may create the conditions for development, amplification, and rapid propagation of an unusually large number of intense extratropical cyclones. Double-sided Rossby wave breaking is identified as a factor in maintaining the jet in this state.

Further analysis of the mechanisms behind clustering at the exit region of the North Atlantic storm track is provided by Priestley et al. (2016). Using the method of Pinto et al. (2013, 2014) applied to ERA-Interim, clustering events within 700 km of 55°N, 5°W are found to be strongly associated with an anomalously strong, extended jet stream flanked by double-sided Rossby wave breaking events. The extent of the clustering event was found to be positively correlated with the 250 hPa wind speed. When clustering is analysed near 65°N at the same longitude, Rossby wave breaking on the right side of the jet exit predominates; conversely, when clustering is analysed near 55°N on the same longitude, Rossby wave breaking is stronger on the north side of the jet exit. Rossby wave breaking is found to peak two days before clustering events, intensifying the jet stream at 250 hPa.

Pinto et al. (2014) analysed the previously discussed periods of intense cyclone clustering subjectively using surface maps to identify the existence of secondary cyclogenesis. Secondary cyclone development was identified in all of the periods analysed, and in all cases the secondary cyclone developed in the right-entrance region of the jet stream as the parent cyclone was occluding. This appears to indicate that intense extratropical cyclone clusters are generated by a combination of a dynamical situation with a quasi-stationary, zonal, intense jet stream, often maintained by double-sided Rossby wave

breaking, and secondary cyclogenesis occurring across the jet exit region.

The sensitivity of the dispersion statistic to the choice of tracking method used was analysed in Pinto et al. (2016), using ERA-Interim data with cyclone tracks identified by members of the IMILAST project (Neu et al., 2013), with the addition of the Hodges (1994, 1995) method. All tracking methods were able to represent the general features of the dispersion statistic spatial patterns. Quantitative differences exist between the methods, but this is largely attributed to variation in the total storm frequency between the methods, rather than the variance. This indicates that, despite using different tracking methodologies, the findings of the previously discussed studies concerning the dispersion statistic of extratropical cyclone frequency in the North Atlantic are comparable.

Although a substantial amount of research has been performed to investigate the nature of extratropical cyclone clustering in the North Atlantic in the present and future climate, the focus of research has been on wind storm risk, where the risk of natural hazards related to clustering has been considered. Due to the existence of trailing fronts, areas at risk from precipitation extremes from extratropical cyclones may be located a large distance from the cyclone centre. It is therefore not sufficient only to analyse clustering of cyclone centres when evaluating the risk from accumulated precipitation. Further research into the influence of clustering on precipitation accumulations would be beneficial, and should use spatial information to identify risk areas that are distant from the cyclone centre.

1.6.2 Stalling

In comparison to clustering, relatively little research has been published which addresses the climatology and causes of stalled extratropical cyclones, despite such cyclones frequently being referenced in association to extreme precipitation accumulations and flooding events (e.g. Hand et al. 2004, Blackburn et al. 2008). In relation to the 2007 UK floods, Blackburn et al. (2008) identified the cause of several periods of prolonged rainfall as being stalled extratropical cyclones due to a quasi-stationary global Rossby wave pattern of wavenumber $n = 6$. A similar scenario was identified by Stadtherr et al. (2016) in relation to the 2014 Balkans floods, which were caused by a Mediterranean cyclone which stalled for a period of four days over the Balkans. This stalling was attributed to a quasi-stationary wavenumber 6 pattern. Stadtherr et al. (2016) indicated that this wave pattern was similar to the situation described by Petoukhov et al. (2016), whereby

quasi-resonant amplification of planetary waves of wavenumber 6-8 may occur.

A quasi-stationary wave pattern that acts to resist the movement of extratropical cyclones is identified in several individual flooding events. However, no systematic evaluation of the mechanisms behind stalling of extratropical cyclones near England and Wales, or of the impact on precipitation due to these cyclones, has yet been performed. Research into stalling patterns and mechanisms in extratropical cyclones could yield valuable information applicable to industrial and policy uses. Additionally, the spatial asymmetry of precipitation associated with extratropical cyclones has not been considered in research to date, and relating our existing knowledge of clustering patterns in extratropical cyclones to the impact on extreme precipitation events (which may be associated with distant extratropical cyclones) would be of great practical value.

1.7 Thesis structure and aims

Precipitation extremes are of great importance to society, and extreme rainfall accumulations from extratropical cyclones are of especially high importance given their ability to generate flooding over very large regions. This thesis therefore aims to investigate the relationship between clustering and stalling of North Atlantic storms, and precipitation extremes over time-scales from 1–31 days in England and Wales, both in the recent historical record and in the future climate. The following questions are addressed:

1. How well are historical England and Wales precipitation events represented in reanalyses?
2. What is the best way to associate precipitation with extratropical cyclones?
3. To what extent is precipitation in England and Wales influenced by clustering and stalling of extratropical cyclones?
4. How well do climate models represent observed relationships between extratropical cyclones and England and Wales precipitation events?
5. How can we expect extreme precipitation events caused by extratropical cyclones to change in the future?

The rest of this thesis is structured as follows:

Chapter 2: The data and methods that have been used are described.

Chapter 3: We address the question of how well reanalysis products represent extreme England and Wales precipitation events. The work presented in this chapter has been published in a peer reviewed journal (Rhodes et al., 2015).

Chapter 4: The development of a new method (“CPA”) for objectively associating cyclones with precipitation events in gridded data will be discussed.

Chapter 5: The CPA method is applied to ERA-Interim, and the nature of historical clustering and stalling is considered.

Chapter 6: The CPA method is applied to HadGEM2-ES (Historical experiment), to better understand the ability of HadGEM2-ES to represent features of clustering / stalling and England and Wales precipitation events that are observed in the historical record.

Chapter 7: The CPA method is applied to HadGEM2-ES (RCP8.5 experiment), to evaluate potential changes in the mechanisms leading to clustering / stalling of rain storms, and the relationship between clustering / stalling and England and Wales precipitation events under a high-emissions future climate scenario.

Chapter 8: The results of this thesis will be discussed, and conclusions drawn. Possible avenues of future research are proposed.

Chapter 2

Data and Methods

The questions posed in Chapter 1 require the analysis of atmospheric data from observation, reanalysis and climate model datasets. In this chapter, the tools and datasets used to address these questions are discussed. Observed precipitation data are discussed in Section 2.1. Reanalysis products that have been used in this study are discussed in Section 2.2. The HadGEM2-ES climate model is introduced in Section 2.3. The objective feature tracking method used to identify extratropical cyclones in reanalysis and climate model data is described in Section 2.4. Finally, the method used to identify extreme events in precipitation time-series is explained in Section 2.5.

2.1 Observational datasets

To understand the nature of precipitation in England and Wales, and to evaluate the output of reanalysis products, historical precipitation observations are required. For this study, daily precipitation data from a rain-gauge based dataset is used for statistical analysis and the identification of regional extreme precipitation events, and data derived from a merged satellite and rain-gauge product are used for evaluation of the spatial distribution of precipitation in reanalyses.

2.1.1 England and Wales Precipitation (EWP)

HadUKP (Hadley Centre UK precipitation, Alexander and Jones 2000) is a series of precipitation datasets that provides area-average precipitation accumulations for the United Kingdom, subdivided into irregular regions according to the regional qualities of precipitation. HadUKP incorporates the EWP (England and Wales Precipitation) series, which provides the longest-running instrumental precipitation record in the world

(Met Office Hadley Centre, 2017). Daily precipitation accumulations for EWP are derived from station observations from the Met Office Integrated Data Archive System (MIDAS, Met Office 2013), and are available from 1931-present.

To account for spatial variability between rain gauge sites, each daily gauge measurement is scaled by the ratio of the station monthly mean to the regional monthly mean (Alexander and Jones, 2000). This method attempts to compensate for the localised mechanisms which can bias individual gauges relative to the surrounding region. Croxton et al. (2006) investigates the quality of EWP data by comparison with observations from 24 surface stations from around the UK. A high correlation is found with all stations in England and Wales, with Scottish and Northern Irish stations reporting lower correlations, as should be expected given the spatial extent of EWP. Several stations were found to report significantly over or under the value reported by EWP but correlation coefficients remained high. The EWP daily period is 0900-0859 UTC.

2.1.2 Global Precipitation Climatology Project (GPCP)

GPCP (Huffman et al., 1997) is a satellite- and rain gauge-derived gridded precipitation dataset. Precipitation is highly spatially variable, so satellite data are used to enhance the spatial representation of precipitation over land, and to estimate precipitation over the oceans, where gauge data are unavailable. Gauge observations obtained from the Global Precipitation Climatology Centre (GPCC) used to constrain satellite precipitation observations over land. The GPCC observations are considered to be reliable, but only provide point estimates of precipitation over land. Satellite observations over the extratropics are based on Special Sensor Microwave/Imager (SSM/I) data from Defence Meteorological Satellite Program satellites in sun-synchronous low-earth orbit, which produce average temporal sampling rates of 1.2 images day⁻¹ (Huffman et al., 1997). Additional, higher temporal frequency observations are obtained from infra-red imaging instruments on board geostationary satellites; however, infra-red imagery is primarily useful for identifying precipitation from deep convection in the tropics. Observations are heavily weighted towards rain gauges where data are available, and is combined with ground-calibrated satellite observations where gauge data is sparse.

Data from GPCP are available at daily resolution on a 1° grid, between 1996-present (Huffman et al., 2001). A low bias in precipitation over the high-latitude oceans was identified in merged satellite and rain gauge derived precipitation datasets by Adler et al. (2001), believed to be due to the high reliance on SSM/I data in these regions.

However, near land masses where precipitation rates are strongly constrained by gauge observations, GPCP is considered to provide a good representation of rainfall distribution.

2.2 Reanalysis

Reanalyses provide a best estimate of the historical state of the atmosphere, based on assimilation of meteorological observations. A consistent data assimilation scheme is used throughout the re-analysed time period to create temporally homogeneous datasets (Trenberth et al., 2008), which provide a range of meteorological data on a global grid. In most reanalysis products, the range of observations to be assimilated into the reanalysis changes through time, as new technologies become available, and as observing networks begin or cease collection of data. Changes to the sources, locations and quantity of observations is therefore a common source of temporal inhomogeneity in reanalysis products (Sterl, 2004).

Most variables are constrained by observations; however, the hydrological cycle is generated by a short-term forecast model. The characteristics of the forecast model can alter the quality of the forecast variables (Parker, 2016). In particular, a forecast spin-up period is common, causing poor estimation of precipitation accumulations (Hawcroft et al., 2012; De Leeuw et al., 2015). It is therefore necessary to use caution when using reanalysis products for studies involving the hydrological cycle. As such, the quality of precipitation representation in two reanalysis products over England and Wales is evaluated further in Chapter 3.

2.2.1 NOAA-CIRES Twentieth Century Reanalysis

20CR is a global reanalysis product covering the period 1871-2012 (Compo et al., 2011). To limit the temporal inhomogeneity generated by the changing availability of meteorological observations, only surface pressure and monthly sea surface temperature (SST) observations are assimilated. The assimilation uses an Ensemble Kalman Filter (Whitaker and Hamill, 2002) at six-hourly intervals. Data are output at T62 resolution ($\sim 2.0^\circ$ in latitude and longitude) with 28 vertical levels. There are few publications to date discussing the performance of the precipitation field of 20CR. Zhang et al. (2013) demonstrated a good performance when compared with other reanalysis projects over southern Africa; however, representation of precipitation in the northern hemisphere

extratropics has not yet been evaluated in the published literature.

Precipitation data in 20CR is output in the form of a precipitation rate averaged over three-hourly periods. A preliminary analysis performed for this study highlighted that the global-mean ensemble-mean precipitation rate oscillates every three hours by $\sim 0.5\text{mm/day}$ ($\sim 20\%$ of the total mean precipitation rate). Precipitation rates were found to be lower at the times of data assimilation (0000, 0600, 1200, 1800 UTC) than at the three-hourly forecast times (0300, 0900, 1500 and 2100 UTC). This implies that spin-up period of the forecast precipitation exists in 20CR. Precipitation rates were therefore taken from forecasts at 0300, 0900, 1500 and 2100 UTC to form a dataset of daily precipitation accumulations.

2.2.2 ECMWF Reanalysis (ERA) Interim

ERA-Interim (ERA-I) (Dee et al., 2011) produces output gridded at T255 resolution ($\sim 0.7^\circ$ in latitude and longitude), with 60 vertical levels. Data are available from 1979–present (with a two to three-month delay for quality assurance). Observations are assimilated using a 4D-VAR data assimilation scheme at 0000 UTC and 1200 UTC. Model forecast parameters (e.g. precipitation accumulations) are produced at six-hourly intervals out to 36 hours (Dee et al., 2011). The precipitation field is known to suffer from spin-up errors at short lead times (Kållberg, 2011), although estimates of the severity of this spin-up error vary (Hawcroft et al., 2012; De Leeuw et al., 2015) and the effect of spin-up on precipitation is known to vary greatly by geographical region (Kållberg, 2011). Good results have been obtained using precipitation forecasts at lead times of 6–12 hours (De Leeuw et al., 2015) and 18–30 hours (Hawcroft et al., 2012; De Leeuw et al., 2015). Due to the 0900–0900 UTC timing of the EWP data, daily data were generated for ERA-I based on the same timings, using sub-daily data. To account for the aforementioned forecast spin-up, daily data were created using sub-daily forecast data at lead times of 18–30 hours from both the 0000 and 1200 UTC analyses. Since forecasts are produced on a 6-hour timestep, a constant rate was assumed between 0600 and 1200 UTC to derive daily precipitation accumulations commencing at 0900 UTC.

Precipitation from ERA-I has previously been evaluated against EWP over England and Wales, and found to systematically underestimate precipitation by approximately 22% on average (De Leeuw et al., 2015). A greater degree of underestimation of daily precipitation accumulation is found for the lower 10th percentile of events in ERA-Interim

relative to EWP. In the upper 10th percentile, the underestimation of daily precipitation accumulations in ERA-Interim reduces slightly. For daily accumulations above the 90th percentile ERA-Interim shows approximately 17% underestimation with respect to EWP. However, the De Leeuw et al. (2015) analysis describes only the frequency distribution of daily precipitation accumulation within the two datasets and does not investigate the ability of the reanalysis to accurately represent the timing of extreme events.

2.3 Climate models

To address the question of how clustering and stalling of extratropical cyclones is likely to affect England and Wales precipitation events in the future climate, a coupled climate model from the Coupled Model Intercomparison Project Phase 5 (CMIP5; Taylor et al. 2012) is analysed. HadGEM2-ES was selected for this project due to the quality of its representation of the location and direction of the North Atlantic storm track (see Section 1.5.1).

2.3.1 HadGEM2-ES

HadGEM2-ES (Hadley Centre Global Environment Model - Earth System) is a coupled climate model which incorporates dynamic vegetation, ocean biology and atmospheric chemistry (Collins et al., 2008). This model is part of the CMIP5 intercomparison project which promotes coordinated experiments using 56 coupled climate models from 29 modelling groups (Taylor et al., 2012).

The HadGEM2 family of models are configurations of the Met Office Unified Model (Easterbrook and Johns, 2009) for climate modelling on centennial time-scales. HadGEM2 can be configured in four levels of complexity (Martin et al., 2011), as shown in Figure 2.1. The Earth System configuration (HadGEM2-ES) is used in this thesis, which includes components for troposphere, land surface and hydrology, aerosols, ocean and sea ice, terrestrial carbon cycle, ocean biogeochemistry, and tropospheric chemistry. A well-resolved stratosphere is not included in the ES configuration due to the prohibitive computational cost of climate model runs on with such a high level of complexity (Martin et al., 2011).

Output from HadGEM2-ES is supplied on a $1.25^\circ \times 1.875^\circ$ latitude/longitude grid, with 38 vertical levels extending to approximately 40 km altitude. HadGEM2-ES is intended

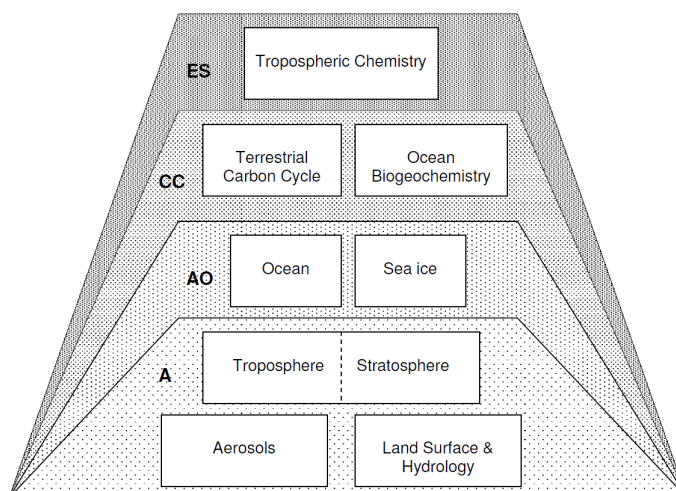


FIGURE 2.1: Processes used in the HadGEM2 model family. From Martin et al. (2011), Fig. 1.

to make improvements against its predecessor, HadGEM1, through improved representation of physical processes; the resolution is identical between the two models. The presence of the Earth System components remove the need for any artificial corrections to the carbon cycle, which were present in HadGEM1 (Collins et al., 2008).

CMIP5 models are used to run a suite of standardised experiments. In this thesis, the Historical and RCP8.5 experiments are used. The Historical experiment covers the period 1860–2005, using forcings from historical records including greenhouse gases, aerosols, volcanic and solar activity (Jones et al., 2011). This experiment is used primarily for model evaluation, and in this thesis will be analysed for its representation of key properties of clustering and stalling in association with England and Wales precipitation events in comparison with ERA-I.

Future projections are modelled using Representative Concentration Pathway (RCP) experiments (Moss et al., 2010; van Vuuren et al., 2011), initiated from the model state at 2005 in the Historical run (Jones et al., 2011). The RCPs are a set of scenarios which provide trajectories of emissions, atmospheric greenhouse gas concentrations, and land use in the twenty-first century. Four RCPs are used in CMIP5 experiments, which culminate in radiative forcing levels of 2.6, 4.5, 6 and 8.5 Wm^{-2} by 2100. RCP2.6 represents a scenario with a high level of mitigation leading to a very low forcing level; RCP4.5 and RCP6 represent mid-range scenarios, and RCP8.5 represents a scenario with increasing greenhouse gas emissions over time, leading to very high radiative forcing by 2100 (van Vuuren et al., 2011). RCP8.5 has been selected for evaluation in this thesis, as the high

radiative forcing is likely to amplify any climate change signal observed.

Whereas the North Atlantic storm track extends from west to east with a prominent south-west to north-east tilt, Zappa et al. (2013b) found that many members of the CMIP5 project generate a storm track that is too zonal in nature. HadGEM2-ES is one of the models that best represents the direction of the North Atlantic storm track (Figure 1.12). In particular it very accurately represents the location of the storm track at the prime meridian, where extratropical cyclones may be expected to have the largest impact on England and Wales. Martin et al. (2011) also finds that HadGEM2-ES represents the North Atlantic storm track well with respect to ERA-40, when analysed using the Blackmon (1976) band-pass filter method to identify the storm tracks (see Section 1.3.4). HadGEM2-ES was selected as the preferred climate model for this analysis due to the high quality of its representation of the location and intensity of the North Atlantic storm track, as analysed by Zappa et al. (2013a,b).

The representation of extratropical cyclone clustering in a selection of CMIP-5 models was analysed by Renggli and Zimmerli (2016). Good agreement was found between this selection of models in terms of number of storms per winter season (DJF), with a mean distribution closely following that of 20CR between 1871–2010. Greater variation was found in correlation between the dynamical intensity of storms within individual seasons, but all models were able to reproduce an increased mean dynamical intensity for cyclones in seasons where a single intense (10 year return period or greater) storm has been identified. These results indicate that distribution of cyclone counts per season is well represented across CMIP5 models, and that CMIP5 models are able to identify the observed phenomenon by which intense cyclones are found to cluster more strongly than weaker cyclones.

To evaluate the ability of HadGEM2-ES to represent clustering and stalling patterns associated with England and Wales precipitation events in the present climate, the Historical experiment was selected for comparison with reanalysis data. For future climate projections, the RCP8.5 experiment was chosen. This represents a high emissions scenario, and is likely to show the greatest response to climate change. However, responses of the atmosphere to a warming climate are non-linear, so it should be noted that other RCP scenarios may yield different results. At the time of analysis, complete sub-daily wind and precipitation data were only available for the r2i1p1 and r1i1p1 ensemble members (Historical and RCP8.5 experiments respectively) for the analysis period required (Historical 1980–2005, RCP8.5 2080–2099), so analysis was performed using only these

ensemble members.

For evaluation of the climate model against reanalysis, the period of greatest overlap between ERA-Interim and the Historical experiment of HadGEM2-ES was selected, giving a 25-year period: 1980–2005. For evaluation of the future climate projection, the final 20 years of the 20th and 21st centuries were selected (1980–1999 and 2080–2099 for Historical and RCP8.5 respectively), giving an identical number of years in both experiments.

2.4 Extratropical cyclone tracking

Objective identification of extratropical cyclones in reanalyses and climate models is a non-trivial problem. Extratropical cyclones are of irregular shape and size, with large variance in propagation speed. Additionally, extratropical cyclones can split and merge with other cyclones (Neu et al., 2013). As such, no commonly-agreed definition of an extratropical cyclone exists. As discussed in Section 1.3.4, numerous feature tracking methods are used in the existing literature, the majority of which identify extratropical cyclones as either local minima of mean sea level pressure (MSLP) or ∇^2 MSLP, or local maxima of relative vorticity at 850 hPa (ξ_{850}). The IMILAST project (Neu et al., 2013) provides an inter-comparison of 15 commonly used tracking schemes (not including Hodges 1994, 1995) and has evaluated the characteristics of the northern- and southern-hemisphere storm tracks as represented in each scheme in its most commonly used configuration. A large amount of variation is identified between the tracking schemes, particularly in terms of the magnitude of seasonal variation in the storm tracks. As no “best track” database exists, the quality of each tracking scheme is largely subjective. In an analysis of the representation of extratropical cyclone clustering in the North Atlantic in ERA-Interim with various tracking schemes (IMILAST members and Hodges 1994, 1995), Pinto et al. (2016) finds a large amount of variation in the spatial distribution of the dispersion statistic (see Section 1.6.1). However, all tracking schemes produced statistically significant regions of under-dispersion in the western North Atlantic and over-dispersion in the eastern North Atlantic.

To objectively track the position of extratropical cyclones in the North Atlantic, the feature tracking algorithm of Hodges (1994, 1995) has been used. This method is used to track minima of MSLP or maxima of ξ_{850} in gridded datasets, and has been used extensively in previous studies that have analysed the behaviour of North Atlantic extratropical cyclones in climate models and reanalyses (e.g. Hoskins and Hodges 2002,

Mailier et al. 2006, Bengtsson et al. 2006, Zappa et al. 2013a). The feature tracking algorithm is able to identify smaller features when tracking maxima of ξ_{850} than minima of MSLP, and features are detected at an earlier stage in the development of the cyclone (Hoskins and Hodges, 2002). ξ_{850} features are also less influenced by the large-scale background flow than MSLP features (Hoskins and Hodges, 2002). As such, ξ_{850} was tracked so as to identify smaller, developing cyclones and frontal waves.

Before features are identified, the vorticity field must be filtered to remove features with wavenumber ≥ 42 , which improves the signal-to-noise ratio and prevents very small-scale features from being tracked. Features of local maximum ξ_{850} are then identified and temporally combined into tracks using a nearest neighbour approach (Hodges, 1994). This occurs directly on the unit sphere, which eliminates the need for re-projection of data which may cause results to be distorted, and is preferable for global datasets (Hodges, 1995). Adaptive constraints are used to vary the maximum distance at which features in consecutive time-steps may be considered to be part of the same track (Hodges, 1999). These constraints specify that the motion of features may not change discontinuously. Therefore, if a rapid change of propagation speed would be required to allow two features to be connected in a single track, the connection is not made and they are treated as two separate features.

The standard approach when using this system is to remove tracks that last less than two days, or that travel less than 1,000 km (e.g. Hoskins and Hodges 2002, Neu et al. 2013). For this study, the minimum movement criterion was removed, so as not to discard tracks of storms which form in the eastern North Atlantic and stall over the UK. This algorithm has been applied to ERA-I and HadGEM2-ES to generate tracks of individual storms in the North Atlantic for analysis of propagation speed and clustering and stalling patterns, and to calculate overall track density across the North Atlantic for the inter-comparison of models. Two regions are defined for analysis of the behaviour of extratropical cyclones: the “Eastern North Atlantic” region (45° – 65° N, 25° W– 10° E), and the “British Isles” region (circle of 700 km radius from 55° N, 5° W, c.f. Pinto et al. 2013). The Eastern North Atlantic region and the British Isles region are displayed in Figure 2.2 as a blue box and red circle respectively.

2.5 Time-series analysis

Analysis of precipitation time-series is used in this thesis for the identification of accumulated precipitation events in England and Wales. Time-series of precipitation are

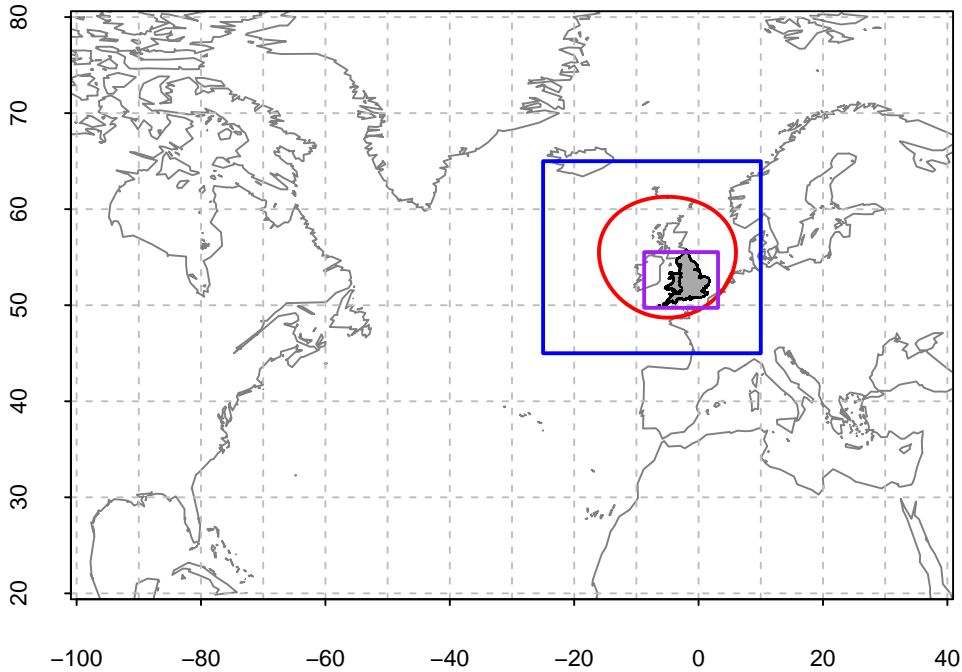


FIGURE 2.2: Regions defined for analysis of spatial data. Blue box: “Eastern North Atlantic region”. Red circle: “British Isles region”. Purple box: “England and Wales region”. Geographical location of England and Wales denoted by shaded map region.

obtained from HadUKP, ERA-I and HadGEM2-ES. Where gridded data are used, a spatial average for each time-step is taken from the England and Wales region (denoted by the purple box on Figure 2.2). Sensitivity analysis was performed to determine the England and Wales domain used for averaging for gridded datasets, based upon the frequency of extreme events observed in EWP that were identified in 20CR and ERA-I. The domain chosen for ERA-I and 20CR is defined by a rectangle bounded by $51.73^{\circ}N - 55.53^{\circ}N$, $8.75^{\circ}W - 3.125^{\circ}E$. This domain is overlaid on the panels in Fig. 3.1. The smaller domain used by De Leeuw et al. (2015) ($50.6^{\circ}N - 54.5^{\circ}N$, $4.5^{\circ}W - 0.7^{\circ}E$) was also considered but found to be less sensitive to extreme events than the domains in Fig. 3.1.

For analysis of the influence of clustering and stalling of extratropical cyclones on England and Wales precipitation events, precipitation accumulations on time-scales from 1–31 days were considered. Having created daily time-series for England and Wales precipitation in each dataset, precipitation accumulations were calculated for 7-, 13- and 31-day periods (representing weekly, fortnightly and monthly periods) using a centred running sum. A variant on the peaks-over-threshold (POT) approach is used to identify precipitation events, whereby precipitation events are identified iteratively, starting at the largest precipitation accumulation. For each “event” identified in the accumulated

time-series, the full duration of the accumulated event is removed from the time-series before the next event is identified, so as to minimise the effect of autocorrelation. Precipitation events are classified as “Extreme wet”, “Wet”, and “Extreme dry” according to the criteria presented in Table 2.1. Whilst there is a fixed number of extreme wet events in each sample, the count of wet and extreme dry events is variable.

2.6 Quantification of periods of cyclone clustering and stalling

The concept of cyclone clustering has been described extensively in the literature with respect to the dispersion statistic of Mailier et al. (2006) (see Equation 1.3). This statistic describes serial clustering (regularity) of extratropical cyclones as the over- (under-) dispersion of cyclone passages as represented as the ratio of the sample variance to the mean. This method is a highly effective descriptor of the regularity of cyclone transits. However, it is not applicable to an event-focussed evaluation, where high-impact precipitation events may be of varying time-scales. For this reason, clustering in this study will be related to the cyclone count during the time-period of an event of length 1–31 days.

Stalling is described using two metrics: the mean cyclone residence time during a precipitation event, and the maximum cyclone residence time during a precipitation event. The former metric describes the overall state of cyclone mobility during a given time-period, where a “stalled” event would be described as one with low overall cyclone mobility. The latter metric defines a “stalled” event as one in which any single cyclone in the time-period is resident for a long period of time, as may occur in situations where a single slow-moving storm is embedded within an otherwise mobile period.

Time-scale (days)	Extreme wet events	Wet events	Extreme dry events
1	Top 60 events	All remaining events >50th percentile	All dry (0 mm) events or bottom 60 (whichever is the larger sample)
7, 13, 31	Top 10 events	All remaining events >50th percentile	All dry (0 mm) events or bottom 10 (whichever is the larger sample)

TABLE 2.1: Criteria for Peaks-Over-Threshold event identification in England and Wales Precipitation time-series. Time-series data are split by season before criteria are applied.

Chapter 3

Can reanalyses represent extreme precipitation over England and Wales?

This chapter is adapted from work published in the Quarterly Journal of the Royal Meteorological Society:

Rhodes, R. I., L. C. Shaffrey, and S. L. Gray, 2015: "Can reanalyses represent extreme precipitation over England and Wales?." *Quart. J. Roy. Meteorol. Soc.*, **141**, 1114-1120.

3.1 Introduction

Obtaining consistent and accurate precipitation records is challenging on account of the range of precipitation observation methods available and the highly localised nature of precipitation events (NOAA NCDC, 2013). At present, the alternatives to using direct observations from rain gauges consist of gridded satellite derived products, pre-processed gridded rain gauge observations, or reanalysis. Satellite derived products, for example the Global Precipitation Climatology Project (Huffman et al., 1997), are necessarily limited to the short period from 1979 to the present day (the "modern satellite era"). It is preferable to include data from a longer period when considering long-term precipitation variability and trends. Global gridded rain gauge products are available for longer periods (e.g. Chen et al. 2002; Becker et al. 2013), but are limited by the spatio-temporal availability of gauge measurements, and the data are necessarily produced on a coarse

grid. Higher resolution gridded gauge products are available regionally, including ENSEMBLES E-OBS (Haylock et al., 2008), which provides gridded observations at 0.25° longitude/latitude over Europe from 1950-2013, and the NCEP Climate Prediction Centre's Unified Gauge-Based Analysis of Precipitation (Higgins et al., 1996, 2000), which provides 0.25° longitude/latitude gridded precipitation data over North America from 1948-2006. However, these products are limited spatially, in terms of both their regional nature and their land-based coverage. The purpose of this study is to determine the ability of re-analysis datasets to represent individual extreme precipitation events over England and Wales.

Reanalysis can be a useful tool for reconstructing precipitation patterns, particularly where events prior to the advent of the modern satellite era are important. Reanalysis has the potential to describe weather conditions over a longer period of time than satellite derived observations, and to produce high resolution, high spatial coverage data relative to gridded gauge observations. The NOAA-CIRES Twentieth Century Reanalysis (20CR)¹ spans the longest time of any currently available reanalysis dataset (Compo et al., 2011), whilst the ECMWF Interim Reanalysis (ERA-I) has a higher resolution than 20CR (Dee et al., 2011). Reanalysis products are generally accepted to reproduce large-scale analysed variables to a good degree of accuracy and large-scale storm systems can reliably be objectively tracked (e.g. Hoskins and Hodges (2002)). Reanalysis products do not directly assimilate observations of precipitation (Kalnay et al., 1996; Dee et al., 2011; Compo et al., 2011); however, precipitation is produced as a short-term forecast variable, typically at a three- to six-hour lead time, and as such is dependent on the model formulation. Given this limitation, accurately representing the peak accumulations of precipitation associated with an extreme precipitation event may be difficult for any reanalysis product. Some previous analysis of ERA-I precipitation over the UK and north-western Europe has been conducted, e.g. De Leeuw et al. (2015). 20CR is a recently developed reanalysis and to date no analysis of precipitation data from 20CR over north-western Europe has been published.

In this chapter the ability of 20CR and ERA-I to represent extreme precipitation events over England and Wales is investigated, focussing on the ability of reanalyses to represent individual events, with accurate timings, found in the observed record on one-, three- and seven- day accumulation time-scales. Precipitation data from ERA-I and 20CR is compared with processed rain gauge data from the England and Wales Precipitation (EWP) dataset (Alexander and Jones, 2000) and gridded precipitation data from the

¹20th Century Reanalysis V2c data provided by the NOAA/OAR/ESRL PSD, Boulder, Colorado, USA, from their Web site at <http://www.esrl.noaa.gov/psd/>

Global Precipitation Climatology Project (GPCP) (Huffman et al., 1997). England and Wales has been selected due to the availability of long-running observations with a high spatial density across the region. A statistical analysis is performed which describes the ability of the reanalysis products to describe extreme precipitation accumulations over a range of accumulation time-scales.

3.2 Data and Methods

To evaluate the ability of ERA-I and 20CR to represent extreme precipitation events, analysis is performed using EWP as a comparison dataset. The definition of “extreme” in this study is based on percentiles of the individual datasets, thus reducing the problem of systematic error. A range of thresholds are considered, from the 90th percentile (hereafter p90) to p99, with a focus on p98 equating to an average of seven events per year with daily accumulations, 2.5 events per year with three-day accumulations, and one event per year with seven-day accumulations.

3.2.1 Hit Rate analysis method

Hit rate analysis depends on a threshold value to give a binary “hit” (e_{hit}) or “miss” (e_{miss}) response for any given event when comparing a model with observations. When the daily precipitation accumulation for a given date is recorded in both the EWP observations and the reanalysis data as above their respective “extreme” thresholds (see Table 3.1 for values), a hit is recorded; conversely when EWP indicates extreme precipitation and the reanalysis data does not, a “miss” is recorded. The ratio of hits to misses is used to create a hit rate, expressed as a percentage:

$$H = 100 \frac{e_{hit}}{e_{total}},$$

where e_{total} is the total number of extreme events identified in the sample of observations, and e_{hit} is the number of occasions when both the observations and the reanalysis product have identified extreme events on the same date.

3.2.2 Accumulation time-scales

A common period of 1979–2010 was chosen to reflect the maximum period of overlap between ERA-I and 20CR. To test the response of the hit rate to events of different time-scales, three accumulation lengths were considered: one, three and seven days.

These varying accumulation lengths reflect both the manner in which precipitation is accumulated (e.g. single, intense cyclone; stalled or clustered cyclones), and the varying flood potentials of catchment areas with differing response times (Lavers et al., 2011). Daily accumulations were calculated from the sub-daily data in the reanalysis products as described in sections 2.2.2 and 2.2.1. Multiple-day accumulations were calculated by taking the sum of daily accumulations, and are dated according to the final day of the accumulation.

3.3 Analysis

3.3.1 Spatial analysis of precipitation data

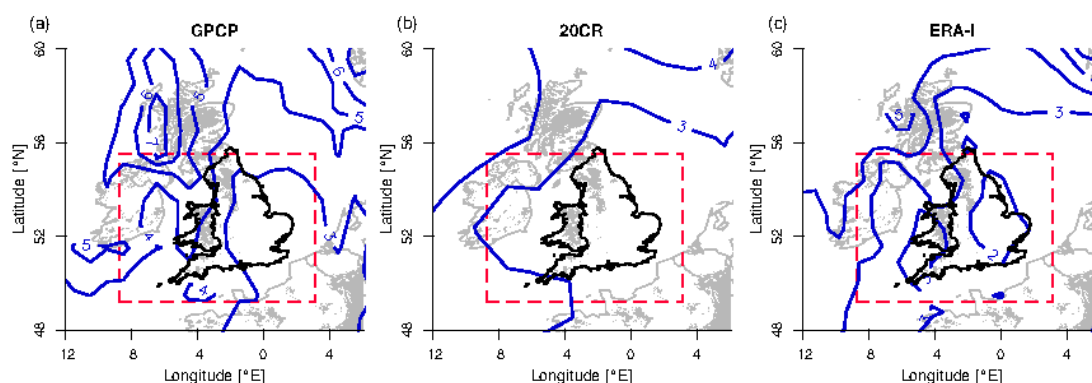


FIGURE 3.1: 1996-2009 DJF mean daily precipitation accumulation contours for (a) GPCP, (b) 20CR, (c) ERA-I. Dashed box indicates spatial extent of data extracted from ERA-I and 20CR. England and Wales are shown with bold coastlines in all figures.

Contours in 1mm intervals. Land with elevation over 200m is shaded grey.

To identify variations in the spatial representation of precipitation between ERA-I, 20CR and observed precipitation, Fig. 3.1 shows the climatological distribution of DJF precipitation across the British Isles in GPCP, ERA-I and 20CR in the period 1996-2009. Using the high-resolution satellite- and gauge-derived observations from GPCP as a comparison, the quality of the spatial representation of precipitation accumulation in ERA-I and 20CR are shown. Both reanalysis products capture some large-scale features, such as the higher accumulations to the west of the UK and Ireland relative to the east. 20CR is unable to represent the precise location and intensity of the regions of increased precipitation over orography in western England and Wales, possibly due to its lower horizontal resolution in comparison to ERA-I. ERA-I represents these smaller-scale features over orography, albeit with a lower precipitation rate than in GPCP. ERA-I also indicates a drier region in the east of England than is indicated by GPCP.

3.3.2 Statistical analysis

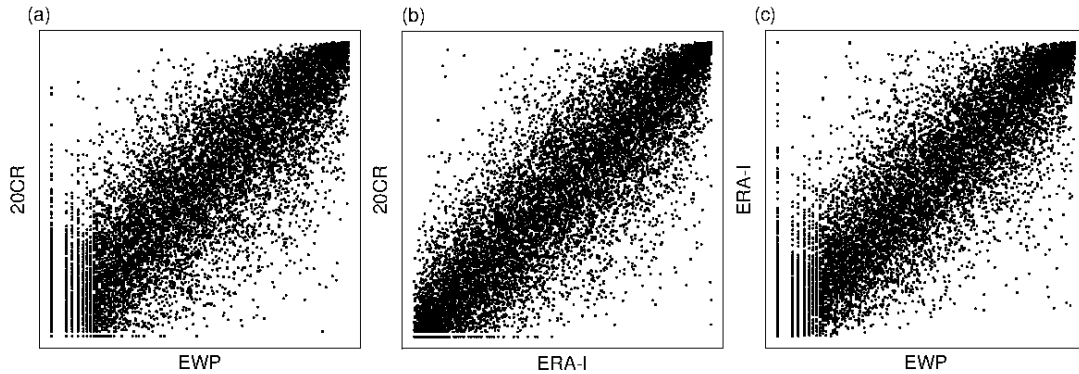


FIGURE 3.2: Rank scatter-plots of daily accumulations in a) 20CR vs EWP b) 20CR vs ERA-I c) ERA-I vs EWP. Note: apparent “binning” of EWP data is due to the two decimal place rounding applied to EWP values as provided.

A rank correlation analysis was performed to check for consistency in the relationships between the three datasets (Fig. 3.2). This analysis assigns a rank to every value in a sample, and checks for correlation with the rank for the same data-point in a second sample. Spearman’s Rank Coefficient (ρ) was calculated for each correlation with results as follows for daily accumulations: 20CR vs EWP $\rho = 0.86$; 20CR vs ERA-I $\rho = 0.87$; ERA-I vs EWP $\rho = 0.88$. High rank correlations are found in all cases, indicating a good relationship between ERA-I/20CR and EWP, and between ERA-I and 20CR. Similar results were found for three- and seven- day accumulations.

3.3.3 Intensity of precipitation accumulations in reanalysis

The values of p98 in ERA-I and 20CR were compared with that of EWP to determine whether these reanalyses correctly represent the magnitude of precipitation accumulation during extreme events. These values, for one-, three- and seven- day accumulations, are listed in Table 3.1.

Both ERA-I and 20CR underestimate the magnitude of p98 one-day accumulations by $\sim 25\%$, and by $\sim 20\%$ for three- and seven- day accumulations. This underestimation is

Accum.	EWP	ERA-I	20CR
1 day	13.62	10.35	10.10
3 day	28.54	22.95	22.59
7 day	53.33	43.58	43.86

TABLE 3.1: Values of the 98th percentile of precipitation accumulation in EWP, ERA-I and 20CR at daily, three-day and seven-day accumulations, 1979-2010.

slightly greater than that found by De Leeuw et al. (2015) for daily precipitation accumulations above the 90th percentile in ERA-I with respect to EWP. Although the precipitation is under-represented, the high rank correlations demonstrated in Section 3.3.2 indicate that the reanalysis is performing consistently relative to observations.

3.3.4 Hit rate analysis for an example time-series

Figure 3.3 gives a time-series example over one month, indicating the frequency with which the two reanalysis datasets represent extreme events. The time series presented here, September-October 2000, was a particularly wet period, with EWP recording five events above p98 in a 30 day period in the daily accumulations, against an average of seven events per year. This plot highlights the range of values reported for each event across the three datasets. Note that an extreme event was recorded by ERA-I on the first day of this time period, when the precipitation accumulation in EWP was well below the p98 threshold. On 19 September, 25 September, and 10 October, EWP records extreme events which are not identified as extreme in either ERA-I or 20CR. Good agreement in all datasets is shown on 26 September and 9 October. The ability of ERA-I and 20CR to represent these extreme events can be characterised by the hit-rate, which indicates the percentage of extreme events in the reanalysis which correspond to an observed extreme event in the same time period.

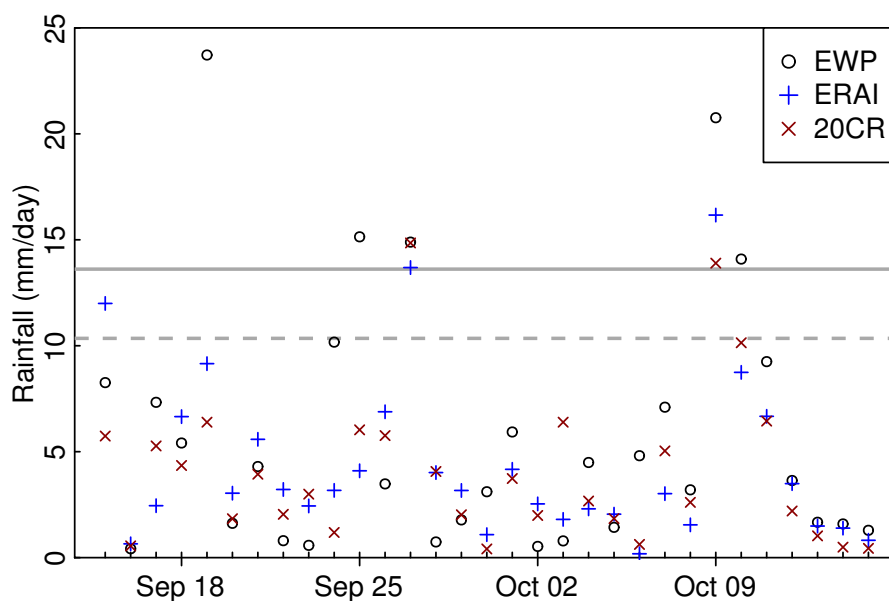


FIGURE 3.3: Example time series indicating the distribution of England/Wales precipitation values from EWP, ERA-I and 20CR across an example wet month (Sep 15–Oct 15 2000). Solid horizontal line indicates p98 value for EWP. Dashed horizontal line indicates p98 value for ERA-I and 20CR (equal to within the accuracy of this diagram).

3.3.5 Hit rate analysis

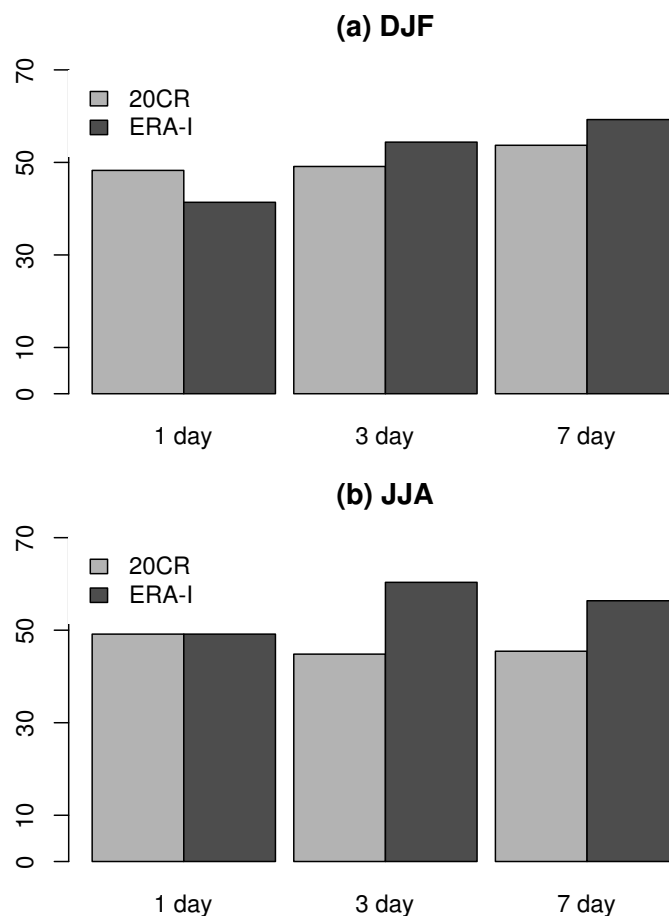


FIGURE 3.4: Hit rates at the 98th percentile threshold in (a) DJF and (b) JJA for ERA-I and 20CR for one-, three- and seven- day accumulations

A hit rate analysis was performed with the threshold set to p98 for ERA-I and 20CR. Hit rates for one-, three- and seven- day accumulations when calculated over the period 1979–2010 are indicated in Fig. 3.4. The most notable result indicated by Fig. 3.4 is the low hit rate value demonstrated by all datasets. ERA-I demonstrates a particularly low hit rate at daily time-scales in DJF, with a hit rate of approximately 40%. The highest hit rate, ~60%, was demonstrated by ERA-I three-day JJA accumulations. Most 20CR results lay within a range of 45–50% hit rate. Tables 3.2 and 3.3 demonstrate the numbers of hits, misses, false alarms and true negatives in the all seasons daily accumulations at the p98 threshold. At the daily accumulation time-scale, 20CR appears to be performing well compared with ERA-I, particularly in the winter months. However, the improvement in ERA-I at the three- and seven- day time-scales may be indicative of an error in the daily accumulations introduced by the interpolation between 0600 and 1200 UTC required to fit ERA-I to a 0900–0900 UTC day. Since a constant rain rate is assumed between 0600 and 1200 UTC, there is the potential for a short, intense period of accumulation to be inappropriately spread evenly between two days rather

than allocated to a single day, thus reducing the hit rate for the daily accumulation. The magnitude of this error should be reduced for longer accumulations, since the uncertain period accounts for less time relative to the length of the accumulation period.

	ERA-I \geq p98	ERA-I $<$ p98
EWP \geq p98	118	116
EWP $<$ p98	116	11,335

TABLE 3.2: Contingency table indicating counts of events where ERA-I recorded values \geq p98. A "hit" is indicated by a value where both ERA-I and EWP recorded values in excess of their respective p98 value.

	20CR \geq p98	20CR $<$ p98
EWP \geq p98	115	119
EWP $<$ p98	119	11,335

TABLE 3.3: Contingency table. As Table 3.2, with data from 20CR.

For three- and seven- day accumulations, both 20CR and ERA-I show an increased hit rate during the winter months, whilst 20CR's hit rate is reduced at longer accumulations in the summer. This may be due to shorter time-scale events in summer which may be poorly represented in 20CR. Conversely, winter precipitation is usually generated by synoptic-scale systems, which can take several days to cross the UK and so may be better represented through a three- or seven- day accumulation.

For 20CR, data for years 1931-1979 (corresponding to the remainder of the available EWP daily data) were also analysed for hit rate at p98 against EWP. Hit rates were in the range 35-45% for one-, three- and seven-day accumulations in DJF and JJA, indicating a decrease in quality for extreme precipitation in 20CR for this earlier time-period.

Having investigated the hit rates of extreme events in 20CR and ERA-I at p98, the sensitivity of the hit rate analysis to the threshold value was analysed between p90 and p99 (Fig. 3.5). Thresholds from p90 to p99 indicate high levels of precipitation accumulation, and occur on average 37 days per year for p90 and 4 days per year for p99. Hit rates decrease with higher thresholds for both reanalyses. Even at p90, neither reanalysis exceeds a 65% hit rate on daily accumulations in either summer or winter. 20CR only achieves a 70% hit rate at three- and seven- day accumulations at the p90 threshold, whilst ERA-I exceeds 70% hit rate in the seven- day accumulations in DJF and JJA at thresholds $p \leq 0.94$. 20CR consistently has higher hit rates than ERA-I in winter daily accumulations and has similar hit rates to ERA-I at longer accumulations and in summer months.

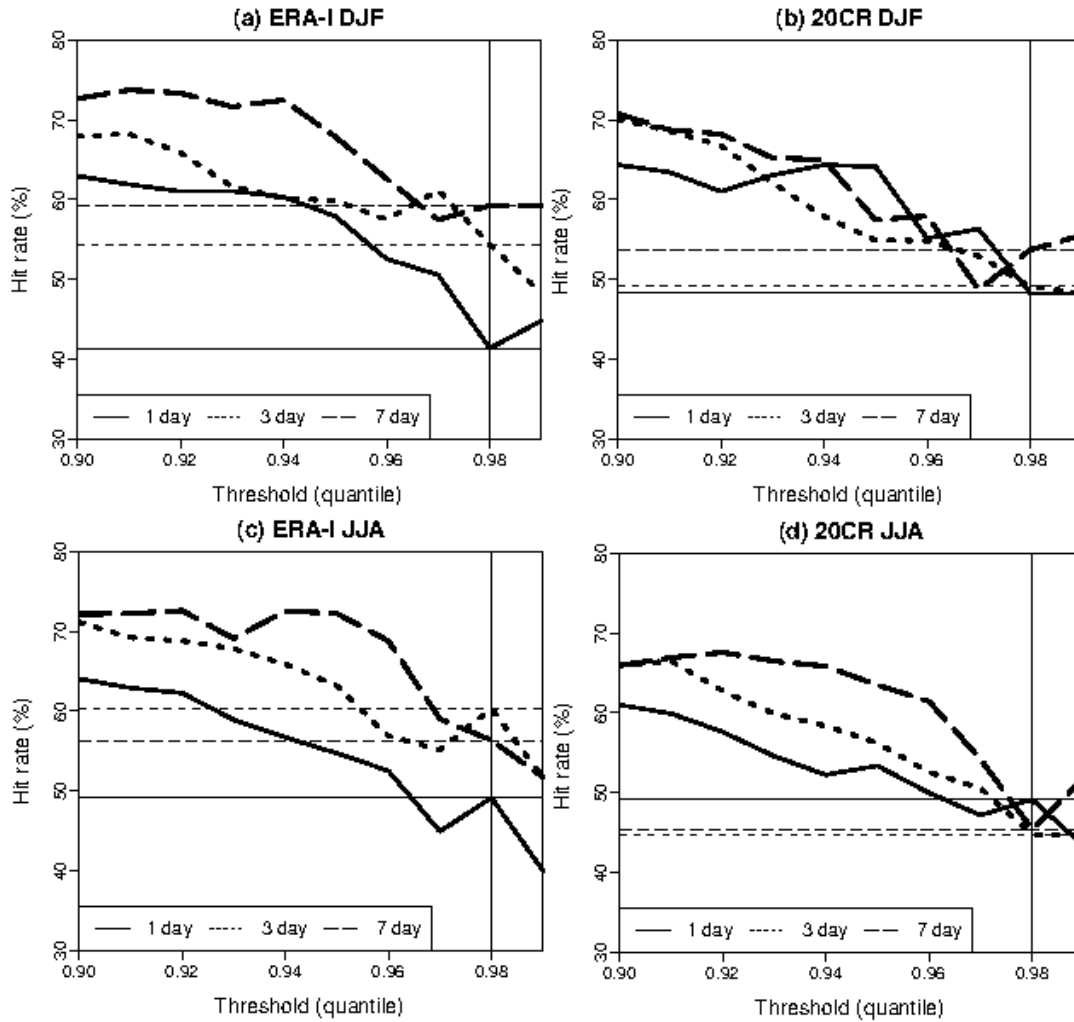


FIGURE 3.5: Hit rates as a function of threshold for ERA-I and 20CR in DJF and JJA seasons. (a) ERA-I DJF (b) 20CR DJF (c) ERA-I JJA (d) 20CR JJA. Vertical lines indicate p98, and horizontal lines indicate the hit rates at p98 for one-, three- and seven-day accumulations.

3.4 Conclusions

The representation of extreme precipitation over England and Wales in the Twentieth Century Reanalysis and in ERA-Interim has been evaluated, using processed rain gauge data from the England and Wales Precipitation dataset as a comparison. The motivation was to assess the usefulness of ERA-I and 20CR for the investigation of historical occurrences of high precipitation accumulations. The main findings of this study are as follows.

- Both ERA-I and 20CR were found to represent many of the large-scale features of climatological DJF precipitation distribution over the British Isles when compared to GPCP, such as the contrast between relatively high precipitation levels in the

west and lower values in the east. However, ERA-I was able to generate more detail, with better representation of localised climatological features. Precipitation rates were lower in 20CR to the west of England and Wales, particularly over mountainous regions where orographic enhancement is important.

- ERA-I and 20CR are highly correlated with each other and with a time-series of daily precipitation totals over England and Wales from EWP, indicating that daily precipitation accumulations are usually well represented over England and Wales in ERA-I and 20CR. The virtually identical rank correlations found for ERA-I and 20CR against EWP are notable, given the limited range of observations assimilated into 20CR.
- Both ERA-I and 20CR produced hit rates for extreme events at the 98th percentile in the range 45-55% for extremes of daily precipitation accumulation. Timing errors are likely to be an important source of error for one-day accumulations. Both reanalysis products showed improved hit rate for longer accumulation time-scales. However, hit rates did not exceed 80% for either ERA-I or 20CR for any accumulation length at p98.

The hit rates of ~45-70% in ERA-I and 20CR suggests that it might be difficult to use 20CR and ERA-I to investigate long term variability of extreme precipitation over England and Wales, in situations where knowledge of the timing of such events is necessary. However, the quality of 20CR's precipitation data appears to be comparable to that of ERA-I, which is encouraging considering the potential usefulness of this long time period dataset. These results suggest that further evaluation is necessary in other regions with extensive observations of precipitation to ascertain the quality of precipitation in reanalysis.

Chapter 4

Development of the Continuous Precipitation Area storm association algorithm

4.1 Introduction

This chapter discusses the development of the Continuous Precipitation Area (CPA) method for associating objectively identified cyclone tracks with events in a given region. The structure of extratropical cyclones is highly asymmetrical and non-uniform, and existing methods may be unsuitable for the purpose of associating a given precipitation event with the extratropical cyclone responsible. In Chapter 3 it was demonstrated that although reanalysis cannot be used to identify individual extreme events as observed in EWP, it can be used to represent the spatial distribution of precipitation. This new method is designed to objectively identify the extent of a storm using spatial patterns in gridded precipitation data, before finding the most appropriate cyclone track for a given event.

Existing methods for identifying the passage of a cyclone in the vicinity of a given region are discussed in Section 4.2. Section 4.3 outlines the criteria for an improved method, and the development of this method is discussed in Section 4.4. The new CPA method is compared against two existing methods in Section 4.5. The parameter sensitivity of the new method is discussed in Section 4.6. Finally, this chapter is summarised in Section 4.7.

4.2 Evaluation of established methods

Prior to the development of the Continuous Precipitation Area (CPA) algorithm, a number of alternative methods of associating the passage of storms with their influence over a region of impact had been developed for various uses. The first of these was the “gate” method, as implemented by Mailier et al. (2006) and Vitolo et al. (2009). Mailier et al. (2006) implemented this method both to analyse cyclone passages across all grid points in a northern hemisphere region ($-180:180^{\circ}\text{E}$, $10:80^{\circ}\text{N}$), and to provide a more thorough analysis at points corresponding to the North Atlantic storm track genesis and lysis regions. The point chosen for the analysis of the storm track lysis region, 0°W , $55^{\circ} \pm 10^{\circ}\text{N}$, provides a “gate” positioned over the British Isles. Extra-tropical cyclone transits over the United Kingdom are treated as a point process occurring at the time at which a ξ_{850} track crosses the meridional line defined by the aforementioned coordinates (Figure 4.1). This method was designed to capture instances of cyclone centres tracking westerly across the United Kingdom, to provide data for a statistical analysis of spatio-temporal serial clustering of cyclones in the western North Atlantic. This method was not designed to take into account the spatially non-uniform influence of individual cyclones, or to provide diagnostics beyond time, location and intensity as expressed by ξ_{850} . Furthermore, it does not take into account a meridional component of cyclone propagation, instead making the assumption that cyclone motion is predominantly zonal and westerly.

The method employed by Pinto et al. (2013) (Figure 4.1) addresses the meridional component of cyclone transit by detecting cyclones which track within a 700km radius of 55°N , 5°W . By utilising a two-dimensional region instead of a one-dimensional gate to track cyclones, this method also allows for analysis of cyclone propagation speeds and direction of propagation. This method was developed for the analysis of the impact on cyclone clustering on windstorm risk, in which the region of maximum intensity is usually close to the location of peak ξ_{850} . However, peak rainfall accumulations may occur on a front at a considerable distance from the cyclone centre and in a highly asymmetrical distribution pattern, indicating that the suitability of this method for analysing cyclone passages associated with precipitation events must be carefully studied.

Hawcroft et al. (2012) evaluates the percentage of precipitation associated with extratropical cyclones in the Northern Hemisphere, and therefore utilises a method designed for the purpose of associating precipitation with a parent cyclone. Like Pinto et al. (2013), Hawcroft et al. (2012) uses a fixed-radius association method, however, in the case of Hawcroft et al. (2012) a radial cap of $12/10^{\circ}$ (DJF/JJA respectively) is applied

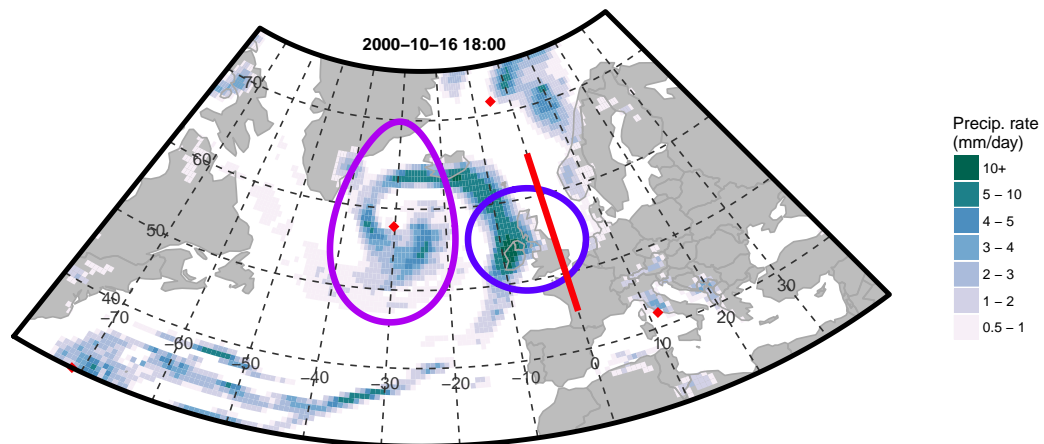


FIGURE 4.1: 0.75° gridded precipitation forecast field from ERA-Interim for 1800 UTC 16 October 2000 over the North Atlantic. Grid cells with precipitation rate $\leq 0.5 \text{ mm day}^{-1}$ not shown. Overlaid with ξ_{850} cyclone track data (red points) and cyclone association gates as used by Mailier et al. (2006) (red meridional line centred on 0°E , 55°N), Pinto et al. (2013) (blue circle of $r=700\text{km}$ centred on 5°W , 55°N), and Hawcroft et al. (2012) (purple line of $r=12^\circ$ about a cyclone centre at 30°W , 58°N). This figure highlights an extreme precipitation event with no attributable cyclone track by previous methods.

from the cyclone centre, with a tighter radius of 5° applied to the analysis of extreme events on the assumption that the peak of precipitation intensity is to be found close to the cyclone centre. This leaves the method unable to identify remote accumulations of precipitation generated by fronts associated with an identified cyclone. It is also noted in the literature that the identified total precipitation accumulations are highly dependent on the radial cap chosen.

A method which enables the analysis of remote precipitation events generated by fronts associated with an extratropical cyclone is presented by Catto and Pfahl (2013). By combining cyclone tracking (Pfahl and Wernli 2012 method) with front tracking (Berry et al. 2011 method, based on Hewson 1997), additional information regarding the spatial structure of extratropical cyclones can be obtained. Precipitation events are categorised as being associated with a cyclone, a front, or both a cyclone and a front. However, as cyclones and fronts are treated as independent features, this method does not directly allow the association of a distant (front-only) precipitation event with a parent cyclone. Because a front is defined as a line feature, plus a 5° search area, this method may lose some spatial information that is available directly from the precipitation field of a gridded dataset. It may also be preferable to use a less computationally expensive method where it is possible to obtain spatial information for a storm using existing data.

A method for identifying contiguous rain areas (CRAs) was described in Ebert and McBride (2000), for the purposes of forecast verification. By creating CRAs based on a user-defined isopleth, objects may be compared between forecast and observed rain fields, allowing for objective analysis of the displacement of features in the forecast. The identification of contiguous rain (or precipitation) features in gridded data using a thresholding technique is an essential component of the method described in this chapter. However, the method must be developed beyond the identification of precipitation areas to identify the most likely cyclone centre to be responsible for the precipitation. In this case, applications to forecast verification are not required. The CPA method was therefore developed independently. This approach gives greater control of the required functionality, and improved understanding of the workings of the method. This development is detailed in the following sections.

4.3 Criteria for storm association algorithm

To identify the cyclone tracks responsible for individual precipitation events in a given region (e.g. England and Wales), a method is required that is able to associate cyclone tracks with the region of interest by analysis of the spatial structure of precipitation features as found in a gridded dataset. Figure 4.1 shows a typical extratropical cyclone interacting with the England and Wales region. The cyclone centre of this event would not be identified as affecting the UK by either the Mailier et al. (2006), Pinto et al. (2013), or Hawcroft et al. (2012) methods due to its position to the west of the British Isles. However, a human observer is able to identify the appropriate cyclone track for this event due to its location enveloped by a continuous rain band with a frontal structure extending eastwards, interacting with England and Wales.

For a new method to improve the association rate between precipitation events in a defined region and the appropriate cyclone centre, precipitation bands must be identified within the gridded precipitation data. These bands should be objectively identified by applying a threshold precipitation rate to identify continuous regions of substantial precipitation. Storm tracks lying within a precipitation band, or within a small, pre-defined radius of a precipitation band, should be taken to be associated with the regional precipitation event. Measures must be taken to prevent multiple cyclone tracks being associated with the same event, for example in a situation where the cyclone tracking algorithm identifies multiple features on a single precipitation band (common in frontal waves and secondary cyclogenesis). The algorithm must also be designed not to associate highly unlikely track points with an event, if it fails to identify a likely track

(e.g. Figure 4.1). A maximum distance limit must therefore be defined to ensure that no tracks are identified that would be physically unable to cause or influence a precipitation event. A conceptual process flow diagram for the CPA method is presented in Figure 4.2.

4.4 Development of CPA algorithm

4.4.1 Identification of Continuous Precipitation Areas

Figure 4.3a shows an example of the input data for a single timestep, during which a well-defined extratropical cyclone is interacting with the England and Wales region, as defined by the purple rectangle (the “interest region”). The algorithm must first objectively isolate the appropriate precipitation band, based on a pre-defined threshold (here 1.5 mm day^{-1}). The algorithm first searches for any precipitation cells within the interest region above the threshold value, and halts if none are found, saving processing time for dry events. If wet cells are present within the interest region, a contouring algorithm is applied with a single level at the precipitation threshold value.

The contouring algorithm produces a number of polygons which correspond to precipitation bands Figure 4.3b. The CPA algorithm identifies any overlap between these polygons and the interest region, and any precipitation bands which interact with the interest region are tagged (thick black contour in Figure 4.3b. Having identified any precipitation bands which interact with the interest region, the algorithm searches for cyclone centres that fulfil one or more of the following criteria:

- Are located within interest region
- Are located within a matched precipitation band
- Are located within a pre-determined distance (250km) from a matched precipitation band or interest region

In the case shown in Figure 4.3b, no cyclone centres lie within the interest region or the matched precipitation band, but one track lies within 250 km of the matched precipitation band (indicated by the red circle of radius 250 km; the cyclone proximity radius).

It is possible that multiple tracks may be present at this stage that fulfil one or more of the above criteria, so the algorithm must choose appropriate track(s) based on their

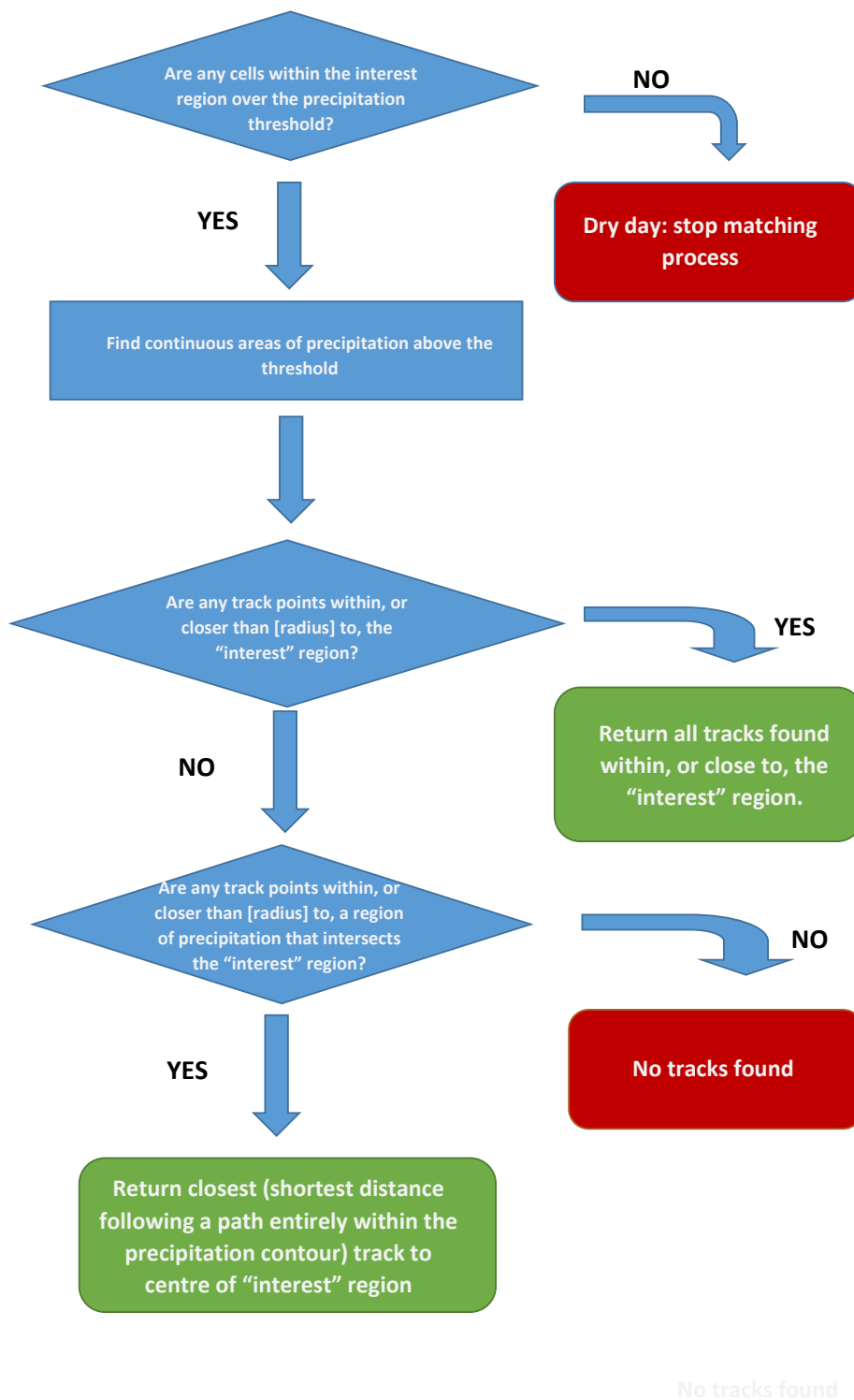


FIGURE 4.2: Flow diagram demonstrating the decision flow of the CPA algorithm.

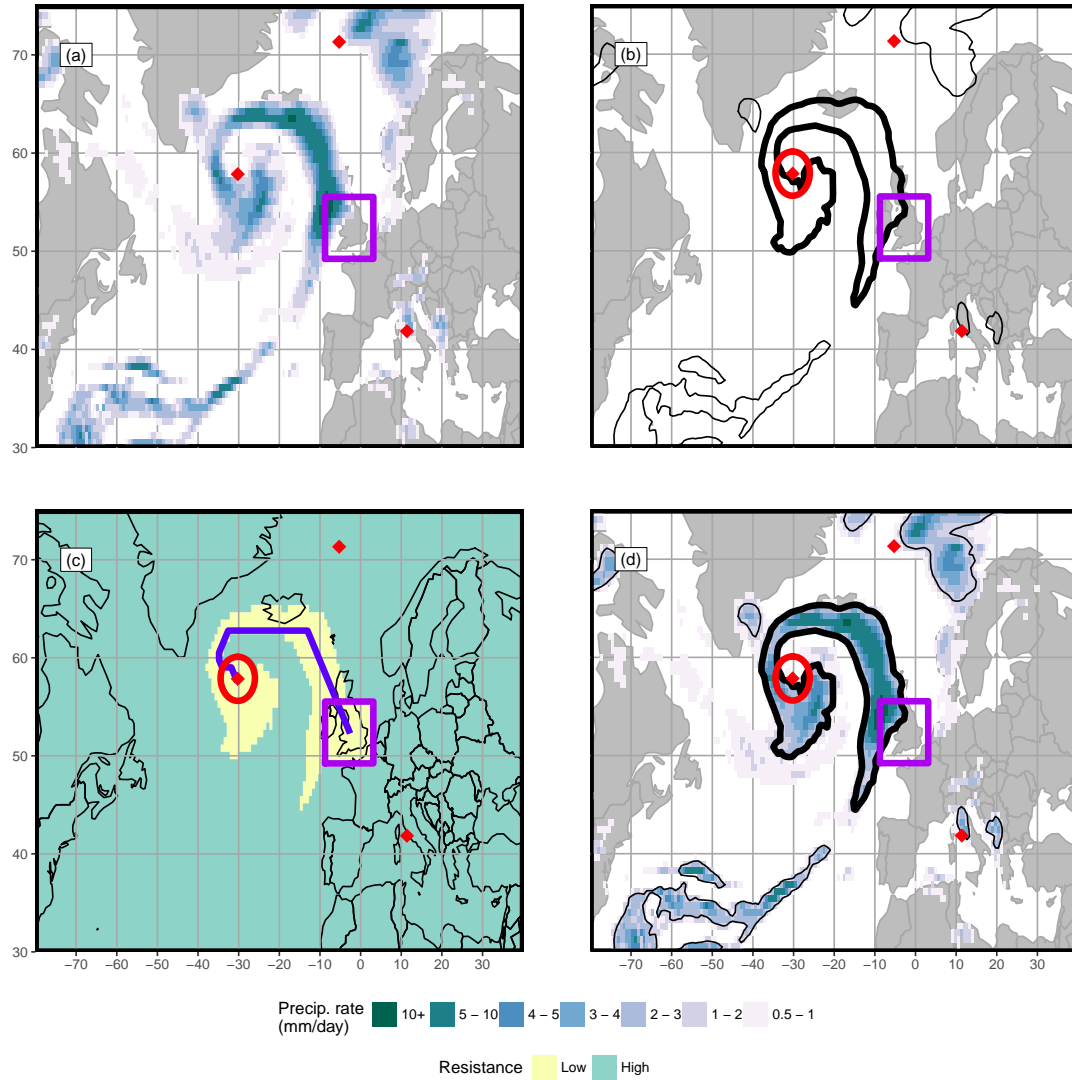


FIGURE 4.3: Demonstration of elements of CPA process for a single event (1800 UTC 16 October 2000). Red points: cyclone centres (Hodges (1994, 1995) on ξ_{850}); red circle: 250 km cyclone proximity radius; contours (thin): regions of precipitation with rate $\geq 1.5 \text{ mm d}^{-1}$; contours (bold): precipitation region associated with England and Wales precipitation event; purple rectangle: England and Wales "interest" region; blue line: shortest path from centre of England and Wales region to matched track point (within precipitation region). (a) Data input to function: gridded precipitation (ERA-Interim), cyclone centres (Hodges on ξ_{850}), interest region. (b) Precipitation regions as identified by the CPA algorithm. (c) Shortest path from interest region to cyclone centre, shown overlaying resistance layer corresponding to matched precipitation region (see Section 4.4.1). (d) Data as output from CPA algorithm: precipitation regions, matched precipitation regions, matched cyclone centres.

position relative to the interest region and the precipitation band(s). Any tracks lying within the interest region, or within a pre-set radius of the interest region (here 250 km), will automatically be recorded as directly associated with precipitation over England and Wales. In this case, all storms directly influencing the interest region are recorded and the matching process ends.

If no “local” (within the interest region) storms are found, the algorithm searches for the shortest path to each track point via a path that lies entirely within the precipitation band. This is achieved by the creation of a rasterised resistance layer (Figure 4.3c). In the resistance layer, all grid cells within the precipitation polygon, the interest region, and the cyclone proximity radius around matched cyclone centres, are set to a very low resistance value (1×10^{-1}). All other points are set to a very high resistance value (1×10^5). A least-cost path-finding algorithm (`shortestPath`; van Etten 2015) is used to approximate the shortest path from the centroid of the interest region to the track point, via a path contained entirely within the precipitation area. This approximation is set to operate on limited degrees of freedom, reducing the smoothness of the curve, to prevent excessive allocation of computing resources towards a problem in which strict accuracy is not critical. Having computed shortest paths to all storm centres associated with the precipitation area, the point that lies closest to the centroid of the interest region, via a path lying entirely within the precipitation band, is selected as the most likely to be of influence to precipitation totals in this region.

Figure 4.3d shows the output of the CPA algorithm. Precipitation areas (including matching status) and cyclone centres (including matching status) are output. In this case, the algorithm appropriately identifies the extratropical cyclone that is associated with precipitation over England and Wales, and chooses an appropriate cyclone centre for this timestep.

4.4.2 Language and structure

The CPA algorithm was designed as a function within the R statistical programming language (Ihaka and Gentleman, 1996; R Core Team, 2015). R is a free, open source programming language, focussed on statistical analysis and highly customisable. Numerous packages are freely available for the automation of common tasks, and R is capable of being used as a Geographic Information System (GIS).

To provide the required output, the function was required to accept input of gridded precipitation data, cyclone track coordinates, and a region of interest (for the purposes of this study, the “region of interest” is a box corresponding to the England and Wales region). Given these inputs, the algorithm performs the following operations:

1. Check for any precipitation above a threshold value within the region of interest
2. Find precipitation bands within gridded precipitation data by applying a single-level contour at a pre-defined threshold value
3. Find cyclone centres located within the interest region, or within a pre-defined distance of a precipitation band
4. Determine most appropriate track point(s) by distance from interest region and position relative to precipitation bands
5. Return “matched” cyclone centres and precipitation bands for analysis

The CPA algorithm was designed to use standardised GIS inputs and outputs, enabling its use with data from a variety of sources. The “SP” package (Pebesma and Bivand, 2005; Bivand et al., 2013) was used to standardise track data inputs and spatial processing. CPA is designed to process data by individual time-step, and can be included in a loop structure for processing large numbers of time-steps. It is also possible to use the CPA function in conjunction with R’s parallel processing capability, which considerably increases its efficiency when used with appropriate hardware on large datasets.

4.5 Comparison with established methods

To investigate the performance of the CPA method in comparison to the “linear”, “circle” and “radial cap” methods proposed by Mailier et al. (2006), Pinto et al. (2013) and Hawcroft et al. (2012) respectively, the association rates for 1-day accumulation precipitation events were considered for all seasons for dry ($p \leq 2$) and extreme wet ($p \geq 98$) events. “Association rate” is defined as the percentage of events during which at least one cyclone has been detected within the radius or across the gate of the respective event, with respect to all events in the set. An ideal method would be expected to approach 0% association rate for dry events, and 100% association rate for DJF extreme wet events (with other seasons demonstrating high extreme wet association rates, allowing for the influence of convective systems, which are more prevalent in the summer months).

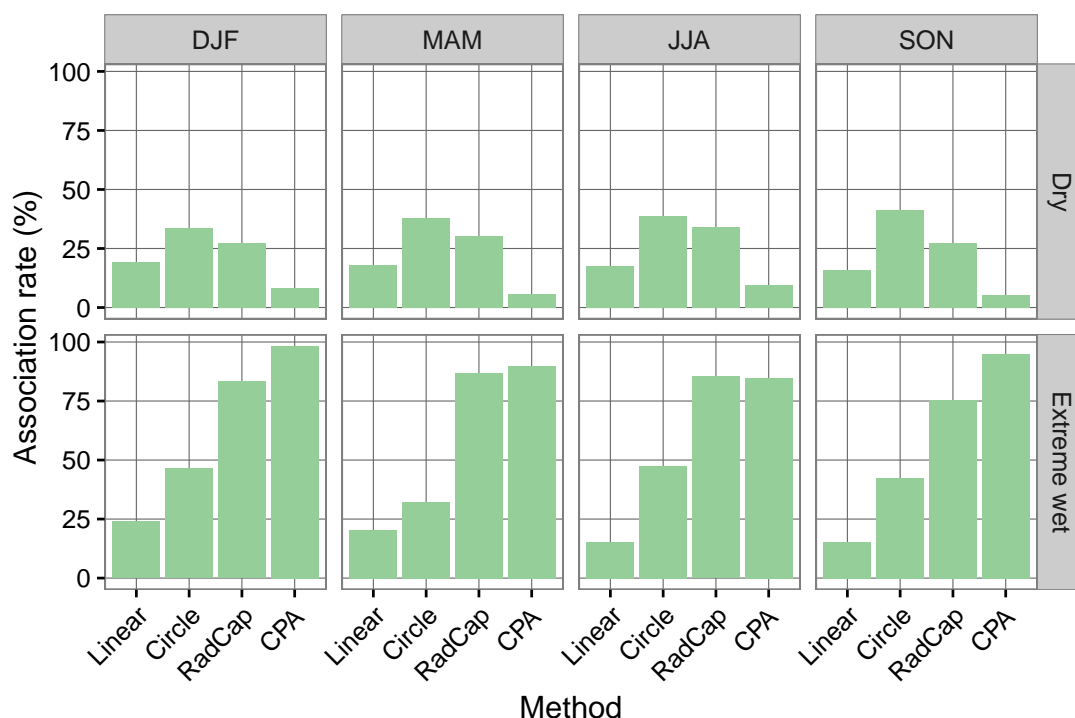


FIGURE 4.4: Association rates for dry and extreme wet events, all seasons. Four storm association methods are demonstrated: “Linear” (meridional linear gate at 0°E , $55 \pm 10^{\circ}\text{N}$); “Circle” (5°W , 55°N , 700km radius); “RadCap” (radial cap, 12° radius centred on cyclone centre); “CPA” (Continuous Precipitation Area method, threshold 1.5 mm d^{-1} , cyclone proximity radius 250km).

Figure 4.4 shows the large variation in association rates found with the different methods. The linear gate method demonstrates very little response to the severity of a precipitation event over England and Wales for any season, indicating that the zonal passage of the centre of an extratropical cyclone is not a reliable indicator for the likelihood of an extreme one-day precipitation event. The circle method with a 700km radius demonstrates an improved response with respect to the linear gate method, for extreme precipitation events in all seasons, but gives a very high (25-50%) association rate for dry events in all seasons. The radial cap method with a cap of 12° performs well for association rate in extreme wet cases, with MAM and JJA association rates comparable with CPA, although lower association rates are found in DJF and SON. However, high (25-30%) association rates are found for dry events in all seasons, indicating that this method may spuriously associate cyclones with regions not experiencing associated precipitation. The CPA method returns considerable improvements in extreme wet association rates for all seasons when compared to both the linear gate and circle methods, and for DJF and SON when compared with the radial cap method. CPA also minimises association rate for dry events in all seasons when compared with all other methods.

Based upon the daily dry and extreme wet event storm association rate, the CPA method was found to be an appropriate method for the analysis of track counts and residence times for extreme precipitation events in ERA-Interim.

4.6 Parameter sensitivity

The CPA method has two pre-defined parameters that may significantly influence its operation. The precipitation threshold value determines how sensitive the algorithm is to low rain rates, and how likely a weakly precipitating system is to be captured as a single precipitation feature. The cyclone proximity radius parameter determines how far outside a precipitation feature a cyclone centre point may lie whilst still being associated correctly with that feature. A large radius may allow spurious association with a distant precipitation feature, whilst too small a radius will prevent the detection of storm centres lying within a dry slot in the structure of the extratropical cyclone.

When testing the sensitivity of the algorithm to its parameters, the ideal setup is considered to be one that consistently associates no cyclone tracks with “dry” ($\leq 2^{nd}$ percentile precipitation) one-day events, and at least one cyclone track with “extreme wet” ($\geq 98^{th}$ percentile precipitation) one-day events. Lower track association rates are expected for extreme wet events in JJA than DJF, owing to the greater prevalence of convective precipitation events during the summer months.

4.6.1 Precipitation threshold evaluation

The CPA algorithm was applied to gridded precipitation in ERA-Interim (1980-2011) with tracking provided by the Hodges (1994; 1995) algorithm applied to maxima of ξ_{850} . Figure 4.5 and Figure 4.6 show the sensitivity of the CPA algorithm to varying precipitation area threshold. As discussed in Section 4.6, the key criteria on test are the absence of associated tracks with “dry” ($\leq p2$ daily precipitation) daily accumulation events, and a near-100% association rate “extreme wet” ($\geq p98$ daily precipitation) daily accumulation events. Furthermore, it is expected that multiple storm passages per day will be a rare event even for $p98$ precipitation events, so the parameters should be set up to prevent regular multiple storm associations. For consistency, a single threshold value was chosen for the analysis of all seasons.

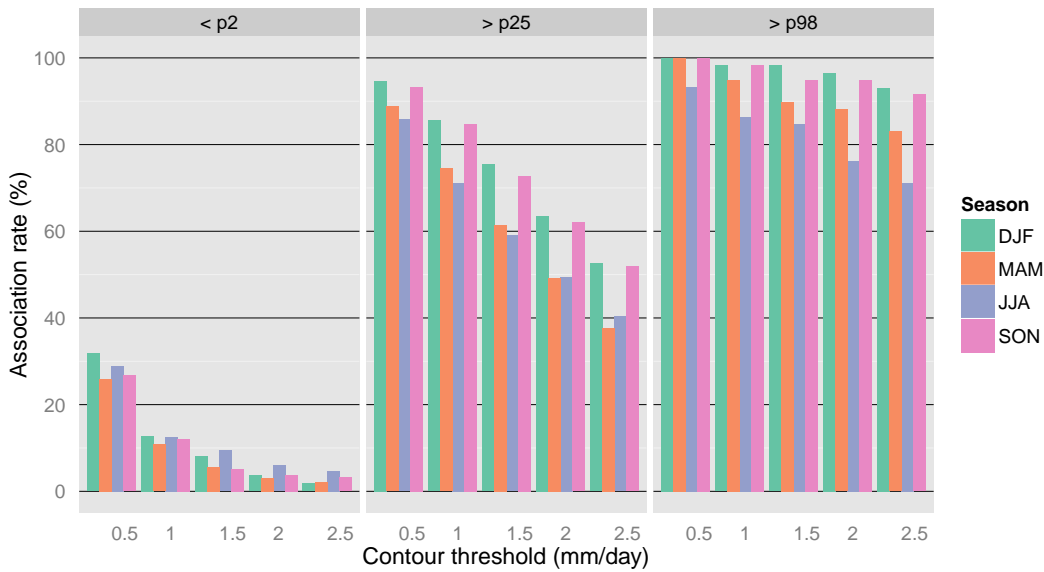


FIGURE 4.5: Association rate by varying precipitation area threshold (threshold value at which precipitation bands are considered to be continuous) for "dry" ($\leq p2$ precipitation), "wet" ($\geq p25$) and "extreme wet" ($\geq p98$ precipitation) one-day accumulation events. Cyclone proximity radius: 250 km.

The sensitivity of association rate to contour threshold is shown for all seasons and event types in Figure 4.5. The association rate is dependant on the contour threshold value for all seasons and all event types, with an increase in association rates particularly evident in dry events going from the 1 mm d⁻¹ to the 0.5 mm d⁻¹ threshold. The dry event association rate decreases to $\leq 10\%$ for all seasons when the threshold increases to 1.5 mm d⁻¹. At this threshold, the extreme wet event DJF association rate is near 100%, although the extreme wet event JJA association rate is less, which may be due to the higher prevalence of convective storms with no associated extratropical cyclone track.

Figure 4.6 shows the sensitivity of the track count per one-day event for different contouring thresholds, for all seasons and all event types. The priority is to minimise over-association with multiple tracks per one-day event in the "wet" and "extreme wet" categories, whilst ensuring that the algorithm does not fail to associate any storms. For instance, the 0.5 mm d⁻¹ threshold causes the majority of DJF extreme precipitation events to be associated with two storms (where different storms are associated with the event for each of the four time-steps in a daily accumulation period), which is a physically undesirable situation. However, by increasing the threshold to 2.5 mm d⁻¹, 20-30% of extreme JJA events have a track count of zero, which is also unlikely. A threshold of

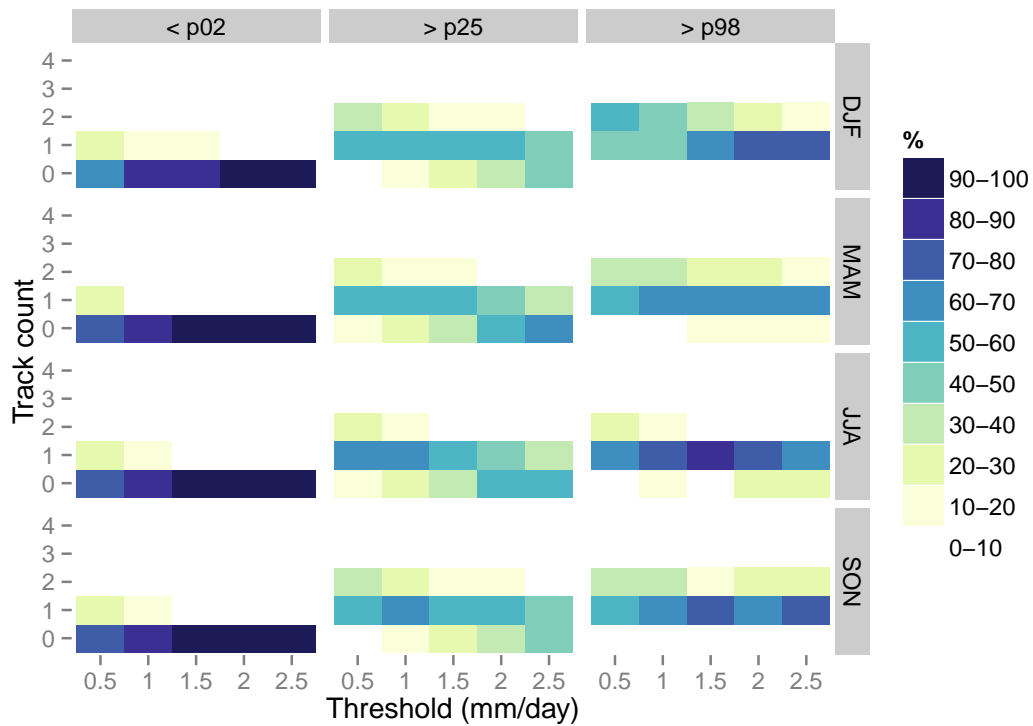


FIGURE 4.6: Percentage frequency of track counts by varying CPA method precipitation area threshold. Cyclone proximity association radius: 250 km. Track counts are shown for “dry”, “wet” and “extreme wet” (≤ 2 , ≥ 25 , ≥ 98 percentile of England and Wales precipitation respectively).

1.5 mm d^{-1} is found to be an appropriate balance between minimising extreme events with no associated storms, maximising single storm count extreme events, and allowing a small number of multiple associations, which is a physically acceptable scenario in a small number of events. Subsequently, based upon Figure 4.5 and Figure 4.6, 1.5 mm d^{-1} was chosen as an appropriate threshold for analysis of precipitation events in England and Wales.

4.6.2 Cyclone proximity radius evaluation

The cyclone proximity radius (r_{cp}) governs how far outside a precipitation region or the interest region a track may be positioned to be considered to be associated with that feature. As with the evaluation of the contouring threshold parameter in Section 4.6.1, the cyclone proximity radius parameter is evaluated to determine an appropriate value which maximises wet and extreme wet event association, minimises dry event association, and minimises multiple track association for one-day events.

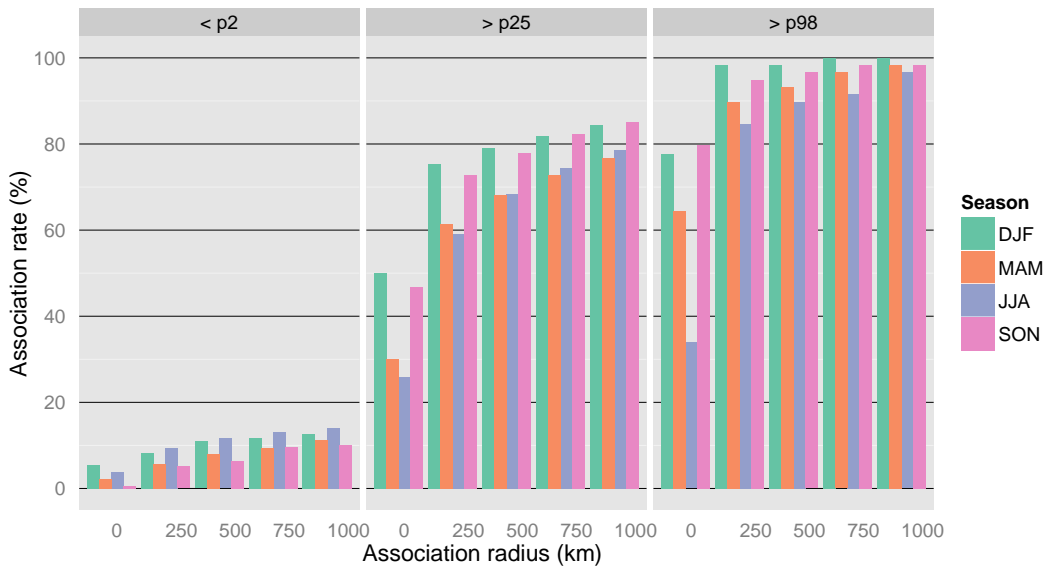


FIGURE 4.7: Association rate by varying cyclone proximity radius (maximum permissible distance between precipitation band and cyclone centre) for “dry” ($\leq p2$ precipitation), “wet” ($\geq p25$) and “extreme wet” ($\geq p98$ precipitation) one-day accumulation events. Precipitation band threshold: 1.5 mm d^{-1} .

Figure 4.7 shows the response of association rate, for all seasons and all event thresholds, to varying cyclone proximity radius (r_{cp}) from 0 to 1,000km. The dry event association rate increases steadily for all seasons with increasing association radius. Wet and extreme wet event association rates increase where $r_{cp} > 0$, with DJF association rates stabilising near 100% for $r_{cp} > 250$ km. JJA association rates remain lower than in other seasons for wet and extreme wet events until a very high radius is used, at which point problems with spurious association with distant features may become prevalent. This may be due to the prevalence of convective precipitation in the summer months, which generates smaller precipitation features which are not physically associated with any cyclone centre.

The influence of the cyclone proximity radius parameter on track counts is demonstrated in Figure 4.8, for all seasons and event thresholds, and with the contour threshold set to 1.5 mm d^{-1} . Altering the cyclone proximity radius appears to have a small effect on the dry events. However, wet and extreme wet events are very sensitive to increasing the radius. A maximum in the count of events associated with a single track is evident at with radius of 250 km for all seasons in the extreme wet category. The likelihood of associating two or more tracks to a single event increases considerably as the r_{cp} is

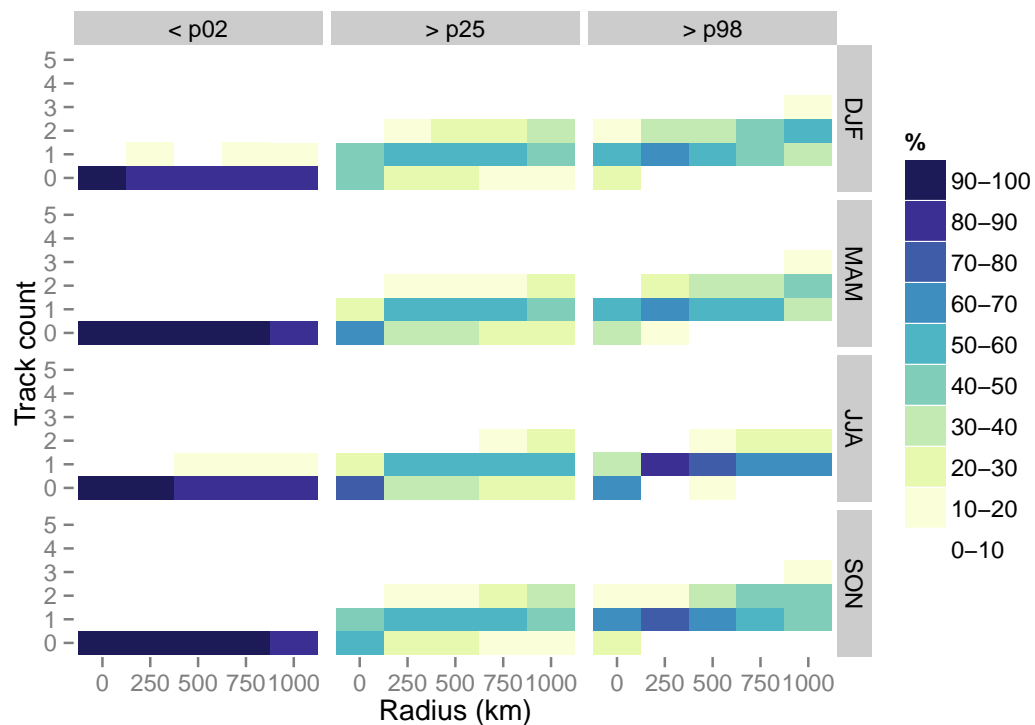


FIGURE 4.8: Percentage frequency of track counts by varying CPA method cyclone proximity radius (maximum permissible distance between precipitation band and cyclone centre). Precipitation band threshold: 1.5 mm d^{-1} . Track counts are shown for “dry”, “wet” and “extreme wet” (≤ 2 , ≥ 25 , ≥ 98 percentile of England and Wales precipitation respectively).

increased above 250 km. A cyclone proximity radius of 250 km was chosen as an appropriate parameter due to its low dry event association rate, high extreme wet event association rate, and minimised one-day event multiple track count rate.

4.7 Summary: CPA algorithm development and evaluation

In this chapter, existing methods for associating precipitation events with cyclones have been discussed and evaluated. The case for developing a new Continuous Precipitation Area (CPA) method has been made, based on its potential for improvements in storm association rate against linear gate (Mailier et al., 2006) and fixed-radius search area methods (Pinto et al., 2013; Hawcroft et al., 2012), reduced computational cost and increased spatial information against the combined storm and front tracking method

(Catto and Pfahl, 2013). The criteria for this system are as follows:

- Full utilisation of existing spatial precipitation data
- Applicable to any product with gridded precipitation output
- Low computational cost
- High storm association rate for extreme precipitation events in the England and Wales region
- Minimal storm association rate for dry events in the England and Wales region
- Minimal over-association rate (two or more cyclones in a daily accumulation period) for extreme events
- Ability to discern most appropriate cyclone centre in systems with multiple embedded cyclone centres

CPA has been evaluated against the linear gate (Mailier et al., 2006), circle (Pinto et al., 2013), and radial cap methods (Hawcroft et al., 2012). CPA performs well for extreme wet event association rate and dry event association rate against all methods tested. The CPA algorithm is not computationally expensive, and is applicable to any gridded dataset. For the purpose of associating cyclone tracks with extremes of precipitation over the England and Wales region, CPA is found both to be an improvement on existing methods, and to be an appropriate method for further analysis of reanalysis and climate model data. The following chapters concern the application of the CPA method to data from ERA-Interim and HadGEM2-ES, to identify behaviours of extratropical cyclone clustering and stalling events in the historical record; to test the ability of a climate model to represent observed clustering and stalling patterns in association with England and Wales precipitation events; and to analyse clustering stalling and England and Wales precipitation events in the RCP8.5 climate scenario in HadGEM2-ES.

Chapter 5

Clustering, stalling, and England and Wales precipitation events in the recent climate

5.1 Introduction

This chapter discusses the analysis of precipitation events in ERA-Interim using the CPA method (Chapter 4). The behaviour of cyclones associated with precipitation events over England and Wales is analysed. Cyclone behaviour is considered in terms of “clustering” and “stalling” episodes, which in turn are represented in terms of cyclone count per event and maximum and/or mean cyclone residence time per event, respectively.

The data and methods used in this chapter are discussed in Section 5.2, including analysis of precipitation events in EWP and the North Atlantic storm track and mean 250-hPa winds in ERA-I. The CPA method is applied to ERA-I with precipitation event timings identified using EWP, and the resulting data are analysed for patterns of clustering and stalling in Section 5.3. A discussion of the results presented in this chapter, and key conclusions, is given in Section 5.4.

5.2 Data

For analysis of precipitation events in England and Wales using the CPA method described in Chapter 4, three inputs are required. A time-series of precipitation data for

England and Wales is used to identify the timing of precipitation events over England and Wales; spatial precipitation data are used to identify rain bands; and cyclone track data are used to identify characteristics of the extra-tropical cyclones associated with England and Wales precipitation event. For further analysis, 250-hPa vector winds from ERA-I are used for analysis of large-scale conditions, including mean jet stream location. Section 5.2.1 discusses the identification of precipitation events in the EWP time-series; Section 5.2.2 discusses the key features of the North Atlantic storm track as represented by the Hodges (1994, 1995) method on maxima of ξ_{850} in ERA-I; and 250-hPa wind vectors are discussed in Section 5.2.3 for seasonal mean and extreme England and Wales precipitation events.

5.2.1 England and Wales precipitation

The ECMWF ERA-Interim reanalysis product was used for all spatial analysis in this chapter. Daily precipitation data from the HadUKP England and Wales Precipitation (EWP) dataset for the period 1 March 1980 to 30 November 2011 were processed according to the time-series analysis method presented in Section 2.5. This categorises precipitation events as “Extreme dry”, “Wet”, and “Extreme wet” through an iterative highest-peaks method (Section 2.5).

For analysis using the CPA method, precipitation events are identified in the EWP time-series (gauge-based observations of precipitation in England and Wales). EWP data are provided on a daily period spanning 0900-0859. Precipitation and cyclone track data are obtained from ERA-I, which provides 6-hourly output at 0000, 0600, 1200, and 1800 UTC. Therefore, to most closely align with the 0900-0859 UTC EWP daily period, data are taken from ERA-I for daily period d from 0600, 1200 and 1800 UTC on day d , and 0000 on day $d + 1$.

The mean event count per year for each event type is shown in Figure 5.1, as determined by season and accumulation period. For short time-scale events, wet event frequency greatly exceeds extreme wet event frequency. However, wet event frequency decreases as event time-scale increases, due to fewer data points being available as the record is divided into longer sections. Extreme dry event count may exceed extreme wet event count in instances where a large number of time periods with zero precipitation are found in the record. An average of 2.8 events extreme wet per year are identified for each season on a one day accumulation time-scale (approximately p98), and an average of

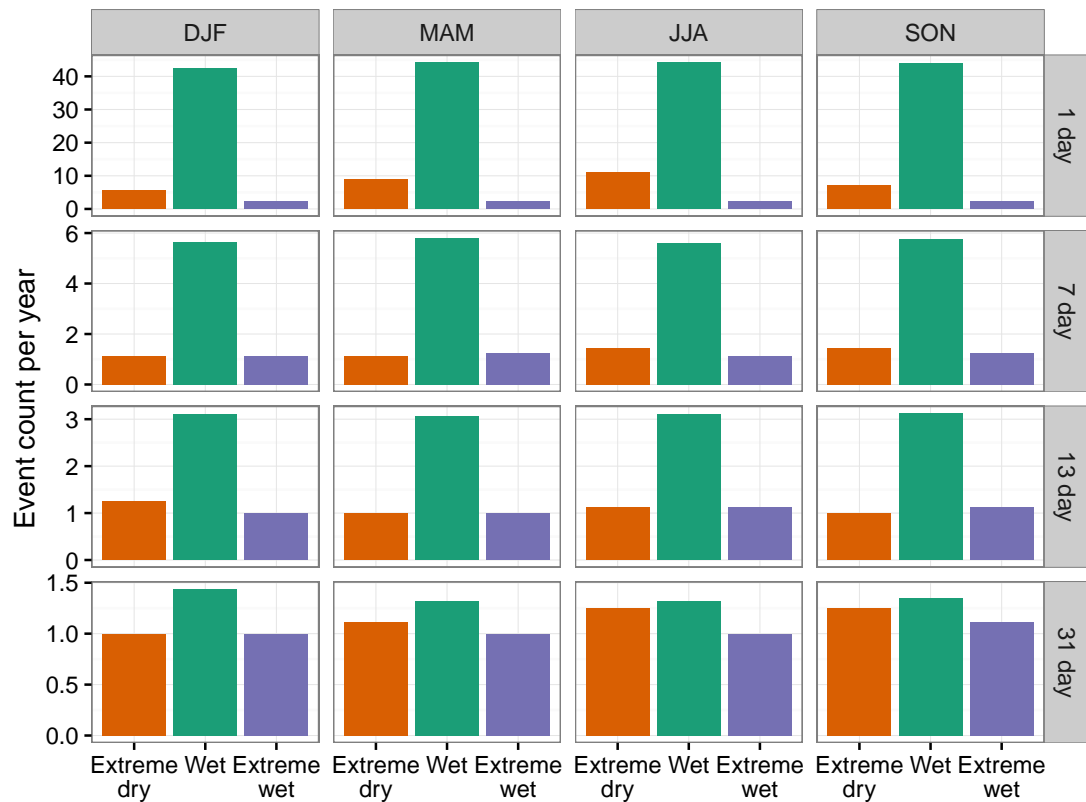


FIGURE 5.1: Mean event count per year for extreme dry, wet, and extreme wet event categories. Y axis varies by row.

1 extreme event per year is identified for each season on 7-, 13- and 31-day accumulation time-scales.

5.2.2 The North Atlantic storm track in ERA-I

Storm tracks were generated using the Hodges (1994, 1995) method on ξ_{850} , with the minimum movement criterion removed to allow the detection of slow moving features (Section 2.4). Storm track densities in ERA-I are displayed by season in Figure 5.2. These density maps highlight the key features of the North Atlantic storm track, with the track densities at a maximum near the east coast of North America, where cyclones are generated primarily through baroclinic processes, and in the lee of Greenland, where cyclones are primarily generated by high orography. The storm track is tilted from south west to north east, and a seasonal cycle is evident with peak track density in winter.

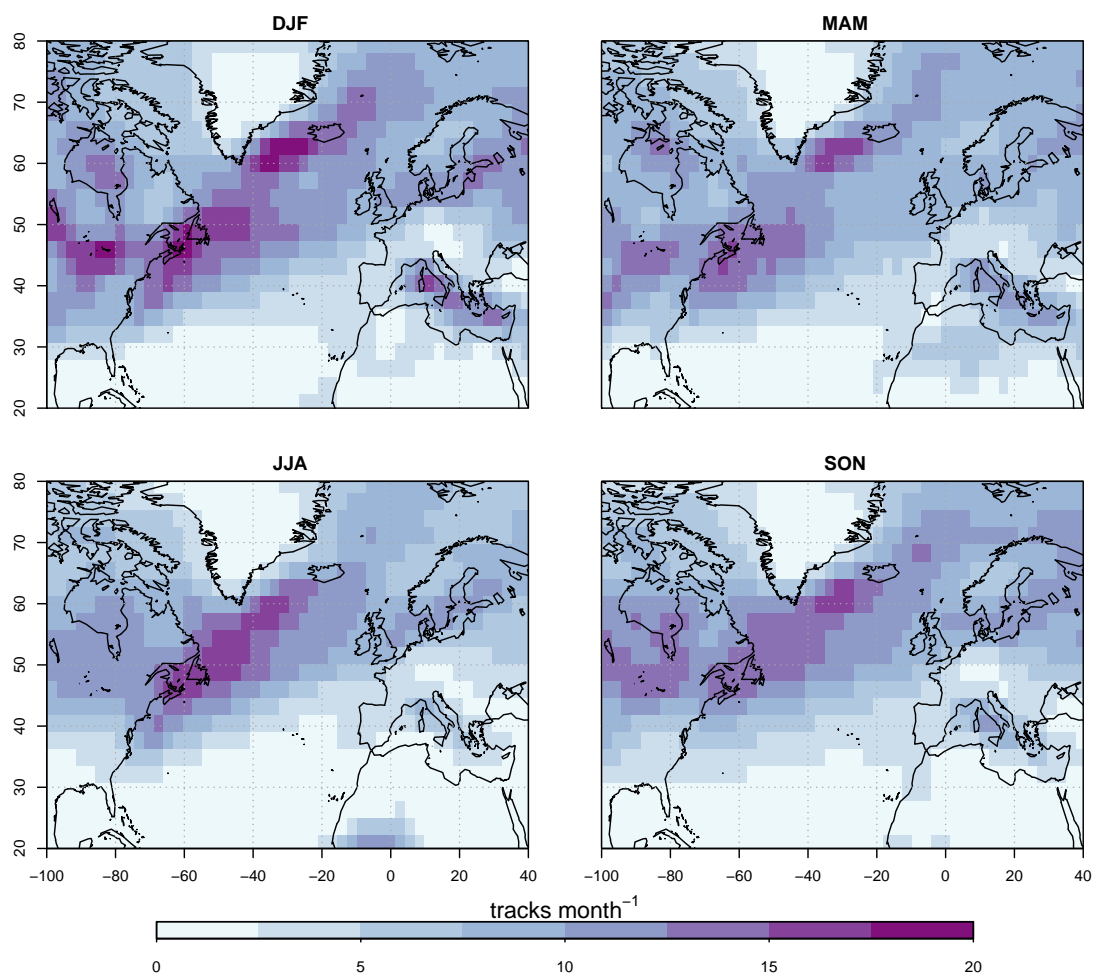


FIGURE 5.2: Seasonal North Atlantic cyclone track density for ERA-I, 1980-2011. Densities are calculated using spherical kernel estimators on a 5° spherical cap using the Hodges (1996) method. Data are then interpolated to a 2° latitude/longitude grid.

5.2.3 250-hPa vector winds

Figure 5.3 shows the mean state of the wind vectors seasonally at 250 hPa, indicating the position of the North Atlantic jet stream. All panels show the mean state being a westerly to south-westerly wind, with an intensity maximum in the western North Atlantic. The meridional tilt of the jet stream is shown to be greatest in DJF, with a more zonal flow prevalent in JJA.

Mean wind vectors for dates associated with one-day extreme wet events over England and Wales are shown in Figure 5.4(a-d), with anomalies against the seasonal mean given in panels (e-h). In DJF, an extension and intensification of the one-day mean 250 hPa jet stream is found (panel a), with a jet exit region over the British Isles and north-western Europe. This synoptic situation is consistent with high rates of cyclogenesis, cyclone

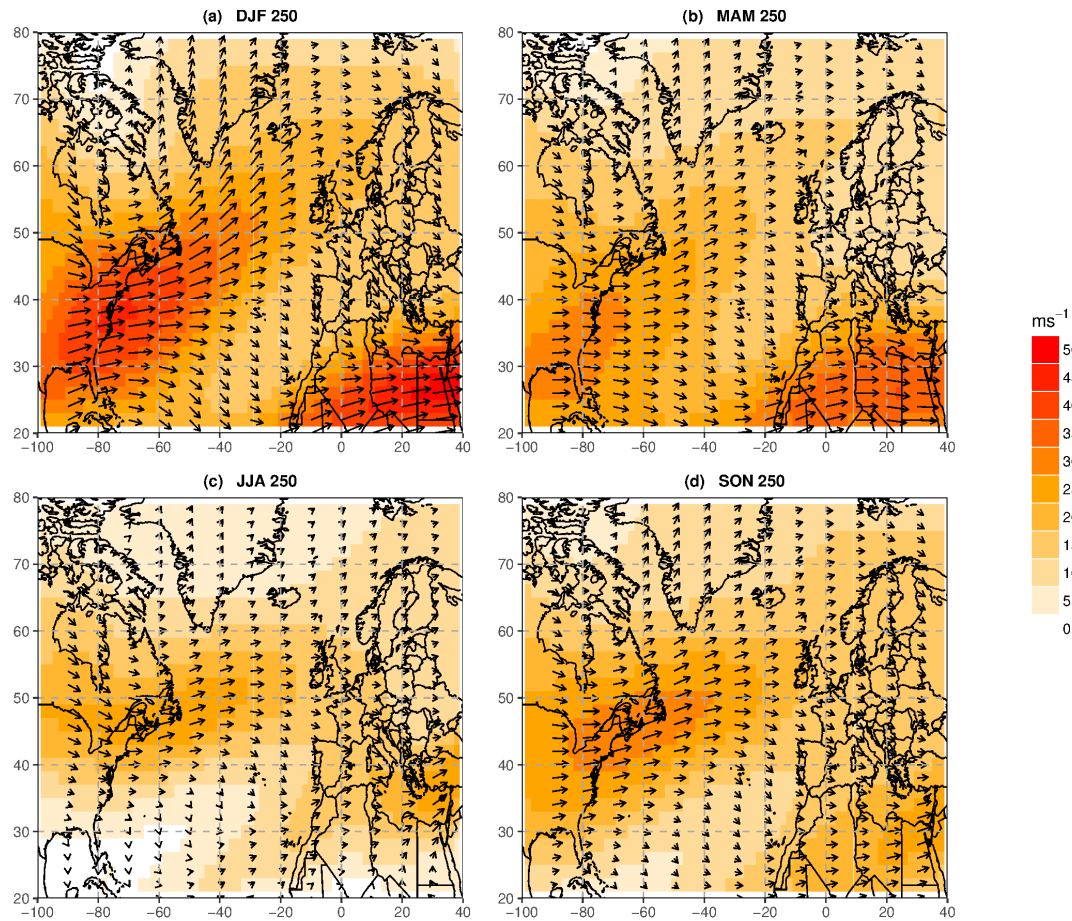


FIGURE 5.3: Seasonal mean vector winds from ERA-I, 1980-2011, 250-hPa. Data are interpolated to a 2° grid.

intensification in the eastern North Atlantic, and a steering flow that acts to direct features toward the England and Wales region. For MAM, JJA and SON, Figure 5.4 shows a similar pattern of vector winds for one-day extreme wet events. Relative to the seasonal mean, these seasons show an extended jet with a prominent wave pattern, approximately equal to a planetary wave of wave-number $n = 6$. This is reminiscent of the quasi-stationary wave pattern observed by Blackburn et al. (2008), which found that a quasi-stationary wave pattern of wave-number $n = 6$ lead to periods of low cyclone mobility over the UK, creating conditions for slow moving, intensely precipitating cyclones to generate flooding over northern and western regions of England and Wales. Stadherr et al. (2016) and Petoukhov et al. (2016) also found similar quasi-stationary wave patterns associated with extreme events in Europe. The 250 hPa MAM vector wind (Figure 5.4[b]) also shows a split jet stream, consistent with blocking over the Azores. The wave pattern found in MAM–SON in the seasonal means is also consistent with a cyclonic flow anomaly relative to the seasonal mean, which is strongest in SON (Figure 5.4h).

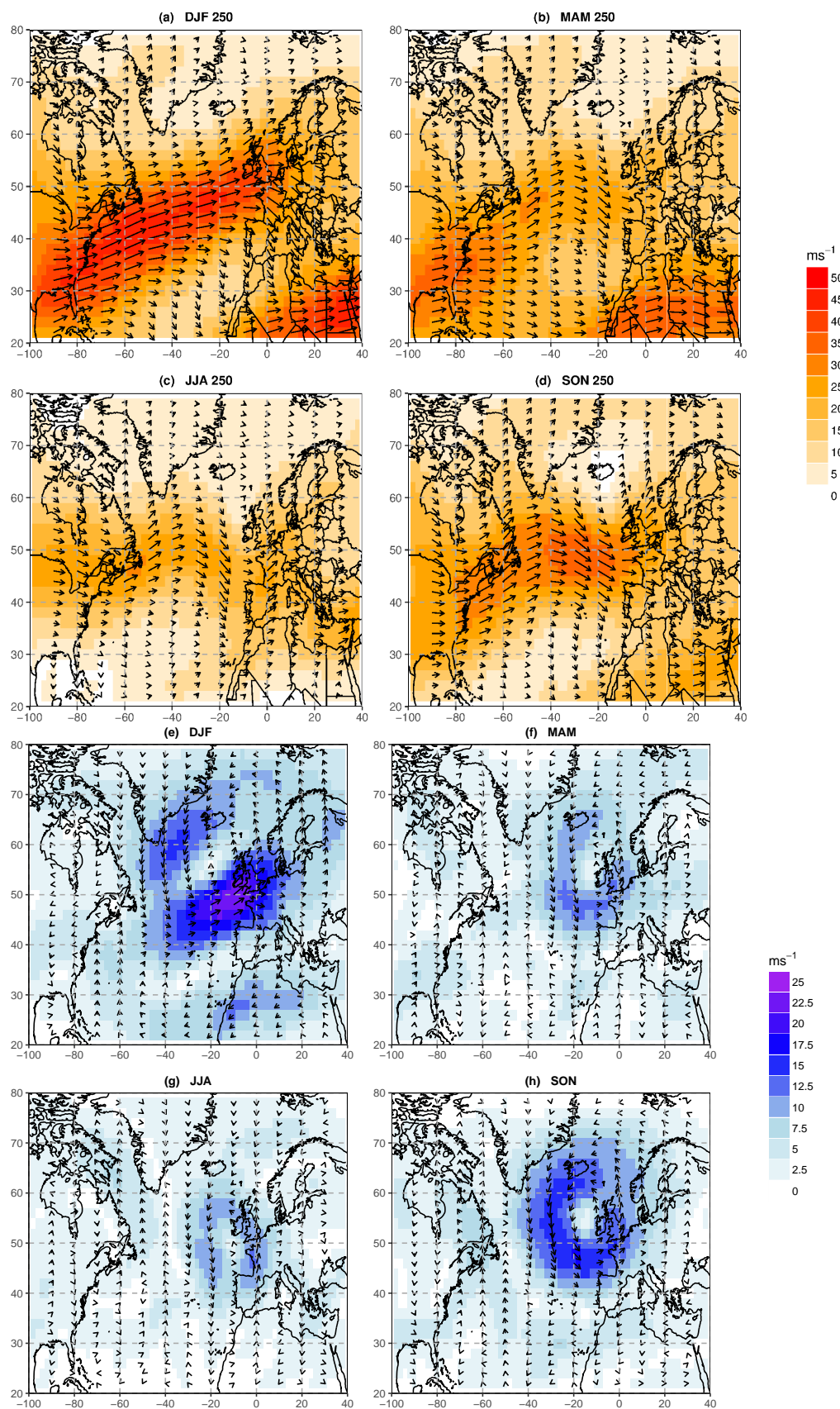


FIGURE 5.4: (a-d): Mean vector winds at 250 hPa from ERA-I, 1980-2011, for one-day extreme wet events. (e-h) Wind vector anomalies against seasonal mean, 1980-2011. Data are interpolated to a 2° grid.

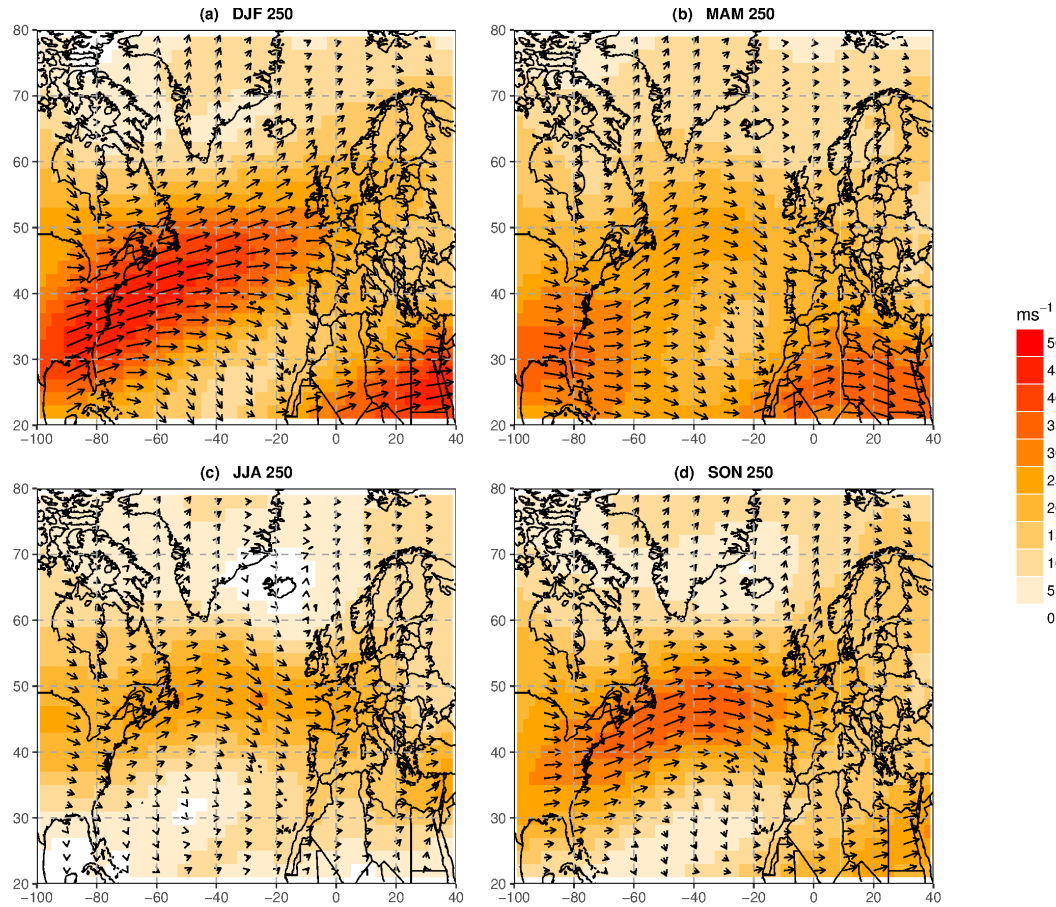


FIGURE 5.5: Mean vector winds at 250 hPa from ERA-I, 1980-2011, for 31-day extreme wet events. Data are interpolated to a 2° grid.

Mean wind vectors for 31-day extreme wet events are shown in Figure 5.5. Some features in the 250-hPa winds are similar to the one-day extreme wet events (Figure 5.4). For DJF, an extension and intensification of the North Atlantic jet at 250 hPa is evident relative to the seasonal mean, with evidence of a direct flow aligned with the England and Wales region. This situation is highly favourable to mobile cyclones, supporting the hypothesis that cyclone clustering is related to extreme rainfall events in DJF at a 31-day time-scale. This is in agreement with Table 5.1, which indicates that DJF 31-day extreme wet events have on average a 40% greater cyclone count than wet events for the same period.

JJA, MAM and SON show a less direct 250-hPa wind flow than DJF. This less direct flow is similar to the wave-like pattern observed in the one-day event mean wind plots, suggesting that this wavenumber $n = 6$ pattern is persistent for long periods of time,

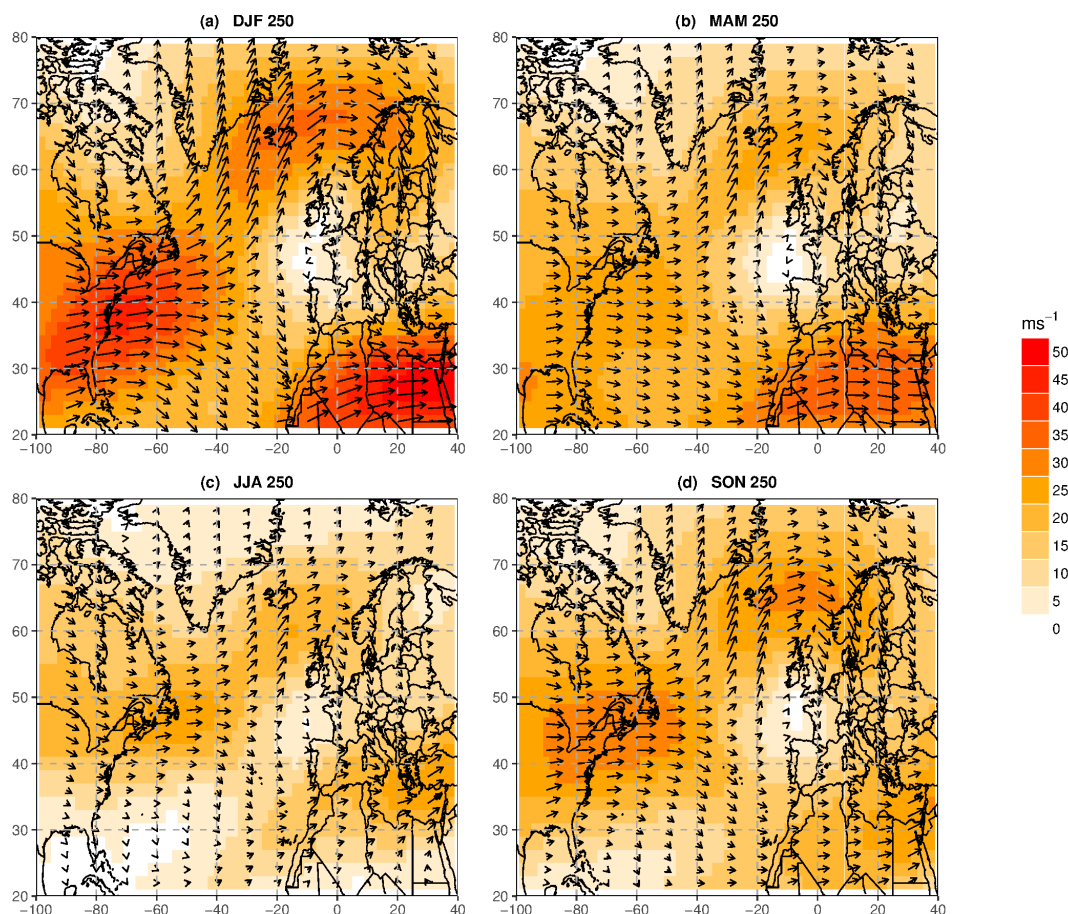


FIGURE 5.6: Mean vector winds at 250 hPa from ERA-I, 1980-2011, for one-day extreme dry events. Data are interpolated to a 2° grid.

and is related to extreme wet events in England and Wales on time-scales of 1–31 days. Extreme wet events at the 31-day time-scale are found to be associated with faster wind speeds across the North Atlantic than the seasonal mean. An intense jet extends in a predominantly zonal direction across the North Atlantic, creating favourable conditions for cyclogenesis and high cyclone mobility.

Extreme dry events in England and Wales, as shown in Figure 5.6, are characterised in all seasons by a split 250 hPa wind flow, with a wind speed maximum to the north of the British Isles. This pattern is consistent with the presence of a blocking high over western Europe. A highly similar pattern is found at 31-day time-scales (not shown), indicating that such situations are persistent on time-scales of 1–31 days.

5.3 Clustering, stalling, and extreme precipitation events in ERA-Interim

The CPA method has been applied to observed and re-analysed data in the recent climate (1979–2005). The timing of precipitation events in England and Wales is determined by analysis of the EWP time-series. In the following analysis, cyclone count per event is used to describe the amount of clustering associated with precipitation events in the EWP time-series. Stalling is defined by the residence times of extratropical cyclones associated with England and Wales precipitation events. The statistical frequency of extratropical cyclone clustering and stalling in conjunction with precipitation events of different intensities are analysed in this section, along with an evaluation of the large-scale conditions at the time of the precipitation events.

5.3.1 Relationship of cyclone clustering to extreme events

For the evaluation of the extent of extratropical cyclone clustering, precipitation accumulation time-scales of 1, 7, 13, and 31 days are considered. Clustering is therefore considered to be a function of event time-scale, as opposed to other clustering metrics (e.g. Mailier et al. 2006) which represent cyclone clustering as over- or under-dispersed events relative to a Poisson distribution with fixed rate. The distribution of cyclone counts per event for wet events is shown in Figure 5.7.

The cyclone count distributions shown in Figure 5.7 indicate that one-day precipitation events are most frequently associated with a single cyclone. The CPA method allows for a maximum of one track to be associated per time-step, leading to a maximum of four unique tracks per day for data with a 6-hour temporal resolution. Instances of more than two tracks being associated with a single one-day precipitation event are shown to be extremely rare.

For accumulation time-scales of 7 and 13 days, the distribution of cyclone count per event approximates a normal distribution around the mean. The distribution pattern is more irregular for 31-day events. This is likely to be due to the small sample size (36-40 events).

The mean cyclone count per event is displayed in Figure 5.8, as a metric of the importance of cyclone clustering for precipitation event intensity on 1-, 7-, 13-, and 31-day

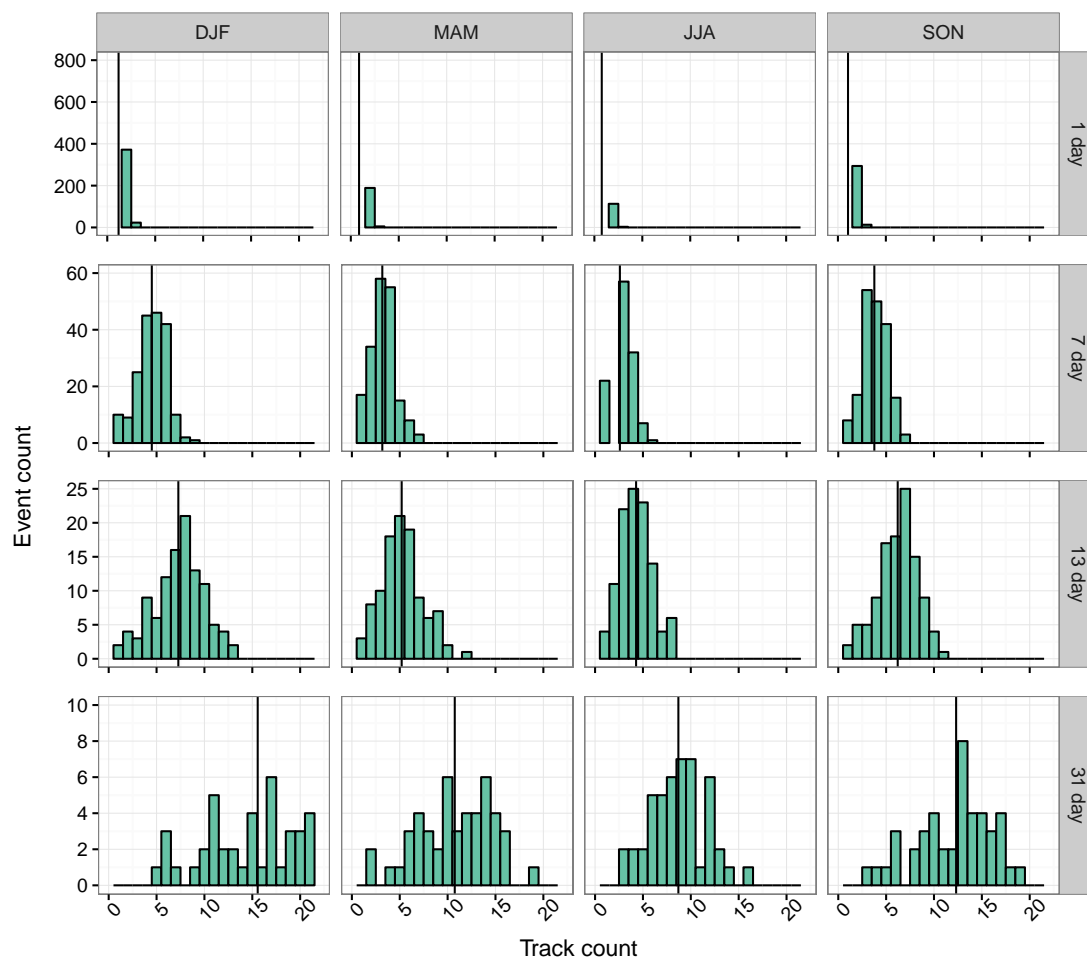


FIGURE 5.7: Histograms of cyclone count for both “Wet” and “Extreme wet” events (combined) for 1-, 7-, 13- and 31-day accumulation periods. Vertical line indicates mean. Bin width: 1 track. Events not associated with any cyclone track are not shown.

time-scales. Error bars display the Standard Error ($SE = \frac{SD}{\sqrt{n}}$, where SD is the sample standard deviation and n is the sample size). This provides a metric of uncertainty which accounts for the variance in sample size between event classifications.

Accumulation period	DJF	MAM	JJA	SON
1 day	19.60	44.20	15.30	16.20
7 day	4.60	34.50	8.50	6.50
13 day	15.70	12.90	-9.80	17.80
31 day	21.80	35.00	26.20	26.40

TABLE 5.1: Percentage difference in mean cyclone count between wet and extreme wet events. Positive value indicates higher mean cyclone count for extreme events. Shading indicates that differences fall within the margin of standard error on the mean. Bold type indicates significant differences by Kolmogorov-Smirnov test between wet and extreme wet samples ($p < 0.05$)

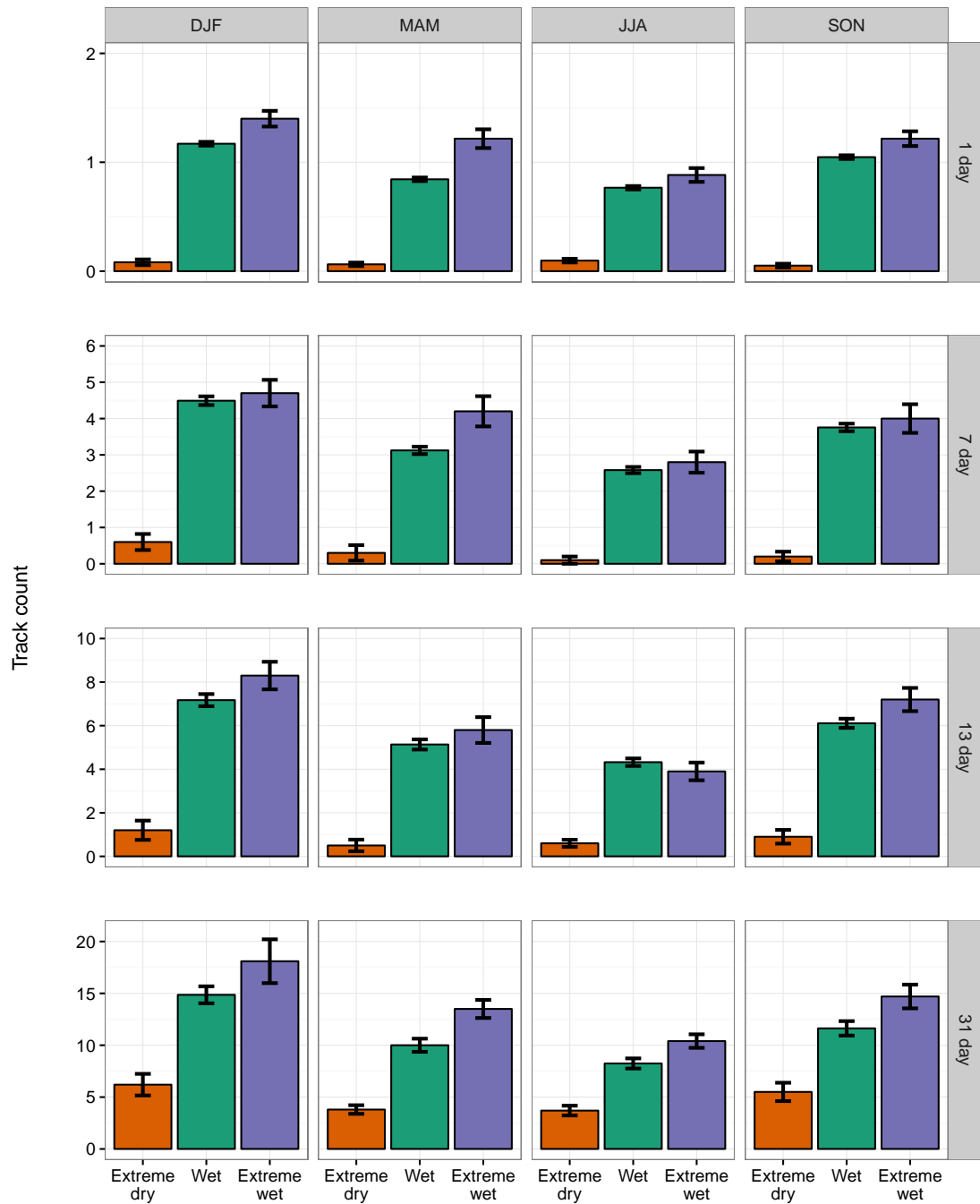


FIGURE 5.8: Bar plot of mean cyclone count per event. Data are plotted by season and accumulation period for 1-, 7-, 13- and 31- day events. All events in the “Extreme dry”, “Wet” and “Extreme wet” categories are shown. Error bars are standard error on the mean. Y-axis differs between rows.

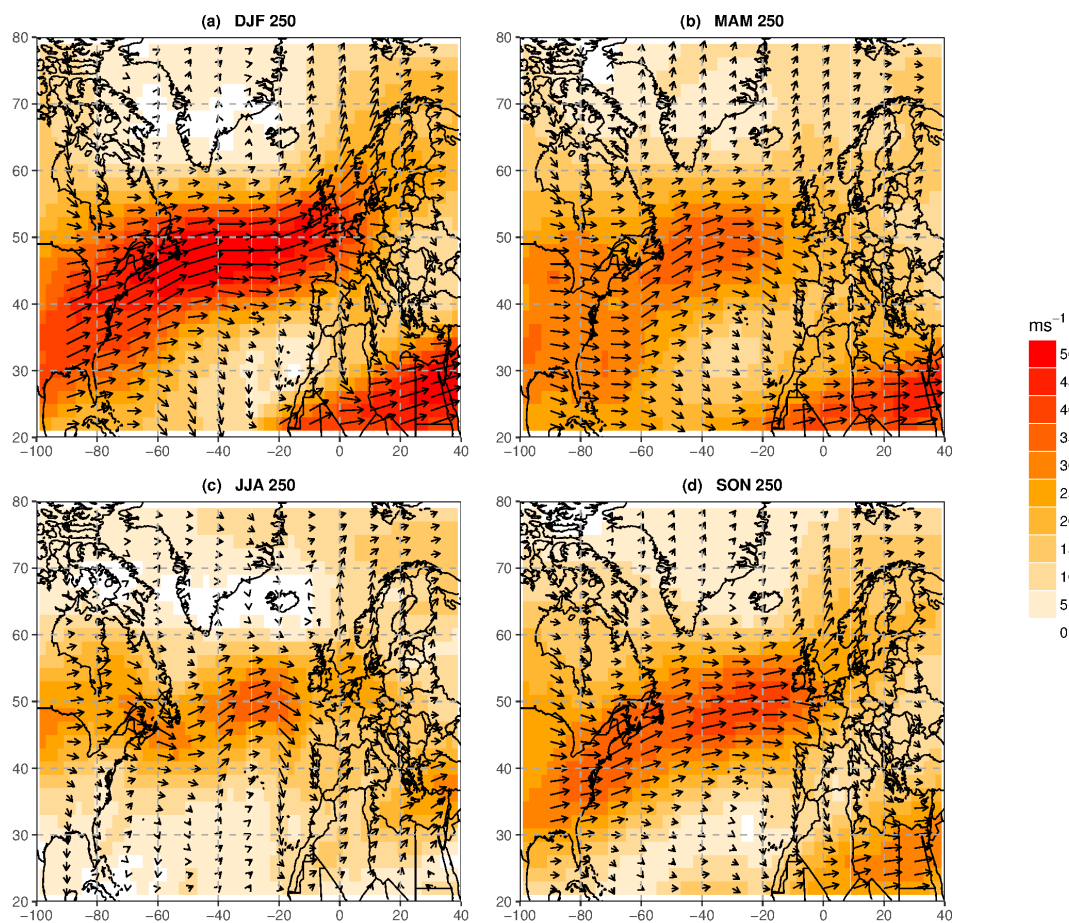


FIGURE 5.9: Mean vector winds from ERA-I, 1980-2011, for 7-day wet/extreme wet events associated with a high cyclone count ($\geq 75^{\text{th}}$ percentile). Data are interpolated to a 2° grid.

For all seasons, mean cyclone count is higher for extreme wet events than for wet events by at least the margin of standard error on the one-day and 31-day time-scales. For MAM, a large (35%) increase in clustering is found at the 7-day time-scale. Cyclone count is found to be associated most strongly with extreme events for all seasons at 31-day time-scales, with the lowest association with cyclone counts found in JJA at 7- and 13-day time-scales. These statistics show that clustering is most relevant for long accumulation period extreme events, whilst little increase in cyclone count is identified in most seasons during the 1–13 day accumulation periods.

To analyse the synoptic-scale conditions associated with cyclone clusters and precipitation events, all wet and extreme wet events have been analysed for cyclone count, with events above the top 25th percentile of cyclone count being considered to be “clustered”. This method returns 7 events for each season at the 31 day time-scale. 7-day time-scale

events are analysed here, to give information about clustering on weekly time-scales.

Wind vectors for clustered 7-day events are shown in Figure 5.9. Features broadly consistent with those found for extreme daily and 31-day events, discussed in Section 5.2.3, are evident, with high 250-hPa wind speeds found across the North Atlantic. A particularly intense jet is found in DJF. The strong jet stream creates favourable conditions for cyclogenesis, intensification and advection of cyclones toward the England and Wales region. In JJA, the wind speeds are higher and the direction more zonal than in the “extreme wet” case (Figure 5.4). This indicates that fast moving cyclones may not be the primary influence on extreme wet precipitation events during JJA.

5.3.2 Relationship of cyclone stalling to extreme events

The frequency distribution of cyclone residence times for both wet and extreme wet events is displayed in Figure 5.10. The longest mean residence times are found in JJA and SON. Mean residence time is approximately one day for all seasons and accumulation periods.

Figure 5.11 shows mean residence time statistics for the three precipitation event categories. The black outlined bars display the mean residence time of all cyclones associated with precipitation events of each category, giving information on the degree of stalling of all cyclones associated with the England and Wales region during each event. This analysis is used to evaluate the influence of conditions which lead to slow moving and/or long lasting cyclones during the full time period of an event. This type of event is shown to be associated with extreme wet conditions on short time-scales, with mean residence time found to be higher in extreme wet events than wet events for all seasons at the one- and seven-day time-scales (see Table 5.2 for percentage differences). Significant increases in mean residence time in extreme wet events are found for all seasons at daily time-scales, whilst the greatest increases in mean residence time are found in JJA, where significance is found at 1–13 day time-scales. The largest increases in mean residence times are found at shorter time-scales and in the summer months, indicating that extreme wet England and Wales events at 1–13 day time-scales during JJA are likely to be associated with long-lived or stalling cyclones.

The solid coloured bars of Figure 5.11 display the mean (over all events) residence time of the longest-lived cyclone associated with each event, giving information of the degree

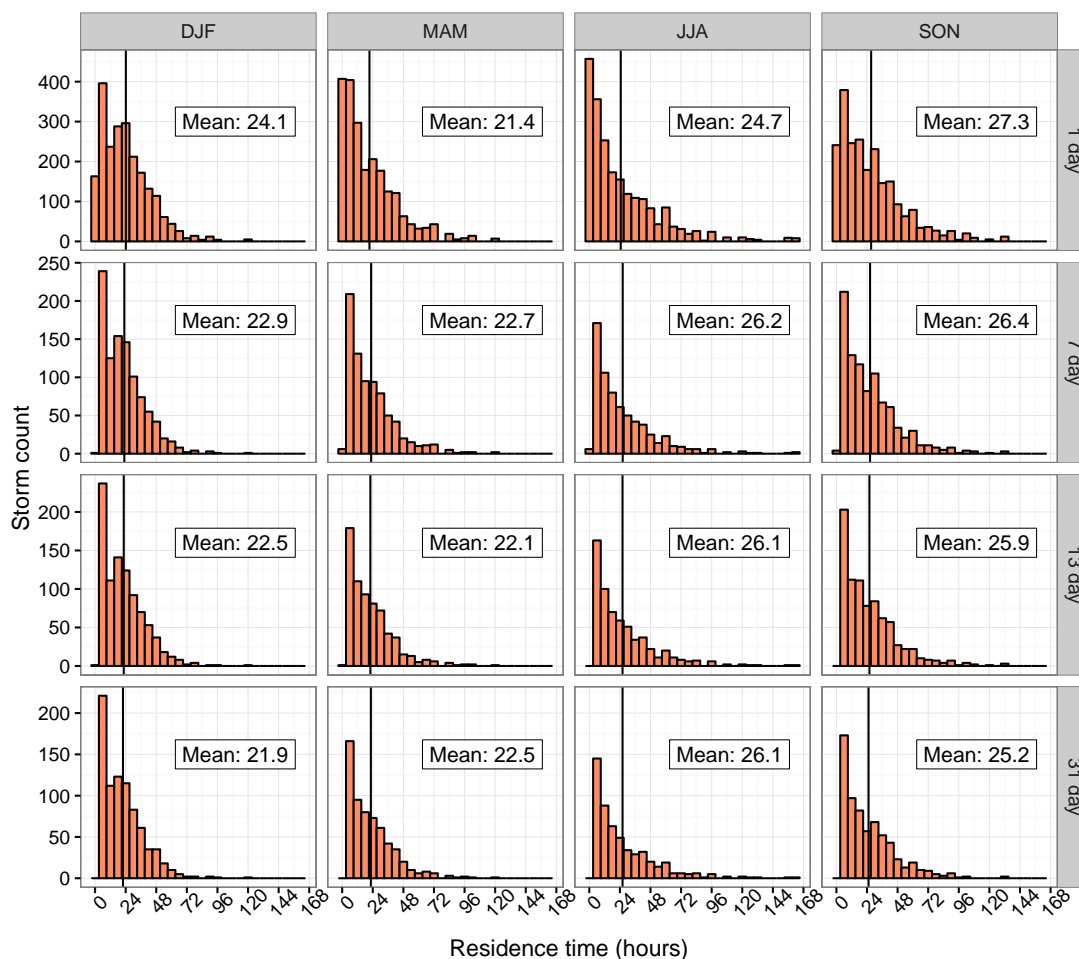


FIGURE 5.10: Histograms of residence times for “Wet” and “Extreme wet” events (combined) for 1-, 7-, 13- and 31-day accumulation periods. Only events which were associated with at least one track are shown. Vertical line indicates mean. Bin width: 6 hours.

Accumulation period	DJF	MAM	JJA	SON
1 day	6.4	12.2	12.2	7.3
7 day	7.0	4.2	16.5	10.9
13 day	2.6	6.4	14.7	5.9
31 day	-0.7	0.9	3.9	0.8

TABLE 5.2: Difference (in %) in mean residence times between extreme wet and wet events. Positive values indicate longer mean residence times in extreme wet events. Grey cells indicate standard error exceeds difference. Bold type indicates significant differences by Kolmogorov-Smirnov test between wet and extreme wet samples ($p < 0.05$)

of stalling of the most “stalled” cyclone of each event (“peak stalling”). This analysis is used to evaluate the influence of a single stalled cyclone during the full time period of an event, which may be embedded within a cluster of faster-moving cyclones. This type of event may have large implications for flood risk, as a single exceptional cyclone within

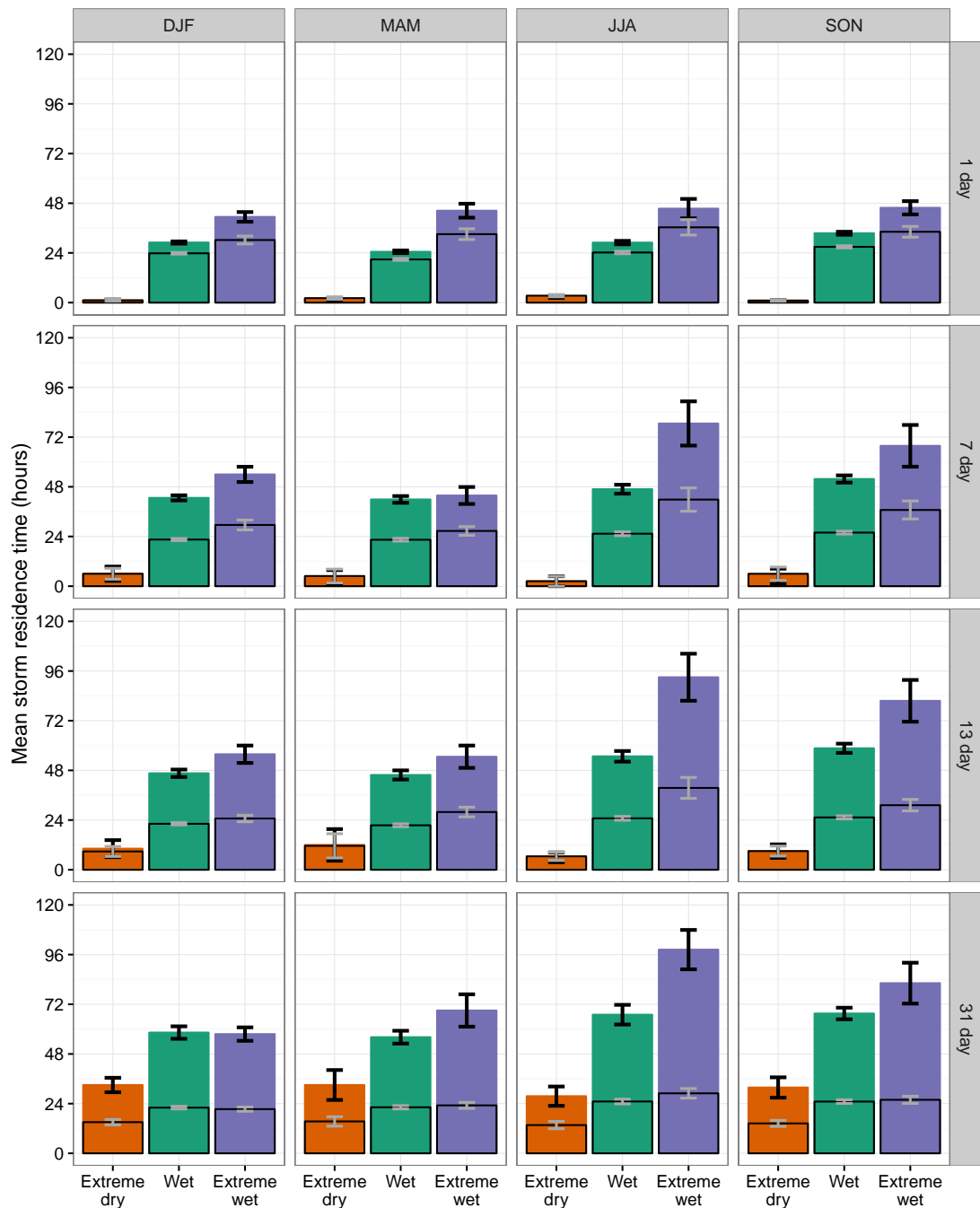


FIGURE 5.11: Overlaid bar plots indicating (1) mean residence time of all cyclones in all events and (2) mean (over all events) of maximum residence time of cyclones in each event. Data set (1) displayed as black outline bars, grey error bars; data set (2) displayed as solid colour bars, black error bars. Data are plotted by season and accumulation period for 1-, 7-, 13- and 31- day events. All events in the “Extreme dry”, “Wet” and “Extreme wet” categories are shown. Error bars are standard error on the mean.

a generally wet period may cause flooding of saturated ground. This type of event was observed during the UK floods of summer 2007 (Blackburn et al., 2008).

Accumulation period	DJF	MAM	JJA	SON
1 day	12.4	19.9	16.4	12.3
7 day	11.3	1.9	31.7	16.0
13 day	9.2	8.8	38.2	22.9
31 day	-0.7	12.9	31.4	14.7

TABLE 5.3: Difference (in %) in mean (over all events) maximum residence time of cyclones in each event (“peak stalling”) between extreme wet and wet events. Positive values indicate higher mean residence times in extreme wet events. Grey cells indicate standard error exceeds difference. Bold type indicates significant differences by Kolmogorov-Smirnov test between wet and extreme wet samples ($p < 0.05$)

Peak stalling is found to be greater for extreme wet events than wet events on one-day time-scales in all seasons (see Table 5.3), supporting the evidence from the previously discussed mean residence times which indicated that stalling is a factor in extreme wet events on short time-scales. The influence of peak stalling on extreme wet events is greatest in JJA, where large differences are evident between wet event and extreme wet peak stalling at time-scales from 1–31 days. These differences are significant at $p < 0.05$ level when measured using the Kolmogorov-Smirnov test. In DJF the difference between wet event and extreme wet event peak stalling reduces with increasing time-scale, indicating that peak stalling is most influential in DJF at 1- and 7-day time-scales.

To analyse the synoptic-scale conditions associated with stalled cyclones and precipitation events, all wet and extreme wet events have been analysed for mean and maximum residence time, with events over the top 25th percentile of both mean and maximum residence time being considered to include at least one “stalled” cyclone. 1- and 7-day events are analysed here, to give information about stalling on daily to weekly time-scales.

Figure 5.12 shows wind vectors for one-day wet and extreme wet precipitation events associated with a long residence time (“stalled”) cyclone. Several features are notably similar to the extreme wet case shown in Figure 5.4, with all seasons showing an extended jet at 250 hPa. However, whereas for DJF 1-day extreme wet events the jet stream extends linearly across the British Isles at a high intensity, in the high residence time case the trajectory of the jet deviates slightly to the south of the British Isles, where it weakens. This pattern may act to drive the cyclone towards the British Isles before slowing down, thus generating an active yet slow-moving cyclone. For MAM, JJA and SON, a trough is evident over the British Isles, which may cause cyclones to

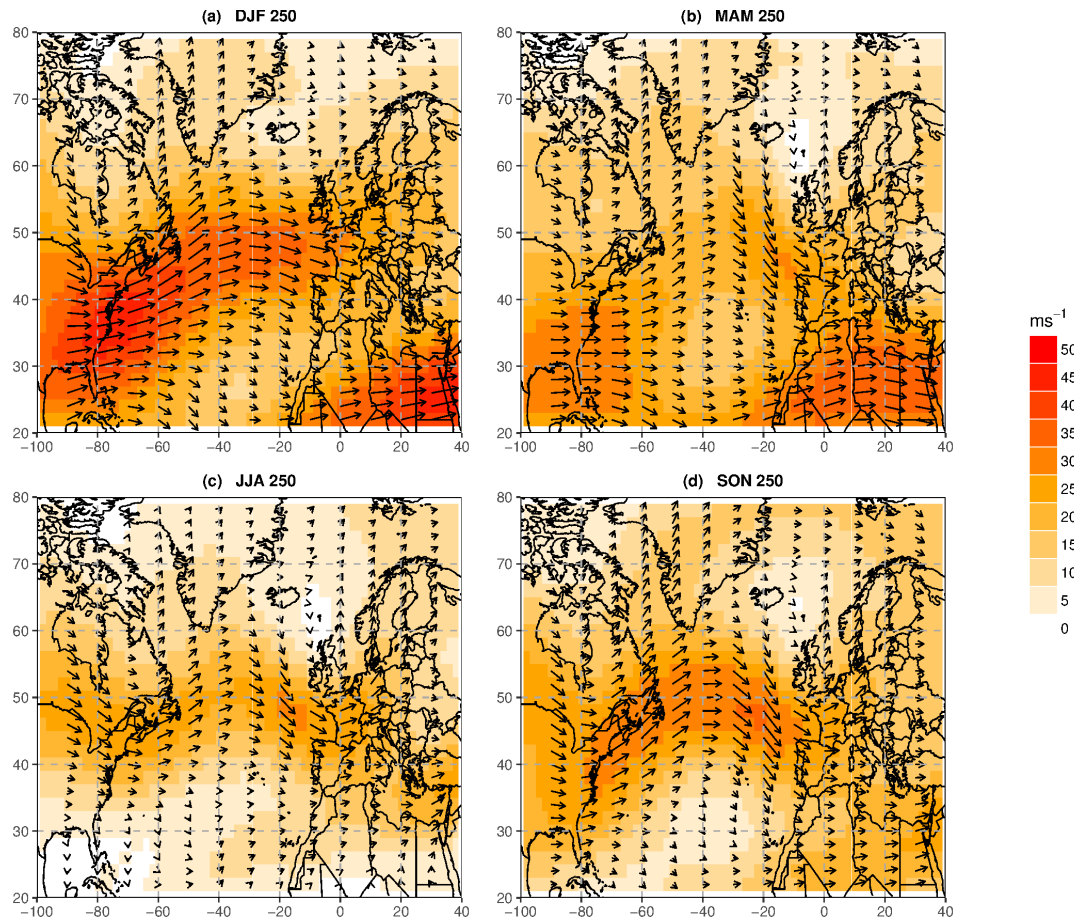


FIGURE 5.12: Mean vector winds at 250 hPa from ERA-I, 1980-2011, for one-day wet/extreme wet events associated with a long residence time cyclone ($\geq 75^{\text{th}}$ percentile). Data are interpolated to a 2° grid.

stall in that position. The 7-day “stalled” event synoptic charts in Figure 5.13 show a similar synoptic situation to the one-day events.

In comparison to dry cases (e.g. Figure 5.6), Figures 5.12 and 5.13 show the absence of a blocking region directly above the British Isles, and a more intense, zonal mean jet stream position across the North Atlantic region. These features might be expected in a “wet” event; however, the absence of a clearly identifiable blocking region is in itself significant when considering the genesis of “stalling” events. A cyclone might be expected to stall due to the presence of a block near the region of interest. However, this appears not to be the dominant cause of stalling in the vicinity of the British Isles. Stalling appears to be more regularly associated with the trough of a quasi-stationary wave on the jet stream and cyclonic upper-level circulation to the north of the British Isles, particularly in the summer months.

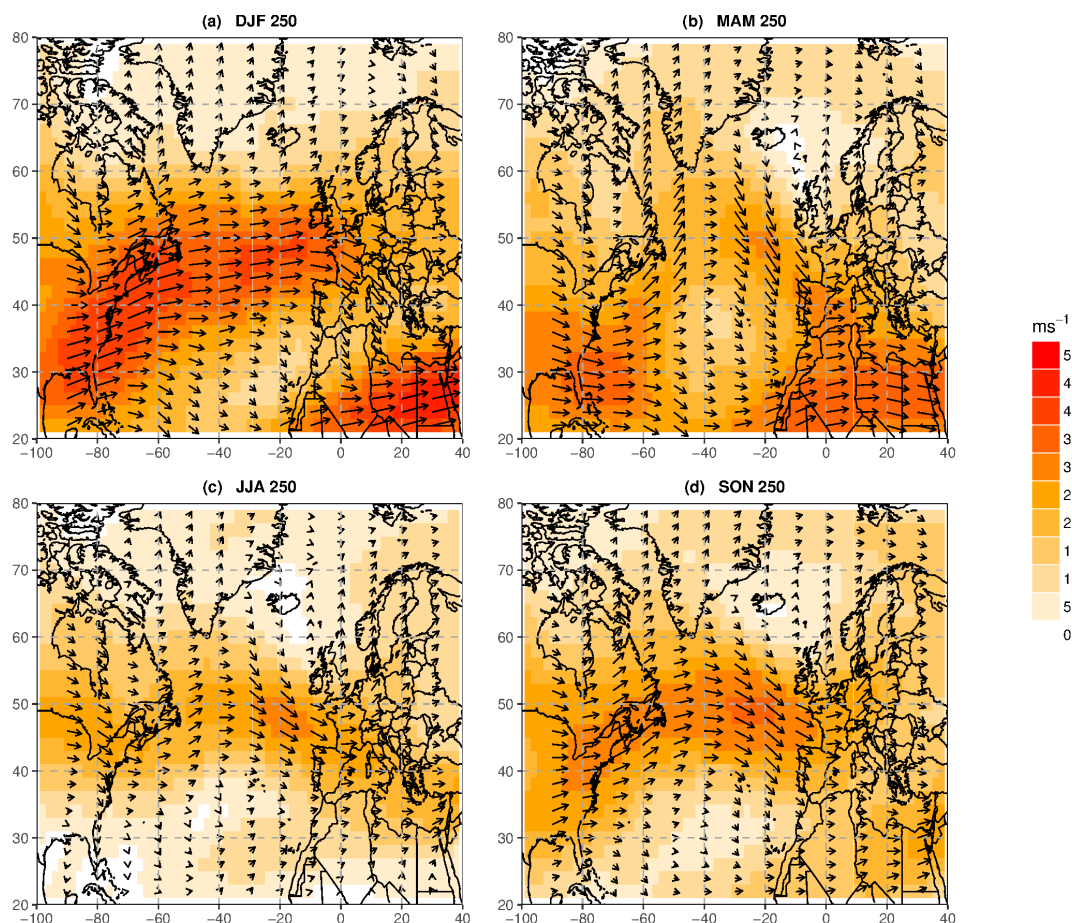


FIGURE 5.13: Mean vector winds at 250 hPa from ERA-I, 1980-2011, for 7-day wet/extreme wet events associated with a long residence time cyclone ($\geq 75^{\text{th}}$ percentile). Data are interpolated to a 2° grid.

5.3.3 Precipitation intensity in extratropical cyclones

The mean precipitation accumulation per unique extratropical cyclone (from EWP) for wet and extreme wet events is shown in Figure 5.14. This method of analysis allows evaluation of the relative importance of individual cyclone intensity and total cyclone count in precipitation events on varying time-scales. Where high values are shown, this indicates that the event category in question tends to be associated either with more intensely precipitating cyclones, or with cyclones that propagate slowly (stall) over the England and Wales region (as discussed in Section 5.3.2). This plot indicates whether cyclone count or cyclone precipitation accumulation is the more important factor in each event classification.

For all seasons, the accumulated precipitation per cyclone for daily events is higher for extreme wet events than for wet events, indicating that extreme daily accumulations

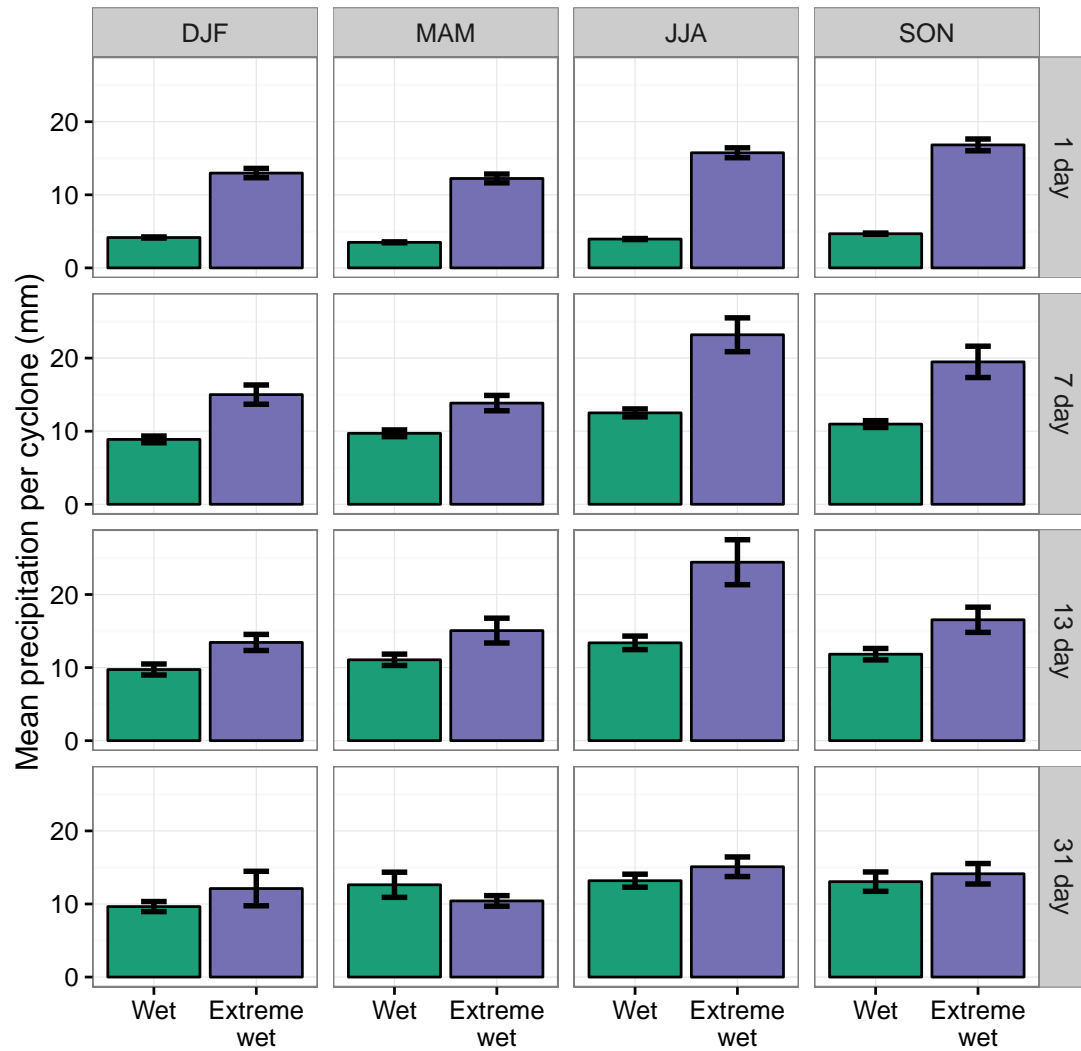


FIGURE 5.14: Bar chart showing mean precipitation accumulation per extratropical cyclone associated with wet and extreme wet events. Error bars show standard error on the mean.

of precipitation are associated with intensely precipitating cyclones. The difference between the precipitation accumulation per cyclone decreases with increasing accumulation period for all seasons, and at the 31-day time-scale little difference is evident between precipitation accumulations per cyclone in wet and extreme wet events. This indicates that for 31-day events, the precipitation rate or residence time of the cyclone is less important than the cyclone count for all seasons. However, in JJA a larger difference between precipitation accumulations per cyclone in wet and extreme wet events is evident for 1–13 day accumulation periods. This indicates that for JJA, extreme precipitation accumulations for 1–13 day periods are more strongly related to the total precipitation accumulation per cyclone. This may be attributed to the longer residence times observed in JJA extreme wet events (Figure 5.11).

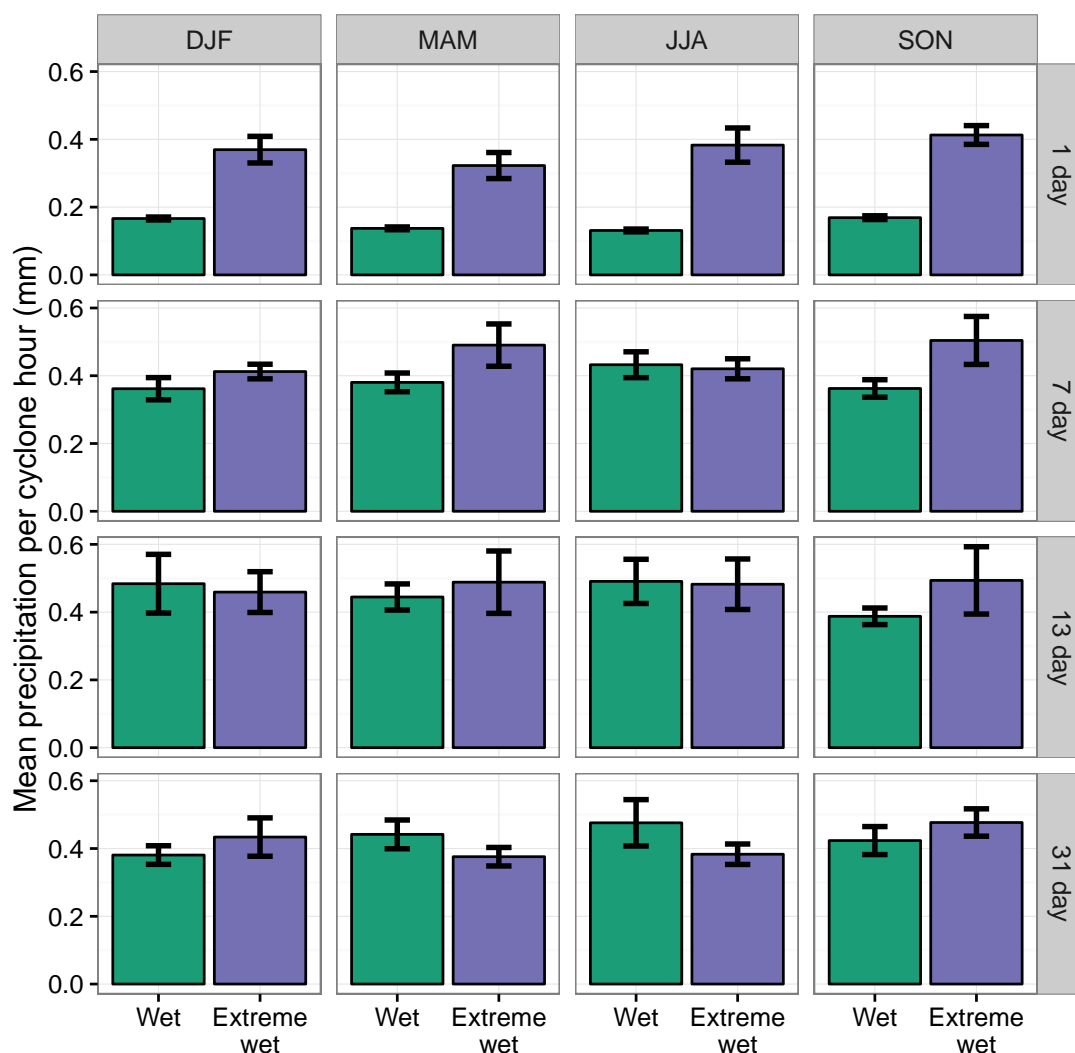


FIGURE 5.15: Bar chart showing mean precipitation accumulation per hour of cyclone residence time, for cyclones associated with wet and extreme wet events. Error bars show standard error on the mean.

These results show that the contribution of individual cyclones to the total accumulated precipitation is most influential at short time-scales and in the summer months. Storm intensity is not strongly influential on the total precipitation accumulation for extreme wet events in any season for 31-day precipitation accumulations, indicating that the total cyclone count is more important than cyclone residence times or precipitation intensity for the development of extreme precipitation events at 31-day accumulation periods.

The mean hourly precipitation rate for wet and extreme wet events is displayed in Figure 5.15, calculated as the total precipitation accumulation divided by the cumulative

residence time of all extratropical cyclones associated with each event. This measurement shows the precipitation intensity of cyclones associated with England and Wales precipitation events. Whereas the statistics of mean precipitation accumulation per extratropical cyclone displayed in Figure 5.14 indicates where large precipitation accumulations are generated by individual cyclones, the hourly precipitation measurement shown in Figure 5.14 gives information on the precipitation rate in these cyclones. For example, an extreme event generated by a single cyclone may be caused by a fast-moving cyclone with a high precipitation rate, or by a slow-moving cyclone with a lower precipitation rate. In Figure 5.15, high values indicate a prevalence of cyclones with a high precipitation rate.

Extreme wet events in all seasons on daily time-scales are found to be associated with cyclones with a higher precipitation rate than wet events in Figure 5.14. At the seven-day time-scale, the equinoctial seasons (MAM and SON) both show larger hourly precipitation accumulations for extreme wet events. On all other time-scales, no significant difference between wet and extreme wet event mean hourly precipitation is found. This indicates that on daily time-scales for all seasons, and on seven-day time-scales for MAM and SON, high precipitation rates are strongly related to extreme precipitation accumulations. However, at longer time-scales, the mean precipitation per cyclone hour reduces for extreme wet events relative to wet events. This indicates that for longer accumulation time-scales, the total cyclone residence time (which may be generated by number or duration of cyclones) is more relevant than individual cyclone precipitation intensity.

5.4 Discussion and conclusions

In this chapter the relationship between extratropical cyclone movement patterns and England and Wales precipitation events has been analysed. Precipitation events were identified in the EWP series of observed England and Wales precipitation. These events were matched with cyclone track data from the output of CPA analysis on ERA-I data for the period 1980-2011. Clustering and stalling were analysed in terms of cyclone count per event, and mean / maximum cyclone residence time per event respectively.

Precipitation events derived from the HadUKP England and Wales Precipitation record have been analysed using data from ERA-I and the CPA method, to determine the influence of cyclone clustering and stalling on the intensity of England and Wales precipitation events. “Clustering” was defined as the total cyclone count associated with

each event over its full time-period. Stalling was defined by two measurements: (1) mean residence time across all cyclones in all events, and (2) mean across all events of the maximum cyclone residence time in each event. Mean cyclone residence time indicates the degree to which all cyclones that interact with England and Wales during the precipitation event are moving more slowly than usual. Maximum cyclone residence time indicates the degree to which the longest-lasting cyclone in the event has stalled. This is designed to highlight cases where a single stalled cyclone is embedded within a series of more mobile cyclones during the course of the precipitation event.

A large amount of variability in the degree of clustering in extreme events is present due to the small sample size of the extreme events. However, DJF and SON showed higher cyclone counts for extreme wet events than wet events on the 13- and 31-day time-scales (Table 5.1). All seasons were found to have a higher mean cyclone count for extreme wet events than wet events on 1- and 31-day time-scales. The increased cyclone count for 1-day time-scales may indicate that extreme wet events are more likely to have multiple cyclone features in the vicinity of England and Wales; for example an intense cyclone may generate a secondary vorticity feature on its fronts. However, the high rates of clustering for longer time-scales may indicate a more mobile synoptic-scale situation, as is indicated by the synoptic-scale wind vector plots in Section 5.3.1. We conclude that over 31-day time-scales for all seasons, and over 13-day time-scales for DJF and SON, cyclone clustering is a factor in generating England and Wales precipitation extremes. Cyclone clustering was found in Section 5.3.1 to be associated with a 250-hPa jet that was stronger, more zonal, and extended toward the east relative to the seasonal mean, which is consistent with the situation described by Priestley et al. (2016) as being conducive to Rossby wave breaking and clustered extratropical cyclones.

In considering the influence of extratropical cyclone stalling, we must consider two different scenarios. The first scenario, represented by the mean residence time over all cyclones in all events, is characterised by a period of low cyclone mobility spanning most or all of the event period. Such situations were found to be associated with extreme wet events at short time-scales (1–13 days) in all seasons, with extreme wet JJA events returning particularly high differentials between wet and extreme wet event mean residence time. At the 31 day time-scale, very little difference between wet and extreme wet event residence times was found for DJF, MAM and SON, with a small increase in JJA extreme wet event mean residence times, indicating that over this time-scale there is little difference in the average stalling of cyclones between wet and extreme wet events..

The second scenario to be considered in the analysis of extra-tropic cyclone stalling is that of a single stalled cyclone embedded within a more mobile period. This situation has been witnessed in flooding events (e.g. summer 2007, November 2009), when precipitation from a mobile series of extratropical cyclones saturates the ground, and a stalled cyclone generates enough precipitation to cause flooding. This situation was found to be more prevalent for extreme wet events than for wet events in all seasons. JJA and SON showed particularly high (12–38%) differentials in mean maximum cyclone residence time between extreme wet and wet events, indicating that the extent of peak stalling in these seasons is particularly influential on precipitation accumulations.

For periods of low cyclone mobility (implied by long cyclone residence times), the 250 hPa jet stream was found to be intensified and extended towards England and Wales relative to the seasonal mean, but to a lesser degree than in the extreme wet event means or the high cyclone count event means. In the “stalled” event means, a trough over Great Britain is evident, represented by a curvature of the jet stream towards the south. In JJA and SON, a wave pattern consistent with a wavenumber $n = 6$ stationary wave is identified in these cases, mirroring the findings of Blackburn et al. (2008). For all seasons, the jet stream core at 250 hPa does not extend beyond the British Isles, unlike that found in the high cyclone count cases. However, there is no significant blocking feature near the British Isles, indicating that cyclone stalling is caused by more complicated situations than a simple blocking region.

The key conclusions of this chapter are as follows:

- Clustered extratropical cyclones are associated with historical extreme precipitation events in England and Wales in all seasons at 31-day accumulation periods. A strong association between clustered extratropical cyclones and extreme wet events is also identified in MAM at the daily accumulation time-scale.
- Stalled extratropical cyclones are most strongly associated with JJA extreme wet events, but stalling is relevant for precipitation extremes for all seasons at short (1–7 day) time-scales.
- Stalled extratropical cyclones embedded within a period of more mobile extratropical cyclones are commonly associated with extreme precipitation events. This phenomenon is particularly evident in JJA, where a significantly increased maximum residence time for extreme wet events is identified for 1–31 day events.
- The position and intensity of the 250-hPa jet stream is associated with the generation of both clustered and stalled periods. An intense, zonal jet stream with

jet exit region located over or to the east of the British Isles is associated with clustered cyclones leading to England and Wales precipitation events. Stalled cyclones are associated with a jet stream exhibiting a wave pattern of approximate wavelength $n = 6$ and an upper-level trough over the British isles.

This chapter has established the relationship between England and Wales precipitation events and clustered and stalled extratropical cyclones in the recent climate. To understand how these relationships are likely to change in the future climate, we must understand which aspects of these relationships are well represented in climate model. Chapter 6 investigates the ability of the HadGEM2-ES climate model to reproduce observed patterns of clustering and stalling in extratropical cyclones associated with England and Wales precipitation events, using a historical run of the model.

Chapter 6

Evaluation of clustering, stalling and England and Wales precipitation events in HadGEM2-ES

6.1 Introduction

In this chapter, the extent to which a climate model can represent the relationship between clustering and stalling of extratropical cyclones and extreme precipitation events over England and Wales is evaluated. To give confidence in the ability of HadGEM2-ES to simulate changes to the storm tracks in a future climate scenario, it must first be analysed against a historical reanalysis. This analysis is intended to highlight any differences in the generation of extreme wet events over England and Wales between HadGEM2-ES Historical and ERA-I, including their ability to represent key features of the North Atlantic storm track, and the relationship between clustering, stalling, and extreme precipitation events in England and Wales.

The CMIP5 “Historical” experiment of HadGEM2-ES had been analysed against ERA-I in terms of its representation of precipitation over England and Wales; 250-hPa vector wind speeds and positions over the North Atlantic and Europe; cyclone track densities

and propagation speeds over the north-eastern Atlantic; and cyclone counts and residence times for cyclones associated with precipitation events in England and Wales, generated from analysis with the CPA method (Chapter 4). For analysis of the HadGEM2-ES Historical experiment, the r2i1p1 ensemble member was selected as data were not available for sub-daily wind and precipitation in other ensemble members at time of analysis. Data for ERA-I, EWP and HadGEM2-ES Historical were evaluated over a common time-period of 1979–2005, representing the longest period of overlap between the three datasets.

The ability of HadGEM2-ES to model precipitation distributions over England and Wales is evaluated in Section 6.2. The representation of the North Atlantic storm track is evaluated in Section 6.3. This analysis includes discussion of the general properties of the North Atlantic storm track in HadGEM2-ES, including 250-hPa wind speeds, cyclone frequency, and extratropical cyclone propagation speeds. Precipitation events in HadGEM2-ES are analysed with respect to the level of clustering and stalling of extratropical cyclones identified using the CPA method in Section 6.4. The role of extratropical cyclone precipitation intensity in the generation of precipitation events in both the climate model and reanalysis is also analysed in this section. Finally, a discussion of the key findings of this chapter is given in Section 6.5.

6.2 England and Wales precipitation in HadGEM2-ES

Histograms of one-day precipitation totals in ERA-I, EWP and HadGEM2-ES are shown in Figure 6.1, for all days with ≥ 1 mm precipitation. For the gridded datasets (ERA-I and HadGEM2-ES), precipitation was spatially averaged over the England and Wales region (Figure 2.2). Both the climate model and the reanalysis represent the shape of the frequency distribution well with respect to EWP. The seasonal means of the daily precipitation accumulations (indicated by the solid black line) are approximately equal between ERA-I and HadGEM2-ES, but lower than EWP for all seasons (values shown in Table 6.1). As an indicator of the ability of each data-set to reproduce extreme events, the 98th percentiles of the distributions are indicated on Figure 6.1 as a dashed line. As with the mean, the 98th percentile value is consistently higher in EWP than in ERA-I and HadGEM2-ES, whilst both ERA-I and HadGEM2-ES return similar 98th percentile values.

The percentage of days with < 1 mm precipitation (“dry days”) in EWP, ERA-I and HadGEM2-ES Historical is shown in Table 6.2. ERA-I and HadGEM2-ES are both found

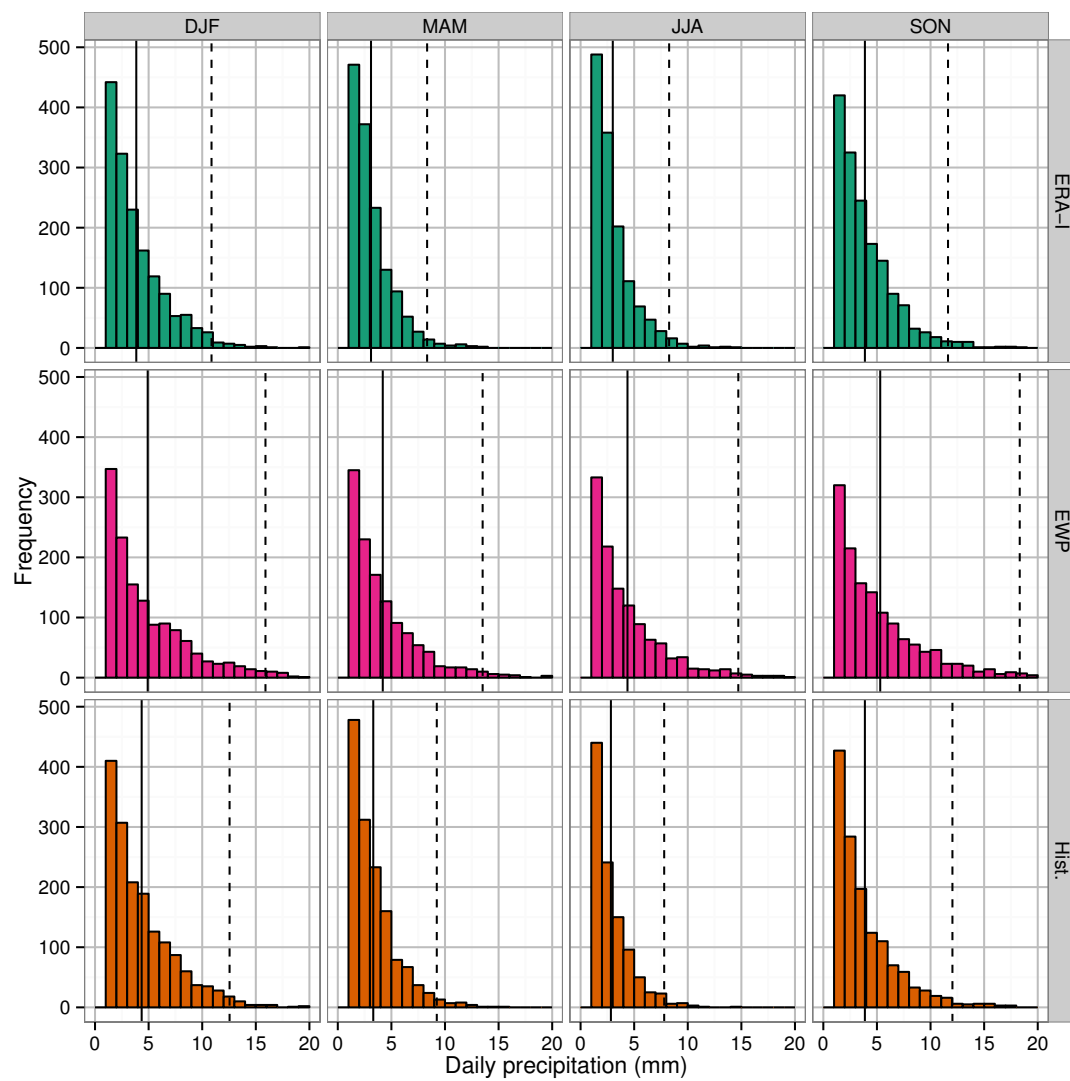


FIGURE 6.1: Histograms of daily precipitation accumulation for wet days (> 1 mm precipitation) in ERA-I (top), EWP (middle), HadGEM2-ES Historical r2i1p1 (bottom). Solid black line indicates mean. Dashed black line indicates 98th percentile. Model precipitation is averaged over a box bounded by 8.75°W - 3.25°E , 49°N - 55.5°N (England and Wales region, Rhodes et al. 2015). Data are taken from a common period of 1 Jan 1980 to 30 Dec 2005.

to underestimate the frequency of dry days relative to EWP. The problem of climate models producing too few dry days and underestimating extreme event intensity is well known (e.g. Dai 2006, Liu et al. 2014, Sivakumar 2011), and thus HadGEM2-ES may be expected not to represent some features of the extreme precipitation distributions observed in the EWP record. ERA-I has also been previously found not to represent the intensity or timing of extreme precipitation well with respect to observations over England and Wales (Rhodes et al. 2015, Chapter 3).

Season	Model	Mean (mm d ⁻¹)	p98 (mm d ⁻¹)
DJF	EWP	2.9	14.1
	ERA-I	2.6	10.1
	HadGEM2-ES	3.2	11.8
MAM	EWP	2.2	11.5
	ERA-I	1.9	7.3
	HadGEM2-ES	2.1	8.33
JJA	EWP	2.2	12.2
	ERA-I	1.8	7.5
	HadGEM2-ES	1.4	6.5
SON	EWP	3.1	15.8
	ERA-I	2.7	10.5
	HadGEM2-ES	2.4	10.9

TABLE 6.1: Mean and 98th percentile (p98) values of daily precipitation in England and Wales Precipitation (“EWP”), ERA-I (“ERA-I”), and HadGEM2-ES Historical r2i1p1 (“HadGEM2-ES”). Data included for 1979–2005.

For further analysis of England and Wales precipitation events in HadGEM2-ES, data were accumulated into 1-, 7-, 13- and 31-day periods and analysed with a Peaks-Over-Threshold method as described in Chapter 5. The minimum value recorded for one-day wet and extreme wet events are also shown in Table 6.3. The minimum extreme wet event values are consistently lower in ERA-I and HadGEM2-ES than in EWP. ERA-I and HadGEM2-ES also both overestimate the frequency of low daily rainfall accumulations (excess drizzle) (not shown). However, HadGEM2-ES and ERA-I compare favourably with each other.

6.3 The North Atlantic storm track in HadGEM2-ES

Before evaluating the ability of HadGEM2-ES to represent clustering and stalling of extratropical cyclones in association with England and Wales precipitation events, it is necessary to consider its representation of the North Atlantic storm track. In this

	EWP %	ERA-I %	HadGEM2-ES %
DJF	43.8	36.9	31.1
MAM	50.9	44.1	41.7
JJA	52.2	45.8	57.4
SON	43.5	35.6	42.6

TABLE 6.2: Dry day frequencies in EWP, ERA-I and HadGEM2-ES (Historical). “Dry day” defined as events with < 1 mm precipitation.

Season	Model	“Wet” minimum	“Extreme wet” minimum
DJF	EWP	1.35	13.19
	ERA-I	1.69	9.54
	HadGEM2-ES	2.12	11.26
MAM	EWP	1.29	10.52
	ERA-I	0.96	6.88
	HadGEM2-ES	1.37	7.84
JJA	EWP	0.85	11.21
	ERA-I	1.19	7.02
	HadGEM2-ES	0.72	6.16
SON	EWP	1.41	15.14
	ERA-I	1.81	9.92
	HadGEM2-ES	1.37	10.14

TABLE 6.3: Minimum values of total daily precipitation accumulation in $mm d^{-1}$ by season for wet and extreme wet events in EWP, ERA-I and HadGEM2-ES, one-day accumulations

section, comparisons are drawn against the North Atlantic storm track in ERA-I, as represented by the location of the 250-hPa jet, and by analysis of features identified by the Hodges (1994, 1995) tracking algorithm.

6.3.1 Seasonal mean vector winds

It is important to consider the representation of 250-hPa wind vectors in HadGEM2-ES, as winds at this level form the North Atlantic jet. The North Atlantic jet plays important roles in cyclogenesis, cyclone propagation speed, and cyclone intensification. Figure 6.2 shows seasonal mean 250-hPa wind vectors over the North Atlantic, in ERA-I and HadGEM2-ES for a common period of 1980-2005. For all seasons in ERA-I, a region of intense 250-hPa wind is found near the north-eastern coast of North America, with the jet extending to the west or north-west from this region. These features indicate the mean state of the North Atlantic jet.

HadGEM2-ES represents the seasonal average 250-hPa vector winds well in comparison to ERA-I in the region of the North Atlantic storm track. The seasonal cycle of wind intensities and directions is well represented, with the strongest winds in DJF and a minimum wind speed in JJA. For DJF a small overestimation of peak wind speeds in the eastern North Atlantic is found in HadGEM2-ES relative to ERA-I, with slightly weaker average wind speeds (7.1% reduction relative to ERA-I) over the British Isles (Table 6.4). The 250-hPa winds in HadGEM2-ES are weaker than in ERA-I in JJA, with

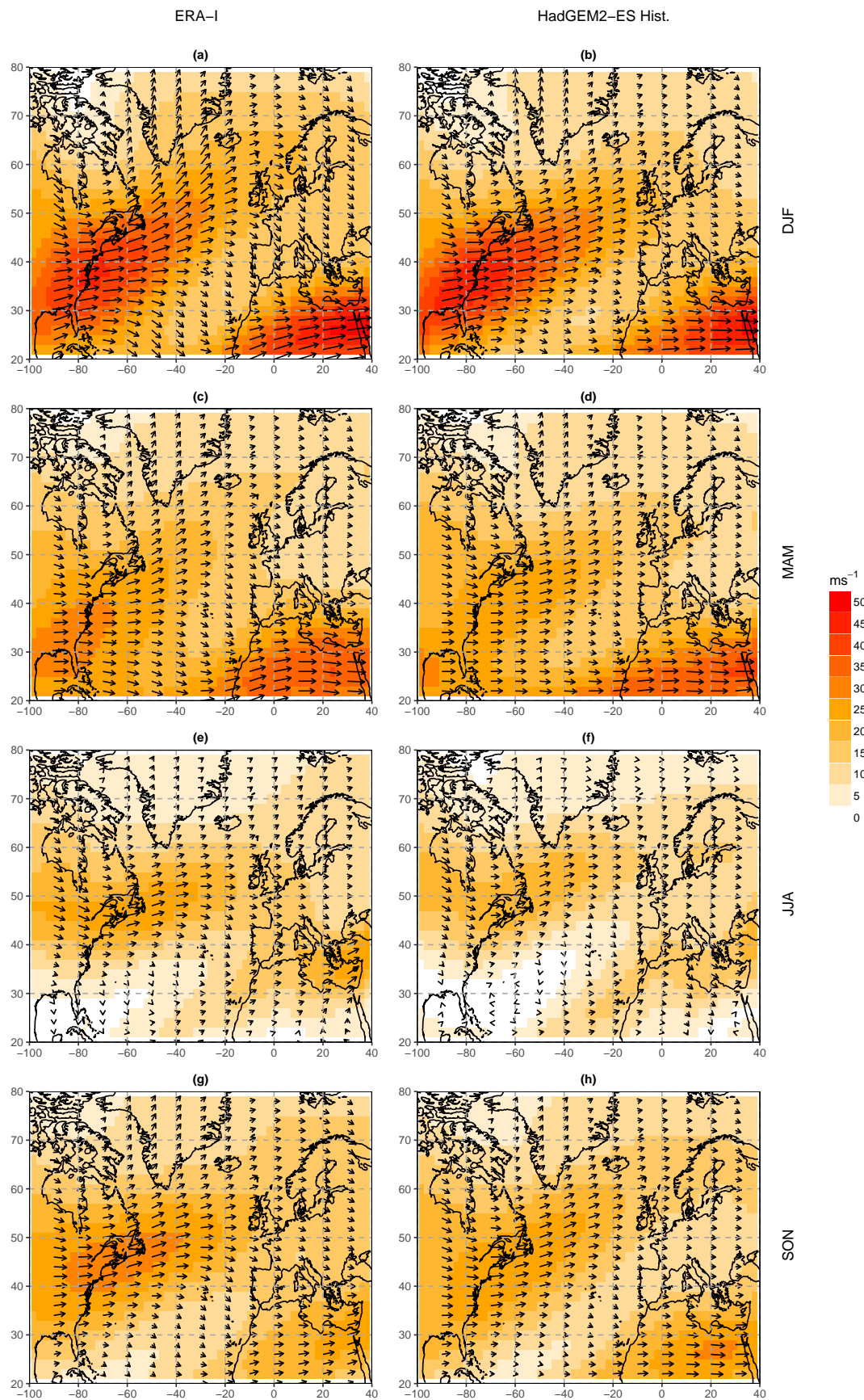


FIGURE 6.2: Seasonal mean 250-hPa vector wind speed and direction in (left) ERA-I and (right) HadGEM2-ES Historical experiment (r2i1p1 ensemble member), 1980-2005.

a reduction in wind speeds relative to ERA-I of 16.8% over the British Isles (Table 6.4).

	ERA-I u (ms^{-1})	HadGEM2-ES u (ms^{-1})	Difference (%)
DJF	19.5	18.1	-7.1
MAM	13.0	14.0	7.9
JJA	14.6	12.2	-16.8
SON	17.2	14.1	-17.7

TABLE 6.4: Seasonal mean 250-hPa vector wind speed, 1980–2005, ERA-I and HadGEM2-ES Historical. Spatial mean of data points within the British Isles region. Positive values of “difference” indicate higher wind speeds in HadGEM2-ES than in ERA-I.

6.3.2 Storm track density in the North Atlantic

Track densities in the North Atlantic region for HadGEM2-ES Historical and ERA-I are shown for a common period of 1980–2005 in Figure 6.3. The main North Atlantic storm track is visible for all seasons, extending approximately from the eastern coast of North America north-west to Iceland. A seasonal cycle is evident in the storm track, with the highest track frequencies in the North Atlantic being found in DJF. For DJF and MAM, two distinct maxima are observed. One maximum is located near the east coast of North America, corresponding to the main baroclinic cyclogenesis zone, and a second maximum is found between the southern tip of Greenland and Iceland, corresponding to an orographic cyclogenesis zone generated by the high orography of Greenland (Hoskins and Hodges, 2002).

HadGEM2-ES represents key features of the storm track in a comparable fashion to ERA-I, including the separate maxima in DJF and MAM. Track frequency anomalies in HadGEM2-ES Historical with respect to ERA-I are shown in Figure 6.4. The anomaly figures indicate little systematic difference between ERA-I and HadGEM2-ES in the North Atlantic region in DJF and MAM, with a low level of signal to noise. In SON, HadGEM2-ES produces a strong maximum of cyclone track frequency close to the southern tip of Greenland, with lower frequencies near the east coast of North America. This anomaly is clear in Figure 6.4, with high percentage anomalies along the eastern coast of Greenland. For JJA the HadGEM2-ES storm track shows a greatly reduced track density when compared with ERA-I, with fewer cyclones tracking directly from the western North Atlantic to the region of the British Isles in HadGEM2-ES than in ERA-I; this is reflected in the low HadGEM2-ES British Isles cyclone count for JJA in Table 6.5. This is consistent with the finding of Zappa et al. (2013a) that indicates a reduced JJA

North Atlantic track density in the CMIP5 models. A lower track density near the British Isles is evident in HadGEM2-ES for SON in Figure 6.4, with cyclone tracks in HadGEM2-ES tending to cluster around the east coast of Greenland to a greater extent than in ERA-I. The low frequency of HadGEM2-ES cyclones tracking directly west-east across the North Atlantic in SON is also noted in Table 6.5.

6.3.3 Number and speed of extratropical cyclones in the Eastern North Atlantic

Table 6.5 shows the number of unique cyclone tracks per month in ERA-I and HadGEM2-ES between 1980–2005 travelling through the British Isles region (Figure 2.2). HadGEM2-ES finds fewer cyclones crossing directly over the British Isles for all seasons. The largest under-estimation is found in JJA, and the smallest under-estimation is found in DJF. For the full period 1980–2005, the Hodges (1995) tracking algorithm on ξ_{850} identifies a total of 2,619 cyclones in ERA-I and 2,214 cyclones in HadGEM2-ES in the British Isles region (15.46% underestimate in HadGEM2-ES); a mean of 87.3 and 73.8 cyclones per year in ERA-I and HadGEM2-ES respectively. These results show that HadGEM2-ES produces too few cyclones in the British Isles region, with a particular deficit in JJA and SON. This finding is in agreement with the findings of Zappa et al. (2013a), which showed that a reduced number of cyclones were identified in the eastern North Atlantic in an evaluation of the CMIP5 multimodel average representation of the Northern Hemisphere storm tracks.

Season	Model	Track frequency (month ⁻¹)	
DJF	ERA-I	8.0	
	Historical	7.6	(-5.0%)
MAM	ERA-I	6.8	
	Historical	6.1	(-10.3%)
JJA	ERA-I	7.0	
	Historical	5.0	(-28.6%)
SON	ERA-I	7.3	
	Historical	5.9	(-19.2%)

TABLE 6.5: Frequency of unique cyclone tracks propagating through the British Isles region (see Figure 6.3). Figures in brackets indicate the percentage difference between ERA-I and HadGEM2-ES Historical (positive values indicate higher track frequency in HadGEM2-ES than ERA-I).

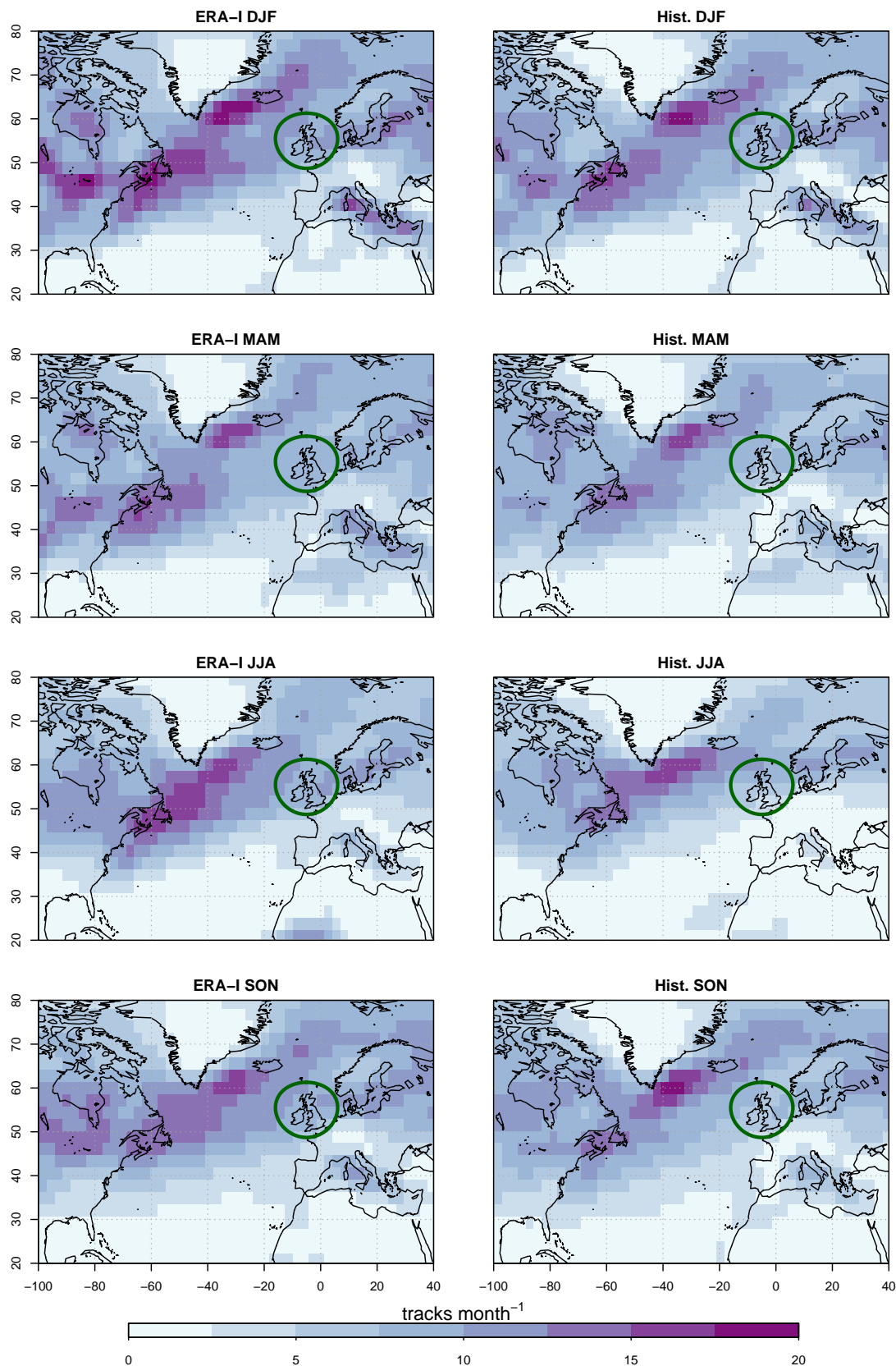


FIGURE 6.3: Storm track density for ERA-I and HadGEM2-ES Historical r2i1p1, for a common period of 1980-2005. Track density was calculated as frequency of unique cyclone tracks on a 5° spherical cap using spherical kernel estimators (Hodges, 1996). Storm tracks identified using the Hodges (1995) method on ξ_{850} . Data interpolated to 2° longitude-latitude grid. Green circle indicates British Isles region

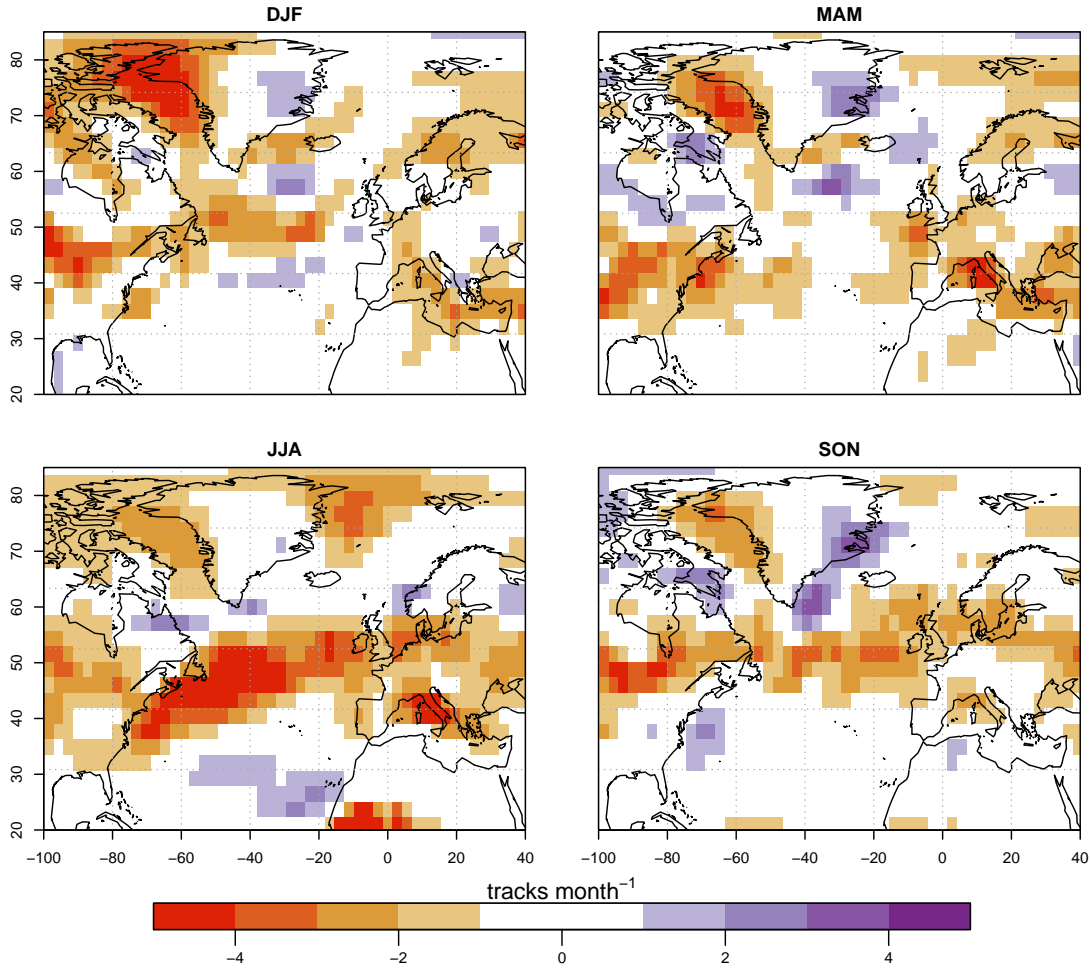


FIGURE 6.4: Track density anomaly in HadGEM2-ES Historical (r2i1p1) data for 1980-2005, with respect to ERA-I for the same period. Densities calculated as per Figure 6.3.

6.3.4 North Atlantic extratropical cyclone propagation speeds

Figure 6.5 shows histograms of extratropical cyclone centre propagation speeds, using the Hodges (1995) tracking scheme on ξ_{850} in ERA-I (top) and HadGEM2-ES (bottom). Speed v on the great circle of Earth radius $R_e = 6378.145 \text{ km}$ is calculated for each time-step i for a cyclone of (longitude,latitude) position (x, y) with a time-step t using a centred-difference equation. The following formulae are used to calculate distances on the great circle, given inputs of longitude/latitude co-ordinates in radians $(x_1, y_1), (x_2, y_2)$, for pairs $(x_{[i-1]}, y_{[i-1]}), (x_{[i]}, y_{[i]})$ and $(x_{[i]}, y_{[i]}), (x_{[i+1]}, y_{[i+1]})$:

$$\begin{aligned}\Delta x &= x_2 - x_1 \\ \Delta y &= y_2 - y_1 \\ a &= \sin \frac{\Delta y_1}{2} + \cos(y_{[i]}) \cdot \cos(y_{[i-1]}) \cdot \sin \frac{\Delta x_1}{2} \\ c &= 2 \arctan_2(\sqrt{a}, \sqrt{1-a}) \\ d &= R_e c\end{aligned}$$

Distances d_1 and d_2 are calculated for the two (longitude,latitude) pairs. The centred difference speed $|v|$ is then calculated as follows:

$$|v| = \frac{d_1 + d_2}{2t}$$

To calculate the frequency distributions of extratropical cyclone propagation speeds, data are analysed using the above equations for cyclones at time-steps during which they are located within the Eastern North Atlantic region (Figure 2.2). Both the climate model and reanalysis capture a similar range and distribution of track speeds; however, the cyclone propagation speed distribution from HadGEM2-ES is more positively skewed than ERA-I (DJF skewness: ERA-I 0.4, HadGEM2-ES 4.4. JJA skewness: ERA-I 0.8, HadGEM2-ES 4.8). Extra-tropical cyclone centres in HadGEM2-ES propagate on average at slower speeds than those in ERA-I. HadGEM2-ES underestimates the mean cyclone propagation speed relative to ERA-I for all seasons, as follows: DJF -23.8%, MAM -18.8%, JJA -19.9%, SON -17.5%. For JJA and SON the underestimation of cyclone propagation speeds in the eastern North Atlantic is of a similar magnitude to the underestimation of mean wind speed ($|\mathbf{u}|_{250}$) over the British Isles, as shown in Table 6.4.

The underestimation of cyclone propagation speed in HadGEM2-ES is consistent with the results of Froude (2010), which found that all ensemble members of the TIGGE (The Observing System Research and Predictability Experiment (THORPEX) Interactive Grand Global Ensemble) project underestimated cyclone propagation speed, with mean error between model and analysis ranging from 10-16 km h⁻¹. The difference between HadGEM2-ES and ERA-I is slightly lower than observed with the TIGGE models, with extratropical cyclones in HadGEM2-ES propagating 7–12 km h⁻¹ slower than ERA-I. Extratropical cyclones in the North Atlantic storm track in HadGEM2-ES move slowest relative to ERA-I in DJF, moving on average 24% slower than cyclones in ERA-I.

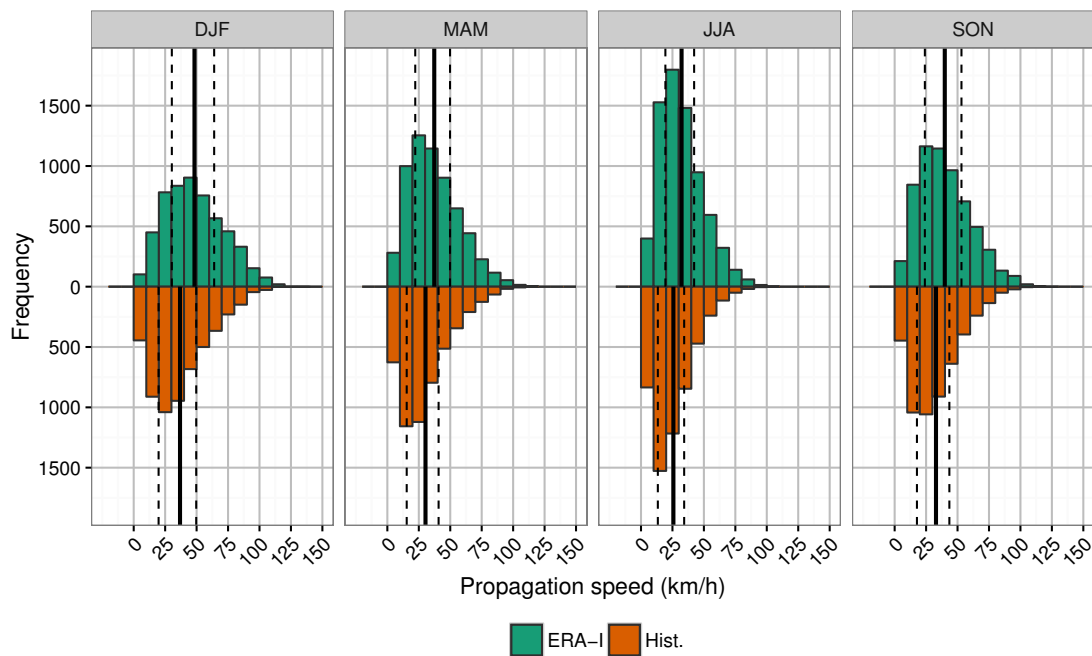


FIGURE 6.5: Histograms of extratropical cyclone speed for all tracks identified within the eastern North Atlantic region (Figure 2.2). ERA-I in green (above line), HadGEM2-ES Historical r2i1p1 in orange (below line). Data analysed for a common period of 1980–2005. Means are marked as solid black line, quartiles are marked as dashed black lines. Samples are binned to 10 km/h intervals and displayed back-to-back for comparison.

6.4 Clustering, stalling, and precipitation events in HadGEM2-ES Historical

To evaluate the ability of HadGEM2-ES to project future conditions related to the North Atlantic storm track, its ability to represent key features in the synoptic-scale wind patterns should be evaluated. Analysis of 250-hPa vector wind speeds and directions has been performed for one-day accumulation “extreme wet” precipitation events, and precipitation events associated with a high ($\geq 75^{th}$ percentile) cyclone count or mean cyclone residence time. The HadGEM2-ES results are evaluated with ERA-I. Data were taken from a common period of 1980–2005.

6.4.1 Extreme England and Wales precipitation events

Before considering the influence of extratropical cyclone clustering and stalling on precipitation events in England and Wales, it is important to know how well HadGEM2-ES represents the large-scale conditions which lead to extreme wet events, regardless of

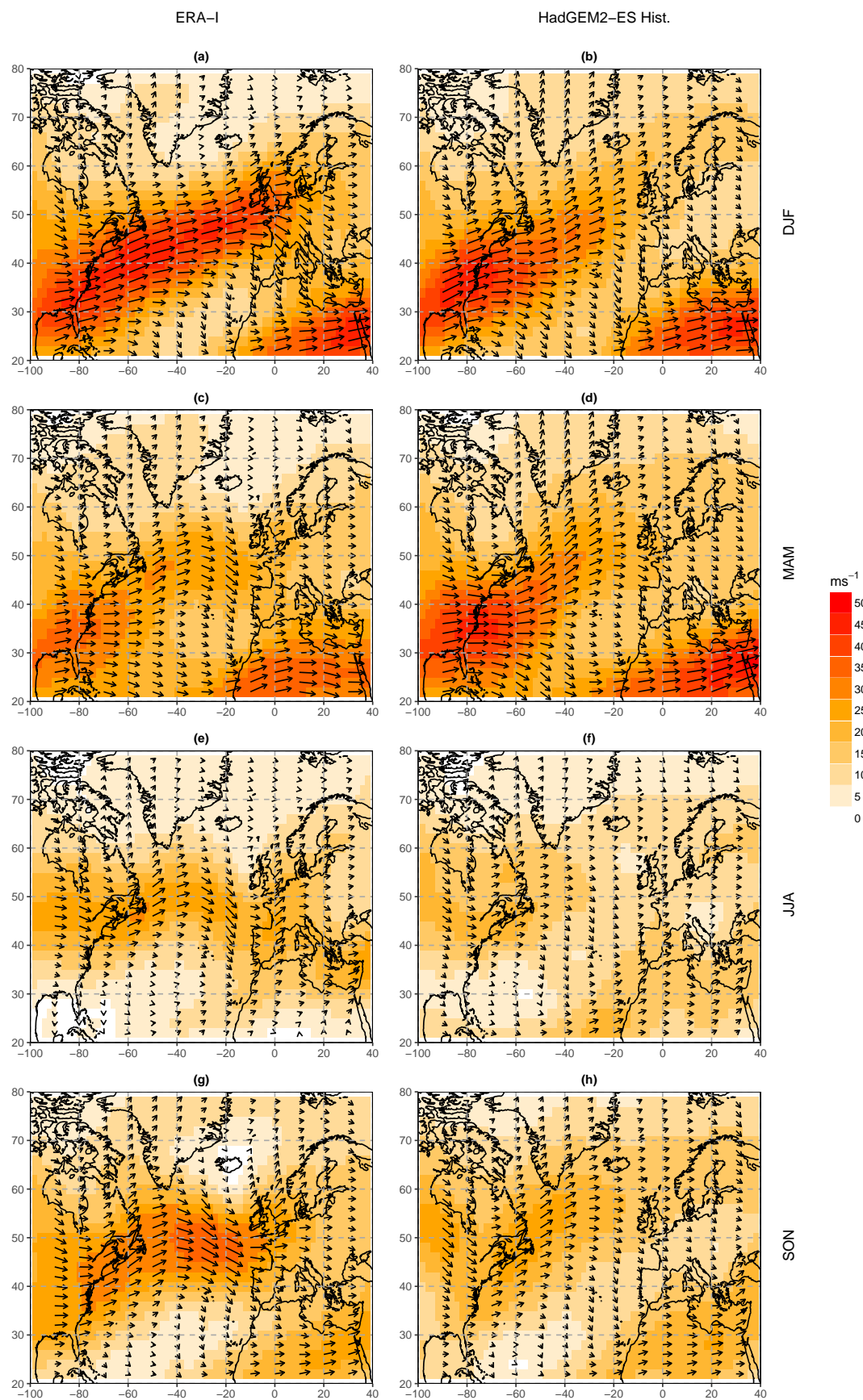


FIGURE 6.6: Mean 250-hPa vector wind speed and direction for days associated with an “extreme wet” one-day precipitation accumulation event, by season. (left) ERA-I and (right) HadGEM2-ES Historical experiment (r2i1p1 ensemble member), 1980-2005.

clustering and stalling patterns. Figure 6.6 shows the mean 250-hPa winds on days with “extreme wet” one-day precipitation events over England and Wales within ERA-I and HadGEM2-ES. When compared with the seasonal mean winds shown in Figure 6.2, each panel shows an extension of the 250-hPa jet toward western Europe, which is associated with the intensification of North Atlantic cyclones, and their propagation towards north-western Europe. However, when comparing “extreme wet” event mean wind patterns between ERA-I and HadGEM2-ES, some differences can be noted. In DJF, HadGEM2-ES shows a similar mean wind pattern to ERA-I, with an intensified jet relative to the seasonal mean, and strong westerly wind speeds near the UK. However, the wind speed in the jet stream is weaker in HadGEM2-ES than in ERA-I, particularly near the British Isles. A region of divergence directly over the British Isles is indicated in both the climate model and reanalysis.

In MAM, JJA and SON, a distinct wave-like pattern is found in the ERA-I 250-hPa vector wind mean, characterised by a ridge in the mid-North Atlantic and troughs over the western coast of North America and near the British Isles. In HadGEM2-ES a similar pattern is found in MAM and SON, with a weaker northerly component at the eastern end of the jet stream. In JJA little of the jet structure can be identified in HadGEM2-ES. Westerly winds are present, but no distinct structure is found in the mean wind speeds. This indicates that the JJA 250-hPa jet stream in HadGEM2-ES is either very weakly represented, or that its position is highly variable in extreme wet cases.

	ERA-I u (ms^{-1})	HadGEM2-ES u (ms^{-1})	Difference (%)
DJF	31.5	16.7	-47.1
MAM	16.6	17.9	7.5
JJA	12.5	8.7	-30.6
SON	22.1	14.6	-33.8

TABLE 6.6: “Extreme wet” one-day event mean 250-hPa vector wind speed, 1980–2005, ERA-I and HadGEM2-ES Historical (r2i1p1 ensemble member). Spatial mean of data points within the British Isles region (Figure 2.2). Positive values of “difference” indicate higher wind speeds in HadGEM2-ES than in ERA-I.

Extratropical cyclone tracks for all 7-day accumulation period extreme wet events in ERA-I and HadGEM2-ES are shown in Figure 6.7. The same tracks are shown at the time of their association with an England and Wales extreme wet precipitation event in Figure 6.8. Storms in both the climate model and reanalysis tend to approach the British Isles from the south-west, with many cyclones making direct crossings of the England and Wales region, particularly in JJA and SON. Some more distant cyclones

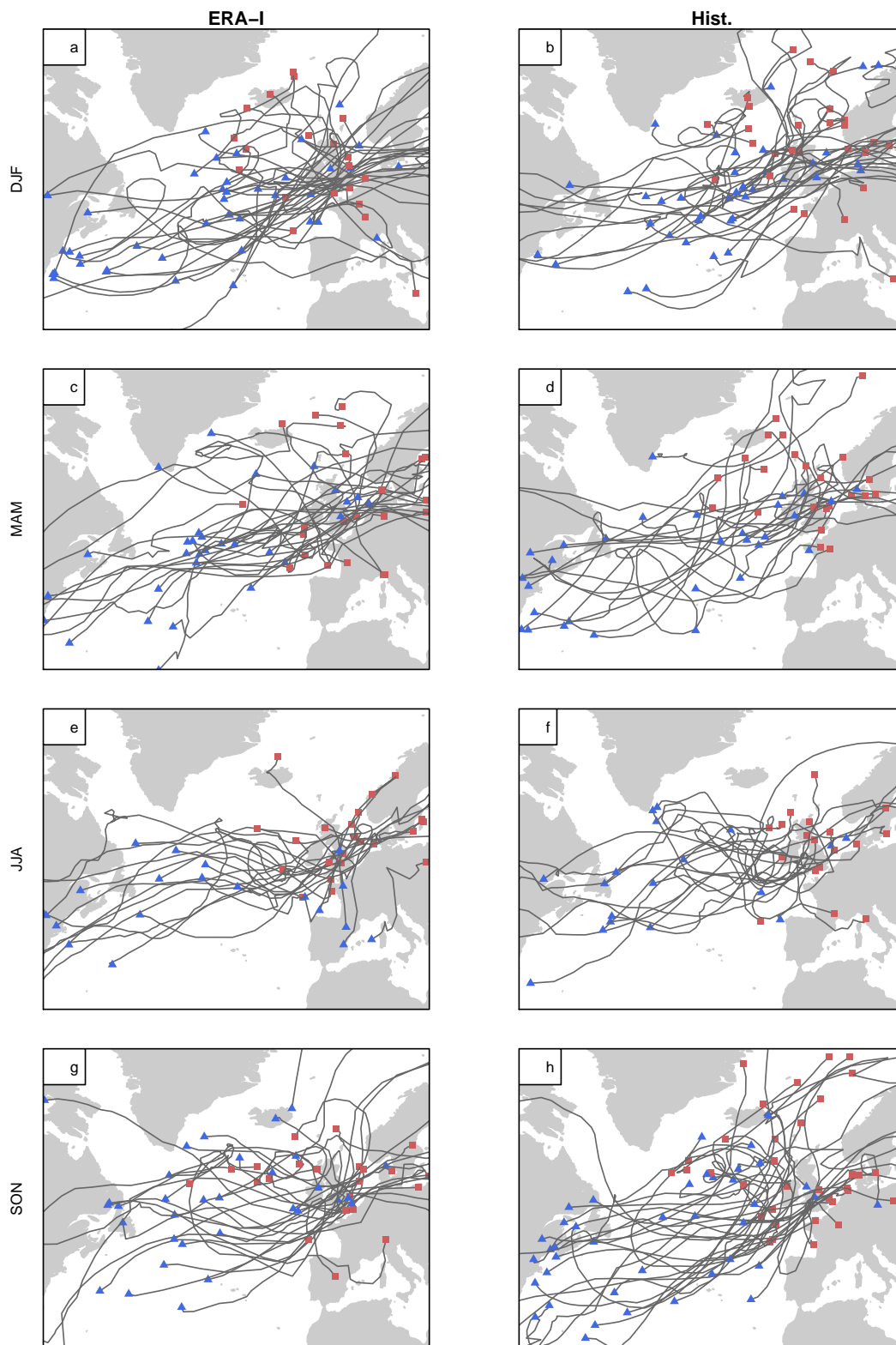


FIGURE 6.7: Cyclone tracks for all cyclones associated with extreme wet 7-day precipitation events in (a,c,e,g) ERA-I and (b,d,f,h) HadGEM2-ES Historical for a common period 1980–2005. Cyclogenesis points marked as blue triangles; cyclolysis points marked as red squares.

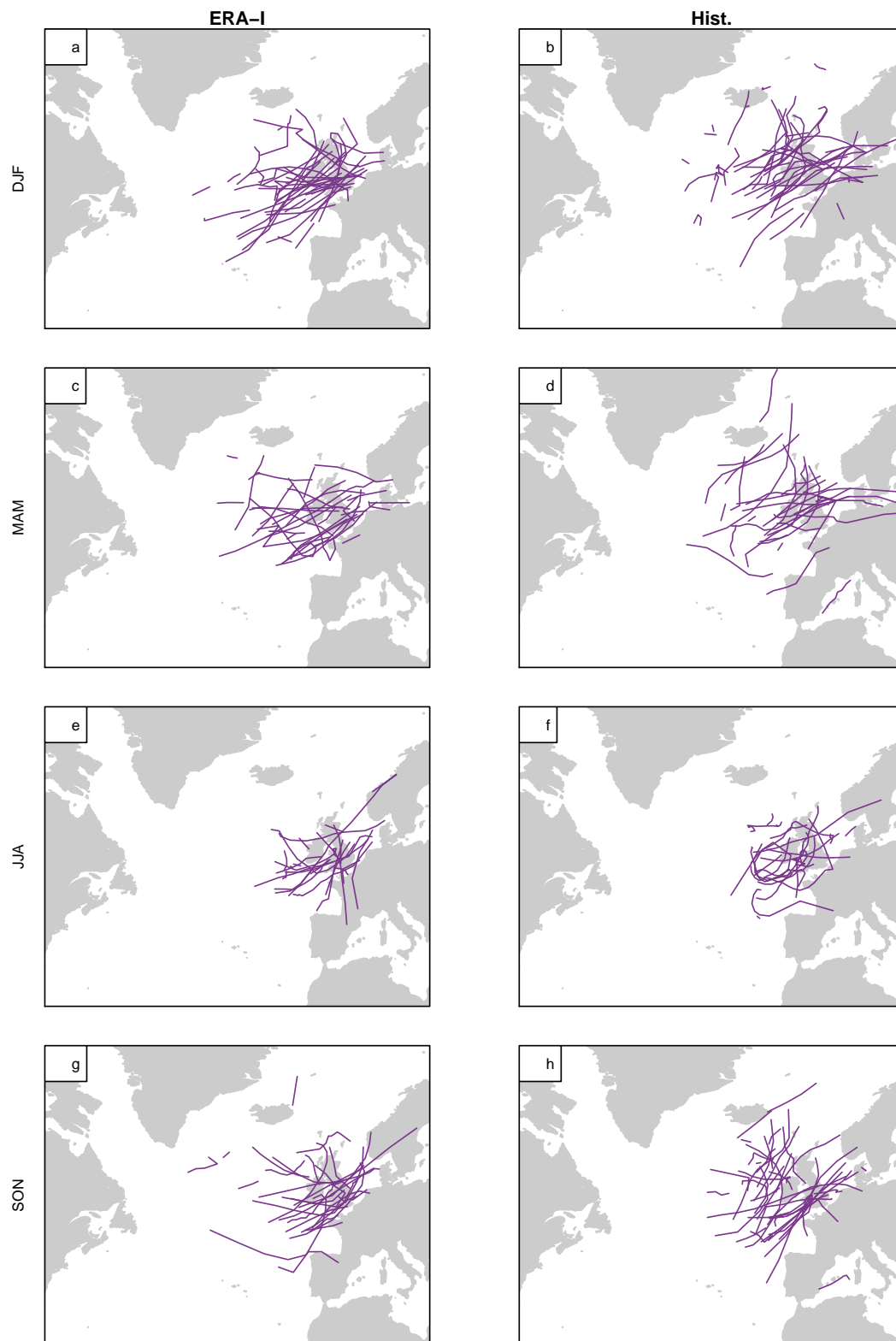


FIGURE 6.8: “Associated” locations of tracks for extreme wet 7-day events in the high residence time categories. (a,c,e,g) ERA-I and (b,d,f,h) HadGEM2-ES Historical, for a common period 1980–2005. Data as per Figure 6.12, locations shown only for times when tracks were associated with an England and Wales precipitation event.

are associated with extreme wet precipitation events in DJF and SON in both the climate model and reanalysis, and in MAM in HadGEM2-ES, indicating the presence of long, interrupted rain bands in the model output. In DJF, cyclones in ERA-I are more likely to directly cross the England and Wales region, whilst HadGEM2-ES has a greater number of cyclones tracking to the north. JJA cyclones in both the climate model and reanalysis are more erratic in their direction of propagation than DJF cyclones, which can be attributed to weaker upper-level jet in JJA (Table 6.6). For SON, ERA-I shows the majority of cyclone tracks crossing directly over the southern England and Wales region at the time of association. In HadGEM2-ES, a large subset of cyclones follow the same pattern, but a second subset of cyclones are located to the north-west of the British Isles at time of association, implying the presence of a precipitation band extending from the cyclone to the England and Wales region. Both the climate model and reanalysis produce broadly similar cyclone tracks for extreme wet precipitation events, with differences being relatively minor.

6.4.2 Clustering in HadGEM2-ES

Mean cyclone count per event, which is used to indicate clustering, is shown for wet and extreme wet England and Wales precipitation events in Figure 6.9. HadGEM2-ES is found to consistently associate a greater number of cyclones with each 7-day wet precipitation event than ERA-I, with the level of overestimation highest being in MAM. For extreme wet precipitation events, HadGEM2-ES does not systematically over- or under-represent cyclone counts with respect to ERA-I. Mean cyclone counts for HadGEM2-ES lie within the range of standard error relative to ERA-I for most seasons and accumulation periods. For 31-day events, ERA-I consistently associates higher cyclone counts to extreme wet events than to wet events. This response is not found in HadGEM2-ES for 31-day accumulations.

To compare the representation of high cyclone count events in HadGEM2-ES and ERA-I, 7-day accumulation period wet and extreme wet England and Wales precipitation events associated with high ($\geq 75^{th}$ percentile) cyclone counts were selected (termed “high cyclone count precipitation events”). Mean wind vectors at 250-hPa are shown in Figure 6.10). In ERA-I, these cases are characterised for all seasons by an increased zonal wind speed at 250-hPa, with strong wind speeds ($> 40 \text{ ms}^{-1}$ in DJF, $> 25 \text{ ms}^{-1}$ in JJA). The jet stream is particularly prominent in DJF, with strong zonal flow over the North Atlantic and a region of divergence over the British Isles. Wind speeds weaken in the summer months, and the jet stream is less zonal, but wind speeds are still fast

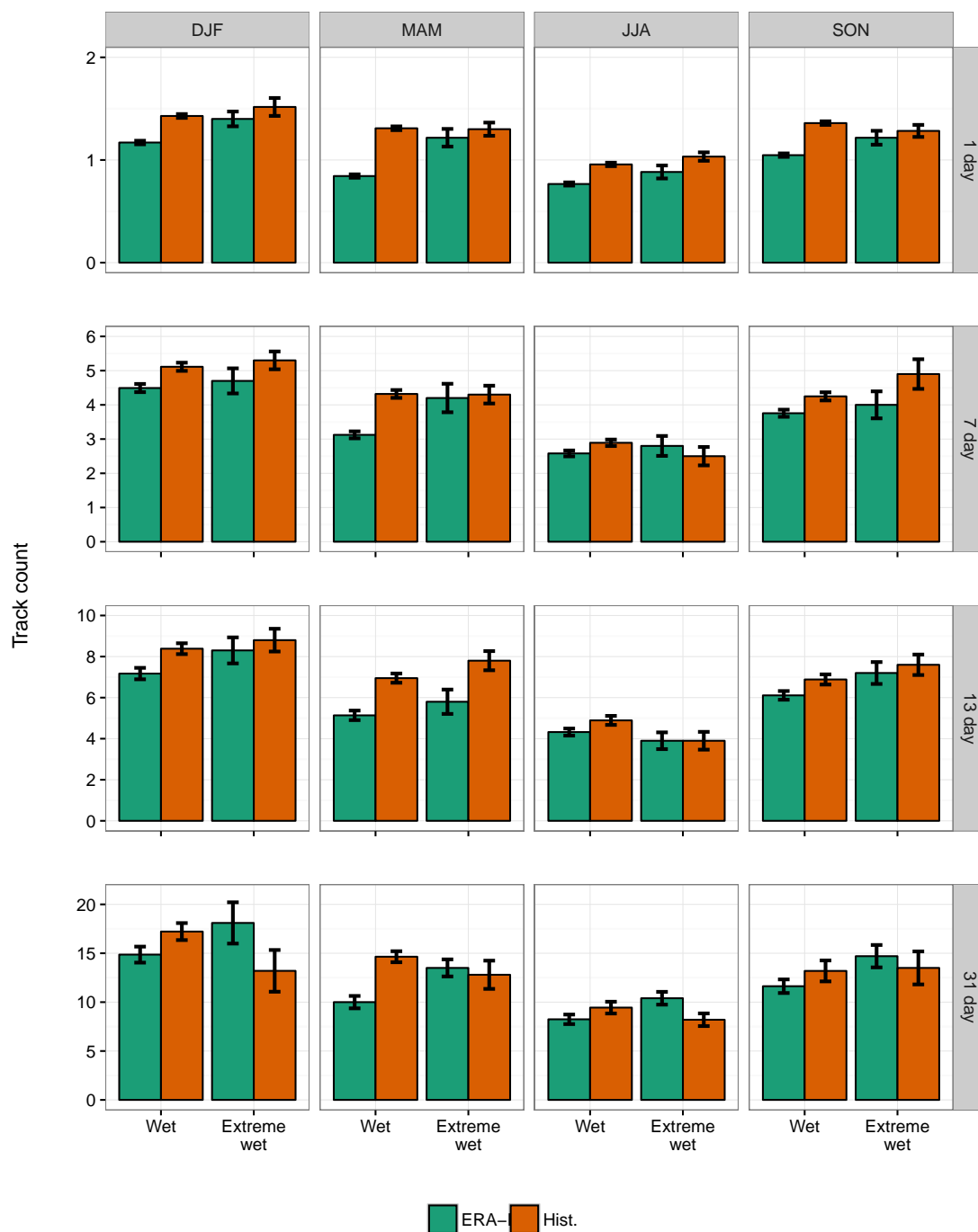


FIGURE 6.9: Mean cyclone count per event for wet and extreme wet events in ERA-I and HadGEM2-ES Historical. Error bars are standard error on the mean.

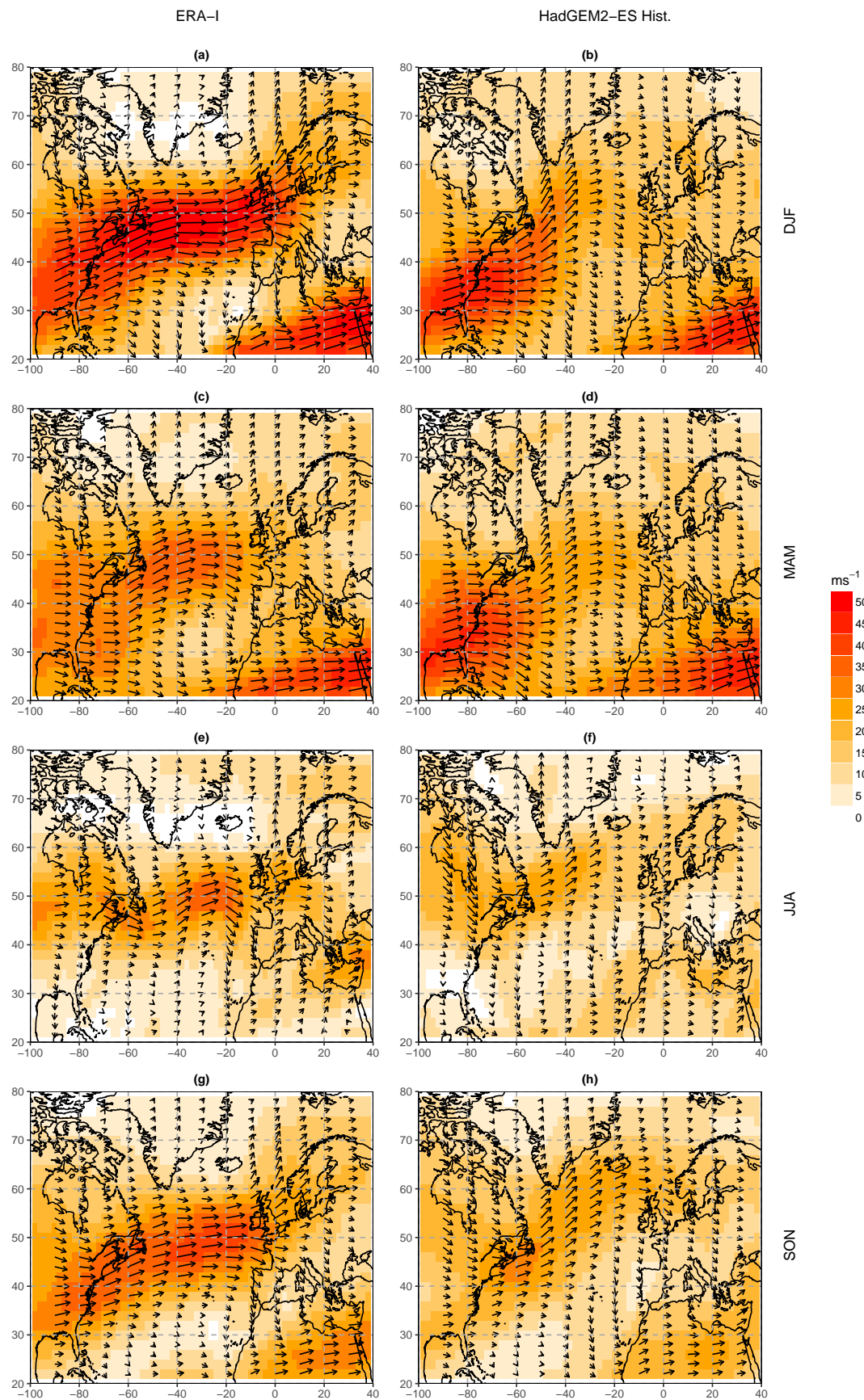


FIGURE 6.10: Mean 250-hPa vector wind speed and direction for days associated with a wet or extreme wet 7-day England and Wales precipitation event, and a high (> 75th percentile) cyclone count. (Left) ERA-I and (right) HadGEM2-ES Historical experiment (r2i1p1 ensemble member), 1980–2005

near the British Isles. In HadGEM2-ES, the 250-hPa vector winds are quite differently represented for high cyclone count cases. In DJF, mean winds are less zonal and slower than in ERA-I. For all seasons, a greater northward component of wind flow is found in the mid-North Atlantic, directing the jet stream north toward Iceland. In DJF, MAM and SON, this northward flow is then observed to curve to the south towards the British Isles. Some evidence of an intensified and extended jet stream is found for all seasons in HadGEM2-ES relative to the seasonal mean.

	ERA-I u (ms^{-1})	HadGEM2-ES u (ms^{-1})	Difference (%)
DJF	36.0	15.7	-56.4
MAM	20.4	15.9	-21.9
JJA	20.0	14.4	-28.4
SON	27.6	17.5	-36.5

TABLE 6.7: High cyclone count wet and extreme wet event mean 250-hPa vector wind speed, 1980–2005, ERA-I and HadGEM2-ES Historical (r2i1p1 ensemble member). Spatial mean of data points within the British Isles region (Figure 2.2). Positive values of “difference” indicate higher wind speeds in HadGEM2-ES than in ERA-I.

Differences in wind speed over the British Isles between ERA-I and HadGEM2-ES for dates with high cyclone counts are shown in Table 6.7. HadGEM2-ES underestimates wind speed near the British Isles for all seasons, with the largest difference being in DJF. Since DJF high cyclone count cases are characterised in ERA-I by an intense jet stream extended across the British Isles, this indicates that HadGEM2-ES generates high cyclone counts associated with England and Wales precipitation events through a different mechanism to ERA-I.

Since Table 6.5 indicates fewer tracks propagating through the eastern North Atlantic for all seasons in HadGEM2-ES relative to ERA-I, the higher mean cyclone count per wet event in HadGEM2-ES cannot be attributed to a higher track density. Figure 6.11 shows histograms of the distance between each track and a point at 55°N 5°E (representing the central point of the British Isles, c.f. Pinto et al. 2013), at the point of closest approach. HadGEM2-ES is found to associate tracks at a greater distance from this point than ERA-I. This suggests that the structure of precipitation bands within HadGEM2-ES are such that continuous bands of precipitation regularly extend to greater distances from the England and Wales region than those found in the ERA-I data. The addition of track associations at greater distances from England and Wales accounts for some of the increased cyclone count in wet events.

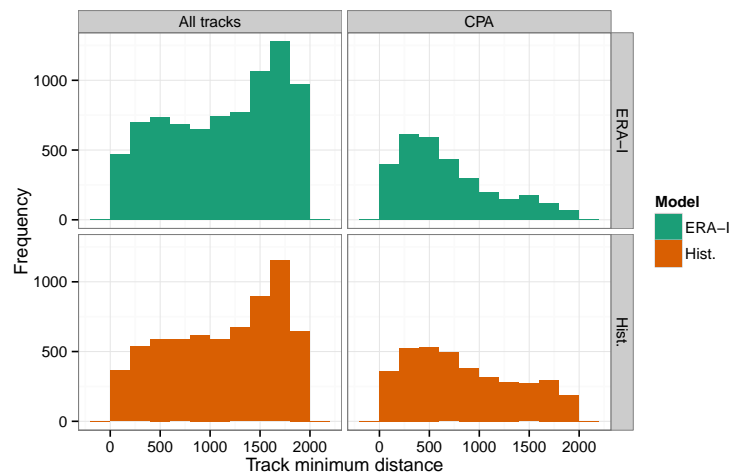


FIGURE 6.11: Histograms of distance to tracks within 2,000km of $55^{\circ}\text{N } 5^{\circ}\text{E}$ at the time of their closest approach. Tracks from ERA-I and HadGEM2-ES are shown. Histograms are shown for “All tracks” (regardless of their association with an England and Wales precipitation event, and for “CPA” tracks, which have been associated with an England and Wales precipitation event by the CPA method.

To investigate the behaviour of cyclone tracks which are associated with high cyclone count events, Figure 6.12 shows the tracks of all cyclones associated with the 10 wettest events in the high- and low- cyclone count precipitation event categories. Figure 6.13 shows the same tracks, for times when they are registered as being associated with an England and Wales precipitation event. In DJF, ERA-I shows predominantly zonal track movements across the North Atlantic, with many cyclones originating in the western North Atlantic. Storms that directly cross the British Isles are concentrated in the central and northern regions, with few tracks travelling to the south. A small number of tracks move northwards towards Iceland in the east North Atlantic, whilst a large number of tracks continue eastward towards the Baltic Sea. By contrast, cyclones in HadGEM2-ES predominantly originate in the east North Atlantic, following a less clearly defined trajectory. This is consistent with the weaker westerly winds found in these cases (Figure 6.10). The formation of intensely precipitating cyclones in the east North Atlantic in HadGEM2-ES is consistent with Dacre and Gray (2009), which identified that many of the most intensely precipitating cyclones that affect the UK are rapidly deepening features originating in this region.

For MAM, JJA and SON, cyclone tracks in ERA-I are less zonal. Tracks which directly cross the British Isles do so at more southerly latitudes than in the DJF cases. This tendency may be consistent with the finding of Hand et al. (2004), that where embedded convection is likely, for example in the summer months, the highest risk of extreme precipitation comes from the northern flank of an extratropical cyclone. Therefore, tracks

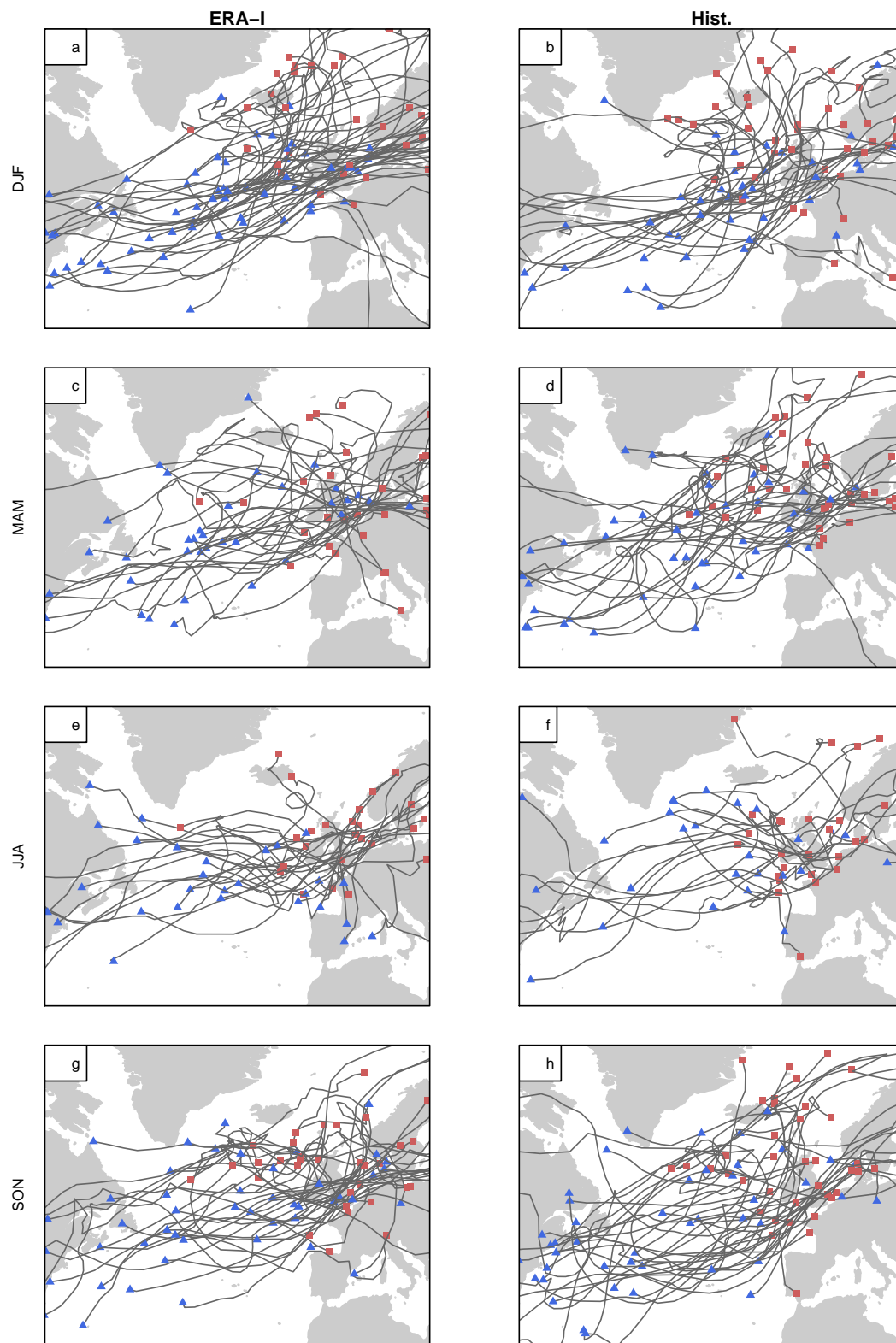


FIGURE 6.12: Cyclones associated with the 10 highest precipitation 7-day accumulation events in the top quartile of cyclone counts for wet & extreme wet events. (a,c,e,g) ERA-I and (b,d,f,h) HadGEM2-ES Historical, for a common period 1980–2005. Cyclogenesis points marked as blue triangles; cyclolysis points marked as red squares.

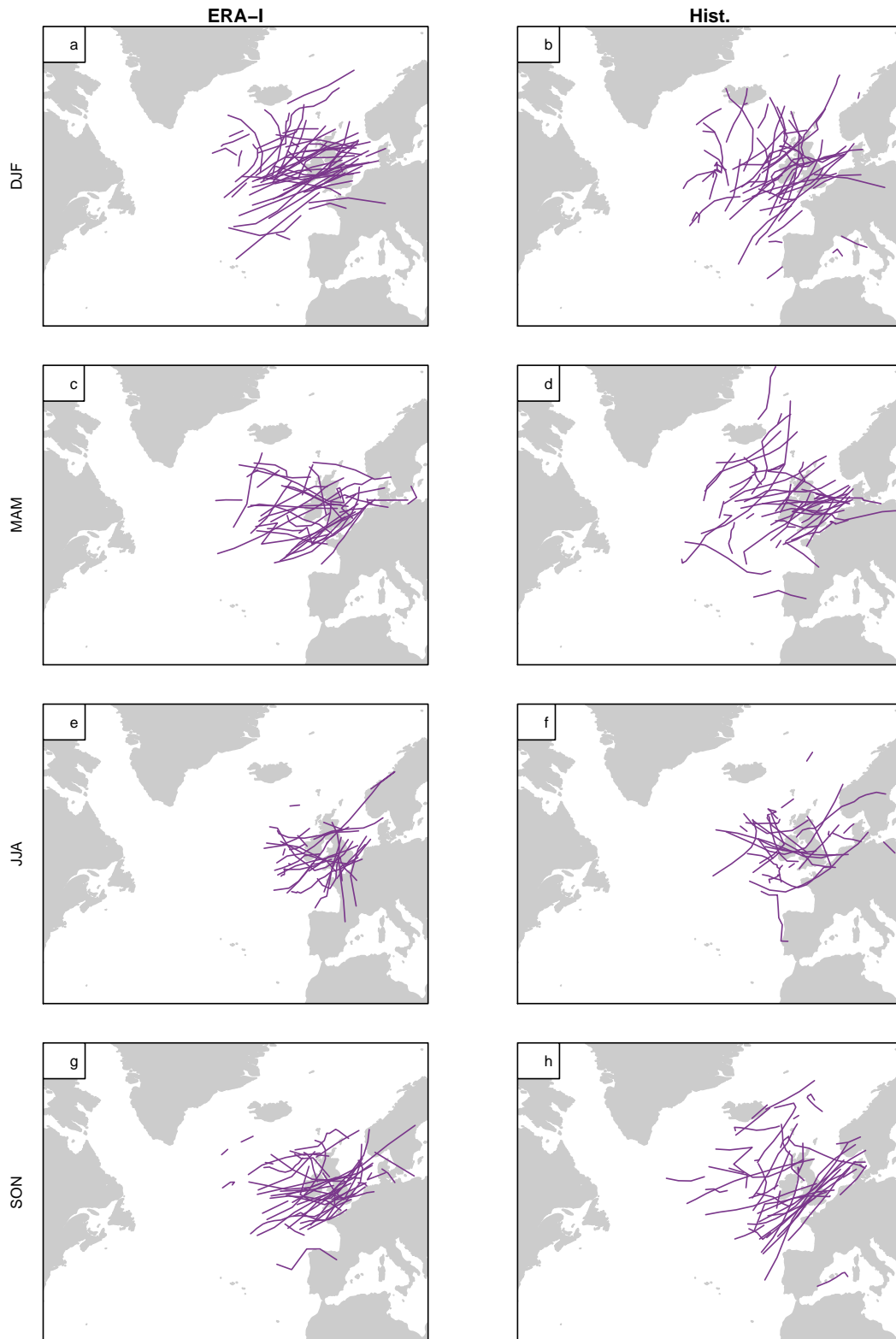


FIGURE 6.13: “Associated” locations of tracks for high cyclone count events with the 10 highest precipitation 7-day accumulation events in the high cyclone count category. (a,c,e,g) ERA-I and (b,d,f,h) HadGEM2-ES Historical, for a common period 1980–2005. Data as per Figure 6.12, locations shown only for times when tracks were associated with an England and Wales precipitation event.

at lower latitudes may be more likely to generate extremes of precipitation across larger parts of the England and Wales region. In HadGEM2-ES, cyclones crossing the British Isles in JJA and SON tend to follow paths further south than those in ERA-I, but track crossings in DJF and MAM are quite evenly distributed. JJA and SON show some evidence of tracks following a curved path across the North Atlantic, with SON also displaying a subset of tracks that originate and/or travel via low latitudes before tracking north-eastwards towards the British Isles. This pattern is conducive to high levels of moisture availability as the cyclone draws warm, humid air north from the tropics.

6.4.3 Stalling in HadGEM2-ES

As discussed in Section 5.3.2, cyclone stalling in association with England and Wales precipitation events is represented by two metrics. Mean residence time per event highlights the overall tendency of all cyclones associated with a precipitation event to stall, whilst the mean of the maximum residence time per event indicates the maximum extent of stalling in a single cyclone per event. The mean of the maximum residence time therefore considers individual cyclones which may have stalled as part of an overall more mobile regime. Both metrics are displayed in Figure 6.14, for ERA-I and HadGEM2-ES Historical, for wet and extreme wet events in a common period 1980–2005. ERA-I shows that mean and maximum residence times are longer for extreme wet than wet events for all seasons at 1- and 7-day accumulation periods, and for JJA at all accumulation periods from 1–31 days.

HadGEM2-ES has longer residence times for all events than ERA-I, which may be related to the slower wind speeds in HadGEM2-ES in the vicinity of the British Isles. However, HadGEM2-ES does not find an increase in mean or maximum residence times per event between wet and extreme wet precipitation events during DJF. Small increases in mean and maximum residence times per event between wet and extreme wet events are found for MAM and SON for 1-day accumulation period events. HadGEM2-ES consistently has higher mean and maximum residence times per event in extreme wet events than in wet events during JJA, for all accumulation periods 1–31 days. Stalling is found to be an important process in the generation of extreme wet events for all seasons at 1- and 7-day accumulation periods in ERA-I, and in JJA for 1–31 day accumulation periods. The maximum cyclone residence time becomes a more important metric than the mean residence time with increasing accumulation period in JJA in ERA-I. For HadGEM2-ES, longer residence times are found in general than in ERA-I, but stalling is only found to be an important process in the generation of extreme events in JJA. In HadGEM2-ES

the relative importance of maximum cyclone residence time per event also increases with increasing accumulation period in JJA, consistent with ERA-I.

Mean wind vectors at 250-hPa are shown for long mean residence time events ($\geq 75^{\text{th}}$ percentile of event mean residence time for both wet and extreme wet events). ERA-I shows, for all seasons, a defined jet stream which defines a curve from the eastern seaboard of north America, north-east towards Greenland/Iceland, and south again towards the British Isles. This curve is most clearly defined in MAM and SON. In DJF, the jet stream is more zonal, but with a pronounced southward deviation in the eastern North Atlantic (whilst the high cyclone count mean wind speed shows a pronounced northward deviation in this area). By contrast, HadGEM2-ES shows a similar situation to the high cyclone count mean (Figure 6.10). This indicates that HadGEM2-ES does not strongly differentiate between situations which lead to high cyclone counts and those which lead to long residence times.

	ERA-I u (ms^{-1})	HadGEM2-ES u (ms^{-1})	HadGEM2-ES overestimation (%)
DJF	23.4	16.7	-28.6
MAM	13.1	17.0	29.6
JJA	11.8	8.0	-32.8
SON	15.4	11.3	-26.9

TABLE 6.8: Long mean residence time wet and extreme wet event mean 250-hPa vector wind speed, 1980–2005, ERA-I and HadGEM2-ES Historical (r2i1p1 ensemble member), for wet and extreme wet events. Spatial mean of data points within the British Isles region.

To demonstrate the movements of long residence time cyclones associated with England and Wales precipitation events, Figure 6.16 shows cyclone tracks from the 10 wettest events from the wet and extreme wet event categories which are associated with long residence time ($\geq 75^{\text{th}}$ percentile of residence time) cyclones. The same tracks are shown for times when they were associated with England and Wales precipitation events in Figure 6.17.

For DJF, ERA generates more zonal cyclone tracks than HadGEM2-ES, corresponding with the stronger zonal 250-hPa wind vectors in ERA-I than in HadGEM2-ES. For both the climate model and reanalysis, cyclogenesis points are spread quite evenly across the North Atlantic, approximately on a line running from the north-east coast of the USA north-west to the British Isles. Cyclolysis in DJF occurs evenly across the eastern North Atlantic. Matching occurs at some distance from the England and Wales region in some

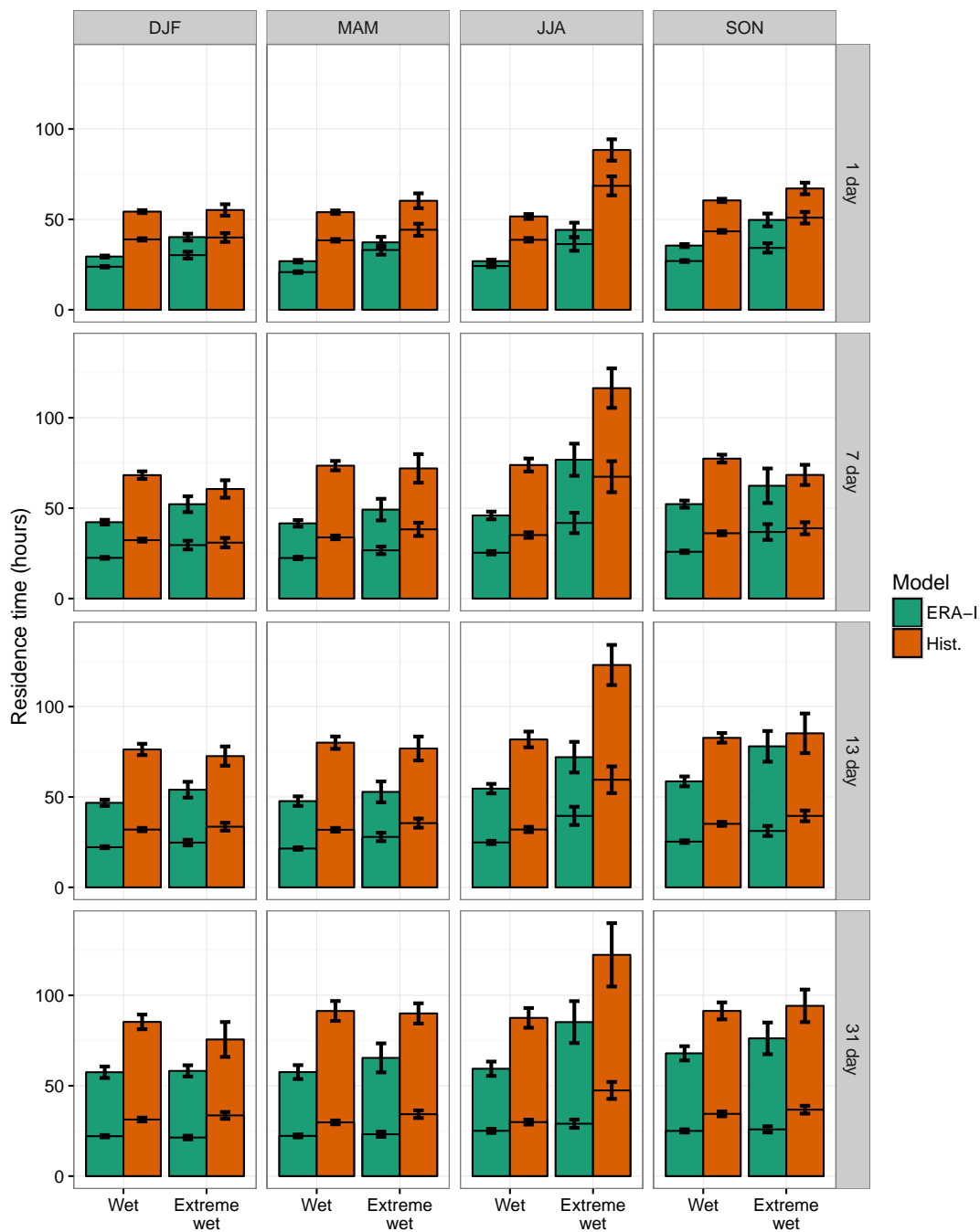


FIGURE 6.14: Means of event maximum residence time (solid colours) and event mean residence time (horizontal lines) in ERA-I and HadGEM2-ES Historical. Error bars are standard error on the mean.

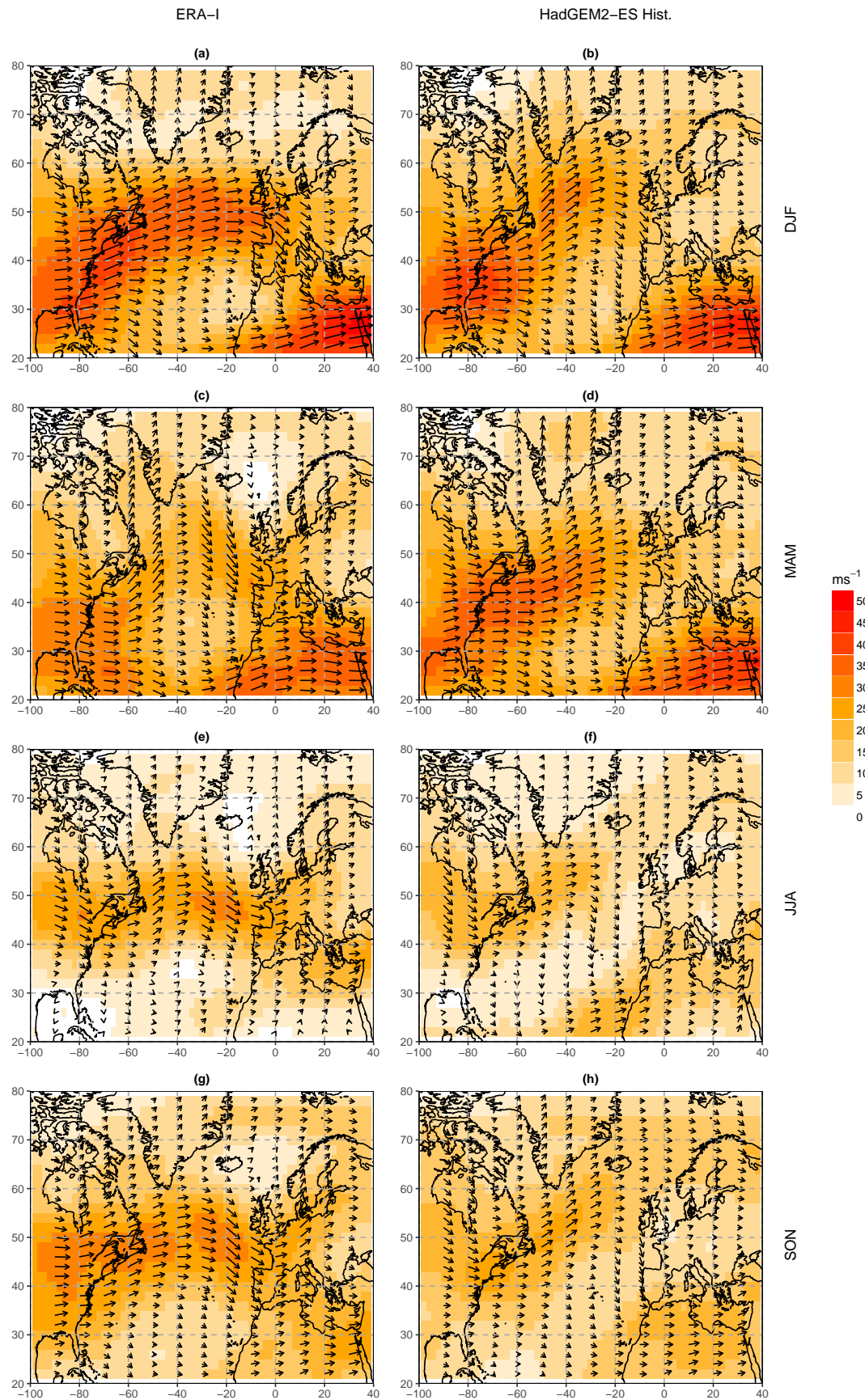


FIGURE 6.15: Mean 250-hPa vector wind speed and direction for days associated with a wet or extreme wet 7-day England and Wales precipitation event, and a high (> 75th percentile) mean cyclone residence time. (Left) ERA-I and (right) HadGEM2-ES Historical experiment (r2i1p1 ensemble member), 1980-2005

cases, suggesting distant storm association by rain bands. A prevalence of matched tracks in both the climate model and reanalysis to the south and west of the British Isles is suggestive of secondary cyclogenesis, with cyclones forming on the fronts of previous storms.

MAM finds more irregular directions of travel in both the climate model and reanalysis, with erratic track movements near the British Isles indicating stalled positions of cyclone centres. In JJA, tracks in both the climate model and reanalysis move approximately west-east before moving erratically in the vicinity of the British Isles.

In JJA, most tracks move directly over the England and Wales region in both ERA-I and HadGEM2-ES, indicating that rainfall in these events is due to the direct impact of the cyclone centre, rather than the fronts of a distant cyclone centre. Both the climate model and reanalysis find that the tracks are associated with England and Wales precipitation events primarily at closer proximity to the England and Wales region than in DJF.

Tracks in SON return to a more zonal nature in both the climate model and reanalysis, with fewer erratic movement patterns. A high density of tracks in ERA-I is found approaching the England and Wales region to the south of Ireland; this is not observed in HadGEM2-ES. Notably, SON tracks in ERA-I have cyclogenesis points to the E/NE of the British Isles, with much cyclogenesis occurring in the Labrador Sea and near the southern tip of Greenland. These cyclogenesis latitudes are much more northern than those observed in DJF, and this pattern is not found in HadGEM2-ES.

6.4.4 Extratropical cyclone precipitation intensity in HadGEM2-ES

Extra-tropical cyclone clustering and stalling have been considered as mechanisms by which extremes of accumulated precipitation may be generated in England and Wales; however, patterns of cyclone movements do not explain every instance of extreme precipitation. ERA-I and HadGEM2-ES have been shown to differ in the mechanisms behind the generation of extreme precipitation in the historical record. Precipitation extremes may be generated by cyclones which do not stall, or form part of a cluster, but simply precipitate intensely over the region. Figure 6.18 shows the mean accumulated precipitation per cyclone associated with precipitation events in ERA-I and HadGEM2-ES.

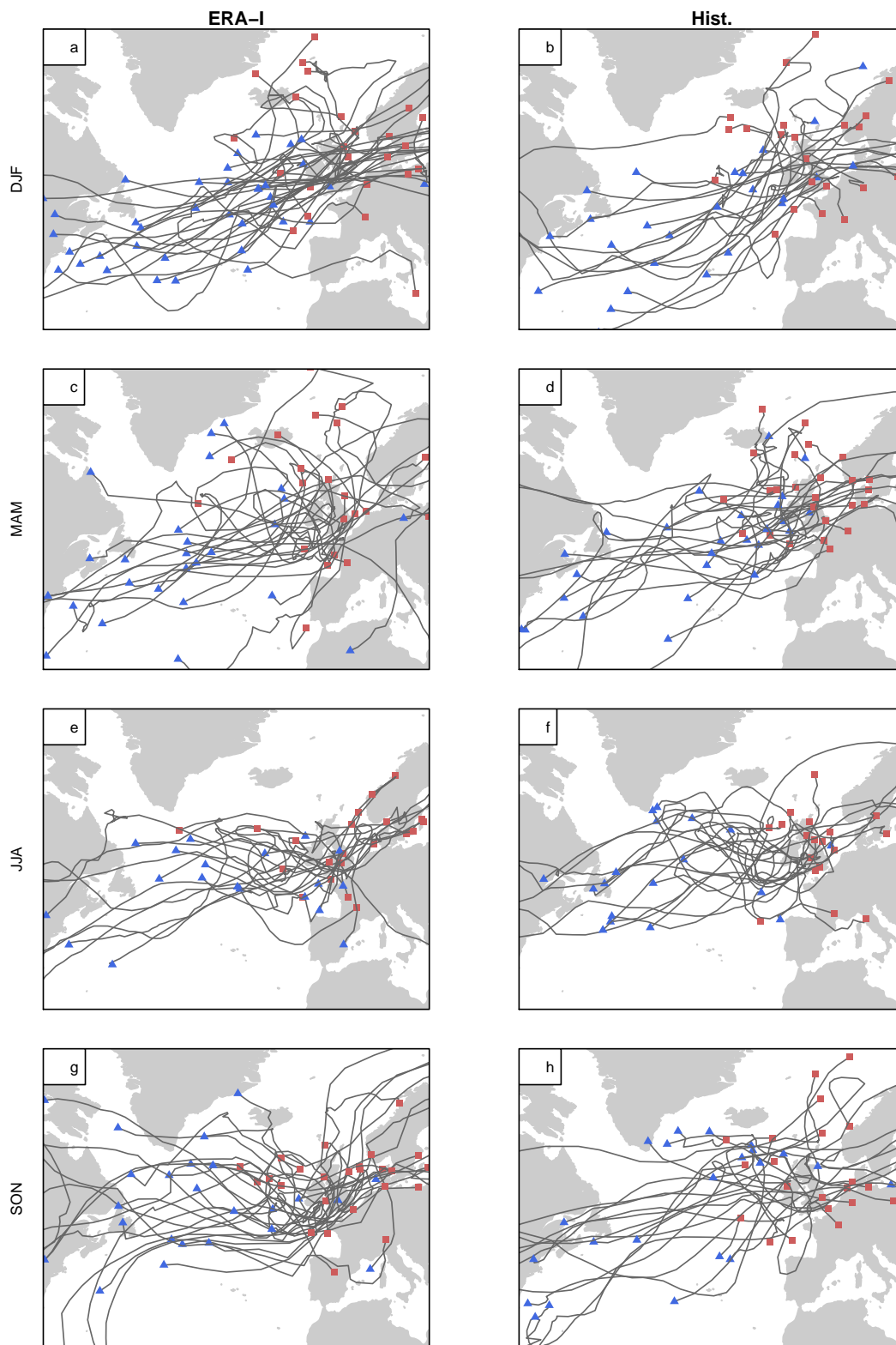


FIGURE 6.16: Full tracks of cyclones associated with the 10 highest precipitation accumulation 7-day events in the high mean residence time category. (a,c,e,g) ERA-I and (b,d,f,h) HadGEM2-ES Historical, for a common period 1980–2005. Cyclogenesis points marked as blue triangles; cyclolysis points marked as red squares.

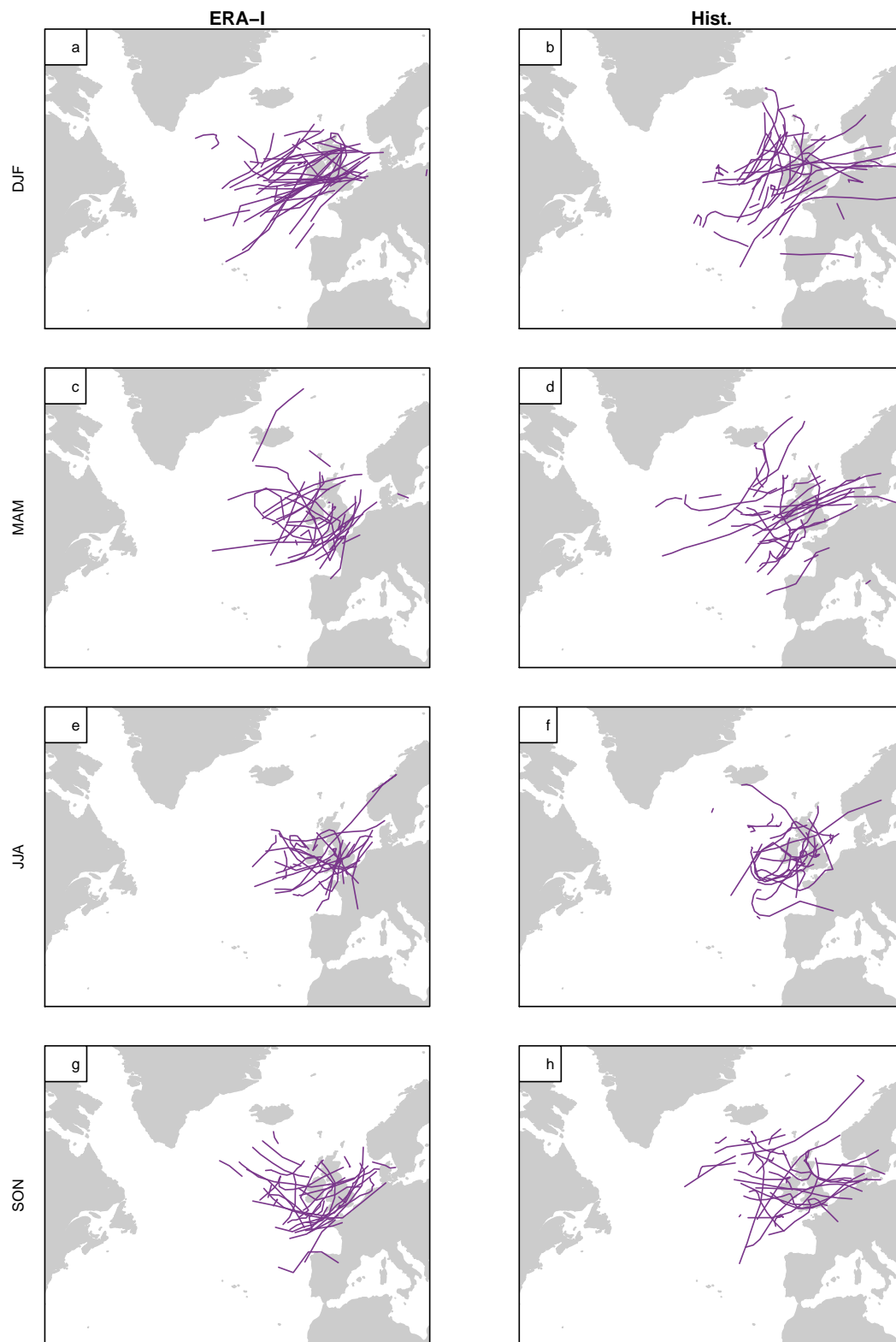


FIGURE 6.17: “Associated” locations of tracks for high mean residence time events with the 10 highest precipitation accumulation 7-day events in the high mean residence time categories. (a,c,e,g) ERA-I and (b,d,f,h) HadGEM2-ES Historical, for a common period 1980–2005. Data as per Figure 6.16, locations shown only for times when tracks were associated with an England and Wales precipitation event.

In DJF, HadGEM2-ES records a larger accumulation of precipitation per cyclone on average than ERA-I, for all accumulation periods, for wet and extreme wet events. In MAM, wet events show a larger accumulation of precipitation per cyclone in HadGEM2-ES than in ERA-I for all accumulation periods, whilst extreme wet events show a larger accumulation of precipitation per cyclone only for 1–7 day accumulation periods. In JJA, the average precipitation per cyclone is slightly reduced in HadGEM2-ES for wet events at all accumulation periods, whilst no systematic change is found for extreme wet events. No systematic change of accumulated precipitation per cyclone is found for wet events in SON, but 1–13 day extreme wet events in HadGEM2-ES have higher precipitation accumulations per cyclone than ERA-I.

Since little systematic difference was found in cyclone counts between HadGEM2-ES and ERA-I, whilst residence times were found to be consistently longer in HadGEM2-ES than ERA-I, these results suggest that where larger volumes of accumulated precipitation per cyclone are identified in HadGEM2-ES, these higher accumulations occur due to the cyclones moving more slowly through the region than is observed in ERA-I. The lack of a consistent sign of difference between HadGEM2-ES and ERA-I in JJA, despite similar cyclone counts and higher residence times in HadGEM2-ES, indicates that a lower precipitation rate is found in summer cyclones associated with England and Wales precipitation events in HadGEM2-ES than in ERA-I.

6.5 Discussion and conclusions

In this chapter we have evaluated the representation of precipitation events in a historical run of HadGEM2-ES, along with the cyclone passages associated with them. ERA-I has been used for comparisons using a common time period, to identify any differences in the representation of extratropical cyclone clustering and stalling associated with England and Wales precipitation events. HadGEM2-ES appears to provide a good representation of England and Wales precipitation events and the North Atlantic storm track, but some differences between HadGEM2-ES and ERA-I have been identified in the importance of clustering and stalling for extreme precipitation events. The key findings of this chapter are summarised as follows:

- Spatially averaged England and Wales precipitation values are similarly distributed between ERA-I and HadGEM2-ES Historical. Both HadGEM2-ES Historical and ERA-I recorded lower mean and 98th percentile precipitation values than EWP, which is considered to be consistent with existing literature concerning climate model and reanalysis precipitation.

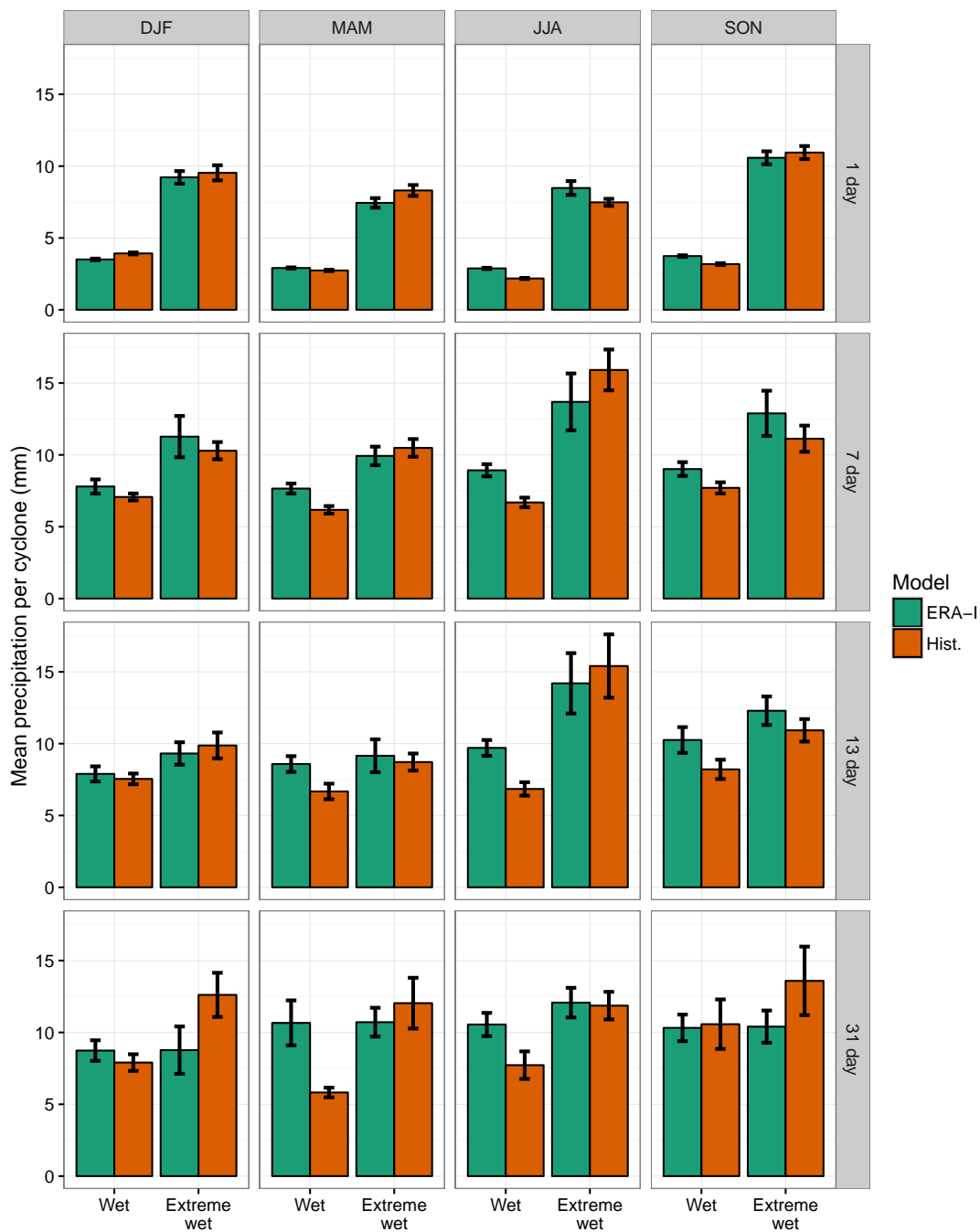


FIGURE 6.18: Mean precipitation per cyclone associated with England and Wales precipitation events, for wet and extreme wet events in ERA-I and HadGEM2-ES Historical. Error bars are standard error on the mean.

- Overall cyclone track spatial distributions highly similar between ERA-I and HadGEM2-ES Historical, particularly in DJF and MAM. HadGEM2-ES Historical has lower cyclone track density than ERA-I in the eastern North Atlantic. Cyclone propagation speeds in the eastern North Atlantic are lower in HadGEM2-ES than in ERA-I, associated with less strong 250-hPa winds.
- Extratropical cyclones matched with England and Wales precipitation events follow similar paths between HadGEM2-ES and ERA-I. Storms associated with extreme England and Wales events are more likely to propagate directly across the England and Wales region in JJA than DJF.
- Higher association rates between England and Wales precipitation events and extratropical cyclones have been found in HadGEM2-ES despite lower overall cyclone count. This is found to be related to HadGEM2-ES associating extratropical cyclones with England and Wales precipitation events at greater distances than in ERA-I.
- Cyclones with long residence times associated with England and Wales precipitation events follow less zonal paths than those associated with high cyclone count events
- Clustering is found to be less important for the generation of extreme precipitation events in HadGEM2-ES, despite higher average cyclone counts associated with precipitation events for all seasons. The situation in HadGEM2-ES Historical is one of lower cyclone mobility associated with extreme England and Wales precipitation events. Although more cyclones tracks are present in HadGEM2-ES Historical, little difference between cyclone counts for wet and extreme wet cases is evident. This appears to be related to a less well defined 250-hPa jet stream position in HadGEM2-ES, which is likely to reduce the frequency at which cyclones transit across the England and Wales region.
- Stalling is found to be less important for the generation of extreme precipitation events in HadGEM2-ES than ERA-I for events in DJF, MAM and SON. Longer residence times are found in HadGEM2-ES for all seasons, which has been linked to slower extratropical cyclone propagation speeds than in ERA-I. In JJA, stalling is found to be important for extreme precipitation events in HadGEM2-ES, with a similar magnitude of change between wet and extreme wet event residence times in both the climate model and the reanalysis.
- Little systematic difference was found between the mean precipitation accumulation per cyclone in ERA-I and HadGEM2-ES, although the precipitation rate from cyclones in JJA was found to be lower in HadGEM2-ES than ERA-I.

Similarities were noted in the representation of seasonal mean cyclone track densities and 250-hPa wind vectors over the North Atlantic in ERA-I and HadGEM2-ES. The distribution of spatially averaged daily precipitation values over the England and Wales region was similar between HadGEM2-ES and ERA-I, although both the climate model and reanalysis recorded lower mean and 98th percentile values than the EWP observational record for the same period.

The behaviour of extratropical cyclones associated with extreme England and Wales precipitation events was found to differ between HadGEM2-ES and ERA-I. HadGEM2-ES appears to generate extreme England and Wales precipitation events through increased cyclone precipitation intensity, with little change to the cyclone count or residence times (except in JJA). Stalling was, however, found to be an important factor in JJA extreme England and Wales precipitation events, with a similar magnitude of response of mean and maximum residence times between wet and extreme wet events in HadGEM2-ES and ERA-I. The weak response of cyclone counts to extreme precipitation events may be associated with the weaker synoptic-scale wind conditions identified in HadGEM2-ES than in ERA-I.

In the next chapter, we will analyse the response of clustering and stalling behaviour and England and Wales precipitation events to the RCP8.5 scenario in HadGEM2-ES. This will highlight the extent to which clustering and stalling behaviour response to changes in the large-scale set-up under a future climate change scenario.

Chapter 7

Climate change projection of clustering, stalling, and England and Wales precipitation events

7.1 Introduction

In this chapter a single ensemble member of the HadGEM2-ES RCP8.5 experiment is evaluated. Using the same techniques applied to ERA-I and the HadGEM2-ES Historical experiment in Chapters 5 & 6 respectively, this chapter aims to investigate changes in the importance of extratropical cyclone clustering and stalling to England and Wales precipitation events under a high emissions scenario in HadGEM2-ES in the last twenty years of the twenty-first century. Analysis of physical processes behind changes in climate model projections is essential to more clearly understand the manner in which the future climate may change. The RCP8.5 experiment was selected for this evaluation as this contains the strongest forcings, and therefore the largest climate response, of any of the CMIP-5 experiments. The r1i1p1 ensemble member was selected as, at the time of analysis, complete sub-daily wind and precipitation data were not available for any other ensemble member.

In this chapter, HadGEM2-ES RCP8.5 data is compared with and contrasted against HadGEM2-ES Historical data to highlight projected changes in the climate system under a high radiative forcing scenario. Twenty-year periods in both models have been selected, covering 1980–1999 and 2080–2099 in the Historical and RCP8.5 experiments respectively, and hence windows of identical length with separation of one century. Note

that these time windows differ from those used in earlier chapters, due to data availability constraints.

7.2 England and Wales precipitation in HadGEM2-ES RCP8.5

Histograms of daily precipitation in HadGEM2-ES Historical and RCP8.5 experiments are shown in Figure 7.1. Data were spatially averaged over the England and Wales region (Chapter 3; Rhodes et al. 2015). Data are included for all days of ≥ 1 mm precipitation (“wet days”).

In Figure 7.1, the RCP8.5 experiment produces increased mean and 98th percentile precipitation values for all seasons. Percentage increases in HadGEM2-ES RCP8.5 relative to Historical are shown in Table 7.1. Daily precipitation in the RCP8.5 experiment is increased for all seasons, with the greatest increase in mean daily precipitation being found in DJF, MAM and SON. Similar increases in 98th percentile precipitation are

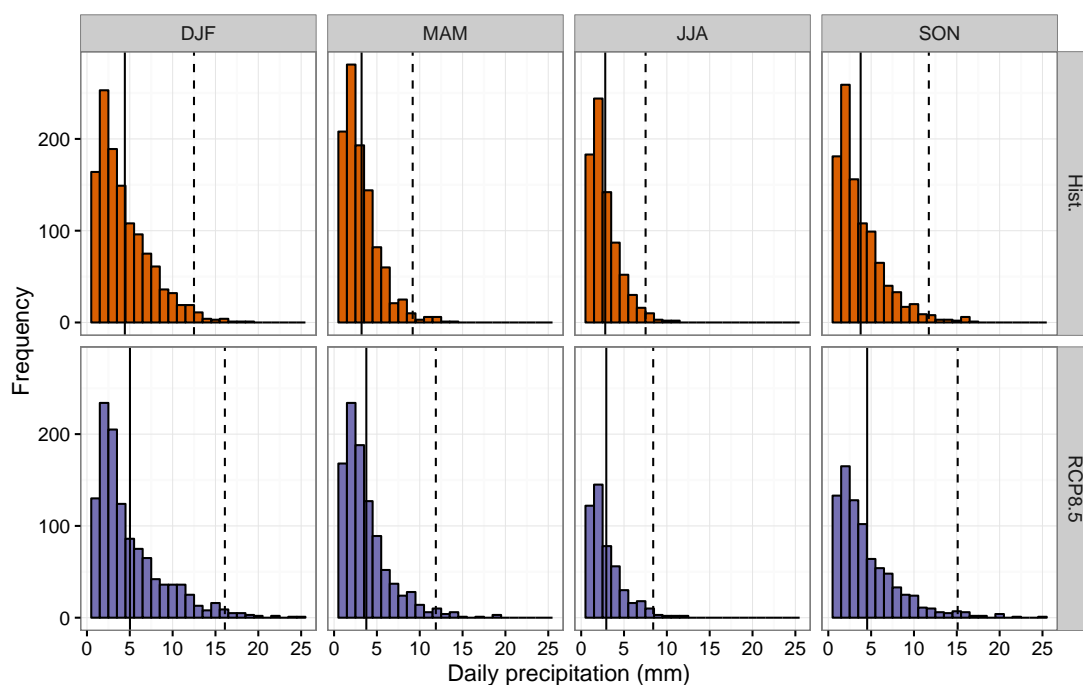


FIGURE 7.1: Histograms of daily England and Wales precipitation accumulation for wet days (> 1 mm precipitation) in HadGEM2-ES Historical r2i1p1 (top) and HadGEM2-ES RCP8.5 r1i1p1 (bottom). Solid black line indicates mean. Dashed black line indicates 98th percentile. Model precipitation is averaged over a box bounded by 8.75°W–3.25°E, 49°N–55.5°N (England and Wales region, Rhodes et al. 2015). Data are taken from 20-year periods 1980–1999 (Historical) and 2080–2099 (RCP8.5).

Season	Mean (%)	98 th percentile (%)
DJF	13.5	28.9
MAM	17.2	29.5
JJA	4.3	11.8
SON	20.1	28.7

TABLE 7.1: Percentage increase in mean and 98th percentile values of daily precipitation in HadGEM2-ES RCP8.5 (r1i1p1) relative to HadGEM2-ES Historical (r2i1p1). Data included for 1980–1999 (Hist.) and 2080–2099 (RCP8.5).

found in DJF, MAM and SON. However, the number of days with < 1 mm precipitation increases for DJF, JJA and SON, with a smaller decrease in dry day frequency in MAM, as shown in Table 7.2. The overall increase in dry day frequency combined with an increase in mean and 98th percentile daily precipitation accumulations indicates that rainfall accumulations are occurring in less frequent, more intense events.

Season	Historical %	RCP8.5 %	% change
DJF	29.5	33.4	13.0
MAM	42.2	42.0	-5.4
JJA	57.2	71.7	19.1
SON	43.9	51.4	11.3

TABLE 7.2: Dry day frequency (< 1 mm precipitation) in HadGEM2-ES Historical and RCP8.5 experiments, 1980–1999 and 2080–2099 respectively.

For further analysis of England and Wales precipitation events, data were accumulated into 1-, 7-, 13- and 31-day periods and analysed with the Peaks-Over-Threshold method as described in Chapter 5. The minimum recorded values for an “extreme wet” event in HadGEM2-ES Historical and RCP8.5 are recorded in Table 7.3. Minimum values for extreme wet events are found to increase in RCP8.5 for DJF, MAM and SON, with a small decrease in JJA. Since the daily p98 precipitation values (Table 7.1) indicate an increase in extreme event intensity for all seasons, this indicates that extreme event anomalies are highly sensitive to the definition of “extreme”.

The projected increase of precipitation accumulations identified here in the RCP8.5 scenario are consistent with the majority of literature on the subject. Held and Soden (2006) identifies a robust increase in global precipitation volumes in a simple climate model under a warmer climate, whilst Beniston et al. (2007) and Lehtonen et al. (2014) find a large amount of uncertainty in projected precipitation over western Europe, with northern regions becoming wetter and southern regions becoming drier, and high uncertainty over the central region between these two regions of large projected changes. In Held and Soden (2006), the increase in precipitation is directly associated with the Clausius Clapeyron effect. Studies using more advanced climate models have found large

Season	Model	“Wet” minimum	“Extreme wet” minimum
DJF	Historical	2.2	10.7
	RCP8.5	2.2	13.1
MAM	Historical	1.3	7.1
	RCP8.5	1.4	9.0
JJA	Historical	0.7	5.6
	RCP8.5	0.3	5.2
SON	Historical	1.3	8.8
	RCP8.5	0.9	10.3

TABLE 7.3: Minimum values of total daily precipitation accumulation in $mm\ d^{-1}$ by season for wet and extreme wet events in HadGEM2-ES Historical and RCP8.5 experiments, one-day accumulations

uncertainties associated with regional precipitation projections, as dynamical influences in the extra-tropical storm tracks vary greatly by model and climate scenario (Harvey et al., 2014, 2015). However, a significant increase in DJF precipitation over the British Isles in the CMIP5 models under the RCP4.5 scenario is identified by Zappa et al. (2013b). Zappa et al. (2013b) also finds that the source of precipitation in extratropical cyclones in the North Atlantic DJF storm track changes under RCP4.5, with precipitation coming predominantly from more intense storms, and fewer weakly precipitating storms being identified. Changes in JJA precipitation are found to be smaller and more uncertain amongst the CMIP5 models.

7.3 Projected changes to the North Atlantic storm track

As identified in Section 7.2, precipitation accumulations are projected to change over England and Wales under the RCP8.5 scenario. Processes causing changes to precipitation due to a warmer climate can be broadly divided into two categories: dynamical and thermodynamic. Dynamical processes include changes to the location and intensity of the storm tracks, for example due to changing equator-pole temperature gradients, whilst thermodynamic processes increase the saturation vapour pressure proportionately with increasing air temperature. Changes in precipitation in the future climate involve the interaction of dynamical and thermodynamic phenomena. In this section, projected changes both to the North Atlantic storm track and to the major sources of moisture for England and Wales precipitation events are evaluated, which may explain the changes in England and Wales precipitation accumulations.

7.3.1 Seasonal mean vector winds

The location and intensity of the North Atlantic storm track is influenced to a great extent by the 250-hPa jet stream. Seasonal mean vector winds at 250-hPa for HadGEM2-ES Historical and RCP8.5 are shown in Figure 7.2, to indicate differences in the mean states of both models. RCP8.5 shows an intensification of the mean North Atlantic jet wind speeds in DJF. The mean state of the 250-hPa jet stream is found to be slightly elongated and intensified in DJF, in agreement with the intensified and elongated DJF jet projected by the CMIP5 multi-model mean (Zappa et al., 2013b). Changes in the jet stream during MAM, JJA and SON are smaller in RCP8.5 than for DJF; this is also expected per the CMIP5 multi-model mean.

The differences between RCP8.5 (2080–2099) and Historical (1980–1999) in HadGEM2-ES are demonstrated clearly in Figure 7.3. These anomaly plots highlight the small mean changes in 250 hPa wind speed near the British Isles for most seasons, with a slight increase (up to 7.5 ms^{-1}) over the British Isles in DJF.

7.3.2 Mean 250-hPa winds associated with extreme England and Wales precipitation events in RCP8.5

Mean 250-hPa wind vectors are shown in Figure 7.4 for one-day events identified as “extreme wet” by the Peaks-Over-Threshold method discussed in Chapter 3. Intensification of the jet is evident in all seasons in the RCP8.5 scenario relative to the Historical experiment. In DJF, the jet is strongly intensified in RCP8.5 relative to Historical, with strong mean wind speeds directly over the British Isles. In MAM, JJA and SON, stronger wind speeds are projected in RCP8.5 than in the Historical experiment, and evidence of the wave pattern identified in Chapter 5 is more prominent. The eastward extension and intensification of the jet is consistent with the conditions found by Priestley et al. (2016) to be conducive to clustering of extratropical cyclones near the UK, as defined by over-dispersion relative to a fixed rate Poisson process.

The intensification of 250-hPa wind speeds for all seasons is highlighted in Figure 7.5. An intensified cyclonic flow near the British Isles is identified for all seasons, with particularly intensified zonal flow south-westerly flow identified near the British Isles in DJF and SON. Enhanced winds of this nature may act to draw moist air from the tropical Atlantic, suggesting a mechanism for the increased 98th percentile precipitation in these seasons. When compared with the seasonal 250-hPa wind anomalies in Figure 7.3, a great deal of intensification is identified for days with extreme precipitation in England and Wales over that which is observed in the seasonal mean synoptic situation.

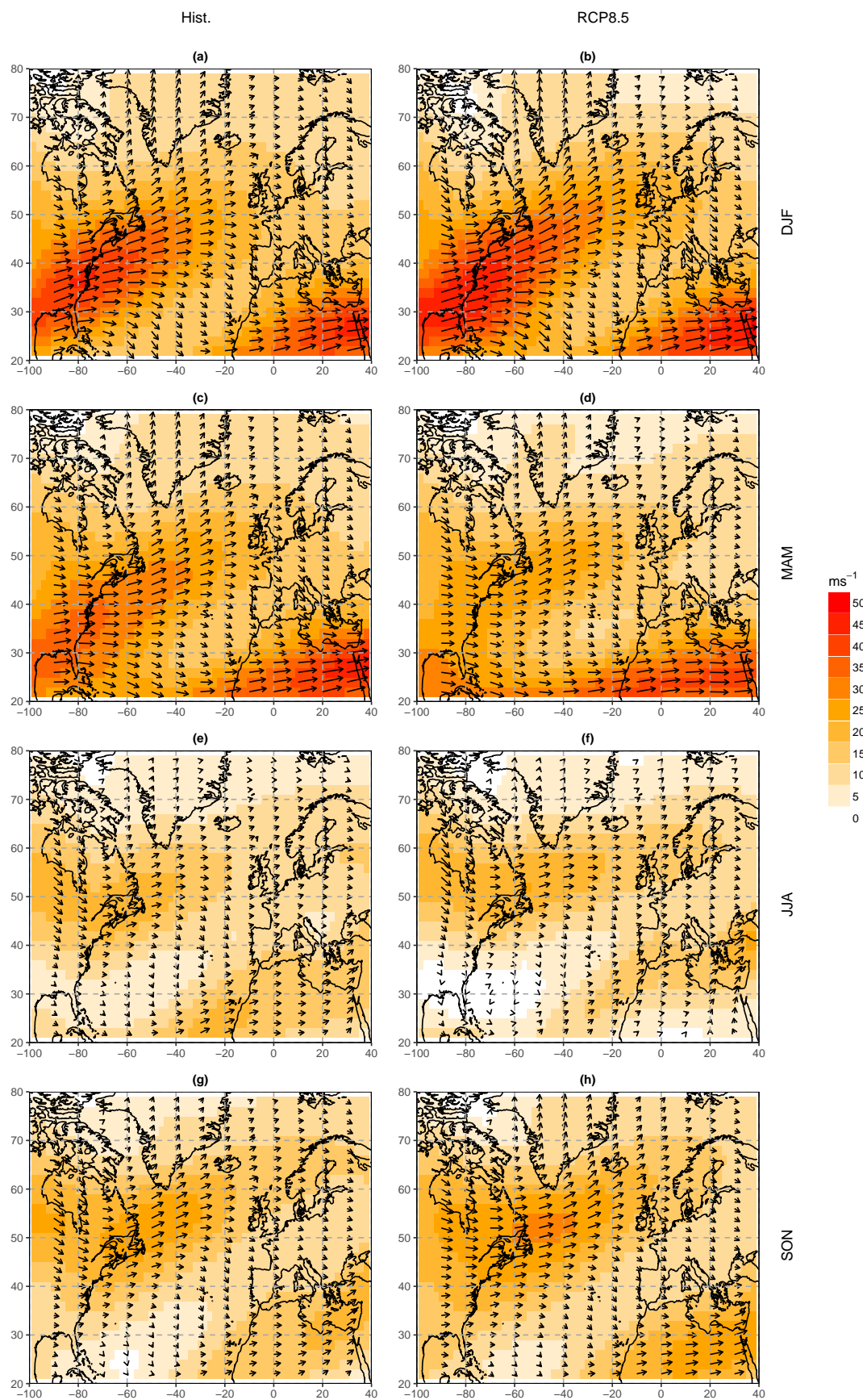


FIGURE 7.2: Seasonal mean 250-hPa vector wind intensity and direction in (left) HadGEM2-ES Historical (1980–1999) and (right) HadGEM2-ES RCP8.5 (2080–2099).

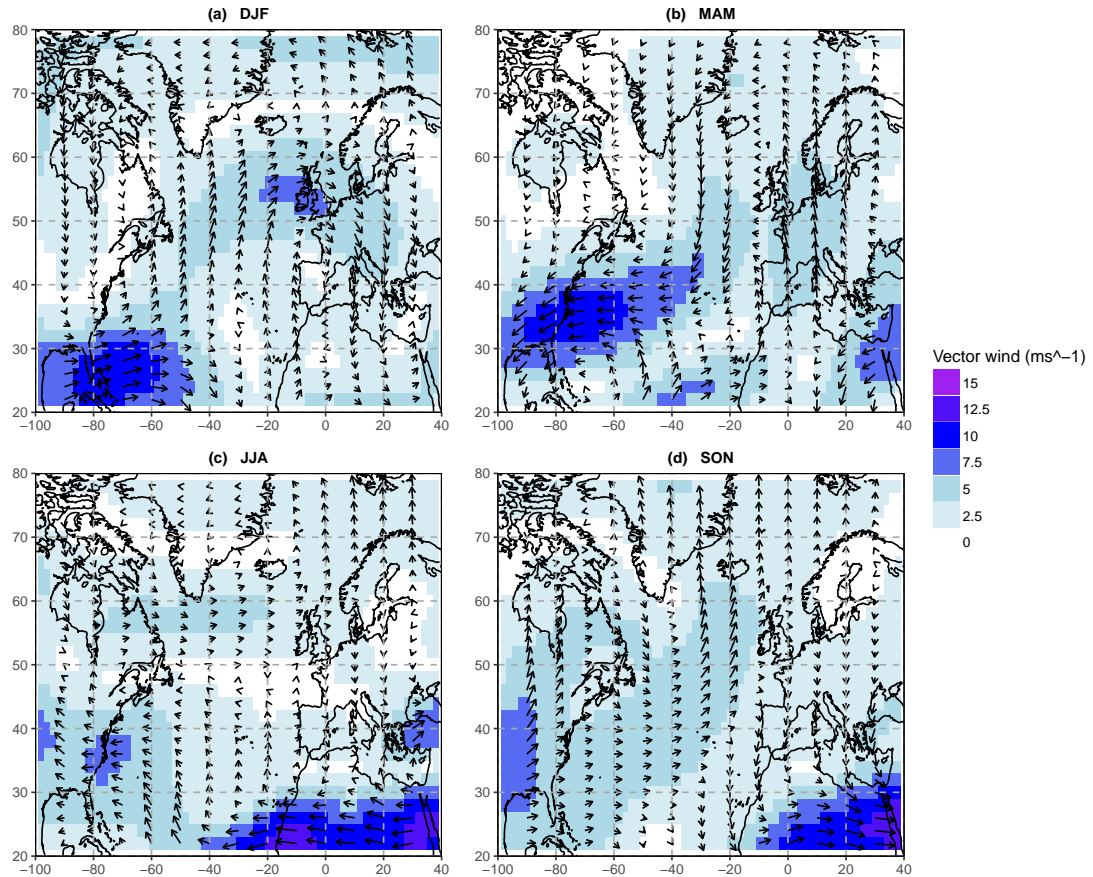


FIGURE 7.3: Anomaly of seasonal mean 250 hPa winds, RCP8.5 2080–2099 minus Historical 1980–1999.

7.3.3 Frequency and propagation speed of North Atlantic Storms

Track density anomalies in the North Atlantic region for HadGEM2-ES RCP8.5 (2080–2099) against Historical (1980–1999) are shown in Figure 7.6. A reduction in cyclone frequency is evident in DJF throughout the main storm track region, with notable decreases evident near the eastern seaboard of North America and in the lee of Greenland. Reduction in cyclone frequency in these locations is notable as these form the main cyclogenesis regions in the North Atlantic. In MAM, a reduction in cyclone track frequency near Iceland is found in the RCP8.5 scenario. In JJA and SON a large increase in cyclone frequency is found near the east coast of Greenland and over Iceland. In JJA, this appears to be related to a reduction in cyclone frequency at lower latitudes, indicating a poleward shift of the storm track, consistent with Yin (2005) and Berry et al. (2011).

Table 7.4 displays the frequency of unique tracks propagating through the British Isles

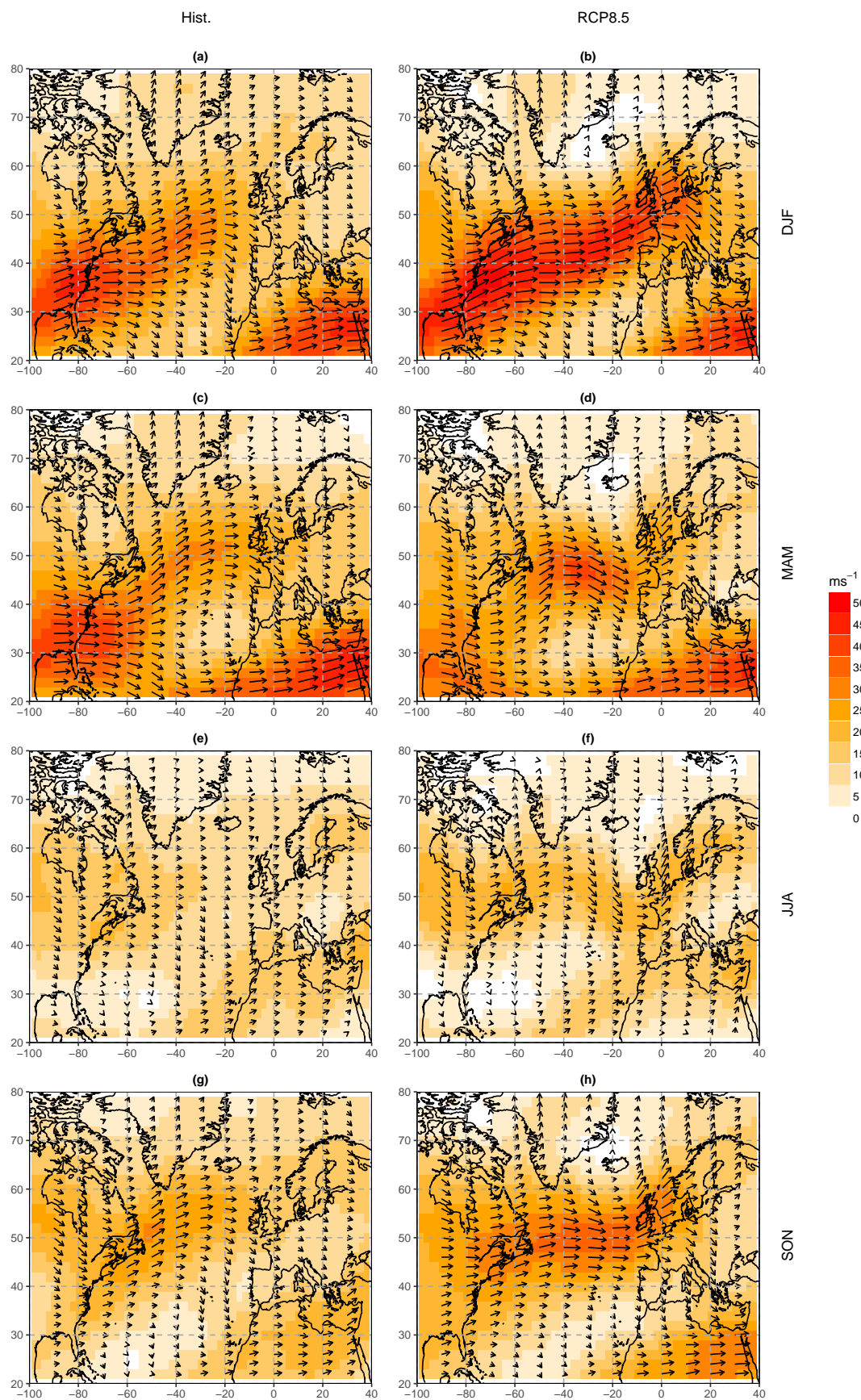


FIGURE 7.4: Extreme wet England and Wales precipitation event mean 250-hPa vector wind intensity and direction in (left) HadGEM2-ES Historical (1980–1999) and (right) HadGEM2-ES RCP8.5 (2080–2099).

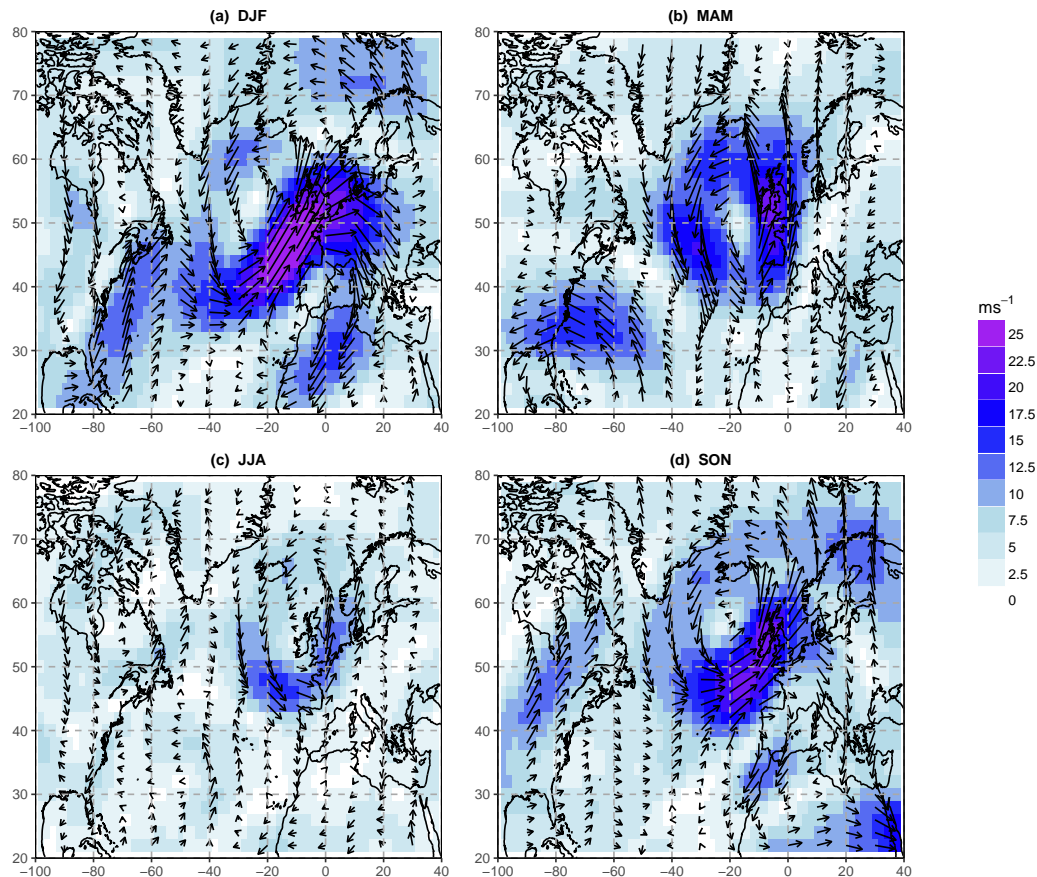


FIGURE 7.5: Anomaly of extreme wet event 250 hPa mean winds, RCP8.5 2080–2099 minus Historical 1980–1999.

region (see green circles marked on Figure 7.6). Small reductions in frequency are identified in DJF, JJA and SON; however, a large amount of noise is present in Figure 7.6. Storm track density is also highly sensitive to the size and location of the search area. The cyclone track density anomalies identified in Figure 7.6 compare favourably with the CMIP5 mean RCP8.5 track density anomaly patterns identified by Zappa et al. (2013b) (see Figure 1.11).

The frequency distribution of cyclone propagation speeds, sampled as the track passes through the “British Isles” search radius (see Figure 7.6, green circle), is shown in Figure 7.7. Very similar distributions are found for all seasons when compared with the Historical experiment. Changes in the mean propagation speed are small, with the largest changes in mean propagation speed found in DJF and JJA, with a 7% increase in both seasons (see Table 7.4).

The changes in cyclone track frequency in the North Atlantic are broadly consistent

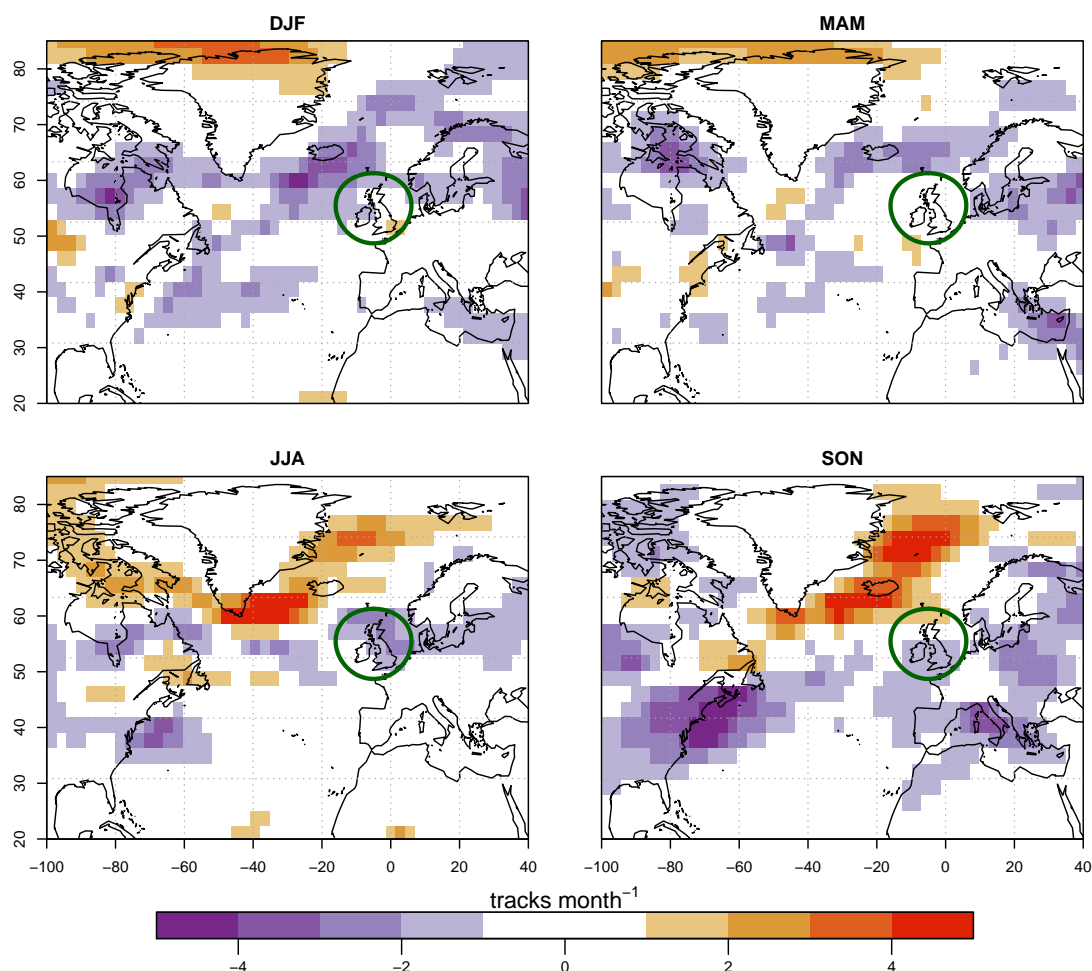


FIGURE 7.6: Storm track density anomaly for HadGEM2-ES RCP8.5 r1i1p1 against HadGEM2-ES Historical r2i1p1, for 20-year periods 1980–1999 (Hist.) and 2080–2099 (RCP8.5). Track density was calculated as frequency of unique cyclone tracks on a 2.5° spherical cap using spherical kernel estimators. Storm tracks identified using the Hodges (1995) method on ξ_{850} . Data interpolated to 2.5° longitude-latitude grid. “British Isles” region indicated by green circle.

with the current literature. JJA and SON exhibit a poleward shift in the storm track, as identified in several climate model evaluations. Held (1993) identified a poleward shift in the storm tracks as a result of a weakening equator-pole temperature gradient in a simple climate model, and this phenomenon was identified in the CMIP3 coupled climate models by Yin (2005). Harvey et al. (2014) identified the equator-pole temperature gradient to be influential in both the lower- and upper-troposphere for changes to the storm track in JJA. In DJF, an overall reduction in cyclone frequency in the North Atlantic is identified in HadGEM2-ES. The reduction in cyclone frequency near Iceland is consistent with the multi-model mean RCP8.5 response identified in CMIP5 models by Zappa et al. (2013b), and thorough review of existing studies of projected changes to the extratropical storm tracks by Ulbrich et al. (2009). However, the small

Season	Model	Track frequency (month ⁻¹)		Mean propagation speed (km h ⁻¹)	
DJF	Historical	7.3		36.4	
	RCP8.5	6.6	(-8.3%)	39.0	(+7%)
MAM	Historical	5.5		31.1	
	RCP8.5	5.5	(0%)	31.3	(+1%)
JJA	Historical	4.7		25.2	
	RCP8.5	3.9	(-15.2%)	26.9	(+7%)
SON	Historical	5.6		33.0	
	RCP8.5	5.4	(-3.6%)	33.7	(+2%)

TABLE 7.4: Frequency and mean propagation speed of unique cyclones propagating through the British Isles region. Figures in brackets indicate the percentage difference between Historical and RCP8.5 experiments (positive values indicate higher track frequency or mean propagation speed in RCP8.5 than Historical).

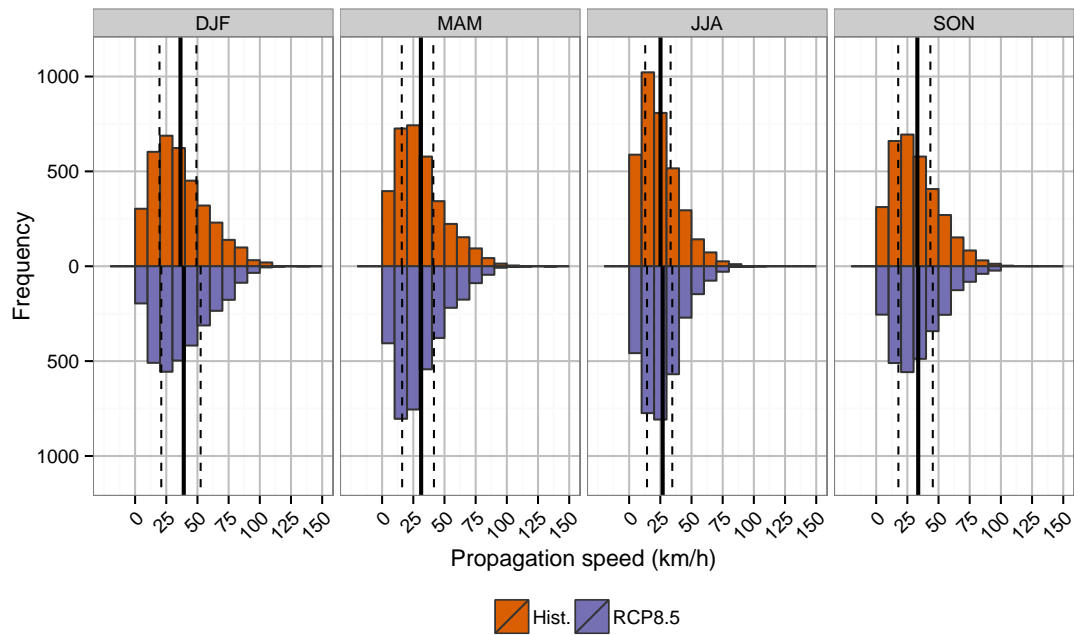


FIGURE 7.7: Histograms of track speed for all tracks identified within a box bounded by 20°W - 10°E and 48°N - 65°N (eastern North Atlantic region). HadGEM2-ES Historical r2i1p1 (above line), HadGEM2-ES RCP8.5 r1i1p1 (below line). Data analysed for a 20-year periods 1980–1999 (Hist.) and 2080–2099 (RCP8.5). Means are marked as solid black line, quartiles are marked as dashed black lines. Samples are binned to 10 km/h intervals and displayed back-to-back for comparison.

increase in cyclone frequency over the British Isles identified by Zappa et al. (2013a) is not evident in the single-model analysis presented here. Harvey et al. (2014, 2015) identifies a large spread in DJF storm track projections with the CMIP3 models, identifying the magnitude of the lower-tropospheric equator-pole temperature gradient as

the primary influence on northern hemisphere DJF storm track location. Zappa et al. (2013a) identifies HadGEM2-ES as one of the CMIP5 models that best represents the tilt of the North Atlantic storm track with respect to reanalysis (see Figure 1.12, model 13).

Storm intensity in HadGEM2-ES (as measured by maximum ξ_{850} or minimum MSLP) is not evaluated here; however, Della-Marta and Pinto (2009) finds a very large increase in storm intensity in the CMIP3 A1B and A2 scenarios in a region covering the British Isles, North Sea and Western Europe, as measured by changing return periods of storms in the 95th percentile of maximum ξ_{850} (no change in intensity as measured by minimum MSLP is identified). However, changes in the dynamical intensity of extra-tropical cyclones do not directly relate to changes in precipitation accumulations, and there is a great deal of variability in projected changes to precipitation accumulations over the western Europe region (Stocker et al., 2013).

7.3.4 Thermodynamic changes in the North Atlantic

As described by Held and Soden (2006), precipitation under a warming climate is projected to increase globally due to increased availability of atmospheric water vapour, as described by the Clausius-Clapeyron relationship. Although the global increase in precipitation is a robust feature of climate model projections, there is a large amount of regional uncertainty (Stocker et al., 2013). Increased saturation vapour pressure (e_s) with increased temperature does not necessarily correspond to increased atmospheric water vapour content, nor does increased atmospheric water content necessarily correspond to increased precipitation. In Section 7.2 we identified strong projected increases in mean and p98 England and Wales wet day precipitation accumulations for DJF, MAM and SON, and a weak projected increase in mean and p98 England and Wales wet day precipitation accumulations for JJA. As track density near the British Isles is projected to decrease or stay the same for all seasons (Figure 7.6 and Table 7.4), the precipitation accumulation per extratropical cyclone, or the number/intensity of convective storms, must increase.

Air temperature and relative humidity anomalies in HadGEM2-ES RCP8.5 relative to Historical are shown in Figure 7.8 (a,b) and (c,d) respectively. Air temperature is effectively directly proportional to saturation vapour pressure in Earth's atmosphere at approximately $7\%^\circ\text{C}^{-1}$ (Held and Soden, 2006). This implies that the spatial pattern of temperature increase in Figure 7.8 (a,b) is analogous with the spatial pattern of

saturation vapour pressure increase. For DJF, a very strong temperature anomaly is found over the Arctic and northern Canada, representing the weakening equator-pole temperature gradient associated with a poleward shift and/or weakening of the northern hemisphere storm tracks (Held, 1993; Yin, 2005; Harvey et al., 2014). DJF temperature anomalies are smallest over the North Atlantic, particularly near the Norwegian Sea; however, the anomaly is always positive in the North Atlantic region, by a minimum of 1°C. In JJA, the strongest temperature anomalies are found at lower latitudes than in DJF, over continental Europe and North America. The average temperature anomaly over the North Atlantic is slightly higher than in DJF. These anomalies indicate that for both DJF and JJA, the potential for moisture availability over the North Atlantic

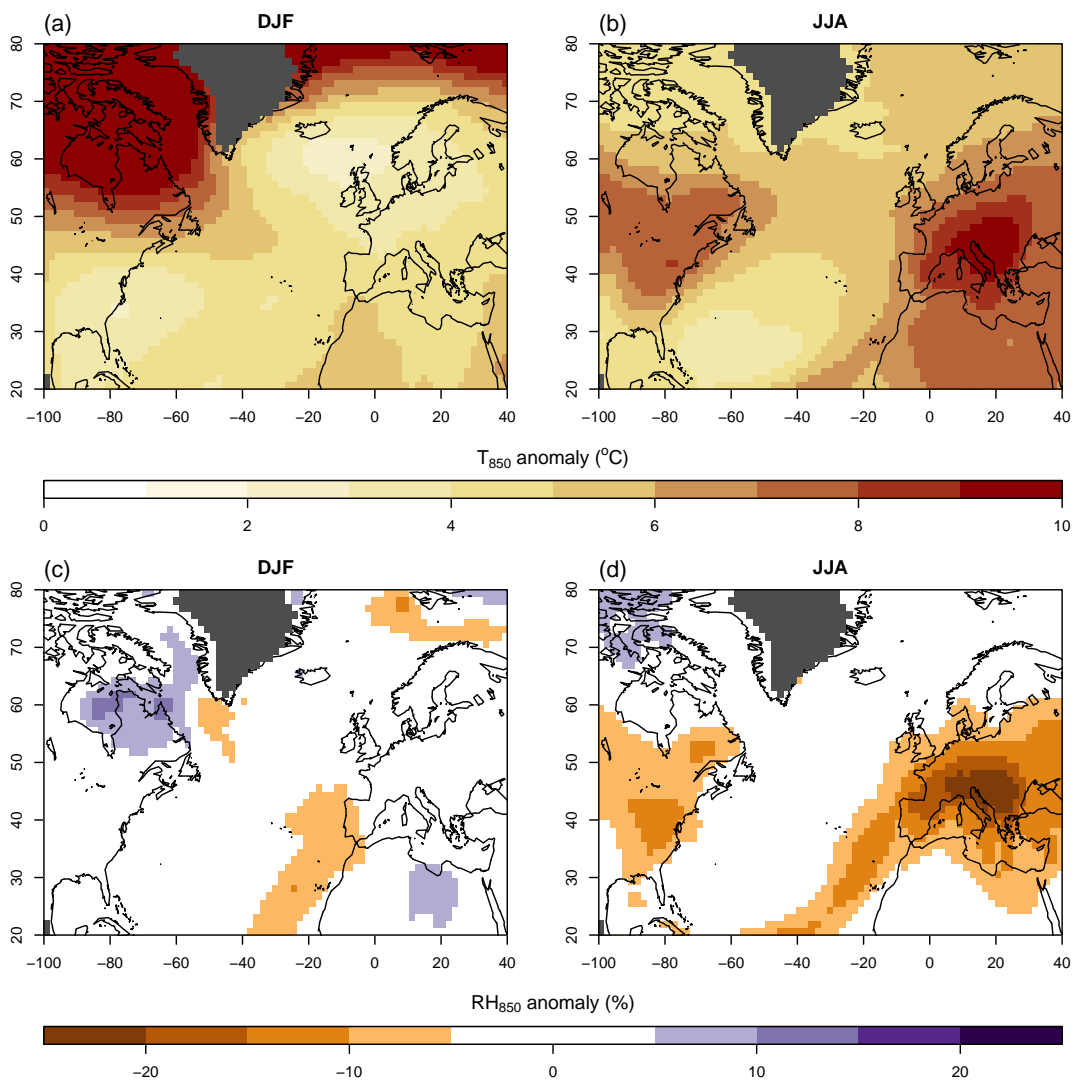


FIGURE 7.8: Anomaly plots of (a,b) 850-hPa air temperature; (c,d) 850-hPa relative humidity; HadGEM2-ES RCP8.5 minus Historical, 2080–2099 and 1980–1999 respectively. Regions where orography intersects with the 850 hPa pressure level are masked in grey. Relative humidity anomalies of magnitude < 5% are omitted for clarity.

increases.

Figure 7.8 (c,d) shows that relative humidity does not vary evenly with temperature. In particular, JJA shows a relative drying of the air (with respect to saturation vapour pressure) over continental Europe and the eastern North Atlantic. This indicates that, despite the atmosphere's increased ability to hold water vapour in the RCP8.5 scenario, moisture availability for some storms which affect England and Wales may not increase. The reduced relative humidity in JJA over coastal western Europe and on a trajectory south-westward from the British Isles is particularly noteworthy. de Leeuw (2014) identified these regions as important sources of atmospheric moisture for summer precipitation events in the UK. The low relative humidity in these regions in RCP8.5 may therefore account for some of the projected reduction in England and Wales JJA precipitation accumulations. By comparison, weak projected relative humidity anomalies are found over the North Atlantic and Europe in DJF, indicating that available moisture scales broadly as expected with projected increases in temperature for DJF.

7.3.5 Relationship between precipitation changes and storm track dynamics

In Figure 7.1, increases in mean and p98 daily precipitation accumulation were noted in all seasons, with the strongest increase found in DJF and the weakest increase in JJA, consistent with the multi-model analysis of CMIP5 climate models by Zappa et al. (2013b). Both DJF and JJA show increases in dry day frequency in England and Wales (+13% and +19% respectively). Large uncertainty is known to exist in projected precipitation changes in the central latitudes of western Europe (Stocker et al., 2013), particularly in the summer months (Zappa et al., 2013b), and precipitation projections in this region are highly sensitive to the location and intensity of the North Atlantic storm track in climate models.

In DJF, the British Isles region is associated with an 8% decrease in extratropical cyclone frequency (Figure 7.6) and 7% increase in mean cyclone propagation speed (Table 6.5). Projected DJF temperature rises by approximately 2°C across the North Atlantic, and relative humidity does not vary greatly in RCP8.5, indicating a projected increase in available moisture in the North Atlantic storm track. The increased England and Wales precipitation projected under the RCP8.5 scenario is suggestive of a situation in which precipitation events due to local extratropical cyclone passages are less frequent, as

demonstrated by the reduction in eastern North Atlantic cyclone frequencies and increase in England and Wales dry days, and in which the precipitation accumulation from cyclones is more intense due to an increase in available moisture, as evidenced by Figure 7.8 and the increased mean and p98 precipitation values in Table 7.1. Zappa et al. (2013b) identifies fewer weakly precipitating extratropical cyclones in the North Atlantic in DJF under the RCP4.5 scenario, and finds that an increasing amount of accumulated precipitation from extratropical cyclones in the North Atlantic comes from intense extratropical cyclones under this scenario in the CMIP5 multi-model analysis.

In JJA, a poleward shift of the North Atlantic storm track is evident, leading to a 15% reduction in track frequency identified in the British Isles region. Extratropical cyclones propagate through the British Isles region on average 7% faster in the RCP8.5 scenario than Historical. Temperature increases in JJA are stronger over the eastern North Atlantic and Europe than in DJF, but a reduction in relative humidity in these regions indicates that the available atmospheric moisture near the eastern end of the storm track may not increase in line with the higher temperatures. The combination of reduced local extratropical cyclone frequency with only weak strengthening of the thermodynamic processes near the England and Wales region may explain the relatively weak increase in JJA mean and p98 precipitation relative to DJF.

7.4 Changes to clustering, stalling, and precipitation events in RCP8.5

In this section, cyclone counts and residence times are analysed to investigate if any overall increase/decrease in clustering/stalling is present in the future climate scenario. Potential causes of changes in precipitation in RCP8.5 are evaluated, including cyclone movements, 250-hPa wind speeds, moisture availability, and the overall precipitation intensity of extratropical cyclones.

7.4.1 Clustering in RCP8.5

Changes in cyclone clustering associated with England and Wales precipitation events in HadGEM2-ES RCP8.5 with respect to Historical are analysed using the CPA method. Figure 7.9 shows the mean cyclone count per precipitation event for wet (left) and extreme wet (right) precipitation events, in HadGEM2-ES Historical and RCP8.5 experiments (orange and purple bars respectively). Wet and extreme wet event cyclone

counts are mostly within the range of standard error in RCP8.5 with respect to Historical, with no consistent pattern of change evident in any season. HadGEM2-ES Historical was previously found to produce associate more unique cyclone tracks per precipitation event than ERA-I (Chapter 6), whilst less difference was found between mean cyclone count in wet and extreme wet events in HadGEM2-ES Historical than in ERA-I, indicating that clustering is a less important process for the generation of extreme precipitation events in HadGEM2-ES than in ERA-I.

The increase in overall cyclone count associated with England and Wales precipitation events in HadGEM2-ES was shown to be related to larger storm association distances in HadGEM2-ES than in ERA-I, whilst the smaller change in cyclone count associated with extreme wet events relative to wet events in HadGEM2-ES was linked to less intense jet stream for extreme wet events in HadGEM2-ES than in ERA-I. Little change in minimum storm association distance is found in RCP8.5 relative to Historical (not shown). HadGEM2-ES generates a stronger 250-hPa jet stream for days with extreme wet precipitation events in England and Wales in RCP8.5 than Historical, but does not reproduce the increased clustering for extreme wet events that is observed in ERA-I. This indicates that the representation of clustering in HadGEM2-ES is dependent on more factors than the location and intensity of the 250-hPa jet stream alone, and that HadGEM2-ES is less likely to generate extreme precipitation events as a result of extra-tropical cyclone clustering than ERA-I.

Accumulation period	DJF	MAM	JJA	SON
1 day	-0.4	0.66	28.84	-9.19
7 day	-3.98	-8.58	3.38	-1.24
13 day	3.28	12.13	-10.52	8.44
31 day	-1.34	-0.44	-19.28	0.70

TABLE 7.5: Percentage difference in mean cyclone count between wet and extreme wet events in HadGEM2-ES RCP8.5. Positive value indicates higher mean cyclone count for extreme events. Significance was not identified between any pair of wet and extreme wet samples at $p < 0.05$ in a Kolmogorov-Smirnov test.

The percentage difference between extreme wet and wet event cyclone counts in RCP8.5 is shown in Table 7.5. Little difference is evident in the cyclone counts between these two event categories, and significance is not identified for any season or accumulation period using the Kolmogorov-Smirnov test. This indicates that HadGEM2-ES does not identify clustering to be a significant influence on the generation of extreme wet precipitation events over England and Wales during the period 2080–2099.

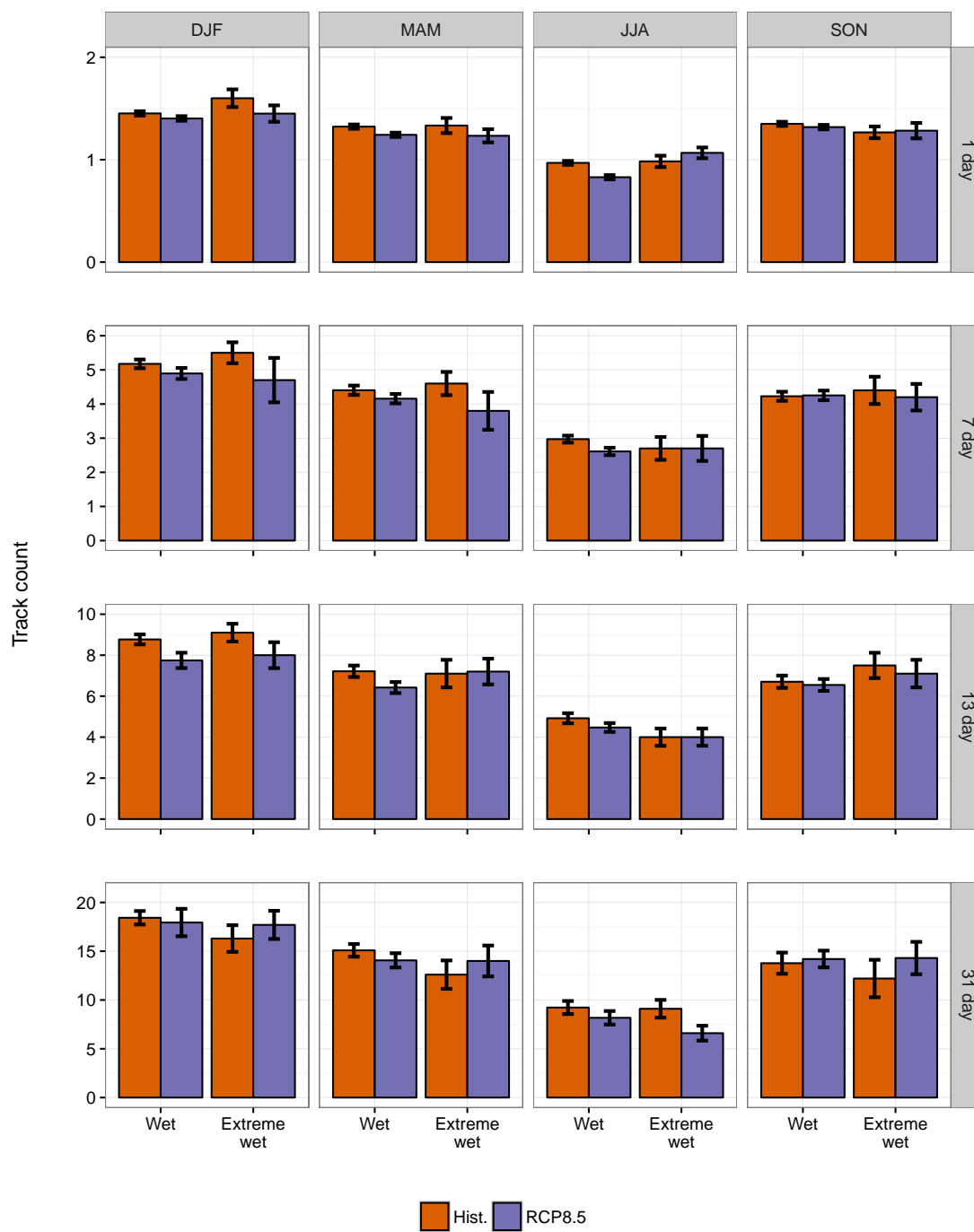


FIGURE 7.9: Mean cyclone count per event for wet and extreme wet events in HadGEM2-ES Historical and RCP8.5, 1980–1999 and 2080–2099 respectively. Error bars are standard error on the mean.

Since no consistent change in cyclone count between wet and extreme wet events in HadGEM2-ES RCP8.5 is observed, this indicates that the role of clustering on extreme wet events is not strongly altered in the future climate as projected by this model run. This is not qualitatively inconsistent with the findings of slightly reduced cyclone clustering throughout the North Atlantic jet region (where clustering is modelled as over-dispersion relative to a fixed-rate Poisson process) in Pinto et al. (2013); however, this method would need to be applied to an ensemble of climate models to establish the significance of these results.

7.4.2 Stalling in RCP8.5

Changes in the residence time of cyclones associated with England and Wales precipitation events in HadGEM2-ES in the RCP8.5 scenario are analysed using the CPA method. For wet and extreme wet events in HadGEM2-ES Historical and RCP8.5 experiments, event mean residence times and mean event maximum residence times are shown in Figure 7.10. Stalling was previously found (in Section 6.4.3) to be associated strongly with JJA extreme precipitation events in HadGEM2-ES (consistent with ERA-I), but to be under-represented with respect to ERA-I for all other seasons.

Accumulation period	DJF	MAM	JJA	SON
1 day	14.81	2.42	88.92	3.63
7 day	14.22	-14.86	80.38	12.64
13 day	7.72	-7.11	17.01	2.83
31 day	25.92	0.96	-2.03	5.15

TABLE 7.6: Percentage difference in mean residence time between wet and extreme wet events in HadGEM2-ES RCP8.5. Positive value indicates higher mean cyclone count for extreme events. Bold type indicates significant differences by Kolmogorov-Smirnov test between wet and extreme wet samples ($p < 0.05$)

Accumulation period	DJF	MAM	JJA	SON
1 day	17.41	3.35	87.56	-0.76
7 day	12.31	-1.75	73.70	-0.57
13 day	30.60	8.28	12.29	2.04
31 day	32.55	-0.07	1.29	12.50

TABLE 7.7: Percentage difference in maximum residence time between wet and extreme wet events in HadGEM2-ES RCP8.5. Positive value indicates higher mean cyclone count for extreme events. Bold type indicates significant differences by Kolmogorov-Smirnov test between wet and extreme wet samples ($p < 0.05$)

In DJF, cyclone mean residence times are slightly reduced for wet events at all accumulation periods in RCP8.5 with respect to Historical, whilst cyclone mean residence times are slightly increased for extreme wet events at all accumulation periods in RCP8.5.

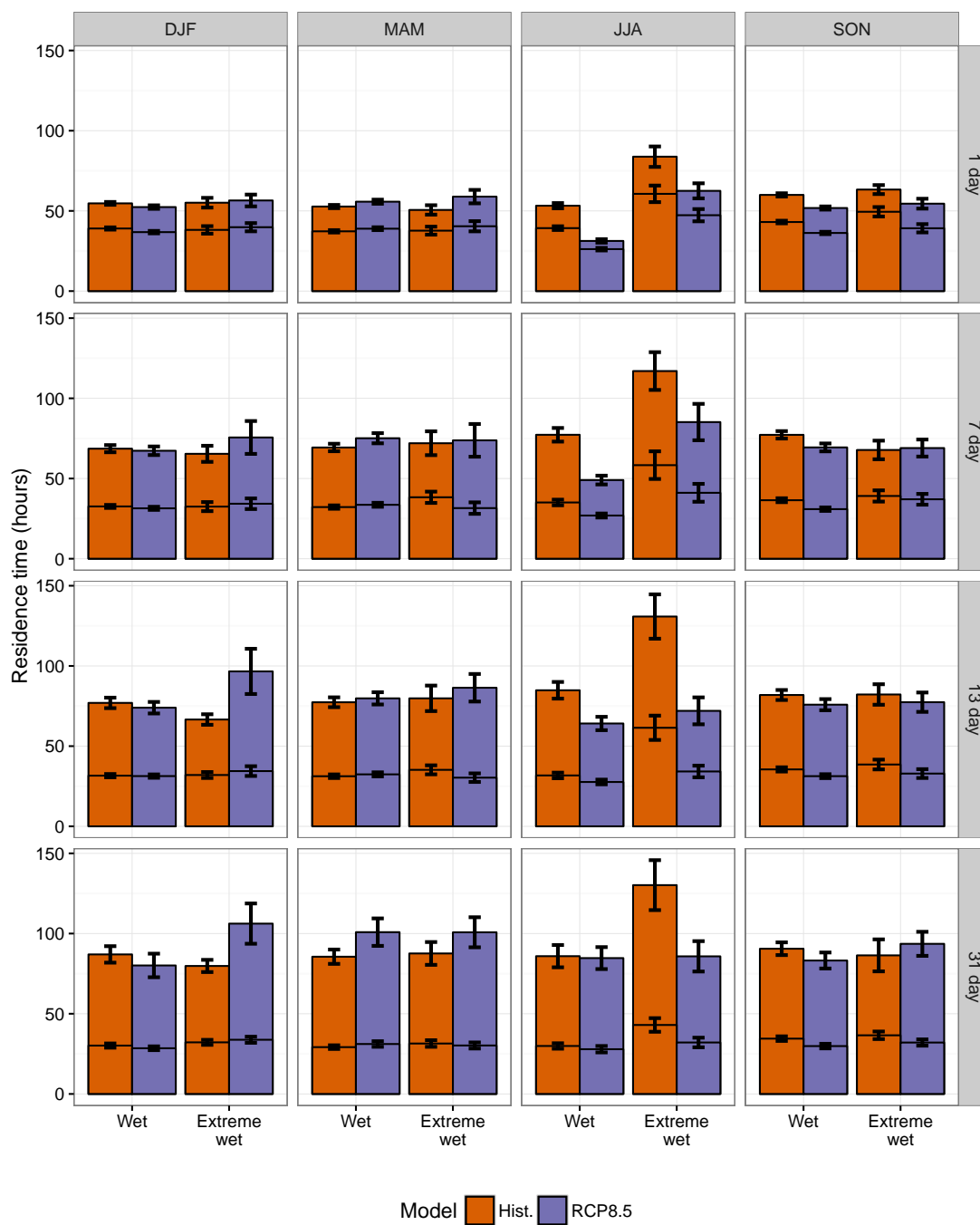


FIGURE 7.10: Means of event maximum residence time (solid colours) and event mean residence time (horizontal lines) in HadGEM2-ES Historical and RCP8.5. Error bars are standard error on the mean.

These changes are mostly within the range of standard error on the mean. The difference between wet and extreme wet event average maximum cyclone residence time increases more strongly, especially at 13–31 day accumulation periods. However, statistical significance is not identified for these events within the RCP8.5 model run (see Tables 7.6 and 7.7). Were significance to be identified in the change in maximum residence time with precipitation intensity, coupled with only a small change in mean residence time, the presence of one or more stalled cyclones associated with extreme wet precipitation events would be indicated, as part of a generally more mobile sequence of cyclones.

In MAM, mean cyclone residence time is increased in RCP8.5 relative to Historical for wet events at all accumulation periods, whilst for extreme wet events the mean cyclone residence time increases for one-day events and decreases for 7–31 day events. This indicates that for extreme precipitation events of 7–31 days, cyclone residence times reduce. This is indicative of more mobile cyclones leading to extreme wet events in the future climate. Maximum cyclone residence times do not show any consistent differences between wet and extreme wet events for either Historical or RCP8.5 across the four accumulation periods (Tables 7.6 and 7.7).

In JJA, large differences are noted between the Historical and RCP8.5 experiments. For wet and extreme wet events, mean and maximum cyclone residence times are reduced in RCP8.5 with respect to Historical. Mean residence times for wet events are reduced by approximately 35% in 1- and 7-day wet events, with smaller reductions for 13- and 31-day accumulation periods. Maximum residence times are reduced for 1–13 day wet events in RCP8.5 with respect to Historical. Extreme wet events also find large reductions in residence time in RCP8.5, with mean residence times reduced by 25–35%. Residence times in RCP8.5 extreme wet events are higher than those in wet events, with significance indicated in an increase in mean and maximum residence times for 1- and 7-day events (Tables 7.6 and 7.7). This indicates that extreme wet events are associated with longer residence time cyclones than wet events in the future climate, at short time-scales.

In SON, mean residence times are reduced for wet and extreme wet events in RCP8.5 with respect to Historical. No significant difference in mean or maximum residence times is identified in RCP8.5 for any accumulation period (see Tables 7.6 and 7.7)

For DJF, MAM and SON, differences in residence times between RCP8.5 and Historical are fairly small. The most notable differences between Historical and RCP8.5 identified in these seasons are an increase in the mean extreme wet event maximum residence

times in DJF (indicating mobile series of cyclones with embedded stalling), and a decrease in the wet and extreme wet event mean residence times in SON, indicating more mobile cyclones associated overall with SON precipitation events. For JJA however, the differences between Historical and RCP8.5 are very much larger. Although extreme wet events in JJA are projected to be associated with longer residence time cyclones than wet events, residence times for all cyclones are greatly reduced relative to the Historical experiment, both in the statistics of mean and maximum residence times. JJA extratropical cyclone propagation speeds are identified as being increased by 7% over the British Isles in RCP8.5 (Figure 7.7), which would suggest a mechanism for the reduction of cyclone residence times. However, a similar increase in cyclone propagation speed is found for DJF, with much less impact on residence times. Also, whilst an intensified jet stream is found in JJA under RCP8.5 (Figures 7.2 and 7.4), a similar pattern of intensification is found in the jet stream for all seasons with much less influence on the associated cyclone residence times.

7.4.3 Extratropical cyclone precipitation intensity in RCP8.5

Precipitation accumulations in England and Wales precipitation events have been found to increase in RCP8.5, both for the mean wet day precipitation accumulation, and for the p98 wet day precipitation accumulations (Figure 7.1). Despite some small changes in clustering patterns in RCP8.5, this change in projected precipitation intensity does not appear to be related to any systematic changes in the number of cyclones associated with England and Wales precipitation events. As such, the precipitation intensity of the cyclones that pass near the England and Wales region must be projected to increase, thus generating increased levels of precipitation regardless of the speed of the cyclones or the extent of clustering. Figure 7.11 shows the mean precipitation per cyclone for wet and extreme wet events in HadGEM2-ES Historical and RCP8.5, calculated as precipitation accumulation per event divided by cyclone count. For all seasons, all accumulation periods, and both climate model experiments, extreme wet events are associated with a greater mean precipitation accumulation per cyclone than wet events. High precipitation intensity is always important in the generation of extreme wet events in the RCP8.5 scenario. It is therefore important to note that, on average, extreme England and Wales precipitation events in HadGEM2-ES are not generated purely by clustered cyclones of average precipitation intensity.

In DJF, mean precipitation per cyclone increases in RCP8.5 with respect to Historical for wet and extreme wet events, for all accumulation periods. Extreme wet events show a larger increase in mean precipitation per cyclone in RCP8.5 than Historical, indicating

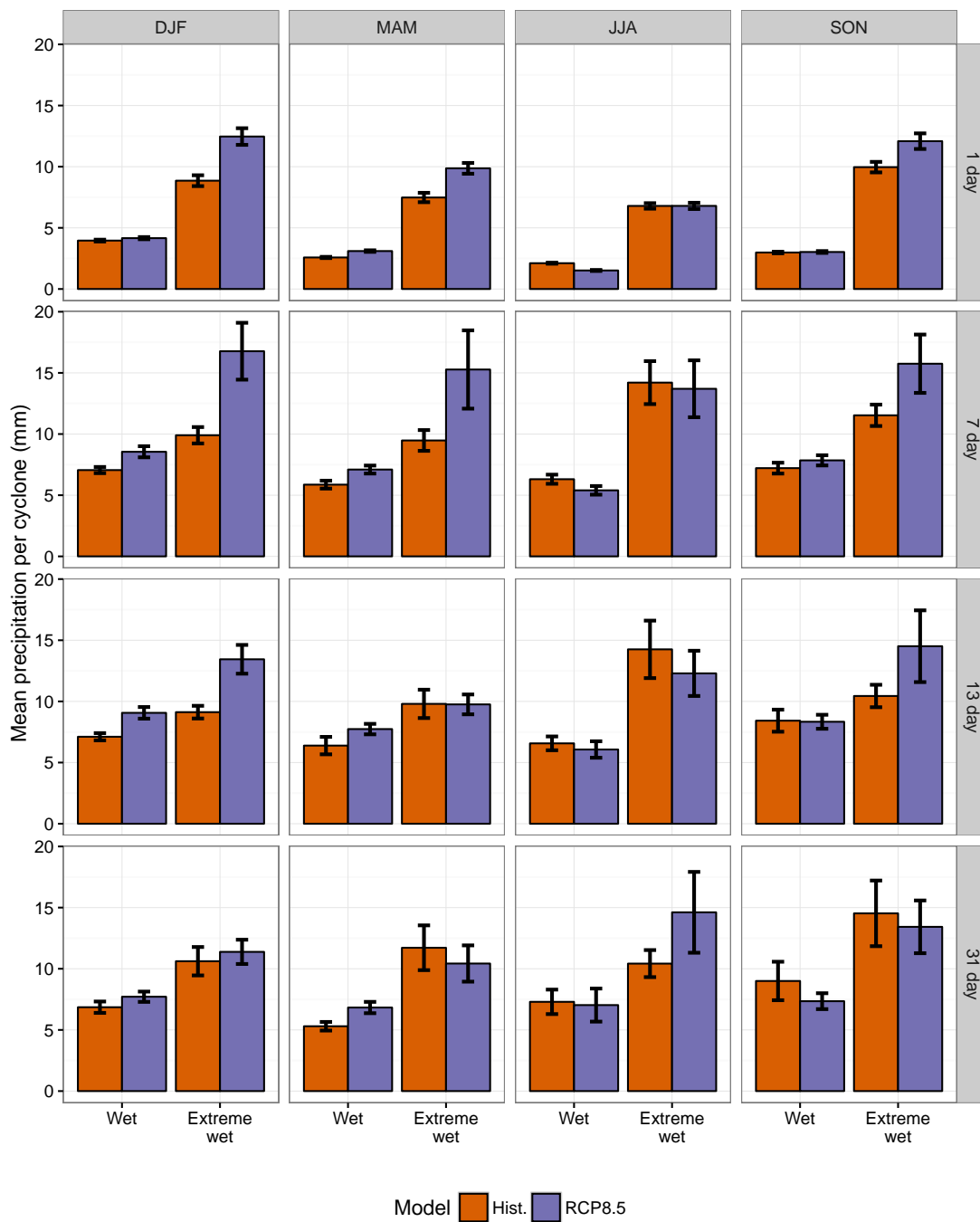


FIGURE 7.11: Mean precipitation per cyclone (total event precipitation accumulation divided by cyclone count) for wet and extreme wet events in HadGEM2-ES Historical and RCP8.5. Error bars are standard error on the mean.

that the precipitation intensity of the most extreme extratropical cyclones is projected to increase in this scenario.

In MAM, a similar pattern is observed to DJF for 1- and 7-day accumulation periods; however, in 13- and 31-day accumulation periods the precipitation intensity of cyclones associated with extreme wet events reduces with respect to the Historical experiment.

In JJA, precipitation intensity is slightly reduced compared to Historical for wet events for all accumulation periods in RCP8.5. Per-cyclone precipitation intensity does increase by a similar proportion in extreme wet events compared to wet events, in RCP8.5 compared to Historical. Despite the lower accumulation of precipitation per cyclone in RCP8.5, a higher precipitation rate is identified when considering the shorter residence times of JJA cyclones when compared to the Historical experiment (Figure 7.10).

In SON, precipitation intensity for wet events in RCP8.5 remains very similar to that observed in Historical. However, for 1–13 day accumulation periods the extreme wet precipitation intensity increases relative to Historical.

For all seasons and accumulation periods, the intensity of precipitation from each cyclone is related to the generation of extreme wet precipitation events in both RCP8.5 and Historical. The increased overall cyclone precipitation intensity found in DJF is consistent with the findings of Bengtsson et al. (2009), which found that winter precipitation in the extratropical storm tracks is likely to come increasingly from extreme events, and Zappa et al. (2013b), which indicated an increase in DJF precipitation near the British Isles in the CMIP5 multi-model mean. This accounts for the higher DJF wet and extreme wet event precipitation intensities, despite lack of notable change in average cyclone counts and mean cyclone residence times. In JJA, little systematic evidence of changes to precipitation per cyclone relative to the Historical experiment is found; however, with the shorter JJA cyclone residence times identified in Section 7.4.2, JJA cyclones are projected to generate higher precipitation rates in RCP8.5.

7.5 Discussion and conclusions

In this chapter, changes in England and Wales precipitation events and their associated storm track activity under the RCP8.5 scenario in HadGEM2-ES have been analysed,

in comparison to the HadGEM2-ES Historical experiment. Changes in daily precipitation accumulations over England and Wales, cyclone frequencies, mean 250-hPa wind patterns, and thermodynamic changes between the Historical and RCP8.5 experiments of HadGEM2-ES were discussed. The CPA method was used to objectively identify cyclones from the Hodges (1994, 1995) algorithm which were associated with precipitation events over England and Wales. Changes in the magnitude of cyclone clustering and stalling relative to HadGEM2-ES Historical were analysed, as well as the response of clustering and stalling characteristics to extreme wet England and Wales precipitation events relative to wet events. Finally, the characteristics of precipitation intensity in extra-tropical cyclones under the RCP8.5 scenario in HadGEM2-ES were evaluated through analysis of the mean precipitation per cyclone for wet and extreme wet events.

The changes in climatological England and Wales precipitation under the RCP8.5 scenario are notably different between winter and summer. DJF exhibits a large increase in mean (+14%) and p98 (+29%) daily precipitation accumulations, and an increase in extreme wet event minimum accumulation where events are selected by the peaks-over-threshold method. Dry day frequency also increases by 13%. The DJF storm track near the British Isles under RCP8.5 is characterised by a reduction in extratropical cyclone frequency (-8%) and an increase in mean extratropical cyclone speed (+7%). The CPA analysis revealed little change in clustering of extratropical cyclones associated with England and Wales precipitation events, despite an extended and intensified jet stream being identified, which is characteristic of clustering of cyclones in the present climate (Priestley et al., 2016). Some evidence of an increase in stalled cyclones embedded within periods of more mobile cyclones was identified for long accumulation period (13–31 day) extreme wet events. These findings are consistent with increased availability of moisture in the warmer atmosphere, scaled approximately per the Clausius-Clapeyron relationship, with extreme precipitation accumulations coming increasingly from intense extratropical cyclones.

By contrast, JJA exhibits small increases in mean (+4%) and p98 (+12%) daily precipitation accumulations, and a slight reduction in minimum precipitation event accumulations as identified by the peaks-over-threshold method. This highlights the importance of consideration of the method used to define “extreme” precipitation events, particularly where data are combined into multi-day periods. JJA dry day frequency increases by 19%. The atmosphere warms by a large amount (5–10°C) over Europe and the eastern North Atlantic in the RCP8.5 scenario, but total precipitation over England and Wales does not increase as might be expected purely based on the Clausius-Clapeyron relationship. This is found to be due to a relative drying of the air over regions known

to be sources of atmospheric moisture for precipitation systems affecting western Europe (de Leeuw, 2014). As with the DJF storm track, extratropical cyclones in JJA are projected to become less frequent near the British Isles, due to a poleward shift of the North Atlantic storm track (as per Yin 2005), and those cyclones which cross the British Isles are projected to propagate on average 7% more quickly, consistent with stronger 250-hPa winds. JJA precipitation events in RCP8.5 show little evidence of increased cyclone count (clustering), but reduced residence times (stalling) are found relative to the Historical experiment. Little change is found in the amount of precipitation per cyclone; however, when combined with the shorter cyclone residence times, an increase in the precipitation rate of cyclones associated with extreme wet JJA events is identified.

An intensification was identified in the mean 250-hPa wind during extreme wet events in England and Wales. This intensification took the form of an increased south-westerly flow in DJF and SON. This pattern, which may be associated with increased moisture transport from the tropical North Atlantic during extreme events, suggests a mechanism for the strongly increased p98 value of daily precipitation (Figure 7.1) between September and May under the RCP8.5 scenario.

Whilst the mean 250-hPa wind is a useful indicator of the dynamical properties of the atmosphere in relation to extratropical cyclone movements and regional precipitation, there are many other variables that might be considered in future studies. In particular, baroclinic instability, upper-tropospheric divergence, and the location of the polar front may be considered in future work to conceptualise more thoroughly the various factors which may influence cyclone movements and cyclone-associated precipitation.

In summary, the key findings of this chapter are as follows:

- An increase in mean and p98 daily precipitation over England and Wales was identified under the RCP8.5 scenario for all seasons. In DJF, MAM and SON this is found to be consistent with atmospheric warming scaling approximately with the Clausius-Clapeyron theorem. In JJA, a reduction in relative humidity in the key moisture source regions for England and Wales precipitation offsets the effect of a large temperature increase in these regions, resulting in a smaller increase of daily precipitation accumulations. The frequency of dry days over England and Wales increases for DJF and JJA, suggesting that the previously identified increases in mean and p98 daily precipitation accumulations are generated by rarer, more intense precipitation events.

- The North Atlantic jet was found to be intensified in RCP8.5 relative to Historical for extreme wet events in all seasons. The strongest increase in wind speeds was identified in DJF and SON, with a notable south-westerly anomalous flow direction. This anomalous flow is found to be greater than that which might be expected due to changes in the seasonal mean flow, and indicates one mechanism by which the p98 daily precipitation value might be expected to increase due to increased water vapour transport from the tropics.
- Cyclone propagation speeds are found to be faster in all seasons under RCP8.5, but cyclone frequencies were lower. In JJA this decrease in cyclone frequency was associated with a poleward shift of the storm track.
- Clustering was not found to be an important process in the generation of extreme precipitation events in England and Wales in RCP8.5. Only small differences were identified between cyclone counts associated with wet or extreme wet precipitation events over England and Wales between RCP8.5 and Historical, with no significance indicated when analysed using the Kolmogorov-Smirnov test.
- The largest change to stalling in extratropical cyclones associated with England and Wales precipitation events occurs in JJA, with an overall reduction in cyclone residence times. Residence times remained significantly higher (KS test $p < 0.05$) for extreme wet events than wet events in JJA at 1–7 day accumulation periods, indicating that stalling is still influential on generating summer precipitation extremes in RCP8.5. Maximum residence times were found to increase in DJF 13–31 day extreme wet events, indicating the presence of stalled cyclones within otherwise more mobile periods.
- Increases in DJF precipitation in RCP8.5 compared to Historical were found to be predominantly caused by larger volumes of precipitation being produced by individual cyclones. In JJA, total precipitation accumulation per cyclone varies little between the two scenarios, but when the shorter mean cyclone residence times are considered, precipitation is found to be generated by cyclones with higher precipitation rates in RCP8.5 than in the Historical experiment.

This analysis has provided information regarding the representation of England and Wales precipitation events in relation to the North Atlantic storm track in the RCP8.5 experiment of HadGEM2-ES. It should be noted that extratropical cyclone clustering in association with England and Wales precipitation events was found to be under-represented relative to ERA-I in Chapter 6. This process may therefore also be under-represented in the RCP8.5 experiment. However, the majority of the key findings are consistent with current literature regarding changes to the nature of precipitation in

north-western Europe, and changes to the North Atlantic storm track. Further analysis using an ensemble of climate models, such as CMIP5, using different RCP scenarios, would be highly beneficial in determining the robustness of the projected changes to England and Wales precipitation identified in this chapter, and would yield valuable information regarding the representation of the relationship between precipitation events and cyclone movements near the storm track exit in climate models. Future work may entail the analysis of variables other than 250-hPa wind to generate a more complete view of the state of the climate during extreme events within the climate model.

Chapter 8

Discussion and conclusions

8.1 Overview

Extratropical cyclones are an important source of precipitation in England and Wales, with the majority of precipitation events in the winter being associated with the passage of an extratropical cyclone or its associated fronts. Extreme precipitation accumulations generated by extratropical cyclones have far-reaching socio-economic impacts. There is a great need from businesses and policy makers to better understand how these precipitation extremes are generated in the present climate, and how these mechanisms may change in the future.

Clustering of extratropical cyclones is a phenomenon that has received considerable research attention in recent years, with several studies finding significant levels of clustering in extratropical cyclones near the North Atlantic jet exit region, including England and Wales (Mailier et al., 2006; Vitolo et al., 2009; Pinto et al., 2013, 2014). The UK floods of winter 2013-14 highlighted the potential risks associated with large precipitation accumulations from clustered storms. Clustering is known to occur more strongly in storms of high dynamical intensity, leading to increased risk to insurance companies from wind-storm losses in clusters of intense storms. However, very little work has considered the impact of clustering on precipitation accumulations.

Stalling is often linked with extreme precipitation accumulations and rapid flooding events (Blackburn et al., 2008; Stadtherr et al., 2016; Petoukhov et al., 2016). Several examples of this have occurred in recent years; the most famous example being the floods of summer 2007, which led to the town of Tewkesbury being entirely cut off by floods,

as well as extensive and damaging flooding across the rest of the country. Although slow-moving storms are mentioned in literature which discusses the cause of floods in Europe (Blackburn et al., 2008; Stadtherr et al., 2016), no systematic study has been performed to identify the climatological nature of stalling, its impact on England and Wales precipitation events, or potential changes to stalling under future climate conditions.

This thesis has aimed to address gaps in our knowledge of how the movement of cyclones, specifically patterns of clustering and stalling, influences precipitation accumulations on time-scales from one day to one month over the England and Wales region. The quality of England and Wales precipitation in reanalysis products and a climate model has been evaluated; a novel method of associating precipitation events with extratropical cyclone centres has been developed; and this method has been applied to reanalysis and climate model data to investigate the influence of clustering and stalling on England and Wales precipitation events. This analysis has been performed with the intention of answering the following questions, posed in Chapter 1:

1. How well are historical England and Wales precipitation events represented in reanalyses?
2. What is the best way to associate precipitation with extratropical cyclones?
3. To what extent is precipitation in England and Wales influenced by the clustering and stalling of extratropical cyclones?
4. How well do climate models represent the observed relationships between extratropical cyclones and England and Wales precipitation events?
5. How might extreme precipitation events caused by extratropical cyclones change in the future?

A discussion of the analysis performed in this thesis is presented in Section 8.2, to respond to the questions posed above. Avenues of potential future research are discussed in Section 8.3.

8.2 Discussion and conclusions

8.2.1 How well are historical England and Wales precipitation events represented in reanalyses?

Reanalysis data is commonly used in evaluation of recent climate conditions (e.g. Mailier et al. 2006; Pinto et al. 2013; Catto et al. 2012; Catto and Pfahl 2013; Hawcroft et al. 2012). Whilst analysis of trends and variability in England and Wales precipitation is usually performed based on data from the high-quality, long-running gauge network available for this region (e.g. Osborn et al. 2000; Alexander and Jones 2000), precipitation data from reanalysis products has great potential for the development of analysis methods which are applicable to other regions. In particular, precipitation data from reanalysis products have been used to investigate the association between extratropical cyclones, fronts, and precipitation in the North Atlantic storm track (Hawcroft et al. 2012; Catto et al. 2012; Catto and Pfahl 2013). Reanalysis products are also of great benefit as the large range of data available from reanalyses allows the identification of extratropical cyclones and precipitation events in the same dataset.

In Chapter 3, the ability of NOAA-CIRES Twentieth Century Reanalysis (20CR; Compo et al. 2011) and ECMWF ERA-Interim (ERA-I; Dee et al. 2011) to represent precipitation over England and Wales was analysed, using data from the Hadley Centre UK Precipitation (HadUKP) England and Wales Precipitation (EWP; Alexander and Jones 2000) series for comparison. Using a hit-rate analysis method, both reanalysis products identified 45–55% of extreme daily precipitation events (where “extreme” is defined as the 98th percentile of each dataset). Hit rates were found to increase for longer accumulation period events, indicating that the timing of precipitation events may be an important factor in the ability of reanalysis products to represent observed events. However, hit rates did not exceed 80% for p98 extreme events on any time-scale (Figure 3.4, indicating that reanalysis is not an appropriate tool for identifying individual extreme events.

The spatial representation of climatological precipitation was found to be similar between 20CR and ERA-I (Figure 3.1), with the north-west to south-east decreasing gradient of climatological precipitation over the British Isles well represented. This was comparable to the spatial distribution of precipitation from the Global Precipitation Climatology Project (GPCP) satellite-derived record, indicating that the spatial representation of climatological precipitation was reasonable in both reanalysis models. However, both reanalysis products underestimated accumulated precipitation relative to GPCP, and

20CR particularly lacked spatial detail due to its coarse resolution. The frequency distribution of daily precipitation accumulations was well represented in both reanalysis products relative to EWP (Figure 3.2), although a systematic underestimation of mean and p98 values, and an over-representation of days of low rainfall accumulation (drizzle), was evident in both reanalysis products.

The usefulness of reanalysis products depends primarily on the intended use. For spatial representation of precipitation features, the reanalysis products evaluated here showed a reasonable level of agreement, representing the climatological distribution of precipitation effectively. However, as a substitute for a high-quality record of observed precipitation accumulations, reanalysis falls short, particularly in instances when it is necessary to identify the timing of extreme precipitation events. In the context of the work presented in this thesis, the spatial representation of precipitation in reanalysis was deemed to be of high enough quality to form a core element of the CPA method, which was developed to identify cyclones in association with precipitation events (Chapter 4). Precipitation observations from the EWP dataset were used to more accurately identify precipitation events in the recent climate.

8.2.2 What is the best way to associate precipitation with extratropical cyclones?

Several methods have previously been used to associate cyclones with regions of potential impact. The simplest existing methods track the east-west passage of cyclones across a meridional gate (Mailier et al., 2006; Vitolo et al., 2009). This method is appropriate for point-process modelling of the transits of extratropical cyclone centres, but does not make allowances for the size of the cyclone, and the potential for damaging impact at a distance from the cyclone centre. Methods using a circle to track cyclone transits (Pinto et al., 2013, 2014; Priestley et al., 2016) or to track precipitation associated with cyclones (Hawcroft et al., 2012) make some allowances for the spatial dimensions of extratropical cyclones, but do not fully account for the distant and highly asymmetric spatial distribution of precipitation associated with extratropical cyclones and the sensitivity to the radius of the search area that this causes. Fully associating precipitation events with extratropical cyclones requires more information regarding the structure of rain bands associated with the cyclone. Additional spatial information regarding the distribution of precipitation from extratropical cyclones was obtained by Catto et al. (2012) and Catto and Pfahl (2013) using front tracking techniques. This method produced high association rates (~90% DJF association rate near British Isles).

It is possible to achieve higher association rates between precipitation events and extratropical cyclones by utilising the spatial information provided by the precipitation output of gridded datasets. In Chapter 4, the CPA method was developed to improve the association rate between England and Wales precipitation events and the extratropical cyclones that were likely to have generated them. CPA applies a threshold precipitation value to gridded data, such as climate model or reanalysis output, to identify contiguous precipitation bands. Precipitation events in a region of interest (England and Wales in this case) are associated with the nearest extratropical cyclone centre that lies within, or close to, the precipitation band that lies over the region of interest. A maximum distance limit is applied to prevent spurious association of very distant events. By utilising the spatial precipitation data available from gridded datasets, association rates between precipitation events and extratropical cyclones are maximised, whilst spurious association with extratropical cyclones is minimised on dry days. The CPA method associates 98% of DJF p98 extreme precipitation events in England and Wales in ERA-I with an extratropical cyclone. 80% of JJA p98 extreme precipitation events in England and Wales in ERA-I are associated with extratropical cyclones; this is expected due to the seasonal cycle of extratropical cyclone activity.

When tested against previously established methods, CPA returns higher association rates between extreme wet England and Wales precipitation events (defined as daily events above the 98th percentile of daily EWP precipitation) and extratropical cyclones in DJF, MAM and SON than all other methods tested (Figure 4.4) (the JJA CPA extreme wet event association rate is very slightly exceeded by a storm-centred 12° radial cap method). Dry day association rates are much lower in all seasons than for other methods, at approximately 5% for all seasons. CPA was found to be only slightly sensitive to precipitation threshold (within ± 0.5 mm of 1.5 mm) for dry and extreme wet event association rates (Figure 4.5) and cyclone counts per daily event (Figure 4.6).

CPA was therefore found to fulfil its purpose of more accurately objectively associating regional precipitation events with extratropical cyclones than methods using a fixed search area, whilst utilising readily available spatial data from gridded atmospheric datasets.

8.2.3 To what extent is precipitation in England and Wales influenced by clustering and stalling of extratropical cyclones?

An analysis of historical precipitation events and associated clustering and stalling patterns in extratropical cyclones was conducted in Chapter 5. This analysis used observed precipitation data from the EWP subset of HadUKP, which is derived from rain gauge observations across England and Wales. These data were combined with spatial precipitation data from ERA-I and the CPA method was used to associate observed England and Wales precipitation events with extratropical cyclones in the reanalysis data, identified and tracked using Hodges (1994, 1995) tracking scheme on ξ_{850} .

Clustering associated with England and Wales precipitation events was characterised by the cyclone count per event. The measurement of cyclone count allows for situations such as winter 2013-14 in the UK to be characterised, when a highly regular series of storms crossed the region, causing wind, flood, and storm surge damage. Whilst this method differs from the established method of identification of storm clusters in the existing literature (Mailier et al., 2006; Vitolo et al., 2009; Pinto et al., 2013, 2014, 2016; Priestley et al., 2016), this is required in order to consider events where regular cyclone passages present a cumulative risk of flood. Track count per event can indicate the level of clustering present in extreme wet events relative to wet events, and the seasonal cycle of clustering associated with precipitation events.

Clustering was found to be an important process governing extreme wet precipitation events in England and Wales in all seasons. The largest differences between cyclone count for wet and extreme wet events were found in DJF, MAM and SON, although some evidence of the influence of clustering on extreme wet precipitation events was identified for JJA (Figure 5.8). Clustering was found to be associated with an intensification and extension to the east of the 250-hPa jet stream. The jet exit was found to be positioned directly above the England and Wales region for clustered extreme wet events. Particularly intense and direct jet stream configurations were found to be associated with DJF and SON extreme wet precipitation events associated with clustered storms; this is consistent with the association between double-sided Rossby wave breaking in the presence of an extended jet stream and clustering near the North Atlantic jet exit region identified by Priestley et al. (2016).

Stalling was defined by two measurements: mean cyclone residence time per event, and maximum cyclone residence time per event. These two measurements describe two distinct types of stalling event. A long mean cyclone residence time per event describes

situations in which the majority of storms associated with a precipitation event are slow moving, indicating a general low level of storm mobility. A long maximum cyclone residence time per event describes a situation where one storm has stalled during the course of the precipitation event; potentially as part of an otherwise more mobile period.

A strong seasonal cycle was identified in the residence times of storms associated with precipitation events in England and Wales (Figure 5.11). Both the mean and maximum cyclone residence time per precipitation event were found to be longer in JJA than in any other season for extreme wet events. Both mean and maximum residence times were very similar between JJA and SON for wet events. Similar mean and maximum residence times were found in wet and extreme wet events in DJF and MAM, and mean residence times were longer in extreme wet events than wet events in both DJF and MAM at 1–13 day accumulation periods. A year-round influence of extratropical cyclone stalling on extreme precipitation events in England and Wales is evident for short accumulation period events. However, in JJA this influence extends to long accumulation period events (1–31 days).

The prevalence of stalling in JJA may be due to the weaker westerly winds present in JJA, which are conducive to the generation of slow-moving extratropical cyclones. However, a wave pattern is strongly evident in the 250-hPa wind vectors for extreme wet precipitation events in MAM, JJA and SON associated with stalled extratropical cyclones. This wave pattern approximates a planetary-scale wave pattern of wave number $n = 6$. An $n = 6$ stationary wave pattern was identified northern hemisphere maps of potential temperature on the dynamical tropopause ($\Theta_{PV=2}$) during the flooding events of summer 2007 by Blackburn et al. (2008), the Northern Hemisphere 300-hPa wind flow during the Balkan floods of 2014 (Stadtherr et al., 2016), and with several extreme precipitation and heatwave events in the summers of 2012 and 2013 (Petoukhov et al., 2016).

The findings presented in this thesis indicate that stalling is a dominant process governing extreme spring–autumn precipitation events in England and Wales. Stalling associated with spring–autumn extreme precipitation events in England and Wales is found to be linked to quasi-stationary planetary-scale waves of wave-number $n = 6$, similar to those identified by Blackburn et al. (2008), Petoukhov et al. (2016) and Stadtherr et al. (2016). Further research would be beneficial to establish the frequency of quasi-stationary planetary-scale waves occurring concurrently with England and Wales precipitation extremes, and the relationship between the amplitude and duration of these waves and the residence times of extratropical cyclones.

8.2.4 How well do climate models represent observed relationships between extratropical cyclones and England and Wales precipitation events?

In Chapter 6 the ability of a historical run of HadGEM2-ES to replicate extratropical cyclone behaviours in association with England and Wales precipitation events was evaluated. Whilst the ability to simulate features of the historical climate is not necessarily an indicator of the ability of a climate model to make accurate projections of the future climate, this analysis is intended to highlight any systematic differences between the mechanisms by which HadGEM2-ES and ERA-Interim generate precipitation affecting England and Wales.

A single climate model from the CMIP5 ensemble was selected for this analysis. Using a multi-model approach (e.g. Zappa et al. (2013b); Economou et al. (2015); Renggli and Zimmerli (2016)) to evaluate the performance of climate models in representing the relationship between extratropical cyclones and England and Wales precipitation would have provided a greater level of confidence in the significance of the results, as well as an indication of the degree of uncertainty inherent in these results. Economou et al. (2015) demonstrates that when considering the full ensemble of CMIP-5 members, considerable quantitative uncertainty exists in the dispersion statistic of extratropical cyclones in the North Atlantic, which may have an effect on the findings of this study. However, Renggli and Zimmerli (2016) indicates that the representation of serial clustering of extratropical cyclones is well constrained between models when only a subset of CMIP-5 is considered, where that subset is known to reproduce large-scale atmospheric dynamics well in the North Atlantic region. The selection of HadGEM2-ES according to the criterion of its representation of the tilt of the North Atlantic storm track gives confidence that these results might be replicated closely by other CMIP-5 models with similar representation of the dynamics of the North Atlantic.

Daily precipitation accumulations in England and Wales were found to be similarly represented in HadGEM2-ES and ERA-I, although both products showed a tendency to over-estimate days of light rain with respect to EWP, and both the reanalysis and the climate model yielded lower mean and 98th percentile precipitation when compared with EWP. HadGEM2-ES represented the location and cyclone frequency of the North Atlantic storm track well in DJF and MAM, but underestimated cyclone frequency near the British Isles by 5%–29% (DJF and JJA respectively) with respect to ERA-I. Extratropical cyclone propagation speeds in the eastern North Atlantic were found to be 18–24% slower for all seasons in HadGEM2-ES than ERA-I. The lower storm frequency

in JJA and SON, and the overall reduction in storm propagation speeds may be associated with weaker wind speeds in the 250-hPa jet in HadGEM2-ES than ERA-I.

The CPA method was applied to HadGEM2-ES (Historical) and ERA-I, and the results were compared to highlight similarities and differences in the nature of storm clustering and stalling associated with England and Wales precipitation events (where precipitation events were identified by model precipitation output). Despite the lower North Atlantic cyclone count in HadGEM2-ES, association rates between England and Wales precipitation events and extratropical cyclones were higher in HadGEM2-ES. This was found to be related to the ability of CPA to associate storms at a greater distance from England and Wales in HadGEM2-ES than in ERA-I. Clustering was found to be less likely to be associated with extreme England and Wales precipitation events in HadGEM2-ES than ERA-I, despite the higher overall cyclone counts associated with England and Wales precipitation events in HadGEM2-ES. Stalling was also found to be less strongly associated with extreme wet events in HadGEM2-ES for DJF, MAM and SON, despite overall longer residence times than in ERA-I. However, a strong link between stalling and extreme wet event generation was found for JJA in HadGEM2-ES for all accumulation periods (1–31 days). The magnitude of the difference between wet and extreme wet event residence times in HadGEM2-ES approximately mirrored that of ERA-I, despite the longer residence times overall in HadGEM2-ES.

In summary, the representation of the North Atlantic storm track, 250-hPa winds, and England and Wales precipitation in HadGEM2-ES closely resembles ERA-I, despite some systematic differences from ERA-I. Extreme England and Wales precipitation events are associated with an extended and intensified 250-hPa jet in both HadGEM2-ES and ERA-I, and similar cyclone counts per precipitation event are found in both HadGEM2-ES and ERA-I, including the seasonal cycle. Clustering is not as important a process for governing extreme England and Wales precipitation events in HadGEM2-ES, and the difference between cyclone counts for wet and extreme wet events is rarely as large in HadGEM2-ES as in ERA-I. Stalling is also represented differently in HadGEM2-ES, with longer average residence times and a stronger seasonal cycle in the importance of stalling for extreme events. Although some aspects of the relationship between clustering, stalling, and extreme precipitation events are represented differently in HadGEM2-ES than in ERA-I, the main features of the North Atlantic storm track are well represented. Therefore there is value in analysis of these events under a high-emissions scenario in HadGEM2-ES, as this can indicate whether changes in thermodynamics or circulation are more important for any future changes in England and Wales precipitation events.

8.2.5 How can we expect extreme precipitation events caused by extratropical cyclones to change in the future?

In Chapter 7 the RCP8.5 experiment of HadGEM2-ES was analysed, to provide information regarding the projected changes to England and Wales precipitation distributions, the North Atlantic storm track, and clustering and stalling of extratropical cyclones in relation to precipitation events in England and Wales. The CPA method was applied to output from the RCP8.5 experiment, allowing direct comparison with the Historical experiment of HadGEM2-ES.

Changes to the North Atlantic storm track, and to precipitation accumulations over western Europe, have been projected by climate models and discussed in previous literature. Zappa et al. (2013b) identified projected changes to the North Atlantic storm track in the CMIP5 multi-model mean, whereby the North Atlantic storm track becomes, on average, more zonal. This leads to an increase in cyclone count near the British Isles. Whilst there is currently high confidence in an intensified global hydrological cycle (Stocker et al., 2013), less certainty exists as to regional magnitude of precipitation change in the future climate.

In HadGEM2-ES RCP8.5, an increase in mean and p98 daily precipitation over England and Wales was identified for all seasons (Figure 7.1). The magnitude of this increase was not uniform in all seasons, with a very much smaller increase in JJA precipitation than in DJF. Investigation of the projected changes to thermodynamic conditions in the North Atlantic indicated that, although air temperature is projected to rise over Europe in the RCP8.5 projection, relative humidity does not rise proportionately. Moisture availability increases more strongly DJF than in JJA. JJA relative humidity is found to be particularly low in regions known to be major moisture source regions for England and Wales precipitation (Figure 7.8), accounting for the small change in JJA mean and p98 daily precipitation accumulations relative to DJF in the RCP8.5 scenario.

Application of the CPA method to RCP8.5 data indicates that clustering does not play a large role in extreme precipitation events over England and Wales in the RCP8.5 projected climate (Figure 7.9). Only small differences in cyclone count between wet and extreme wet events were found in RCP8.5. Consistent with the analysis of the Historical experiment presented in Chapter 6, stalling was found to be strongest in JJA, but, consistent with faster storm propagation speeds, JJA residence times were found to be shorter than in the Historical experiment (Figure 7.10). Extreme wet events in DJF

were found to have longer maximum cyclone residence times for 13–31 day accumulation periods. This is suggestive of a period of mobile storms, with one or more slow-moving storms embedded within it. This situation is highly similar to the situation that generated the flooding in summer 2007, during which a very mobile period brought large accumulations of precipitation to England and Wales, and a slow-moving storm with intense precipitation caused flooding on previously saturated ground.

Consistent with the greater availability of atmospheric moisture in DJF in the RCP8.5 projection, increases in DJF precipitation accumulations were found to be predominantly associated with greater volumes of precipitation per cyclone, as opposed to an increased number of cyclones (Figure 7.11). Little change was found in the amount of precipitation from JJA cyclones, but, when combined with the shorter residence times identified in JJA, this indicates that JJA cyclones precipitate at a faster rate in RCP8.5 than in the historical climate.

Analysis of the RCP8.5 run of HadGEM2-ES indicates that future changes in England and Wales DJF precipitation are governed more by the thermodynamic influences under a warming climate than changes to atmospheric dynamics, such as clustering and stalling patterns in extratropical cyclones. Strong temperature increases in DJF and are associated with a proportionate increase in atmospheric moisture availability, as demonstrated by the lack of change of relative humidity in Figure 7.8. In JJA, a reduction in relative humidity in the main moisture source regions limits the potential increase of precipitation due to a strongly warming climate. In JJA, reduction of mean cyclone residence times introduce a secondary dynamical influence governing precipitation accumulations. These findings must also be considered in the context of the known limitations of HadGEM2-ES, including the lower importance of clustering in generating extreme England and Wales precipitation events relative to ERA-I. It would therefore be useful to analyse further climate models to test the robustness of these findings.

8.3 Future work

In this section, potential avenues of future research will be discussed in terms of three unanswered questions related to the research presented in this thesis.

8.3.1 How does the influence of extratropical cyclone clustering and stalling on precipitation events vary throughout Europe?

A new method for investigating the link between regional precipitation events and extratropical cyclone clustering and stalling has been developed for this project, and utilised to evaluate the role of clustering and stalling on England and Wales precipitation accumulations. England and Wales was chosen as the region to evaluate primarily due to the existence of a long-running, high quality data-set of precipitation observations, processed to give a homogeneous data series on an appropriate spatial scale for this analysis. Given the ability of the CPA method to be applied to any gridded dataset, there would be value in analysing other regions where similar high-quality precipitation observations are available. One such application would be to utilise the E-OBS (Haylock et al., 2008) daily gridded rain gauge data, which is available for European land areas (and some Mediterranean coastal regions) between 1 January 1950 and 31 August 2016. By applying CPA to precipitation data across a larger area, regional climatologies of the influence of clustering and stalling cyclones on precipitation events across Europe could be generated.

In Hand et al. (2004) precipitation events are categorised as convective, frontal or stratiform; such classification within CPA would give useful information regarding the origin of the precipitation. ERA-I provides data concerning the origin of precipitation (convective/stratiform) which, combined with orographic data, could be used to objectively categorise the source of precipitation in each case.

In ERA-Interim, clustering was identified as a more important process than the precipitation intensity of extratropical cyclones in governing the generation of 31-day extreme precipitation events in England and Wales (Chapter 5). It would be beneficial to evaluate the robustness of this relationship by applying this analysis to different reanalysis products, time periods, or regions of Europe.

8.3.2 What causes extratropical cyclones to stall?

In Chapter 1, we established that a large gap exists in the present literature concerning stalling in extratropical cyclones. In Chapter 5 we established that cyclones associated with extreme England and Wales precipitation events in the summer are resident for approximately 50% longer than cyclones associated with non-extreme precipitation events. Therefore, analysis of the causes and climatological frequency of stalling extratropical

cyclones near the exit of the North Atlantic jet would be highly beneficial.

Blackburn et al. (2008), Petoukhov et al. (2013), Petoukhov et al. (2016) and Stadtherr et al. (2016) have all identified the existence of quasi-stationary planetary waves of wavenumber 6–8 concurrently with extreme precipitation events, in limited studies of notable extreme weather events. Petoukhov et al. (2013) and Petoukhov et al. (2016) hypothesise that quasi-stationary planetary waves of this type may self-amplify through a mechanism of quasi-resonant amplification. A systematic analysis of the importance of large amplitude quasi-stationary planetary waves to the generation of extreme England and Wales precipitation events due to stalled cyclones could be conducted by combining the zonal wave number calculation of Petoukhov et al. (2013) with CPA. The strength of the association between quasi-stationary planetary waves and extratropical cyclone stalling could be established by regressing extratropical cyclone residence time onto the amplitude of the $n=6,7,8$ wave components.

8.3.3 How is the influence of clustering and stalling of extratropical cyclones on precipitation represented in CMIP5 models?

This study has been limited to the analysis of a single climate model, HadGEM2-ES. This has produced some valuable insights into the manner in which this climate model performs when generating England and Wales precipitation events, in relation to its representation of the North Atlantic storm track. However, there would be clear benefit from applying this method to other climate models in the CMIP5 project, and to other RCP experiments, to both determine the robustness of these results to the model chosen, and to identify any differences in climate response under alternative emissions scenarios. HadGEM2-ES was found to display biases in its representation of the influence of extratropical cyclone clustering and stalling on England and Wales precipitation events when compared with ERA-I. Therefore it would be beneficial to extend this analysis to the historical scenarios of other models in the CMIP5 project, to allow more complete evaluation of mechanisms that are important for the generation of observed clustering patterns.

Due to the size of the CMIP5 project, it may be desirable to focus further analysis on a subset of models which best represent features which are essential for the accurate representation of extratropical cyclones near England and Wales. For detailed analysis of projected changes to the North Atlantic storm track, Zappa et al. (2013b) selected four models from the CMIP5 project which best represented the location and tilt of the

North Atlantic storm track: HadGEM2-ES, HadGEM2-CC¹, EC-EARTH (Hazeleger et al., 2010) and MRI-CGCM3 (Yukimoto et al., 2012). Since representing the location of the North Atlantic storm track is essential for analysis of clustering, stalling and precipitation characteristics of storms near England and Wales, selecting models according to similar criteria would be preferable. At the time of writing, sub-daily precipitation data is not available for EC-Earth RCP8.5. Therefore, MIROC-5 (Watanabe et al., 2010) and GFDL CM3 (Donner et al., 2011) are proposed as alternative models due to their ability to closely resemble the North Atlantic storm track tilt as observed in reanalysis (Zappa et al., 2013a). Additionally, an evaluation of the ability of the CMIP6 models (Eyring et al., 2016) to represent clustering and stalling should be considered upon release of data (projections expected 2018–2020).

In this thesis, only the RCP8.5 scenario has been evaluated, which represents a high-emissions scenario leading to high levels of warming. This scenario was chosen to provide the strongest climate change signal. However, as the storm track responds non-linearly to climate change it would be highly beneficial to apply this analysis to other RCP scenarios. Several studies of the North Atlantic storm track under climate change (e.g. Harvey et al. 2012; Zappa et al. 2013b; Pinto et al. 2013) focus on the RCP4.5 scenario, as this provides a mid-level estimate of future climate conditions. For the highest level of inter-comparability with existing literature, RCP4.5 should be considered in any further analysis.

¹This model has very similar characteristics to HadGEM2-ES, and was included in Zappa et al. (2013b) to reduce sampling uncertainty

Bibliography

- Adler, R. F., C. Kidd, G. Petty, M. Morissey, and H. M. Goodman, 2001: Intercomparison of global precipitation products: The third precipitation intercomparison project (PIP-3). *Bull. Amer. Meteor. Soc.*, **82**, 1377–1396.
- Alexander, L., and P. Jones, 2000: Updated precipitation series for the UK and discussion of recent extremes. *Atmos. Sci. Lett.*, **1**, 142–150.
- Allen, M. R., and W. J. Ingram, 2002: Constraints on future changes in climate and the hydrologic cycle. *Nature*, **419**, 224–232.
- Becker, A., P. Finger, A. Meyer-Christoffer, B. Rudolf, K. Schamm, U. Schneider, and M. Ziese, 2013: A description of the global land-surface precipitation data products of the Global Precipitation Climatology Centre with sample applications including centennial (trend) analysis from 1901-present. *Earth Syst. Sci. Data*, **5**, 71–99.
- Bengtsson, L., K. I. Hodges, and N. Keenlyside, 2009: Will extratropical storms intensify in a warmer climate? *Int. J. Climatol.*, **22**, 2276–2301.
- Bengtsson, L., K. I. Hodges, and E. Roeckner, 2006: Storm tracks and climate change. *Int. J. Climatol.*, **19**, 3518–3543.
- Beniston, M., and Coauthors, 2007: Future extreme events in European climate: An exploration of regional climate model projections. *Climatic Change*, **81**, 71–95.
- Berry, G., M. J. Reeder, and C. Jakob, 2011: A global climatology of atmospheric fronts. *Geo. Res. Lett.*, **38**.
- Bivand, R. S., E. Pebesma, and V. Gomez-Rubio, 2013: *Applied spatial data analysis with R, Second edition*. Springer, New York, USA.
- Bjerknes, J., 1919: On the structure of moving cyclones. *Mon. Wea. Rev.*, **47**, 95–99.
- Bjerknes, J., and H. Solberg, 1922: Life cycle of cyclones and the polar front theory of atmospheric circulation. *Geofys. Publ.*, **3**, 1–18.

- Blackburn, M., J. Methven, and N. Roberts, 2008: Large-scale context for the UK floods in summer 2007. *Weather*, **63**, 280–288.
- Blackmon, M. L., 1976: A climatological spectral study of the 500 mb geopotential height of the Northern Hemisphere. *J. Atmos. Sci.*, **33**, 1607–1623.
- Browning, K., 1997: The dry intrusion perspective of extra-tropical cyclone development. *Meteor. Appl.*, **4**, 317–324.
- Browning, K., and N. Roberts, 1994: Structure of a frontal cyclone. *Quart. J. Roy. Meteor. Soc.*, **120**, 1535–1557.
- Carlson, T. N., 1980: Airflow through midlatitude cyclones and the comma cloud pattern. *Mon. Wea. Rev.*, **108**, 1498–1509.
- Catto, J., 2010: Extratropical cyclones in HiGEM: Climatology, structure and future predictions. Ph.D. thesis, University of Reading.
- Catto, J., C. Jakob, G. Berry, and N. Nicholls, 2012: Relating global precipitation to atmospheric fronts. *Geo. Res. Let.*, **39**.
- Catto, J., and S. Pfahl, 2013: The importance of fronts for extreme precipitation. *J. Geophys. Res.: Atmos.*, **118**, 10–791.
- Charney, J. G., 1947: The dynamics of long waves in a baroclinic westerly current. *J. Meteor.*, **4**, 136–162.
- Chatterton, J., C. Viavattene, J. Morris, E. Penning-Rowsell, and S. Tapsell, 2010: The costs of the summer 2007 floods in England. Tech. rep., Environment Agency, Bristol, UK.
- Chen, M., P. Xie, J. E. Janowiak, and P. A. Arkin, 2002: Global land precipitation: A 50-yr monthly analysis based on gauge observations. *J. Hydrometeorol.*, **3**, 249–266.
- Collins, W., and Coauthors, 2008: Evaluation of the HadGEM2 model. Tech. rep., Hadley Cent., Exeter, UK.
- Compo, G. P., and Coauthors, 2011: The twentieth century reanalysis project. *Quart. J. Roy. Meteor. Soc.*, **137**, 1–28.
- Cox, D. R., and V. Isham, 1980: *Point Processes*, Vol. 12. Chapman & Hall/CRC, Boca Raton, USA.
- Croxtton, P., K. Huber, N. Collinson, and T. Sparks, 2006: How well do the central England temperature and the England and Wales precipitation series represent the climate of the UK? *Int. J. Climatol.*, **26**, 2287–2292.

- Dacre, H. F., P. A. Clark, O. Martinez-Alvarado, M. A. Stringer, and D. A. Lavers, 2015: How do atmospheric rivers form? *Bull. Amer. Meteor. Soc.*, **96**, 1243–1255.
- Dacre, H. F., and S. L. Gray, 2009: The spatial distribution and evolution characteristics of North Atlantic cyclones. *Mon. Wea. Rev.*, **137**, 99–115.
- Dai, A., 2006: Precipitation characteristics in eighteen coupled climate models. *Int. J. Climatol.*, **19**, 4605–4630.
- de Leeuw, J., 2014: On the origin of summer precipitation variability in the uk. Ph.D. thesis, University of Reading.
- De Leeuw, J., J. Methven, and M. Blackburn, 2015: Evaluation of ERA-Interim reanalysis precipitation products using England and Wales observations. *Quart. J. Roy. Meteor. Soc.*, **141**, 798–806.
- Dee, D. P., and Coauthors, 2011: The ERA-Interim reanalysis: Configuration and performance of the data assimilation system. *Quart. J. Roy. Meteor. Soc.*, **137**, 553–597.
- DEFRA, 2014: *Winter 2013/14 severe weather recovery progress report*. London, UK, Department for Communities and Local Government, URL https://www.gov.uk/government/uploads/system/uploads/attachment_data/file/380573/Winter_2013-14_severe_weather_recovery_progress_report.pdf.
- Della-Marta, P. M., and J. G. Pinto, 2009: Statistical uncertainty of changes in winter storms over the North Atlantic and Europe in an ensemble of transient climate simulations. *Geo. Res. Lett.*, **36**.
- Deveson, A. C. L., K. A. Browning, and T. D. Hewson, 2002: A classification of FASTEX cyclones using a height-attributable quasi-geostrophic vertical-motion diagnostic. *Quart. J. Roy. Meteor. Soc.*, **128**, 93–117.
- Donner, L. J., and Coauthors, 2011: The dynamical core, physical parameterizations, and basic simulation characteristics of the atmospheric component AM3 of the GFDL global coupled model CM3. *J. Climat.*, **24**, 3484–3519.
- Eady, E., 1949: Long waves and cyclone waves. *Tellus*, **1**, 33–52.
- Easterbrook, S., and T. Johns, 2009: Engineering the software for understanding climate change. *Comput. Sci. Eng.*, **PP**, 1.
- Ebert, E., and J. McBride, 2000: Verification of precipitation in weather systems: Determination of systematic errors. *J. Hydrol.*, **239**, 179–202.
- Eckhardt, S., A. Stohl, H. Wernli, P. James, C. Forster, and N. Spichtinger, 2004: A 15-year climatology of warm conveyor belts. *Int. J. Climatol.*, **17**, 218–237.

- Economou, T., D. Stephenson, J. Pinto, L. Shaffrey, and G. Zappa, 2015: Serial clustering of extratropical cyclones in a multi-model ensemble of historical and future simulations. *Quart. J. Roy. Meteor. Soc.*
- Eyring, V., S. Bony, G. A. Meehl, C. A. Senior, B. Stevens, R. J. Stouffer, and K. E. Taylor, 2016: Overview of the Coupled Model Intercomparison Project Phase 6 (CMIP6) experimental design and organization. *Geosci. Model Dev.*, **9**, 1937–1958.
- Froude, L. S., 2010: TIGGE: Comparison of the prediction of northern hemisphere extratropical cyclones by different ensemble prediction systems. *Weather Forecast.*, **25**, 819–836.
- Gray, S. L., and H. F. Dacre, 2006: Classifying dynamical forcing mechanisms using a climatology of extratropical cyclones. *Quart. J. Roy. Meteor. Soc.*, **132**, 1119–1137.
- Hand, W., N. Fox, and C. Collier, 2004: A study of twentieth-century extreme rainfall events in the United Kingdom with implications for forecasting. *Meteor. Appl.*, **11**, 15–31.
- Harrold, T., 1973: Mechanisms influencing the distribution of precipitation within baroclinic disturbances. *Quart. J. Roy. Meteor. Soc.*, **99**, 232–251.
- Harvey, B., L. Shaffrey, T. Woollings, G. Zappa, and K. Hodges, 2012: How large are projected 21st century storm track changes? *Geo. Res. Let.*, **39**.
- Harvey, B. J., L. C. Shaffrey, and T. J. Woollings, 2014: Equator-to-pole temperature differences and the extra-tropical storm track responses of the CMIP5 climate models. *Clim. Dynam.*, **43**, 1171–1182.
- Harvey, B. J., L. C. Shaffrey, and T. J. Woollings, 2015: Deconstructing the climate change response of the northern hemisphere wintertime storm tracks. *Clim. Dynam.*, **45**, 2847–2860.
- Hawcroft, M., L. Shaffrey, K. Hodges, and H. Dacre, 2012: How much Northern Hemisphere precipitation is associated with extratropical cyclones? *Geo. Res. Let.*, **39**.
- Haylock, M., N. Hofstra, A. Klein Tank, E. Klok, P. Jones, and M. New, 2008: A European daily high-resolution gridded data set of surface temperature and precipitation for 1950–2006. *J. Geophys. Res.: Atmos.*, **113**.
- Hazeleger, W., and Coauthors, 2010: EC-Earth: A seamless earth-system prediction approach in action. *Bull. Amer. Meteor. Soc.*, **91**, 1357–1363.
- Held, I. M., 1993: Large-scale dynamics and global warming. *Bull. Amer. Meteor. Soc.*, **74**, 228–241.

- Held, I. M., and B. J. Soden, 2006: Robust responses of the hydrological cycle to global warming. *Int. J. Climatol.*, **19**, 5686–5699.
- Hewson, T. D., 1997: Objective identification of frontal wave cyclones. *Meteor. Appl.*, **4**, 311–315.
- Hewson, T. D., 1998: Objective fronts. *Meteor. Appl.*, **5**, 37–65.
- Hewson, T. D., and U. Neu, 2015: Cyclones, windstorms and the IMILAST project. *Tellus A*, **67**.
- Higgins, R. W., J. E. Janowiak, and Y.-P. Yao, 1996: *A gridded hourly precipitation data base for the United States (1963-1993)*. NCEP/Climate Prediction Centre, 46 pp.
- Higgins, R. W., W. Shi, E. Yarosh, and R. Joyce, 2000: *Improved United States precipitation quality control system and analysis*. NCEP/Climate Prediction Center, 40 pp.
- Hinman, R., 1888: *Eclectic Physical Geography*. Van Antwerp, Bragg and Co., 382 pp.
- Hodges, K., 1994: A general method for tracking analysis and its application to meteorological data. *Mon. Wea. Rev.*, **122**, 2573–2586.
- Hodges, K., 1995: Feature tracking on the unit-sphere. *Mon. Wea. Rev.*, **123**, 3458–3465.
- Hodges, K. I., 1996: Spherical nonparametric estimators applied to the UGAMP model integration for AMIP. *Mon. Wea. Rev.*, **124**, 2914–2932.
- Hodges, K. I., 1999: Adaptive constraints for feature tracking. *Mon. Wea. Rev.*, **127**, 1362–1373.
- Hodges, K. I., B. J. Hoskins, J. Boyle, and C. Thorncroft, 2003: A comparison of recent reanalysis datasets using objective feature tracking: Storm tracks and tropical easterly waves. *Mon. Wea. Rev.*, **131**, 2012–2037.
- Hoskins, B. J., and K. I. Hodges, 2002: New perspectives on the Northern Hemisphere winter storm tracks. *J. Atmos. Sci.*, **59**, 1041–1061.
- Hoskins, B. J., and P. J. Valdes, 1990: On the existence of storm-tracks. *J. Atmos. Sci.*, **47**, 1854–1864.
- Huffman, G., and Coauthors, 1997: The global precipitation climatology project (GPCP) combined precipitation dataset. *Bull. Amer. Meteor. Soc.*, **78**, 5–20.

- Huffman, G. J., R. F. Adler, M. M. Morrissey, D. T. Bolvin, S. Curtis, R. Joyce, B. Mc-Gavock, and J. Susskind, 2001: Global precipitation at one-degree daily resolution from multisatellite observations. *J. Hydrometeorol.*, **2**, 36–50.
- Hughs, T., and S. Gambrill, 2012: Summer floods in the UK: Comparing 2012 and 2007. Tech. rep., AIR Worldwide, London, UK.
- Hulme, M., 1992: A 1951–80 global land precipitation climatology for the evaluation of general circulation models. *Clim. Dynam.*, **7**, 57–72.
- Hulme, M., T. J. Osborn, and T. C. Johns, 1998: Precipitation sensitivity to global warming: Comparison of observations with HadCM2 simulations. *Geo. Res. Let.*, **25**, 3379–3382.
- Huntington, T. G., 2006: Evidence for intensification of the global water cycle: review and synthesis. *J. Hydrol.*, **319**, 83–95.
- Ihaka, R., and R. Gentleman, 1996: R: a language for data analysis and graphics. *J. Comp. Graph. Stat.*, **5**, 299–314.
- Joly, A., and Coauthors, 1997: The Fronts and Atlantic Storm-Track Experiment (FASTEX): scientific objectives and experimental design. *Bull. Amer. Meteor. Soc.*, **78**, 1917–1940.
- Jones, C. D., and Coauthors, 2011: The HadGEM2-ES implementation of CMIP5 centennial simulations. *Geosci. Model Dev.*, **4**, 543–570.
- Kalnay, E., and Coauthors, 1996: The NCEP/NCAR 40-year reanalysis project. *Bull. Amer. Meteor. Soc.*, **77**, 437–471.
- Kistler, R., and Coauthors, 2001: The NCEP-NCAR 50-year reanalysis: Monthly means CD-ROM and documentation. *Bull. Amer. Meteor. Soc.*, **82**, 247–267.
- Kållberg, P., 2011: Forecast drift in ERA-Interim. Tech. rep., ECMWF, Reading, UK.
- Lavers, D. A., R. P. Allan, E. F. Wood, G. Villarini, D. J. Brayshaw, and A. J. Wade, 2011: Winter floods in Britain are connected to atmospheric rivers. *Geo. Res. Let.*, **38**.
- Legg, T., 2011: Changes to the selection of stations used in the compilation of the United Kingdom Precipitation (HadUKP) series. Climate memorandum, Met Office National Climate Information Centre. URL http://www.metoffice.gov.uk/hadobs/hadukp/cm29_HadUKP_revisions_vn2.doc.

- Lehtonen, I., K. Ruosteenoja, and K. Jylhä, 2014: Projected changes in European extreme precipitation indices on the basis of global and regional climate model ensembles. *Int. J. Climatol.*, **34**, 1208–1222.
- Li, M., T. Woollings, K. Hodges, and G. Masato, 2014: Extratropical cyclones in a warmer, moister climate: A recent Atlantic analogue. *Geo. Res. Let.*, **41**, 8594–8601.
- Liu, Z., A. Mehran, T. J. Phillips, and A. AghaKouchak, 2014: Seasonal and regional biases in CMIP5 precipitation simulations. *Clim. Res.*, **60**, 35–50.
- Mailier, P. J., D. B. Stephenson, C. A. Ferro, and K. I. Hodges, 2006: Serial clustering of extratropical cyclones. *Mon. Wea. Rev.*, **134**, 2224–2240.
- Martin, G. M., and Coauthors, 2011: The HadGEM2 family of Met Office Unified Model climate configurations. *Geosci. Model Dev.*, **4**, 723–757.
- Meehl, G., C. Covey, T. Delworth, M. Latif, B. McAvaney, J. Mitchell, R. Stouffer, and K. Taylor, 2007: The WCRP CMIP3 multi-model dataset: A new era in climate change research. *Bull. Amer. Meteor. Soc.*, **88**, 1383–1394.
- Meehl, G. A., G. J. Boer, C. Covey, M. Latif, and R. J. Stouffer, 2000: The coupled model intercomparison project (CMIP). *Bull. Amer. Meteor. Soc.*, **81**, 313–318.
- Met Office, 2011: *Flooding — Summer 2007*. Exeter, UK, Met Office, URL <http://www.metoffice.gov.uk/about-us/who/how/case-studies/summer-2007>.
- Met Office, 2012: *Heavy rainfall/flooding in the Lake District, Cumbria - November 2009*. Exeter, UK, Met Office, URL <http://www.metoffice.gov.uk/climate/uk/interesting/nov2009>.
- Met Office, 2013: MIDAS land surface stations data (1853–current). *NCAS Br. Atmos. Data Cent.*, URL <http://catalogue.ceda.ac.uk/uuid/220a65615218d5c9cc9e4785a3234bd0>, accessed: 18/09/2013.
- Met Office, 2015: *Winter storms, January to February 2014*. Exeter, UK, Met Office, URL <http://www.metoffice.gov.uk/climate/uk/interesting/2014-janwind>.
- Met Office Hadley Centre, 2017: HadUKP — UK regional precipitation series. *Met Office Hadley Centre observations datasets*, URL <http://www.metoffice.gov.uk/hadobs/hadukp/>, accessed: 15/01/2017.
- Mills, T. C., 2016: Modelling rainfall trends in England and Wales. *Cogent Geosci.*, **2**, 1–8.
- Moss, R. R. H., and Coauthors, 2010: The next generation of scenarios for climate change research and assessment. *Nature*, **463**, 747–756.

- Murray, R. J., and I. Simmonds, 1991: A numerical scheme for tracking cyclone centres from digital data. Part I: Development and operation of the scheme. *Aust. Meteorol. Mag.*, **39**, 155–166.
- Neu, U., and Coauthors, 2013: IMILAST: a community effort to intercompare extratropical cyclone detection and tracking algorithms. *Bull. Amer. Meteor. Soc.*, **94**, 529–547.
- NOAA NCDC, 2013: GHCN - Monthly version 3: Homogeneity adjustment. *National Oceanographic and Atmospheric Administration*, URL <http://www.ncdc.noaa.gov/ghcnm/v3.php>, accessed: 23/09/2013.
- Osborn, T. J., M. Hulme, P. D. Jones, and T. A. Basnett, 2000: Observed trends in the daily intensity of United Kingdom precipitation. *Int. J. Climatol.*, **20**, 347–364.
- Parker, W. S., 2016: Reanalyses and observations: What’s the difference? *Bull. Amer. Meteor. Soc.*, **97**, 1565–1572.
- Pebesma, E. J., and R. S. Bivand, 2005: Classes and methods for spatial data in R. *R News*, **5**, 9–13.
- Petoukhov, V., S. Petri, S. Rahmstorf, D. Coumou, K. Kornhuber, and H. Joachim-Schellnhuber, 2016: The role of quasi-resonant planetary wave dynamics in recent boreal spring-to-autumn extreme events. *Proc. Natl. Acad. Sci. U. S. Amer.*, **113**, 6862–6867.
- Petoukhov, V., S. Rahmstorf, S. Petri, and H. J. Schellnhuber, 2013: Quasiresonant amplification of planetary waves and recent northern hemisphere weather extremes. *Proc. Natl. Acad. Sci. U. S. Amer.*, **110**, 5336–5341.
- Petterssen, S., and S. J. Smebye, 1971: On the development of extratropical cyclones. *Quart. J. Roy. Meteor. Soc.*, **97**, 457–482.
- Pfahl, S., and H. Wernli, 2012: Quantifying the relevance of cyclones for precipitation extremes. *Int. J. Climatol.*, **25**, 6770–6780.
- Pinto, J. G., N. Bellenbaum, M. K. Karremann, and P. M. Della-Marta, 2013: Serial clustering of extratropical cyclones over the North Atlantic and Europe under recent and future climate conditions. *J. Geophys. Res.: Atmos.*, **118**, 12–476.
- Pinto, J. G., I. Gómara, G. Masato, H. F. Dacre, T. Woollings, and R. Caballero, 2014: Large-scale dynamics associated with clustering of extratropical cyclones affecting western Europe. *J. Geophys. Res.: Atmos.*, **119**, 13,704–13,719.

- Pinto, J. G., S. Ulbrich, T. Economou, D. B. Stephenson, M. K. Karremann, and L. C. Shaffrey, 2016: Robustness of serial clustering of extratropical cyclones to the choice of tracking method. *Tellus A*, **68**.
- Pinto, J. G., U. Ulbrich, G. Leckebusch, T. Spanghel, M. Meyers, and S. Zacharias, 2007: Changes in storm track and cyclone activity in three SRES ensemble experiments with the ECHAM5/MPI-OM1 GCM. *Clim. Dynam.*, **29**, 195–210.
- Pitt, M., 2008: The Pitt Review - Learning lessons from the 2007 floods. *Cabinet Office Independent Review*.
- Plant, R., G. C. Craig, and S. Gray, 2003: On a threefold classification of extratropical cyclogenesis. *Quart. J. Roy. Meteor. Soc.*, 2989–3012.
- Priestley, M. D. K., J. G. Pinto, H. F. Dacre, and L. C. Shaffrey, 2016: Rossby wave-breaking, the upper-level jet and serial clustering of extratropical cyclones in Western Europe. *Geo. Res. Let.*, 1–8.
- R Core Team, 2015: *R: A Language and Environment for Statistical Computing*. Vienna, Austria, R Foundation for Statistical Computing, URL <https://www.R-project.org/>.
- Radinovic, D., 1986: On the development of orographic cyclones. *Quart. J. Roy. Meteor. Soc.*, **112**, 927–951.
- Ramos, A. M., R. Tomé, R. M. Trigo, M. L. Liberato, and J. G. Pinto, 2016: Projected changes in atmospheric rivers affecting Europe in CMIP5 models. *Geo. Res. Let.*, **43**, 9315–9323.
- Renard, R. J., and C. Clarke, 1965: Experiments in numerical objective frontal analysis. *Mon. Wea. Rev.*, **93**, 774–781.
- Renfrew, I. A., A. J. Thorpe, and C. H. Bishop, 1997: The role of the environmental flow in the development of secondary frontal cyclones. *Quart. J. Roy. Meteor. Soc.*, **123**, 1653–1675.
- Renggli, D., and P. Zimmerli, 2016: Misfortune seldom comes alone: Winter storm clusters in Europe. Tech. rep.
- Rhodes, R., L. Shaffrey, and S. Gray, 2015: Can reanalyses represent extreme precipitation over England and Wales? *Quart. J. Roy. Meteor. Soc.*, **141**, 1114–1120.
- Rivals, H., J.-P. Cammas, and I. A. Renfrew, 1998: Secondary cyclogenesis: The initiation phase of a frontal wave observed over the eastern Atlantic. *Quart. J. Roy. Meteor. Soc.*, **124**, 243–267.

- RMS, 2014: 2013–2014 winter storms in Europe. Tech. rep., RMS, London, UK.
URL http://forms2.rms.com/rs/729-DJX-565/images/ws_2013_2014_europe_winter_storms.pdf.
- Robson, A. J., T. K. Jones, D. W. Reed, and A. C. Bayliss, 1998: A study of national trend and variation in UK floods. *Int. J. Climatol.*, **18**, 165–182.
- Schaller, N., and Coauthors, 2016: Human influence on climate in the 2014 southern England winter floods and their impacts. *Nat. Clim. Change*, **6**, 627–634.
- Schemm, S., and M. Sprenger, 2015: Frontal-wave cyclogenesis in the North Atlantic: A climatological characterisation. *Quart. J. Roy. Meteor. Soc.*, **141**, 2989–3005.
- Schultz, D. M., 2001: Reexamining the cold conveyor belt. *Mon. Wea. Rev.*, **129**, 2205–2225.
- Shapiro, M. A., and D. A. Keyser, 1990: *Fronts, jet streams, and the tropopause*. NOAA ERL WPL.
- Sivakumar, B., 2011: Global climate change and its impacts on water resources planning and management: Assessment and challenges. *Stochastic Env. Res. and Risk Assessment*, **25**, 583–600.
- Smith, A., P. Bates, J. Freer, and F. Wetterhall, 2013: Investigating the application of climate models in flood projection across the UK. *Hydrol. Processes*, **28**, 2810–2823.
- Stadherr, L., D. Coumou, V. Petoukhov, S. Petri, and S. Rahmstorf, 2016: Record Balkan floods of 2014 linked to planetary wave resonance. *Sci. Adv.*
- Sterl, A., 2004: On the (in)homogeneity of reanalysis products. *Int. J. Climatol.*, **17**, 3866–3873.
- Stocker, T., and Coauthors, 2013: *Climate Change 2013: The Physical Science Basis. Contribution of Working Group I to the Fifth Assessment Report of the Intergovernmental Panel on Climate Change*. Cambridge University Press, Cambridge, UK and New York, USA.
- Taylor, K. E., R. J. Stouffer, and G. A. Meehl, 2012: An overview of CMIP5 and the experiment design. *Bull. Amer. Meteor. Soc.*, **93**, 485–498.
- Thorncroft, C., and B. Hoskins, 1990: Frontal cyclogenesis. *J. Atmos. Sci.*, **47**, 2317–2336.
- Trenberth, K. E., A. Dai, R. M. Rasmussen, and D. B. Parsons, 2003: The changing character of precipitation. *Bull. Amer. Meteor. Soc.*, **84**, 1205–1217.

- Trenberth, K. E., T. Koike, and K. Onogi, 2008: Progress and prospects for reanalysis for weather and climate. *Eos*, **89**, 234–235.
- Ulbrich, U., G. Leckebusch, and J. Pinto, 2009: Extra-tropical cyclones in the present and future climate: A review. *Theor. Appl. Climatol.*, **96**, 117–131.
- Ulbrich, U., J. G. Pinto, H. Kupfer, G. C. Leckebusch, T. Spanghel, and M. Reyers, 2008: Changing northern hemisphere storm tracks in an ensemble of IPCC climate change simulations. *Int. J. Climatol.*, **21**, 1669–1679.
- Uppala, S. M., and Coauthors, 2005: The ERA-40 re-analysis. *Quart. J. Roy. Meteor. Soc.*, **131**, 2961–3012.
- van Etten, J., 2015: *gdistance: Distances and Routes on Geographical Grids*. URL <https://CRAN.R-project.org/package=gdistance>.
- van Vuuren, D. P., and Coauthors, 2011: The representative concentration pathways: An overview. *Climatic Change*, **109**, 5–31.
- Vitolo, R., D. B. Stephenson, I. M. Cook, and K. Mitchell-Wallace, 2009: Serial clustering of intense European storms. *Meteorol. Z.*, **18**, 411–424.
- Wang, X. L., Y. Feng, R. Chan, and V. Isaac, 2016: Inter-comparison of extra-tropical cyclone activity in nine reanalysis datasets. *Atmos. Res.*, **181**, 133–153.
- Watanabe, M., and Coauthors, 2010: Improved climate simulation by MIROC5: Mean states, variability, and climate sensitivity. *J. Climat.*, **23**, 6312–6335.
- Wernli, H., and C. Schwierz, 2006: Surface cyclones in the ERA-40 dataset (1958–2001). Part I: Novel identification method and global climatology. *J. Atmos. Sci.*, **63**, 2486–2507.
- Whitaker, J. S., and T. M. Hamill, 2002: Ensemble data assimilation without perturbed observations. *Mon. Wea. Rev.*, **130**, 1913–1924.
- Wilby, R. L., K. J. Beven, and N. Reynard, 2008: Climate change and fluvial flood risk in the UK: More of the same? *Hydrol. proc.*, **22**, 2511–2523.
- Yin, J. H., 2005: A consistent poleward shift of the storm tracks in simulations of 21st century climate. *Geo. Res. Lett.*, **32**.
- Yukimoto, S., and Coauthors, 2012: A new global climate model of the Meteorological Research Institute: MRI-CGCM3 -model description and basic performance-. *J. Meteorol. Soc. Japan*, **90A**, 23–64.

-
- Zappa, G., L. C. Shaffrey, and K. I. Hodges, 2013a: The ability of CMIP5 models to simulate North Atlantic extratropical cyclones. *Int. J. Climatol.*, **26**, 5379–5396.
- Zappa, G., L. C. Shaffrey, K. I. Hodges, P. G. Sansom, and D. B. Stephenson, 2013b: A multimodel assessment of future projections of North Atlantic and European extratropical cyclones in the CMIP5 climate models. *Int. J. Climatol.*, **26**, 5846–5862.
- Zhang, Q., H. Körnich, and K. Holmgren, 2013: How well do reanalyses represent the southern African precipitation? *Clim. Dynam.*, **40**, 951–962.